GluA3-mediated Synaptic Plasticity and Dysfunction in the Cerebellum and in the Hippocampus

Carla Maria da Silva Matos

Lay-out Guus Gijben

Printed by Proefschriftmaken.nl
ISBN 978-94-6380-545-2

GluA3-mediated Synaptic Plasticity and Dysfunction in the Cerebellum and in the Hippocampus

GluA3-gemedieerde synaptische plasticiteit en disfunctie in het cerebellum en hippocampus

THESIS

to obtain the degree of Doctor from the
Erasmus University Rotterdam
by command of the
rector magnificus

Prof.dr. R.C.M.E. Engels

and in accordance with the decision of the Doctorate Board.
The public defence shall be held on
Wednesday 20th November 2019 at 11.30 hrs

by

Carla Maria da Silva Matos,
born in São João da Madeira, Portugal

Erasmus University Rotterdam

Erasmus

Doctoral Committee

Promotors:
Prof. Dr. C.I. De Zeeuw
Prof. Dr. H.W.H.G. Kessels

Copromotor:
Dr. B.H.J. Winkelman

Reading Committee:
Prof. Dr. Christiaan Levelt
Prof. Dr. Maarten Frens
Prof. Dr. Maarten Kamermans

To June

Table of Contents

Chapter 1

1

General Introduction

GENERAL INTRODUCTION

The ultimate goal in neuroscience is to uncover the biological basis and the mechanisms by which we perceive the world and act upon it, and by which we remember and learn. Learning and memory refer to the processes of acquiring, retaining and retrieving information in the central nervous system, ultimately leading to the formation of stable long-term memories. In the pursuit to understand the neural basis for learning and memory, it is crucial to grasp the relationships between behavior, behavioral learning, neuronal signals and circuit, and plasticity mechanisms.

This thesis explores the multiple roles of the GluA3 AMPA receptor (AMPAR) subunit, in both normal function and dysfunction, and in two distinct brain structures, the cerebellum and the hippocampus. From here it argues the relevance of this receptor subunit in the general mechanisms of learning and memory. The discussion draws conclusions regarding the differentiated ways the cerebellum and the hippocampus process learning and memory, emphasizing pertinent aspects for each structure.

We start by introducing the relevant concepts underlying learning and memory. We explore behavior as a byproduct of learning and a reflex of brain activity, and we look at learning and memory as the expression of changes in the synaptic connections between neurons, and their strengthening and weakening. We focus our attention at the excitatory glutamatergic activity, particularly the one mediated by AMPARs. Subsequently, we analyze these concepts for the cerebellum, looking at its function in the adaptation of locomotion and vestibulo-ocular reflex (VOR), and emphasizing the particular cases of long-term potentiation (LTP), long-term depression (LTD) and the parallel fiber-Purkinje Cell (pf-PC) synapse. We then shift to the hippocampus, looking at its role in encoding and retrieval of memories, and emphasizing the influence of arousal and stress. Lastly, we look at what happens when synaptic dysfunction arises, namely in Alzheimer's disease (AD).

1.1 The Brain

The remarkable range of human behavior and the complexity of the environment humans have been able to create for themselves depends on a sophisticated system of sensory receptors connected to a highly flexible neuronal machine: the brain.

Composed by millions of neurons, this structure is able to discriminate an enormous variety of events in the surrounding environment and appropriately interact with them. The continuous stream of information captured by these sensory receptors is then organized by the brain into perceptions, which then can be used to engage the appropriate and relevant behavioral responses. The functions of the brain depend not only on the ability of neurons to transmit signals to other cells, but also on their ability to appropriately respond to signals received from other cells and systems.

Experiences can lead to changes in behavior. Because behavior is driven by brain activity, changes in behavior must correspond to changes inside the brain. Indeed, virtually all behavior is the result of brain function; brain function is, in its turn, a sum of a set of operations. Brain activity underlies not only relatively simple motor behaviors (such as walking or eating) but also the complex cognitive actions that we attribute to humans, such as thinking, speaking or purposely creating works of art.

The challenge in science, and in neuroscience in particular, consists in explaining behavior in terms of brain activity, parsing it into the individual particular moves and actions of this structure: understand, on one hand, how the brain manages to trigger a coordinate motion of millions of particular neuronal cells to produce a specific and deliberate behavior; and, one another hand, uncover the way these individual cells are influenced by the whole, by the environment, and react in accordance to it.

It is widely known that the brain is organized into regions, each made up of large groups of neurons. Highly complex behaviors can be traced to specific regions of the brain and understood in terms of the functioning of those groups of neurons. The brain provides a centralized control of the nervous system, allowing rapid and coordinated responses to changes in the environment. This responsiveness can be as complex as sophisticated, controlling behavior based on complex sensory input, which require the information integrating capabilities of a centralized brain.

1.1.1 Behavior and experience - learning and memory

Whilst learning concerns the acquisition of a certain skill or knowledge, memory is the expression of what is acquired and stored. Behavior and experience are intrinsically connected to learning and memory because they constitute the interface between those latter processes and the outside world. Memory can be subdivided in different types, each underlying different types of learning and

controlled by different brain regions. Hippocampal memories, for example, concern mostly the declarative type, while cerebellar learning deals mostly with procedural memory. A simplified way to distinguish these two is by looking at the following example: if we remember a certain aspect of a specific drawing lesson (i.e., what happened, when and where), that is an example of explicit memory; the improved drawing skill as a result of that same lesson is an example of procedural memory.

Since famously advanced by Hebb that "cells that fire together wire together" (as summarized by Lowel & Singer, 1992), it is thought that experiences can modify synapses - the places of interconnection between neurons -, favoring and strengthening some neuronal pathways within a circuit and consequently weakening others. Accordingly, learning and memory are expressed as changes in the synaptic connections between neurons; the modifiability of specific connections contributes to the adaptability of behavior.

An obvious first step in any attempt to uncover how the individual responses of a network of cells give rise to complex behaviors is to understand how neurons are wired together to support those behaviors. Indeed, a major aim in neuroscience is to link systems-level analyses of learning with cellular analyses of plasticity. This top-down approach basically means connecting the observation that neurons can undergo modifications that lasts a relative short period of time, with the fact that much learning results in behavioral changes that can endure for many years. The main question is what patterns of neuronal activity are necessary and sufficient to induce synaptic plasticity in the awake behaving animal. This implies that such neuronal signals must transduce the sensory stimuli that guide learning into the cellular changes that encode memory.

1.1.2 The synapse: synaptic plasticity and transmission

Communication between neurons underlies both the basic and the higher-order processes essential for normal brain function. This communication occurs at a highly specialized site of contact between a presynaptic nerve terminal and a postsynaptic neuron: the synapse.

Though C.S. Sherrington first proposed on theoretical grounds that neurons connect with each other at a "synapsis" (Sherrington, 1890; Foster, 1897), this notion famously got widely accepted when Ramón y Cajal postulated that neurons are not just continuous tissue that goes throughout one point of the body to the other, connecting different parts, but that they actually communicate with each other (Ramón y Cajal, 1933; Sutherland, 1996; Shepherd, 2010).

It took several decades before the first experimental studies on synapses were carried out, first at the neuromuscular junction (Dale, Feldberg and Vogt, 1936); a couple more years later, the first pictures were published of synaptic vesicles and synaptic ultrastructure (e.g. De Robertis, 1954). Right from these studies, it was possible to observe that information is transmitted in the form of a chemical message released from the presynaptic terminal and received by specific receptors in the postsynaptic membrane, where the message is processed, integrated and propagated (Gray, 1959; Klemann and Roubos, 2011). From these, it was postulated that synapses result from the differential distribution and concentration of specific presynaptic and postsynaptic protein components, whose precise organization gives rise to proper function (Scannevin and Huganir, 2000).

Neurons are able to convey unique information because they form specific networks. In these specific connections between neurons, neuronal activity produces long-term changes by modifications in the functions of a set of these prewired connections. This ability of synapses to change their strength constitutes synaptic plasticity; it is long thought that synaptic plasticity encodes memories.

1.1.3 LTP and LTD

Long-term potentiation (LTP) and long-term depression (LTD) at excitatory synapses are thought to underlie experience-dependent learning and memory. These synaptic plasticity mechanisms are best characterized at hippocampal CA1 synapses, where they are used and manipulated in animal models of human neurodevelopmental, neuropsychiatric, and neurological disorders (Richard L. Huganir and Nicoll, 2013). The most prevalent forms of LTP and LTD are induced by calcium influx through postsynaptic NMDA receptors (NMDARs) and are expressed by long-lasting increases or decreases, respectively, in the synaptic localization and function of AMPARs (Collingridge *et al.*, 2010; Richard L. Huganir and Nicoll, 2013).

LTP comprises the strengthening of synapses resulting from recent patterns of activity. In the basis of this mechanism are patterns of synaptic activity that produce a long-lasting increase in the signal transmission between two neurons. A model for the induction of LTP is best described as a binding of glutamate to NMDARs coupled with depolarization of the postsynaptic membrane, which relieves the magnesium channel block, resulting in the entry of calcium through the NMDAR and a rise in spine calcium (Nicoll, Kauer and Malenka, 1988). Considerable evidence indicates that CaMKII is the primary downstream

target following calcium entry through the NMDAR, and it is both necessary and sufficient for LTP. Two interesting areas of research concern the activity-dependent translocation of CaMKII to the synapse and the role of CaMKII as a memory molecule. Accordingly, elevated calcium in the spines recruits CaMKII to the postsynaptic density (PSD) (Lisman, Yasuda and Raghavachari, 2012); the activation of CaMKII during LTP induction is only transient, returning to baseline within a few minutes (Lee *et al.*, 2009). This finding implies that the persistence of LTP must rely on signaling cascades downstream of CaMKII.

LTD is, in essence, the opposite of LTP in terms of its effects on the synapse. It consists in an activity-dependent reduction in the efficacy of neuronal synapses lasting hours or longer following a long patterned stimulus (Volianskis *et al.*, 2015). The role of LTD has been extensively studied in the cerebellum (Ito, 1982; Hansel and Linden, 2000), among other regions (see Massey and Bashir, 2007 for a comprehensive review), as for example the hippocampus (Dudek & Bear, 1993). In terms of the process, cerebellar LTD, unlike hippocampal LTD, does not require NMDAR activation and is induced by the coincident activation of mGluR1 receptors and voltage-gated calcium channels that in turn activate protein kinase C (PKC) (Linden and Connor, 1991; De Zeeuw *et al.*, 1998), resulting in synaptic depression.

The main differentiator between LTP and LTD is proposed to be the magnitude and duration of the calcium signaling. High levels of calcium activate the low-affinity kinase CaMKII to initiate the phosphorylation of PSD proteins, ultimately resulting in enhanced transmission (for LTP). On the other hand, modest levels of calcium selectively engage the high-affinity phosphatase calcineurin, resulting in the dephosphorylation of PSD proteins and a reduction in transmission (for LTD) (Lisman, 1989). This classic model has been challenged in recent years in studies that showed that LTD does not require calcium influx. Instead, glutamate binding to the NMDAR without opening of the channel leads to the expression of LTD (Nabavi *et al.*, 2013; Dore, Aow and Malinow, 2016).

1.1.4 AMPA Receptors

Glutamate is the most abundant neurotransmitter in the nervous system, mediating fast synaptic transmission. In the CNS, the majority of fast excitatory glutamatergic neurotransmission is mediated by AMPARs (Dingledine *et al.*, 1999), that underpin cognitive processes like learning and memory (Derkach *et al.*, 2007; Anggono and Huganir, 2012; Haglerød *et al.*, 2017). AMPAR dysfunction

underlies neurological disorders such as stroke and epilepsy (Sarro *et al.*, 2005; Kwak and Weiss, 2006; Bowie, 2008).

AMPARs are tetrameric complexes, composed by four subunits (GluA1 to GluA4) that assemble into functional homo- or heteromeric channels, and that are permeable to sodium and calcium (only AMPARs without GluA2 are calcium permeable) (Hollmann and Heinemann, 1994; Bettler and Mulle, 1995; Traynelis *et al.*, 2010). It is known that GluA1 can form homomers (composed by four GluA1 subunits) though it is most often seen forming heteromers with GluA2. These GluA1/GluA2 AMPARs are designated here as GluA1-containing AMPARs. GluA3 forms heteromers with GluA2. These GluA2/GluA3 AMPARs are commonly called GluA3-containing AMPARs. The distribution of these subunits throughout the brain varies according to the region and type of neuron one is looking at.

Plasticity mediated by synaptic trafficking of AMPARs plays an important role in the acquisition of declarative memories. More specifically, GluA1-containing AMPARs are crucially involved in several forms of experience-dependent plasticity (Kessels and Malinow, 2009). It is known that GluA1-dependent synaptic plasticity is mediated by active trafficking (Shi *et al.*, 2001; Makino and Malinow, 2011) and by changes in conductance and open probability at the single receptor level (Benke *et al.*, 1998; Derkach, Barria and Soderling, 1999). GluA1 is inserted into synapses upon the induction of LTP or the formation of fear memories; a selective blockade of GluA1 trafficking impairs LTP and memory formation (Rumpel *et al.*, 2005; Mitsushima *et al.*, 2011). Consequently, LTP and the formation of fear memories are severely impaired in GluA1-deficient mice (Humeau *et al.*, 2007).

The GluA1 subunit's primary relevance for learning can be attributed to its unique structure. This subunit contrasts with GluA2 and GluA3 by presenting a long cytoplasmic tail (contrary to GluA2 or GluA3) that contains several unique phosphorylation sites by which trafficking of GluA1 to synapses can be regulated. An example of a phosphorylation trigger is protein kinase A (PKA), which lowers the threshold for LTP and facilitates memory formation (Hu *et al.*, 2007; Crombag *et al.*, 2008; Qian *et al.*, 2012). An activation by PKA can happen following activation of beta-adrenergic receptors (ß-ARs), which leads to the activation of adenylyl cyclases, producing a rise in intracellular cyclic AMP (cAMP).

In the hippocampus, cortex and amygdala, both LTP and learning depend on the trafficking of GluA1-containing AMPARs to synapses (Rumpel *et al.*, 2005; Nedelescu *et al.*, 2010; Makino and Malinow, 2011; Mitsushima *et al.*, 2011).

However, GluA3-containing AMPARs don't seem to contribute much to synaptic currents, synaptic plasticity or learning (Meng, Zhang and Jia, 2003; Humeau *et al.*, 2007; Adamczyk *et al.*, 2012). Though attempts were made to show its relevance for learning and memory processes, AMPA GluA3-mediated currents were never found to be present and/or relevant. Nevertheless, GluA3-containing AMPARs are present in most brain regions, including the hippocampus, cortex, amygdala, striatum, thalamus, brain stem, olfactory bulb, nucleus accumbens and cerebellum (Breese *et al.*, 1996; Reimers, Milovanovic and Wolf, 2012; Schwenk *et al.*, 2014), suggesting that GluA3-plasticity may be operative throughout the brain.

Whereas AMPAR subunit rules for synaptic plasticity have been extensively studied in relation to declarative learning, it is unclear whether these rules apply to cerebellum-dependent motor (procedural) learning. It is known that AMPAR plasticity occurs at pf-PC synapses reflecting the expression of LTP or LTD (Kakegawa and Yuzaki, 2005; Steinberg *et al.*, 2006), but the full functional significance of it and the precise molecular pathways underlying this plasticity remain to be further elucidated (Gao, van Beugen and De Zeeuw, 2012). In addition, the specific roles of GluA1- and/or GluA3-containing AMPARs in plasticity of PCs have hardly been studied (Kakegawa and Yuzaki, 2005; Douyard *et al.*, 2007; Bats, Farrant and Cull-Candy, 2013)

1.2 The Cerebellum

The cerebellum offers a unique opportunity for understanding the neural basis of learning and memory. This structure has a defined circuit and the cell types within it are well identified, allowing a mapping of the convergence of motor and sensory signals, required for motor learning. This facilitates the study of the role of individual neurons but also of the synaptic plasticity mechanisms involved in learning.

Despite its small size, the cerebellum contains more than half of the brain's neurons (Herculano-Houzel and Lent, 2005). While different regions within the cerebellum are connected to different parts of the brain, the pattern of wiring within the cerebellar cortex is highly consistent, receiving input from sensory systems of the spinal cord and from other parts of the brain and integrating these inputs to fine-tune motor activity.

The current view about the cerebellum is that different cerebellar regions play a crucial role in controlling distinct behaviors, for example voluntary limb movements, balance, locomotion and eye movements (Morton and Bastian, 2004). This view

is based on the anatomy of cerebellar afferent and efferent connections as well as neural recording and lesion studies. More specifically, it has been proposed that different modules of the cerebellum use different encoding schemes to form and express their respective memories (De Zeeuw and Ten Brinke, 2015), offering an enriched way to acquire and control sensorimotor processes with its specific challenges in the spatiotemporal domain.

In line with its role in adaptive control of skilled movements and motor learning, and looking at a more detailed view, the cerebellum receives vestibular, sensory and motor information, which are conveyed from the entire body to the cerebellar cortex where they converge to Purkinje cells (PC). Organized in a repeating pattern, PCs receive input signals from two types of fibers. The first type comprises thousands of weak inputs from the parallel fibers (pf) of the granule cells (GC); pf relay proprioceptive, somatosensory and vestibular information reaching the cerebellum via mossy fibers (MFs), originating from several pre-cerebellar nuclei in the brainstem and spinal cord (Ichikawa *et al.*, 2016). Each PC receives another dramatically different type of signal: an extremely strong input from a single climbing fiber (Ichikawa *et al.*, 2016). The climbing fiber serves as a "teaching signal", inducing long-lasting changes in the strength of parallel fiber inputs (Marr, 1969; Albus, 1971; Ito, 1989, 2001; Hansel, Linden and D'Angelo, 2001). It ascends into the cerebellum from the brainstem. Climbing fibers run perpendicular to the pfs, giving rise to a characteristic crystallin structure (Morton and Bastian, 2004). Unlike most other neurons in the brain (van Vreeswijk and Sompolinsky, 1996), PCs produce two different types of spikes: complex spikes and simple spikes (Welsh *et al.*, 1995; Medina and Lisberger, 2008). The complex spikes reflect the activation of the climbing fibers, whereas the simple spikes can be triggered by the other main afferent input to the cerebellar cortex, the mossy fiber-parallel fiber (MF-pf) pathway (Medina and Lisberger, 2008). It has been previously shown that synaptic plasticity at the parallel fiber afferents of PCs (i.e., at the pf-PC synapse) crucially contributes to motor learning (Schonewille *et al.*, 2010).

The arrangement of cells in the cerebellar cortex is highly invariant across the entire structure, making it impossible to subdivide the cerebellum based only on cortical anatomy. Instead, the cerebellum is divided into distinct functional zones based on afferent and efferent connectivity (Jansen and Brodal, 1940; Ito, 1984; Voogd and Glickstein, 1998).

Based on different behavioral abnormalities that resulted when each region was lesioned, Fulton and Dow (Botterell and Fulton, 1938, 1938; Dow, 1938) first proposed three divisions: the vestibulocerebellum, responsible for the vestibular function (Dow, 1938; Voogd and Barmack, 2006); the spinocerebellum, that controls locomotion (Botterell and Fulton, 1938, 1938); and the cerebrocerebellum, that is involved in the voluntary control of body parts (Botterell and Fulton, 1938, 1938).

1.2.1 Cerebellar learning and memory: adaptation

In our daily life, we all subtly benefit from the fine work performed by the cerebellum. It allows us to fine tune our movements during daily actions in response to environmental changes, and while executing complicate tasks such as walking, playing the violin, or painting. The process of producing visual art as in a drawing or a painting are a paradigmatic case of this type of learning, as it requires a refined and over-time perfected eye-hand coordination.

As we see here, this structure deals with a procedural type of learning. The type of memories involved are adaptive, meaning that they constitute a constant refinement of previous memories; this implies that these memories have to be flexible for this adaptation to occur.

The cerebellum also exerts control over the flexibility of these behaviors: cerebellar integrity is critical for trial-and-error adaptation of motor behaviors to new contexts. One hypothesis for this adaptability of the motor patterns is that the cerebellum processes sensory inputs and makes immediate alterations of ongoing movement patterns (Allen and Tsukahara, 1974; Shimansky *et al.*, 2004), acting as a real-time sensory processing device (Bower, 1997) and modulating motor responses in a reactive, feedback manner based on sensory perturbations. An alternative hypothesis is that the cerebellum predicts alterations in the movements patterns using trial-and-error practice (Thach, Goodkin and Keating, 1992); this is consistent with the cerebellar widespread capacity for plasticity (Ito, 1989, 2000; Hansel, Linden and D'Angelo, 2001) and the behavioral evidence that cerebellar damage interferes with many forms of practice-dependent motor adjustments (McCormick, Steinmetz and Thompson, 1985; Horak and Diener, 1994; Martin *et al.*, 1996; Lang and Bastian, 1999). The reactive or feedback-driven adaptations differ importantly from predictive adaptations in that they occur more quickly in response to ongoing afferent feedback (i.e., do not require practice) and are not stored by the nervous system (i.e., do not produce aftereffects) (Morton and Bastian, 2006).

The cerebellum is essential for well-researched and characterized forms of learning, such as the proper coordination of posture and locomotion (Thach, Goodkin and Keating, 1992; Welsh *et al.*, 1995) and the adaptation of the VOR (Raymond, Lisberger and Mauk, 1996). Both the cerebellar circuitry and the learned behaviors it mediates are more complex than once thought. Appreciating and linking the complexities of both is bringing us closer than ever to understanding how specific mechanisms of plasticity contribute to learning.

1.2.1.1 Locomotion

Locomotion is a mechanically demanding task; the cerebellum plays an important role in the spatiotemporal control of the complex multi-joint movements required for the coordination of this behavior. To accomplish it, the cerebellum must synchronize motor signals through projections to the cerebral cortex via thalamus (Allen and Tsukahara, 1974) and to the spinal cord via the brainstem (Llinas, 1964; Azim *et al.*, 2014; Esposito, Capelli and Arber, 2014).

When the integrity of the cerebellum and its circuits is perturbed, the motor output is severely impaired, often resulting in ataxia and dystonia (see Morton and Bastian, 2004 for a comprehensive review). Several studies have shown that cell type-specific abnormalities in cerebellar micro circuitry can result in pronounced impairments in locomotion performance and adaptation as well as interlimb coordination (Lalonde and Strazielle, 2007; Hoogland *et al.*, 2015; Machado *et al.*, 2015; Vinueza Veloz *et al.*, 2015; Darmohray *et al.*, 2019).

1.2.1.2 VOR adaptation

Adaptation of compensatory eye movements is one of the most widely studied forms of cerebellar motor learning and serves to stabilize gaze (Anzai, Kitazawa and Nagao, 2010; Schonewille *et al.*, 2011; Blair *et al.*, 2013). The VOR stabilizes images on the retina by causing eye rotation in the opposite direction to head turns. Motor learning mediated by the cerebellum calibrates the VOR by modifying the amplitude of the reflex whenever retinal image motion is associated persistently with head turns (Gonshor and Melvill, 1973; Ito *et al.*, 1974; Miles and Fuller, 1974; Gauthier and Robinson, 1975). If head turns are paired with image motion in the same direction as the head turn, then a learned decrease is induced in the amplitude of the VOR. If head turns are paired with image motion in the opposite direction from the head turn, then a learned increase is induced in the amplitude of the VOR (Raymond and Lisberger, 1998). These changes are documented by computing the gain of the VOR, defined as the ratio of eye movement amplitude

to head movement amplitude during passive head turns in darkness. Learning in the VOR is associative: it depends on the pairing of head turns and image motion.

1.2.2 LTP and LTD in the cerebellum: the pf-PC synapse

Accumulating evidence indicates that cerebellar LTP is necessary for procedural learning. However, little is known about its underlying molecular mechanisms.

As seen above, it is widely believed that LTP- and LTD-type synaptic plasticity mechanisms act in concert to mediate several types of learning in brain regions such as the hippocampus, amygdala and cerebral cortex (Malinow and Malenka, 2002; Takahashi, Svoboda and Malinow, 2003; Rumpel *et al.*, 2005; Nedelescu *et al.*, 2010; Makino and Malinow, 2011; Nabavi, Fox, Alfonso, *et al.*, 2014). For cerebellar learning, LTD at the pf to PC synapse has historically been considered the dominant plasticity mechanism (Linden and Connor, 1995; Ito, 2002). The theory of pf-PC LTD was originally based on models by Marr (1969), later elaborated by Albus (1971), suggesting that the cerebellar matrix consisting of parallel fibers and orthogonally oriented climbing fibers is optimally designed for entraining and modifying PC output. Ito and colleagues (1982) confirmed these ideas by showing that the combined activation of these two inputs resulted in a persistent depression of pf-evoked EPSCs in PC (Ito, 1982; Linden and Connor, 1995). Their findings indicated that induction of LTD during visuo-vestibular training could persistently modify the gain and phase of the simple spike activity of the floccular PC that drive the VOR (Nagao, 1989).

Previous studies proposed a role for cerebellar LTP in the context of bidirectional gain modulation (Boyden *et al.*, 2006). This work suggested that gain-down modulation of the eye movements might require pf-PC LTP, and conversely, gain-up modulation would require LTD. The possible role of LTP at the pf to PC synapse in cerebellar motor learning has been also suggested by various other cell-specific mouse mutant studies (Andreescu *et al.*, 2005; Schonewille *et al.*, 2010; Peter *et al.*, 2016). However, these studies tackled more upstream PC processes, which involved the nuclear estrogen receptor, cytosolic protein phosphatase calcineurin and subsynaptic protein shank2, and as a consequence they suffered from various side-effects that prevented definitive conclusions (Gao *et al.*, 2012). Regarding the induction of this long-term synaptic strength changes, at the cerebellar pf synapses onto PCs, LTD induction was shown to be PKCα (Leitges *et al.*, 2004), cGKI (Feil *et al.*, 2003) and α/βCaMKII dependent (Hansel *et al.*, 2006; van Woerden *et al.*, 2009), whereas LTP requires the activation of PP1, PP2A, and calcineurin (Belmeguenai and Hansel, 2005).

The potential correlation between LTD induction and cerebellar motor learning was subsequently supported by a series of studies in mouse mutants in which both processes were affected concomitantly (Alba *et al.*, 1994; Kim and Thompson, 1997; De Zeeuw *et al.*, 1998; Feil *et al.*, 2003; Koekkoek *et al.*, 2003; Boyden *et al.*, 2006). Still, these studies were not conclusive. Pharmacological blocking of LTD did not affect another type of cerebellar motor learning, namely eyeblink conditioning (Welsh *et al.*, 2005). Besides that, training without instructive signals from the climbing fibers partially allowed VOR adaptation (Ke, Guo and Raymond, 2009). Although the simple spike suppression observed at early stages of some forms of motor learning in-vivo may suggest LTD occurrence (Yang and Lisberger, 2014; ten Brinke *et al.*, 2015), an increasing amount of studies suggest that LTD is not a strict requisite for motor learning (Schonewille *et al.*, 2011; Hesslow *et al.*, 2013). In fact, a recent paper by Boele and colleagues (Boele *et al.*, 2018) showed that actually only a concurrent disruption of pf-PC LTD and molecular layer interneurons-PC feed-forward inhibition could affect cerebellar-dependent adaptation (in the case of this study, eyeblink conditioning). In this sense, it rejects the idea that a single form of neural plasticity is essential and sufficient, and it supports the notion that synaptic and intrinsic plasticity synergistically contribute to form a temporal memory in the cerebellum (Gao, van Beugen and De Zeeuw, 2012), highlighting that both processes can compensate for each other's deficits.

1.3 The Hippocampus

The ability to learn spatial relationships and to modify stored representations when the world changes is essential for survival (Anderson, Grossrubatscher and Frank, 2014). Declarative or explicit memories, the conscious memories of facts and events, are mediated by the hippocampal memory system. This structure is widely known as crucial for the generation of new declarative long-term memories (Abel and Nguyen, 2008). It also has long been known to be involved in higher order cognitive functions, most notably memory formation and spatial navigation (Milner and Scoville, 1957; O'Keefe and Dostrovsky, 1971). It constitutes only a fraction of the cortical areas, and it has a relatively organized structure, receiving input from and sending information back to multimodal associational cortical areas (Acsády and Káli, 2007).

As with many brain regions, the hippocampus is highly interconnected (Amaral and Witter, 1995). These connections include a large number of feed-forward connections, which begin with a projection from the entorhinal cortex to all of the hippocampal subdivisions. Information also propagates along multiple internal pathways, including the Mossy fibers of the dentate gyrus that project to areas

CA2 and CA3, and the Schaffer collaterals from area CA3 to area CA1. In addition, there are a number of recurrent networks within the hippocampal circuit (Yang *et al.*, 2014).

The hippocampal regions, which differ in their connectivity with subcortical structures (Amaral and Witter, 1995), also vary along the dorsoventral axis. Most studies of the rodent hippocampus have focused on the more physically accessible dorsal region, which is noted for neurons that represent specific locations in space ("place cells") and is thought to be important for spatial navigation and memories involving spatial context. In contrast, the less-studied intermediate and ventral hippocampus may play an important role in anxiety and emotional memories (Fanselow and Dong, 2010).

1.3.1 Hippocampal learning and memory: encoding and retrieval

The brain has an impressive storage capacity for declarative episodic memories; with hundreds of new experiences encoded every day, years later we may still be able to retrieve details of some of those experiences. The ability to store large numbers of experiences with minimal interference is thought to depend on neural network properties of the hippocampus, which can be described as an autoassociative network with strong intrinsic connectivity (D. and Skey, 1971; McNaughton and Morris, 1987; Treves and Rolls, 1994).

The contribution of hippocampal circuits to high-capacity episodic memory is often attributed to the large number of orthogonal activity patterns that may be stored in these networks (Alme *et al.*, 2014). With these orthogonalizing representations, hippocampal networks are thought not only to minimize interference but also to maximize the number of experiences that can be stored in the same network. Memories are stored in this network by strengthening connections between cells that were active at the encoding stage. These cells are then thought to be reactivated during memory retrieval following stimulation of a subset of the ensemble (Alme *et al.*, 2014).

At the synapse level, protein phosphatases are required for postsynaptic LTD induction at the excitatory synapses of the hippocampal neurons, whereas kinases are required for postsynaptic LTP induction (Mulkey, Herron and Malenka, 1993; Lisman and Zhabotinsky, 2001). In this region, protein phosphatase 1 (PP1), the activity state of which is indirectly controlled by calcium/calmodulin-activated protein phosphatase 2B (calcineurin or PP2B), has been suggested to act in concert with the α isoform of calcium/calmodulin-dependent kinase II

(αCaMKII) to provide a molecular switch regulating the phosphorylation state of AMPA receptors (Lisman and Zhabotinsky, 2001; Malleret *et al.*, 2001).

1.3.2 Arousal and stress

Norepinephrine (NE), also known as noradrenaline, is the neurotransmitter on the basis of the noradrenergic system. Its general function is to mobilize the brain and body for action, regulating neuronal activity and promoting long-term memory changes through the modulation of synaptic plasticity and memory consolidation. NE plays an essential role in the regulation of arousal, attention, cognitive function and stress reactions. It also functions peripherally, as a hormone, as a part of the sympathetic nervous system, in the "fight or flight" response (Hussain and Maani, 2019).

During emotional events and states of heightened arousal, NE release reaches high levels. NE can either be released from the presynaptic terminal to the synaptic cleft via exocytosis, or convert to epinephrine (E) in neurons that contain the enzyme phenylethanolamine-N-methyl transferase (Hussain and Maani, 2019). Both NE and E bind to three classes of adrenergic receptors, the α1, the α2, and the β adrenergic receptors (β-AR) (Hein, 2006; Gelinas and Nguyen, 2007).

β-AR signaling has long been considered to play a crucial role in memory processing (Bouret and Sara, 2005; Tronson and Taylor, 2007; Otis, Fitzgerald and Mueller, 2013; Hagena, Hansen and Manahan-Vaughan, 2016). It is well known that β-AR activation by NE primes an increase in neuronal membrane excitability, leading to a rise in intracellular cyclic adenosine monophosphate (cAMP) levels through the activation of adenylyl cyclases, in a PKA-dependent manner (Cahill *et al.*, 1994; Hu *et al.*, 2007; Mueller, Porter and Quirk, 2008; Sara, 2009). It has been shown that β-ARs significantly modulate LTP in the hippocampus (Thomas *et al.*, 1996; Gelinas *et al.*, 2008) and modulation of LTP by β-AR likely represents a cellular mechanism for the storage of emotionally arousing events. In fact, recent studies have provided a clue to the mechanisms that underlie hippocampus involvement in emotional memory by pointing out a potential role of β-AR as a switch that selectively promotes synaptic plasticity in this structure (Papaleonidopoulos and Papatheodoropoulos, 2018).

1.4 Alzheimer's disease

Alzheimer's disease (AD) is a chronic neurodegenerative disease. Patients with AD display progressive dementia, with cognitive decline and memory impairment (Terry *et al.*, 1991; Brown *et al.*, 1998; Selkoe, 2002; Coleman, Federoff and Kurlan,

2004; Scheff *et al.*, 2006). Synaptic perturbations, and neuronal degeneration and loss are considered to be the best correlate of AD-dementia (Price, 1986; DeKosky and Scheff, 1990; Terry *et al.*, 1991; Sze *et al.*, 1997; Price and Sisodia, 1998).

AD is characterized by the presence of intraneuronal neurofibrillary tangles and extracellular deposits in plaques of β amyloid (Aβ), a small peptide with a high propensity to form aggregates. Though the exact causes of AD have remained unclear, the amyloid hypothesis, first proposed more than 30 years ago (Glenner and Wong, 1984), has steadily received increasing support (Beyreuther and Masters, 1991; Selkoe, 1991, 2011; Hardy and Higgins, 1992; Sisodia and Price, 1995) (for views against this hypothesis, see Marx, 1992; Oda *et al.*, 1994, 1995). The amyloid hypothesis proposes that build-up of Aβ is crucial to the pathogenesis of the disease (Selkoe, 2000). The potential neurotoxicity of Aβ, as well as the damaging effects on neuronal function of the accumulation of excessive amounts of this peptide, have been shown extensively (Yankner, Duffy and Kirschner, 1990; Pike *et al.*, 1991, 1993). Through the use of neuronal preparations with Aβ in various aggregate states, it has been shown that it elicits electrophysiological changes (Cullen *et al.*, 1997; Freir, Holscher and Herron, 2001; Kim *et al.*, 2001; Stéphan, Laroche and Davis, 2001). Transgenic expression of human genes linked to elevated Aβ1-42 (one of the forms of Aβ) has resulted in mice that exhibit certain AD-like molecular, cellular, and behavioral phenotypes (Hsiao *et al.*, 1995, 1996; Moran *et al.*, 1995).

Evidence suggests that synapse degeneration starts at the dendritic spine level (Harris and Kater, 1994; Carlisle and Kennedy, 2005; Segal, 2005), though it's likely that AD dementia starts even before loss of synapses by spine changes. In both AD patients and transgenic mouse AD models, a decrease in spine density has been observed (Ferrer and Gullotta, 1990; Moolman *et al.*, 2004; Spires *et al.*, 2005; Jacobsen *et al.*, 2006).

Even with this evidence, it's still unknown how exactly Aβ participates in the cascade of cellular events that results in progressive cognitive decline in AD patients. It has been shown that neuronal activity modulates the formation and secretion of Aβ peptides in hippocampal slice neurons that overexpress APP, a precursor for Aβ (Kamenetz, Tomita, Hsieh, Seabrook, Borchelt, Iwatsubo, Sisodia, Malinow, *et al.*, 2003). Besides that, Aβ seems to selectively depress excitatory synaptic transmission onto neurons that overexpress APP as well as nearby neurons that do not. Interestingly, this synaptic depression depends on NMDAR activity (Kamenetz, Tomita, Hsieh, Seabrook, Borchelt, Iwatsubo, Sisodia, Malinow, *et al.*,

2003; Shankar *et al.*, 2007; Lu *et al.*, 2011; Kessels, Nabavi and Malinow, 2013) and can be reversed by blockade of neuronal activity (Kamenetz, Tomita, Hsieh, Seabrook, Borchelt, Iwatsubo, Sisodia and Malinow, 2003). Moreover, the NMDAR-dependent synaptic depression triggered by Aβ oligomers happens through the removal of AMPARs and NMDARs from synapses (Snyder *et al.*, 2005; Nabavi *et al.*, 2013). A blockade of AMPAR endocytosis prevents depletion of NMDARs and a loss of spines (Hsieh *et al.*, 2007; D. Miyamoto *et al.*, 2016), suggesting that the removal of AMPARs from synapses is critical for this pathway to induce synaptic failure.

1.5 Scope of this thesis

In this thesis, we aim at exploring the roles of the GluA3 AMPA receptor subunit in the cerebellum and in the hippocampus, as well as its role in Alzheimer's disease. Departing from these concepts, we raise the questions we set to answer, establishing the scope of this thesis. After this, the experimental chapters that form this thesis are presented. Lastly, we engage in a discussion where we aim to answer relevant questions and argue about pertinent topics arised throughout the thesis.

In Chapter 2, we review the most relevant issues regarding the cerebellum and its role in locomotion. We look into neuro-anatomical studies, clinical reports and cell-specific rodent studies to describe the modules and the relevant networks that take part in the act of locomotion. Lastly we discuss the significance of locomotion control in highlighting the modular organization of the spinocerebellum, and how it contrasts beautifully with that of the vestibulocerebellum, which controls VOR adaptation.

In Chapter 3, we follow this lead and shift to VOR adaptation. Here, we explore the impact of different manipulations at the GC level of the cerebellum in this cerebellum-dependent task. We show that there's no impact on VOR adaptation for these manipulations, strengthening the idea proposed before that a minority of functionally intact GCs is sufficient for the maintenance of basic motor performance, and extending this idea that these might also be enough for some level of adaptation.

In Chapter 4, we show that adaptation of the VOR is dependent on GluA3-containing AMPARs in PCs of the cerebellum. We also demonstrate that the induction and expression of LTP at the pf-PC synapse is triggered by a rise in cAMP through Epac-mediated activation of postsynaptic GluA3-containing AMPARs, and that

this process involves a change in conductance and open probability of the GluA3 subunit channel.

In Chapter 5, we report on the physiological function of a newly identified form of hippocampus synaptic plasticity in the CA1 region, dependent of GluA3-containing AMPARs. We show that these GluA3-dependent currents are low under basal conditions, but get increased by β-AR activation during arousal. We propose that GluA3-plasticity in the hippocampus regulates memory retrieval.

In Chapter 6, we reveal that GluA3-containing AMPARs play a crucial role in the Aβ-mediated deficits exhibited by Alzheimer's disease. We show that the expression of amyloid-β-mediated synaptic and cognitive deficits require the presence of GluA3.

In Chapter 7, we expand on the findings described in Chapter 6 and show that oligomeric Aβ-driven synaptic depression and spine loss in AD critically depend on protein interactions at the PDZ-binding domain in the GluA3 c-tail. We conclude that oligomeric Aβ causes cognitive decline by corrupting the trafficking of synaptic GluA3-containing AMPARs.

Finally, the main conclusions of this thesis are thoroughly exposed and discussed in Chapter 8.

1

Chapter 2

Cerebellar Modules and Networks Involved in Locomotion Control

Carla da Silva Matos[1*], María Fernanda Vinueza Veloz[2*], Tom J. H. Ruigrok[2] and Chris I. De Zeeuw[1,2]

[1] Netherlands Institute for Neuroscience, Royal Netherlands Academy of Arts & Sciences, Amsterdam, The Netherlands

[2] Dept. of Neuroscience, Erasmus MC, Rotterdam, The Netherlands

* These authors contributed equally to this work.

Correspondence should be addressed to CIDZ (c.dezeeuw@erasmusmc.nl).

ABSTRACT

Modern neuroscience is paving the way for new insight into cerebellar functions including the control of cognitive, autonomic and emotional processes. Yet, how the cerebellum coordinates basic motor behavior such as locomotion is still only partly understood. Here, we will review the role of the cerebellum in locomotion from the perspective of neuro-anatomical and clinical reports as well as cell-specific rodent studies. Evidence has been emerging that different modules and networks exert synergistic roles in the preparation, performance, adaptation and consolidation of locomotion, highlighting their contribution to interlimb coordination and the accuracy, efficiency and regularity of locomotion patterns.

INTRODUCTION

Whereas the cerebellum does not initiate movement, it does facilitate the acquisition and performance of well-timed, smooth and efficient movements aimed at a specific target in space and/or proper coordination with respect to other body parts. Accordingly, typical signs of cerebellar dysfunction include deficits in the acquisition and performance of such movements. In the initial stages of mild cerebellar disease, deficits are predominantly reflected in the inability to adapt the amplitude and timing of movements to new environmental challenges or to acquire new associative motor behaviors. However, when cerebellar degeneration progresses, performance deficits emerge, often leading to full-blown ataxia (De Zeeuw et al., 2011). The name ***ataxia*** literally means "without order" and highlights the robust coordination deficits of this disorder, while setting it apart from the inability to move (***paralysis***), a disorder occurring in non-cerebellar diseases such as amyotrophic lateral sclerosis or stroke of the cerebral motor cortex.

Modular organization: evidence from neuro-anatomical and clinical studies

The cerebellar cortex can be divided into distinct functional sagittal zones identified by their specific afferent and efferent connections (Voogd and Glickstein, 1998). Each zone of cerebellar Purkinje-cells projects to a specific cerebellar or vestibular nucleus, which in turn inhibits the olivary subnucleus that provides the climbing fibers to the Purkinje-cells of the corresponding zone (De Zeeuw et al., 2011). These topographically organized triangular loops are referred to as olivocerebellar modules.

Lesion studies of the cerebellum or inferior olive in mammals suggest that most, if not all, modules are involved in locomotion, but probably each in a specific way. The medial zones of the cerebellum (A, B) regulate posture and balance by controlling extensor tone and modulate related rhythmic muscular activity by controlling spinal interneurons (Mori et al., 1999; Pijpers et al., 2008; Horn et al., 2010). By contrast, the intermediate zones (C1 to C3) are more relevant for controlling the trajectory, reflexes, timing and amplitude of limb movements (Chambers and Sprague, 1955; Yu and Eidelberg, 1983). Similarly, the lateral zones (D1 and D2) also play a minimal role in controlling balance and undisturbed walking, but seem to be involved in the adaptation of locomotion patterns to unusual and complex circumstances, especially when visual guidance is needed (Thach et al., 1992; Aoki et al., 2013). Indeed, retrograde transneuronal tracer

studies show that multiple modules are involved in the control of individual hindlimb muscles (Fig. 1; Ruigrok et al., 2008).

Clinical studies of cerebellar patients suffering from focal lesions following stroke or resection of tumors also indicate that all olivocerebellar modules contribute to locomotion in specific ways. Here, too, lesions in the medial zones affect balance, posture and undisturbed gait, whereas those in the intermediate and lateral zones deregulate leg placement and interlimb coordination as well as planning and gait adaptation to demanding circumstances (Schoch et al., 2006; Morton and Bastian, 2007; Ilg et al., 2008). Moreover, similar to animal studies, lesions affecting the cerebellar nuclei in humans are more difficult to compensate for than lesions affecting solely the cerebellar cortex (Morton and Bastian, 2004; Konczak et al., 2005; Schoch et al., 2006). Together, the cerebellar cortex and nuclei may act as an internal model of the motor apparatus, allowing sensorimotor predictions of body state in the future following particular motor commands (Wolpert et al., 1995; Bastian, 2006).

Network organization: evidence from cell-specific rodent studies

The cerebellar cortex is a continuous sheet of repeated networks of neurons folded into folia. Its most remarkable structural feature is the orthogonal arrangement of many of its cells and afferents. The dendrites and axons of Purkinje-cells, axons of molecular layer interneurons, ascending axons of granule-cells, dendritic domains of Golgi-cells as well as the climbing-fibers and Bergmann glia-sheaths are all predominantly oriented in sagittal planes, whereas the parallel-fibers originating from the ascending granule cell axons are orthogonally oriented in a medio-lateral direction (De Zeeuw et al., 2011). In this respect, the mossy-fibers exhibit a somewhat ambiguous distribution in that they can show sagittally oriented input patterning as occurs in large parts of the anterior lobe, whereas in other parts they traverse multiple modules (Gao et al., 2012). Interestingly, the sagittally oriented mossy-fiber inputs also entail some of the areas involved in locomotion, such as those receiving input from the spinal cord and dorsal column nuclei (Gerrits et al., 1985).

The Purkinje-cells are most critical for operations at the network level of the cerebellar cortex; deleting these cells in rodents leads to irregular and smaller movements of the limbs just like those of other body parts such as the eyes (De Zeeuw et al., 2011; Vinueza Veloz et al., 2014). Their climbing-fiber input has been suggested to carry an error signal affecting the strength of their parallel-fiber inputs (Marr, 1969; Albus, 1971). With regard to adaptation of locomotion

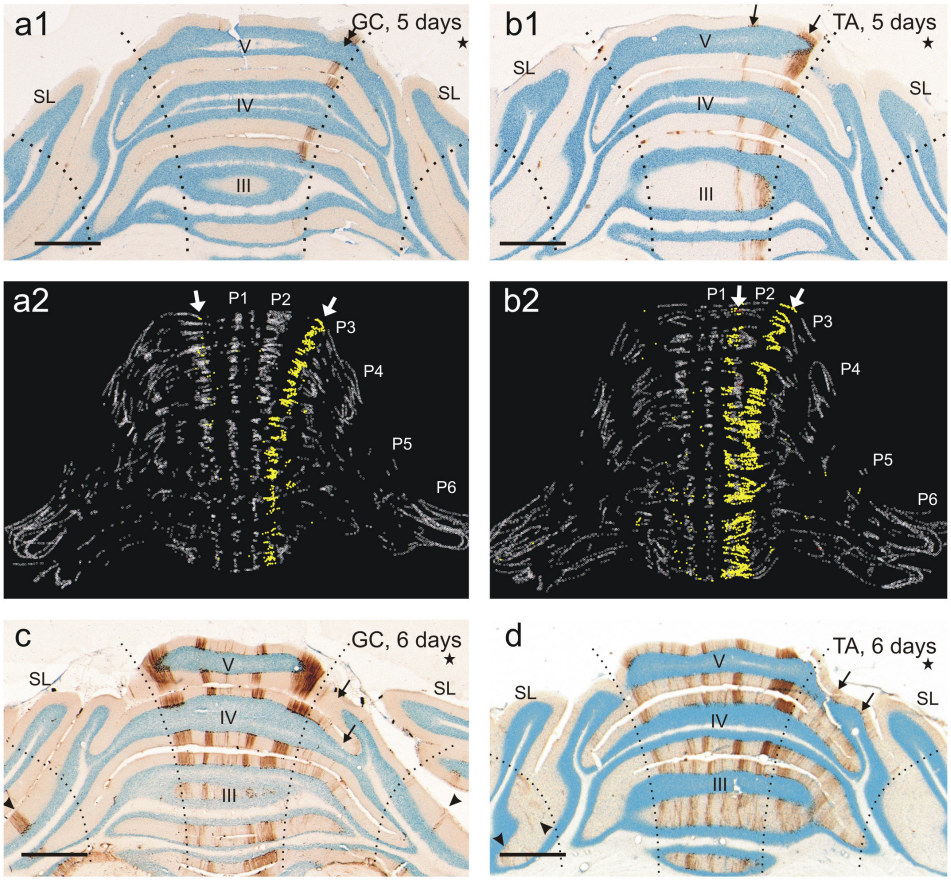

Figure 1. Multiple cerebellar modules are involved in the control of single hindlimb muscles. **a1**, **b1** Injection of the retrogradely and transneuronally transported rabies virus into either the gastrocnemius (GC) or anterior tibial (TA) muscles of the rat resulted in zonal labeling of vermal Purkinje cells after five days survival time. **a2, b2** These zones adhered to the zebrin pattern as demonstrated in a plot of the anterior lobe based on ten superposed double labeled sections. This enabled identification of the labeled zones. Note that virtually all rabies-labeled cells are zebrin-negative. Minor differences exist between patterns resulting from GC and TA injections. Yellow dots, rabies-labeled Purkinje cells; grey dots, zebrin-positive cells; red dots, double labeled cells. **c,d** Lengthening the survival time to allow for a single more transsynaptic passage also labeled Purkinje cells in the paravermis (arrows) and hemispheres (arrowheads). III, IV, V, vermal lobules; SL, simple lobule; star, injected side; stippled lines indicate approximate lateral border of vermis and paravermis; scale bar: 500 µm. Adapted from Ruigrok et al., 2008.

patterns, intrinsic plasticity of Purkinje-cells and long-term potentiation (LTP), but not long-term depression (LTD), of the parallel fiber-Purkinje-cell synapse appear to be essential (Schonewille et al., 2011; Vinueza Veloz et al., 2014). Moreover, processing at the level of the interneurons in both the granular layer and molecular layer also appears to contribute to gaiting patterns, albeit less prominently and predominantly during demanding tasks (Galliano et al., 2013; Vinueza Veloz et al., 2014). Likewise, electrotonic coupling of neurons in the inferior olive is also critical for fast modification of locomotion reflexes (Van Der Giessen et al., 2008). Thus, although Purkinje-cells and their potentiation are most critical for generating accurate, efficient, and consistent walking patterns, their input structures also all play a relevant role; and this role is most prominent during interlimb coordination and obstacle crossings (Stroobants et al., 2013; Vinueza Veloz et al., 2014). Indeed, the cerebellar networks operate in a distributed synergistic fashion allowing for ample possibilities of compensation (Gao et al., 2012).

Acknowledgements

This work was supported by the Dutch Organization for Medical Sciences (ZonMw), Life Sciences (ALW), Senter (Neuro-Bsik) and ERC-adv of the European Community.

REFERENCES

Albus JS (1971) A theory of cerebellar function. Mathematical Biosciences 10:25-61.

Aoki S, Sato Y, Yanagihara D (2013) Lesion in the lateral cerebellum specifically produces overshooting of the toe trajectory in leading forelimb during obstacle avoidance in the rat. Journal of neurophysiology 110:1511-1524.

Bastian AJ (2006) Learning to predict the future: the cerebellum adapts feedforward movement control. Current opinion in neurobiology 16:645-649.

Chambers WW, Sprague JM (1955) Functional localization in the cerebellum. II. Somatotopic organization in cortex and nuclei. AMA archives of neurology and psychiatry 74:653-680.

De Zeeuw CI, Hoebeek FE, Bosman LW, Schonewille M, Witter L, Koekkoek SK (2011) Spatiotemporal firing patterns in the cerebellum. Nature reviews Neuroscience 12:327-344.

Galliano E, Gao Z, Schonewille M, Todorov B, Simons E, Pop AS, D'Angelo E, van den Maagdenberg AM, Hoebeek FE, De Zeeuw CI (2013) Silencing the majority of cerebellar granule cells uncovers their essential role in motor learning and consolidation. Cell reports 3:1239-1251.

Gao Z, van Beugen BJ, De Zeeuw CI (2012) Distributed synergistic plasticity and cerebellar learning. Nature reviews Neuroscience 13:619-635.

Gerrits NM, Voogd J, Nas WS (1985) Cerebellar and olivary projections of the external and rostral internal cuneate nuclei in the cat. Exp Brain Res 57:239-255.

Horn KM, Pong M, Gibson AR (2010) Functional relations of cerebellar modules of the cat. The Journal of neuroscience : the official journal of the Society for Neuroscience 30:9411-9423.

Ilg W, Giese MA, Gizewski ER, Schoch B, Timmann D (2008) The influence of focal cerebellar lesions on the control and adaptation of gait. Brain : a journal of neurology 131:2913-2927.

Konczak J, Schoch B, Dimitrova A, Gizewski E, Timmann D (2005) Functional recovery of children and adolescents after cerebellar tumour resection. Brain : a journal of neurology 128:1428-1441.

Marr D (1969) A theory of cerebellar cortex. The Journal of physiology 202:437-470.

Mori S, Matsui T, Kuze B, Asanome M, Nakajima K, Matsuyama K (1999) Stimulation of a restricted region in the midline cerebellar white matter evokes coordinated quadrupedal locomotion in the decerebrate cat. Journal of neurophysiology 82:290-300.

Morton SM, Bastian AJ (2004) Cerebellar control of balance and locomotion. The Neuroscientist : a review journal bringing neurobiology, neurology and psychiatry 10:247-259.

Morton SM, Bastian AJ (2007) Mechanisms of cerebellar gait ataxia. Cerebellum 6:79-86.

Pijpers A, Winkelman BH, Bronsing R, Ruigrok TJ (2008) Selective impairment of the cerebellar C1 module involved in rat hind limb control reduces step-dependent modulation of cutaneous reflexes. The Journal of neuroscience : the official journal of the Society for Neuroscience 28:2179-2189.

Schoch B, Dimitrova A, Gizewski ER, Timmann D (2006) Functional localization in the human cerebellum based on voxelwise statistical analysis: a study of 90 patients. NeuroImage 30:36-51.

Schonewille M, Gao Z, Boele HJ, Veloz MF, Amerika WE, Simek AA, De Jeu MT, Steinberg JP, Takamiya K, Hoebeek FE, Linden DJ, Huganir RL, De Zeeuw CI (2011) Reevaluating the role of LTD in cerebellar motor learning. Neuron 70:43-50.

Stroobants S, Gantois I, Pooters T, D'Hooge R (2013) Increased gait variability in mice with small cerebellar cortex lesions and normal rotarod performance. Behavioural brain research 241:32-37.

Thach WT, Goodkin HP, Keating JG (1992) The cerebellum and the adaptive coordination of movement. Annual review of neuroscience 15:403-442.

Van Der Giessen RS, Koekkoek SK, van Dorp S, De Gruijl JR, Cupido A, Khosrovani S, Dortland B, Wellershaus K, Degen J, Deuchars J, Fuchs EC, Monyer H, Willecke K, De Jeu MT, De Zeeuw CI (2008) Role of olivary electrical coupling in cerebellar motor learning. Neuron 58:599-612.

Vinueza Veloz MF, Zhou K, Bosman LW, Potters JW, Negrello M, Seepers RM, Strydis C, Koekkoek SK, De Zeeuw CI (2014) Cerebellar control of gait and interlimb coordination. Brain structure & function.

Voogd J, Glickstein M (1998) The anatomy of the cerebellum. Trends in neurosciences 21:370-375.

Wolpert DM, Ghahramani Z, Jordan MI (1995) An internal model for sensorimotor integration. Science 269:1880-1882.

Yu J, Eidelberg E (1983) Recovery of locomotor function in cats after localized cerebellar lesions. Brain research 273:121-131.

2

Chapter 3

Granule Cells in VOR Adaptation

Carla da Silva-Matos[1,6], Nicolas Gutierrez-Castellanos[2], Sandra Goebbels[3], Jeroen J. Dudok[4], Jan Wijnholds[5], Martijn Schonewille[6], Chris I. De Zeeuw[1,6], Beerend H. J. Winkelman[1,7]*

[1] Netherlands Institute for Neuroscience, Amsterdam, The Netherlands
[2] Champalimaud Neuroscience Programme, Champalimaud Centre for the Unknown, Lisbon, Portugal
[3] Max Planck Institute of Experimental Medicine, Department of Neurogenetics, Göttingen, Germany
[4] Vrije Universiteit Amsterdam, Faculty of Science, Dept. of Environment and Health, Amsterdam, The Netherlands
[5] Leiden University Medical Center, Dept. of Ophthalmology, Leiden, The Netherlands
[6] Erasmus University Medical Center, Dept. of Neuroscience, Rotterdam, The Netherlands
[7] Erasmus University Medical Center, Dept. of Ophthalmology, Rotterdam, The Netherlands

* Correspondence should be addressed to Beerend H. J. Winkelman, Netherlands Institute for Neuroscience, Meibergdreef 47, NL-1105 BA Amsterdam, The Netherlands, b.winkelman@nin.knaw.nl

ABSTRACT

Cerebellar granule cells are known to play a pivotal role in cerebellar learning. They form the input layer of the cerebellum and supply Purkinje cells with the contextual information necessary for motor learning. Several genetic manipulations targeting the granule cells of the cerebellum have been screened for their role in cerebellar learning. While mouse lines with a clear phenotype are regularly reported in the literature, others in which a clear phenotype is absent remain for most part unpublished. This publication bias may potentially skew the conclusions drawn from the body of published data. Here, we report five transgenic mouse models targeting the cerebellum, specifically granule cell function, that show no significant effect on vestibulo-ocular reflex adaptation, a cerebellar motor learning paradigm. These results place previous reported experiments in a different light, providing support to the notion that non-significant results play a crucial role in understanding and interpreting significant experiments and should be seen as equally publishable.

1. INTRODUCTION

Based upon the neuron count, the cerebellum is the largest sensorimotor structure in the brain, participating in both motor and non-motor domains. It is extensively connected with other brain structures, namely the brainstem and spinal cord, and projects to and from limbic regions including the amygdala, hypothalamus, prefrontal cortex and periaqueductal grey (Anand, Malhotra, Singh, & Dua, 2017; Snider & Maiti, 1976). Its highly homogenous neuronal circuitry and crystalline-like anatomical cytoarchitecture, as well as the fact that these are built from a small number of cell types, makes the cerebellum an attractive system to study fundamental principles of neural development, organization, function and disease (Eccles, 1970; Herrup & Kuemerle, 1997; Ito, 1984; Ramón y Cajal, 1911; Sillitoe & Joyner, 2007; Wang & Zoghbi, 2001). A summarized schematic representation of cerebellar organization is presented in Figure 1.

The cerebellar granule cell (GC) is a major cell type, accounting for as many as half of all neurons in the central nervous system (CNS) (Fox & Barnard, 1957). Cerebellar GCs are known to play a pivotal role in cerebellar learning. Receiving input from mossy fiber afferents, they form the input layer of the cerebellum and supply Purkinje cells with contextual information necessary for motor learning (Galliano et al., 2013; Gao et al., 2012; Giovannucci et al., 2017; Hansel, Linden, & D'Angelo, 2001; Mapelli, Gandolfi, Vilella, Zoli, & Bigiani, 2016).

Classical theories of cerebellar function emphasize that the pattern of GC connectivity and their presence in a staggering number in the cerebellar cortex makes the GCs perfectly suited to produce high-dimensional representations, in which each sensorimotor-context is encoded by a unique pattern of activity in the GC population and a slight change in context strongly alters the pattern of activity. Marr and Albus hypothesized that GCs are sparse coding – in which the fraction of active neurons is low at any one time – which facilitates cerebellar learning (Marr, 1969; Albus, 1971; see also Schweighofer, Doya and Lay, 2001 for theoretical work on this topic).

Vestibulo-ocular reflex (VOR) adaptation is a particularly well-characterized cerebellum-dependent learning task. The VOR evokes eye movements in the direction opposite to head movement, thus serving to continuously stabilize vision relative to space with the purpose of reducing the slip of visual images on the retina (Ito, 1998; Killian & Baker, 2002; Voogd & Barmack, 2006). Because of its involvement in motor-coordination mechanisms, control of the VOR has been

regarded as a characteristic feature of cerebellar function and extensively used as a model system for studying cerebellar operation and plasticity (Ito, 1998)

In various mouse models, genetic manipulations have been studied that target, directly or indirectly, GC function and plasticity and their particular role in cerebellar learning. Galliano et al. provided evidence that only a fraction of functionally intact GCs is sufficient for the maintenance of basic motor performance, whereas acquisition and stabilization of sophisticated motor memories requires higher numbers of healthy GCs, controlling PC firing (Galliano et al., 2013). On the other hand, Seja and colleagues pointed to a specific role for GCs in the consolidation of phase-reversal learning learning of the VOR, a paradigm in which the VOR is extensively adapted until it reverses direction. They showed that ablation of Kcc2 from GCs impaired consolidation of long-term VOR phase-reversal learning, whereas baseline performance, short-term gain-decrease learning and gain consolidation remained intact (Seja et al., 2012).

The published mouse models described above are typical examples of genetic perturbations that produce a behavioral phenotype concerning cerebellum-dependent motor adaptation. We tested several additional transgenic mouse lines, however, which showed no clear phenotype. Publication-bias towards positive results is notorious in the scientific literature, and a potential snag for correct interpretation of the whole body of literature on cerebellar motor adaptation. In this article, we therefore report on five transgenic mouse models that showed no effect on cerebellar adaptation. These models are either GC-specific (Gabra6-cre) knockouts for NeuroD1, Mpp3, and Gabrg2, or global, with an expected impact on cerebellar plasticity: a global knockout for MDGA1 and a global knockin of Gabrg2 with a disabling point mutation. A summary of these mouse models that include description, role and (possible) effect is presented in Table 1. A schematic representation of their targets in the cerebellar anatomy is depicted in Figure 1. After a brief description of each transgenic mouse model, we present the results regarding performance and adaptation of the VOR, and we compare these models with GC manipulation models published previously, discussing the possible implications and limitations.

Transgenic mouse models

Granule cell specific knockout mice were generated using cre-expression under the promotor for the GABA-A receptor subunit alpha 6 ($Gabra6^{cre}$), which is selectively expressed in cerebellar granule cells and cochlea nuclei (Aller et al., 2003; Laurie, Seeburg, & Wisden, 1992; Varecka, Wu, Rotter, & Frostholm, 1994).

NeuroD1 [Gabra6^{cre}/NeuroD1$^{loxP/loxP}$] is a conditional knockout mouse model of the NeuroD1/Beta2 transcription factor, a transcriptional factor that plays a role in the development of the cerebellum (Chae, Stein, & Lee, 2004; Cho & Tsai, 2006; J.-K. Lee et al., 2000). Knocking-out this gene leads to the inactivation of the NeuroD1 gene in post-migratory cerebellar GCs and a subset of brainstem nuclei (Goebbels et al., 2005). Differences in NeuroD1 expression correlate with the regulation of proliferative activity and GC laminar distribution within the cerebellum of different species (D'Amico, Boujard, & Coumailleau, 2013). In the mouse, at post-natal stages, NeuroD1 was clearly detected in both external and internal granular layers of the cerebellum, and the internal granular layer expression was shown to stably persist until adulthood (Goebbels et al., 2006; J.-K. Lee et al., 2000; Miyata, Maeda, & Lee, 1999; Schwab et al., 2000; Yokoyama et al., 1996).

Mpp3 [Gabra6^{cre}/ Mpp3$^{loxP/loxP}$] is a GC-specific Mpp3 knockout mouse model. MPP3 is highly expressed by cerebellar GCs. In the retina, Mpp3 has a role in the maintenance of retinal integrity by regulation of cell adhesion between photoreceptors and Müller glia cells, and has been proposed as a functional candidate gene for inherited retinal degenerations (Kantardzhieva, Alexeeva, Versteeg, & Wijnholds, 2006). Global Mpp3 removal results in a loss of the apical protein complex and disruption of adherens junctions, cell migration and layering patterns (Cappello et al., 2006; Dudok, Sanz, Lundvig, & Wijnholds, 2013; Imai et al., 2006; Kadowaki et al., 2007). Aberrant migration or connectivity of interneurons is associated with a number of neurodevelopmental disorders, such as autism, schizophrenia, and mental retardation (Di Cristo, 2007; Levitt, 2005; Rossignol, 2011).

α6-gamma2 [Gabra6^{cre}/ Gabrg2$^{loxP/loxP}$] is a GC-specific knockout of the GABA(A) receptor γ2 subunit, and GABA point mutation [Gabrg2$^{Y365/7F}$] is a global knock-in of a point-mutated GABA(A) receptor γ2 subunit, in which two tyrosine residues (Y365/7) are mutated. The γ2 subunit negatively regulates endocytosis of GABA(A) receptors and enhances synaptic inhibition (Jurd & Moss, 2010), hence mutation of these residues results in aberrant synaptic GABA(A) receptor trafficking. Alterations in the number and/or function of GABA(A) receptors can have significant effects on memory and cognition (Jurd and Moss, 2010), and GABA(A) receptor γ2 subunits are reportedly reduced in subjects with autism (Fatemi et al., 2014). GABA(A) receptors that contain a γ2 subunit (in association with α1, α2 or α3 subunits) are the predominant subtypes that mediate phasic synaptic inhibition (Farrant & Nusser, 2005; Wu et al., 2013). One important function of phasic inhibition is the generation of rhythmic activities in neuronal

networks (Farrant & Nusser, 2005). The induction of rebound potentiation, a cerebellar plasticity mechanism that contributes to motor learning, is dependent on GABA(A) receptors (Hirano, Yamazaki, & Nakamura, 2016). The inhibition of GCs by the Golgi-cells, involved in the process through which the Golgi-cells exert an extensive control on spatio-temporal signal organization and information storage in the granular layer playing a critical role for cerebellar computation, is done via GABA(A) receptor (D'Angelo, 2008; Yaeger & Trussell, 2015).

Table 1. Transgenic mouse models

Transgenic mouse model	Description	Role of its main target	Effects of *ko/ki*
NeuroD1 [Gabra6^{cre}/ NeuroD1$^{loxP/loxP}$]	GABA(A) receptor α6 subunit promoter conditional NeuroD1/ Beta2 knockout	NeuroD1/Beta2 is a transcription factor that plays critical roles in the development of the cerebellum.	Efficient inactivation of the NeuroD1 gene in post-migratory cerebellar GCs and a subset of brainstem nuclei. Possible effect on GC maturation.
Mpp3 [Gabra6^{cre}/ Mpp3$^{loxP/loxP}$]	GABA(A) receptor α6 subunit promoter conditional Mpp3 knockout	Mpp3 is a member of a family of membrane-associated proteins termed MAGUKs (membrane-associated guanylate kinase homologs). MAGUKs interact with the cytoskeleton and regulate cell proliferation, signaling pathways, and intracellular junctions.	Disruption of the apical protein complex and adherents' junctions, cell migration and layering patterns in the GC layer.
GABA point mutation [Gabrg2$^{Y365/7F}$]	Global knockin of point-mutated GABA(A) receptor γ2 subunit	γ2 subunit is involved in the phospho-dependent GABAAR membrane trafficking and receptor number at inhibitory synapses, critically shaping neuronal activity by regulating the cell surface accumulation of GABAARs at inhibitory synapses and consequently the efficacy of synaptic inhibition.	(Possible) Ablation of the rebound potentiation (a type of inhibitory long-term potentiation [iLTP] of Purkinje cells) through the disruption of the regulation of synaptic GABAARs via signaling pathways that lead to the activation of Fyn kinase / CaMKII pathway.
α6-gamma2 [Gabra6^{cre}/ Gabrg2$^{loxP/loxP}$]	GABA(A) receptor α6 subunit promoter conditional GABA(A) receptor γ2 subunit knockout	Same as above, conditional to GCs.	Elimination of GC phasic inhibition (the γ2 subunit is required to target the receptors to the postsynaptic membrane).
MDGA1 [Mdga1$^{-/-}$]	Global knockout of Mdga1	MDGA1 is a negative regulator of inhibitory synapse development.	Unimpeded binding between neuroligin-2 and neurexin, facilitating inhibitory synapse formation.

MDGA1 [Mdga1$^{-/-}$] is a global knockout mouse model of MDGA1, a gene implicated in the formation of neural networks and essential for neural cell migration and axon guidance (Takeuchi, Hamasaki, Litwack, & O'Leary, 2007; Takeuchi & O'Leary, 2006). MDGA1 is strongly expressed in the cerebellum (Lein et al., 2006; Litwack, Babey, Buser, Gesemann, & O'Leary, 2004), specifically in the GC layer (H.-K. Lee, 2012) though some studies show expression confined to the Purkinje cell layer (for this see https://www.proteinatlas.org/ENSG00000112139-MDGA1/tissue/cerebellum). This gene is also associated with autism (Pettem, Yokomaku, Takahashi, Ge, & Craig, 2013) and schizophrenia (Song, Kim, Kim, Choi, & Lee, 2012), the latter a condition well known to be associated with cerebellar abnormalities (Yeganeh-Doost, Gruber, Falkai, & Schmitt, 2011), and in particular with GC abnormalities. MDGA1 binds neuroligin-2 at the inhibitory synapses, and interferes with the interaction of neuroligin and neurexin, stopping inhibitory synapse development (Kim et al., 2017). RNAi-mediated knockdown of MDGA1 selectively increases inhibitory but not excitatory synapse density, identifying MDGA1 as one of few known negative regulators of synapse development with a unique selectivity for inhibitory synapses (Pettem et al., 2013)

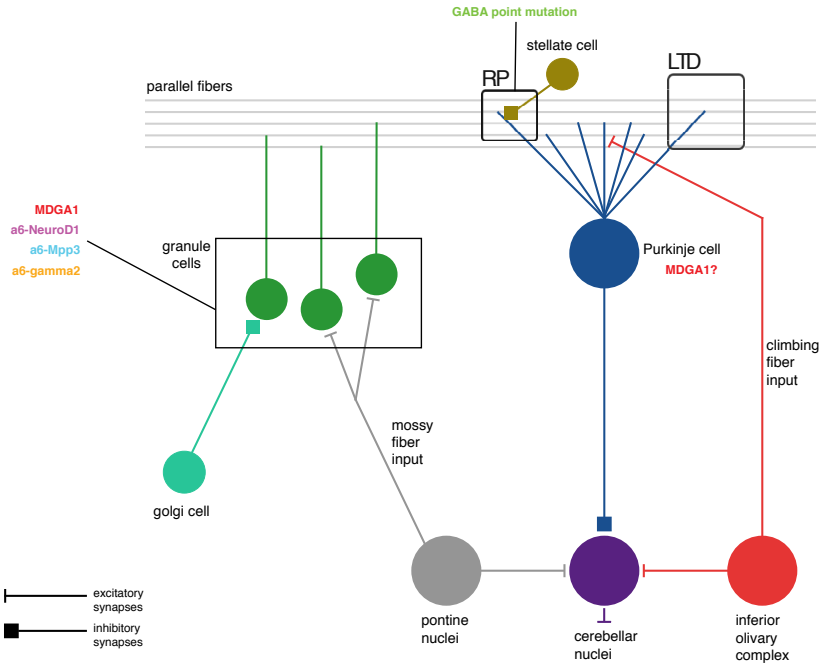

Figure 1. Cerebellar anatomy and schematic representation of the transgenic mouse models and its targets.

2. MATERIALS AND METHODS

2.1. Animals

Inbred breeding colonies were used to obtain the experimental mice. Male adult mice were selected from these colonies. MDGA1 global knockout (KO) mice [Mdga1$^{-/-}$], kindly provided by Dr. David Ginty, were generated as described before (Ishikawa et al., 2011) and maintained on a C57BL/6 background. NeuroD1 GC conditional knockout (CKO) mice [Gabra6^{cre}/NeuroD1$^{loxP/loxP}$] were generated by crossing the floxed *Neurod1* line (Goebbels et al., 2005), kindly provided by Dr. Goebbels, with the *Gabra6*-cre line (Fünfschilling & Reichardt, 2002). GABA-gamma2-Y365/7F, a global knockin of point-mutated GABA(A) receptor γ2 subunit [Gabrg2$^{Y365/7F}$] mouse, was kindly provided by Dr. Trevor Smart and Dr. Stephen Moss, and was generated as previously described (Tretter et al., 2009). A6cre-gamma2, a conditional GC-specific of the GABA-A γ2 subunit knockout [Gabra6^{cre}/Gabrg2$^{loxP/loxP}$], was kindly provided by Dr. Mark Farrant, Dr. William Wisden and Dr. Peer Wulff, and were generated by crossing a *Gabra6-cre* line with the *γ2I77lox*, as described before (Aller et al., 2003). Mpp3 GC conditional knockout mice [Gabra6^{cre}/Mpp3$^{loxP/loxP}$] were generated by crossing a *Gabra6-cre* line (Fünfschilling & Reichardt, 2002) with the floxed Mpp3 line (Dudok et al., 2013), and were maintained on a C57BL/6 background. Mice were kept on a 12-hour light/12-hour dark cycle and had *ad libitum* access to food and water.

2.2. Animal preparation and experimental setup

Mice were tested in two different labs: one located at the department of neuroscience at the Erasmus MC University, Rotterdam, The Netherlands, the other in the Motionlab located at the department of cerebellar coordination and cognition at the Netherlands Institute for Neuroscience, Amsterdam, The Netherlands. Mice were surgically prepared for chronic head restrained experiments by attaching an immobilizing construct (pedestal) on their skulls. The specifics of the surgical procedures were as described before (de Jeu & De Zeeuw, 2012; Gutierrez-Castellanos, Winkelman, Tolosa-Rodriguez, De Gruijl, & De Zeeuw, 2013). In short, mice were anaesthetized using isoflurane (initiation 4%, maintenance 2%, with O2), the skin covering the frontal, parietal and interparietal bones was shaved and incised along the rostro-caudal midline. Mdga1$^{-/-}$, Gabrg2$^{Y365/7F}$ and Gabra6^{cre}/Gabrg2$^{loxP/loxP}$ mice, tested in Rotterdam, were equipped with a U-shaped pedestal design (brass, 6 × 4 mm) with a magnet inside (neodymium, 4 × 4 mm, MTG, Weilbach, Germany), using Optibond (Kerr, Salerno, Italy) and Charisma (Heraeus Kulzer, Hesse, Germany). Gabra6^{cre}/NeuroD1$^{loxP/loxP}$ and Gabra6^{cre}/Mpp3$^{loxP/loxP}$ mice, tested in Amsterdam, were equipped with an aluminium head fixation

pedestal with integrated neodymium magnet using Superbond C&B (Sun Medical, Japan). After surgery, mice were allowed to recover for at least 72 hours before experiments. During the experiment, the mice were placed head-fixed in a holder tube on a vestibular motion platform (Amsterdam: R2000 "Rotopod"; Parallel Robotic Systems Corporation, Hampton, VA, USA; Rotterdam: custom-build vertical axis turntable with Harmonic Drive servo motor). Left eye orientation was measured using video pupil tracking with a table-fixed CCD camera (Amsterdam: Pulnix TM-6710CL, 120 frames/s; infrared (IR) illumination, 850 nm LED, 6.5 cm distance from the eye; Rotterdam: Commercial eye tracker, frames/s, ISCAN Inc.). A visual stimulus was generated by either placing a motorized rotating drum with an illuminated black-and-white random pattern on the inside over the subject animal (Rotterdam). Otherwise (Amsterdam) the visual stimulus was projected panoramically onto 3 back projection screens (width-height.147x118 cm) surrounding the table. The projected pattern was computer generated and consisted of a field of green dots (1 radius), arranged on a virtual sphere, centered on the subject, and rotated about the vertical axis during visual stimulation (i.e., "yaw" motion). Pilocarpine (2%) eye drops were applied before the experiment to limit pupil dilatation in darkness. Each mouse was habituated to the setup for a period of up to three training days before the experimental data were collected. All data of the experiments described below were acquired and analyzed in a blinded fashion with respect to the genotype. All experiments were conducted in-line with the European guidelines for the care and use of laboratory animals (Council Directive 2003/65/CE, Council Directive 86/6009/EEC). The experimental protocols were approved by the Animal Experiment Committee (DEC) of the Royal Netherlands Academy of Arts and Sciences (KNAW).

2.3. Baseline compensatory eye-movements protocols [VOR, OKR, VVOR]

To test baseline oculomotor performance, the vestibulo-ocular reflex (VOR), the optokinetic reflex (OKR), and VOR in the light (or visually-aided VOR [VVOR]) were measured before the start of the VOR adaptation experiment. VOR and OKR were evoked by either rotating the table in the dark and the screen in the light, respectively. VVOR, combining visual and vestibular input, was tested by VOR stimulation in the light in a similar manner. Hence, the horizontal VOR was then characterized in both darkness and light using sinusoidal rotation about the vertical axis. Mdga1$^{-/-}$, Gabrg2$^{Y365/7F}$ and Gabra6^{cre}/Gabrg2$^{loxP/loxP}$ were tested using a constant amplitude of 5° at frequencies ranging between 0.1 and 1.0 Hz; Gabra6^{cre}/NeuroD1$^{loxP/loxP}$ and Gabra6^{cre}/Mpp3$^{loxP/loxP}$ were tested at frequencies ranging between 0.0625 and 4 Hz, presented in a sequence of increasing order,

holding peak velocity constant at 18.85°/s for each frequency, matching the peak velocity of the vestibular stimulus used during adaptation training (see below).

2.4. VOR adaptation protocol

Cerebellar motor learning was evaluated in a multiple day paradigm aimed at adapting the gain and the phase of the VOR towards a reversal of the normal eye movement response. Mice were subjected to a VOR cancellation stimulus on the first day (in-phase sinusoidal movement at 0.6 Hz, 5° amplitude of both the table and the visual surround) and a VOR reversal stimulus on subsequent days (2-4), where the amplitude of the visual surround was increased to 7.5° (day 2) and 10° (days 3 and 4). Gabra6^{cre}/NeuroD1$^{loxP/loxP}$ and Gabra6^{cre}/Mpp3$^{loxP/loxP}$ were trained using 10º amplitude of the visual surround on one additional day (10º, days 3 to 5). The amplitude of the turntable remained constant at 5° amplitude (18.85°/s peak velocity). Training sessions consisted of 6 VOR measurements (30 cycles, 50 seconds, in darkness) that were alternated with 5 periods of visuo-vestibular mismatch training (300 cycles, 500 seconds). Before, in between, and after the 10 min training sessions, the VOR was tested (in the dark) to evaluate the training effect. After the training sessions, animals were kept in total darkness during the consecutive training days to prevent active extinction of the adapted VOR. The eye movement response was expressed as gain and phase relative to head movement, which was calculated using multiple linear regression of eye velocity to in-phase and quadrature components of the turntable velocity trace. Gain of the eye movement response was defined as the ratio between the eye velocity and the table velocity magnitudes. Phase was expressed in degrees and offset by 180°, so that a phase of 0° indicates an eye movement that is in-phase with contraversive head movement; positive phase values indicate phase leads.

2.5. Data analysis

Online image analysis was performed to extract the location of pupil edges and corneal light reflections (Sakatani & Isa, 2004) using custom-built software for LabVIEW (National Instruments, Austin, TX, USA). Angular eye velocity was computed offline using custom software written for Matlab (The Mathworks Inc, Natick, MA, USA) using the computation outlined elsewhere (Stahl, 2002; Stahl et al., 2000). Saccadic eye movements, quick-phases of the vestibular nystagmus and eye blink artifacts were removed using a 50º/s velocity threshold and 200ms margins at each threshold crossing. Stimulus cycles could be located using recorded trigger pulses that indicated the start of a new cycle. Eye velocity during each stimulus cycle was independently fit with a cosine function, using multiple linear regression. Gain and phase values from each fit were transformed into

phasor values for further analysis using Euler's formula. Movement artifacts were excluded on the basis of the computed residual norm of the sinusoidal fits. Cycles with >25% of missing data or a residual norm of the sinusoidal fit that exceeded 1000 were discarded.

2.6. Statistics

For statistical analysis of the behavioral data, we used Matlab (The MathWorks Inc., Natick, MA, 2000), with the statistical toolbox and the CircStats toolbox for analysis of circular data. Differences in mean gain were tested for significance using a two-sample Student's T-test; differences in mean phase were tested using a two-sample Watson-Williams test; differences in mean gain and phase, taken together as phasor values, were tested using a two-sample Hotelling's T^2-test. For single tests, a p-value less than 0.05 was considered significant. For multiple comparison tests (baseline measurements at a range of frequencies) we used the Holm-Bonferroni correction. During VOR phase-reversal training, the learning trajectory in polar coordinates is close-to linear (Gutierrez-Castellanos, Winkelman, Tolosa-Rodriguez, De Gruijl, et al., 2013). We therefore evaluated the total learning extent as the relative shift over this linear trajectory, expressed as units of gain, computing the difference between the average value of the last three catch trials on the final training day and the naïve VOR at the start of the VOR adaptation training (Gutierrez-Castellanos, Winkelman, Tolosa-Rodriguez, De Gruijl, et al., 2013).

3. RESULTS

3.1 Intact baseline performance

To test for differences in baseline oculomotor behavior, we subjected each mouse to a set of visual and vestibular stimuli before the start of the adaptation training. We evaluated the performance over a range of frequencies of the OKR (Figure 2), VOR (Figure 3), and VVOR (Figure 4).

All mice were able to stabilize the images on their retina and/or gaze with respect to a moving visual field (i.e. optokinetic reflex or OKR), as schematized (Figure 2A). Differences in mean gain were tested for significance using a two-sample Student's T-test; differences in mean phase were tested using a two-sample Watson-Williams test; differences in mean gain and phase, taken together as phasor values, were tested using a two-sample Hotelling's T^2-test. After the Holm-Bonferroni correction for multiple comparison tests (baseline measurements at a

range of frequencies), no differences were found for any of the lines and for the different frequencies tested (P > 0.05); both gain (Figures 2B and 2D) and phase (Figures 2C and 2E) values of these mutants (colored symbols) were then comparable to their wildtype controls (opaque symbols). The OKR showed a typical gain and phase decrease with frequency.

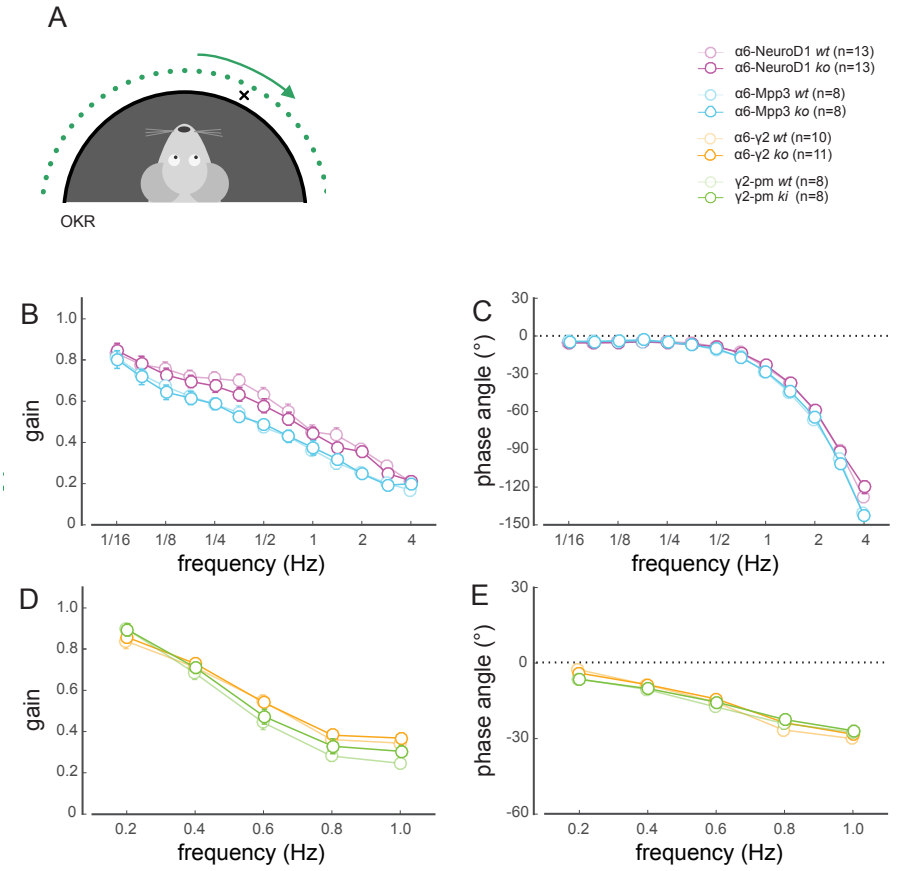

Figure 2. Optokinetic reflex (OKR) eye movement behavior of 4 mouse models before VOR adaptation. (A) Scheme of the setup for the OKR protocol. Panels in each row show different protocols for the OKR stimulation: (B-C) Plots showing the eye movement gain and phase responses to the OKR stimulation measured at frequencies ranging between 0.625 and 4 Hz. Peak velocity of the OKR stimulus was 18.85º/s, matching the table peak velocity of the adaptation paradigm. (B) Gain and (C) phase of the OKR. Pink traces (α6-NeuroD1 mice), and blue traces (α6-Mpp3 mice). (D-E) Plots showing the eye movement gain and phase responses to the OKR stimulation measured at frequencies ranging between 0.2 and 1 Hz. Peak amplitude of the optokinetic stimulus was 5º. (D) Gain and (E) phase of the OKR. Orange traces (α6-γ2 mice), and green traces (γ2-pm mice). Colored symbols: *ko/ki* mice. Opaque symbols: *wt* mice. Error bars indicate standard error of the mean. Profiles were marginally shifted relative to each other along the abscissa to avoid overlapping error bars.

Mice were also able to stabilize their gaze with respect to their head movements (i.e. the vestibulo-ocular reflex in the dark or VOR: Figure 3, scheme in Figure 3A). Differences in mean gain were tested for significance using a two-sample Student's T-test; differences in mean phase were tested using a two-sample Watson-Williams test; differences in mean gain and phase, taken together as phasor values, were tested using a two-sample Hotelling's T2-test. After the Holm-

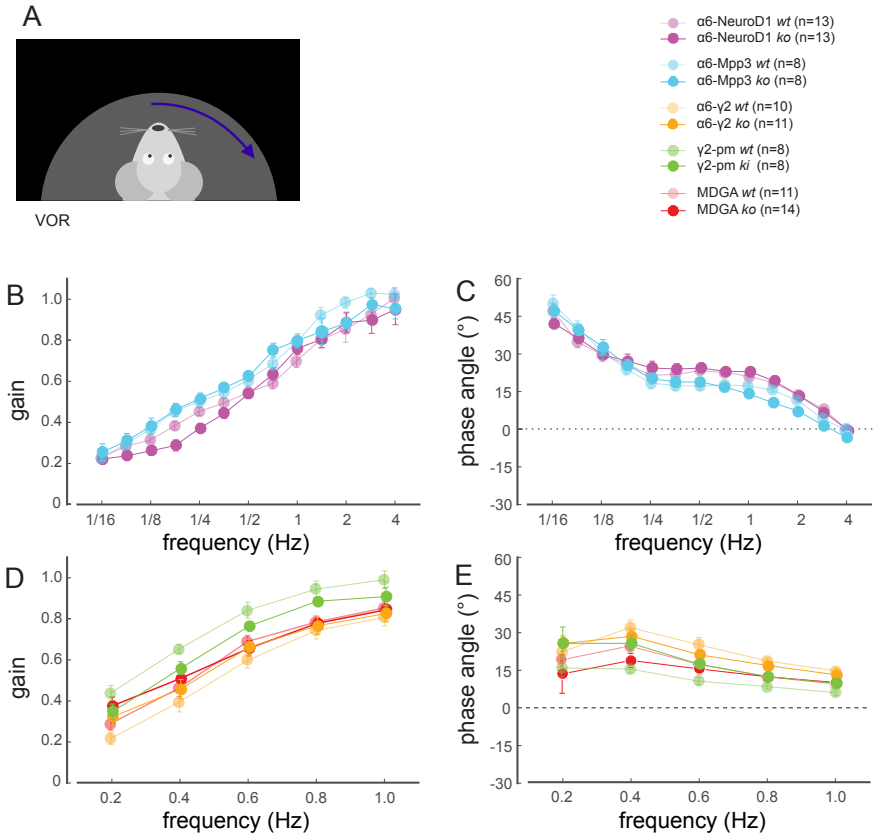

Figure 3. Vestibulo-ocular reflex eye movement behavior in the 5 mouse models before phase reversal training. (A) Scheme of the setup for the VOR stimulation protocol. Panels in each row show different protocols for the VOR stimulation: (B-C) Plots showing the eye movement gain and phase responses to the VOR stimulation measured at frequencies ranging between 0.0625 and 4 Hz. Peak velocity of the VOR stimulus was 18.8°/s, matching the table peak velocity of the adaptation paradigm. (B) Gain and (C) phase of the VOR. Pink traces (α6-NeuroD1 mice), and blue traces (α6-Mpp3 mice). (D-E) Plots showing the eye movement gain and phase responses to the VOR stimulation measured at frequencies ranging between 0.2 and 1 Hz. Peak amplitude of the vestibular stimulus was 5°. (D) Gain and (E) phase of the VOR. Orange traces (α6-γ2 mice), green traces (γ2-pm mice) and red traces (MDGA mice). Colored symbols: *ko/ki* mice. Opaque symbols: *wt* mice. Error bars indicate standard error of the mean. Profiles were marginally shifted relative to each other along the abscissa to avoid overlapping error bars.

Bonferroni correction for multiple comparison tests (the baseline measurements at a range of frequencies), we found instances where the data were marginally significant: the phase of γ2-pm *ki* mice at 0.4 Hz, and the phase of the α6-Mpp3 mouse at 1.4 Hz and 2 Hz. No other differences were found for any of the lines and for the different frequencies tested ($P > 0.05$); both gain (Figures 3B and 3D) and phase (Figures 3C and 3E) values of these mutants (colored symbols) were otherwise comparable to their wildtype controls (opaque symbols). The VOR showed a typical gain increase with frequency and phase lead at the low-frequency range.

Lastly, mice showed near optimal image stabilization during head movement in the light (i.e. VVOR; Figure 4). Differences in mean gain were tested for significance using a two-sample Student's T-test; differences in mean phase were tested using a two-sample Watson-Williams test; differences in mean gain and phase, taken together as phasor values, were tested using a two-sample Hotelling's T^2-test. After the Holm-Bonferroni correction for multiple comparison tests (with baseline measurements at a range of frequencies), no differences were found for any of the lines and for the different frequencies tested ($P > 0.05$); both gain (Figures 4B and 4D) and phase (Figures 4C and 4E) values of these mutants (colored symbols) were comparable to their *wt* controls (opaque symbols).

In summary, all the mouse models displayed intact basic oculomotor behavior in the three stimulation protocols: OKR, VOR and VVOR. None of the comparisons between these mice and their control littermates showed a significant difference in any of these paradigms.

3.2 VOR adaptation in α6-NeuroD1 *ko* mice

Following the measurement of the baseline performance, mice were tested using VOR phase-reversal adaptation. Under this paradigm, mice learn to shift the phase of their VOR in response to sinusoidal visuo-vestibular mismatch stimulation, in which the visual stimulus moves in the same direction as the vestibular stimulus (i.e. in-phase), yet at a greater amplitude (Figure 5A).

After the 1h long training sessions, α6-NeuroD1 *ko* and their *wt* littermates followed the same learning curves (Figures 5B and 5C), indicating that these transgenic mice have the ability to modify their VOR gain after short-term visuo-vestibular training that is comparable to their wildtype littermates.

Six catch trials (1 min each) were recorded in between five training blocks of the visuovestibular training signal (8 min each; scheme in Figure 5D). No differences were found in the initial VOR gain displayed by the *ko* mice and their *wt* littermates (Figure 10, P=0.680).

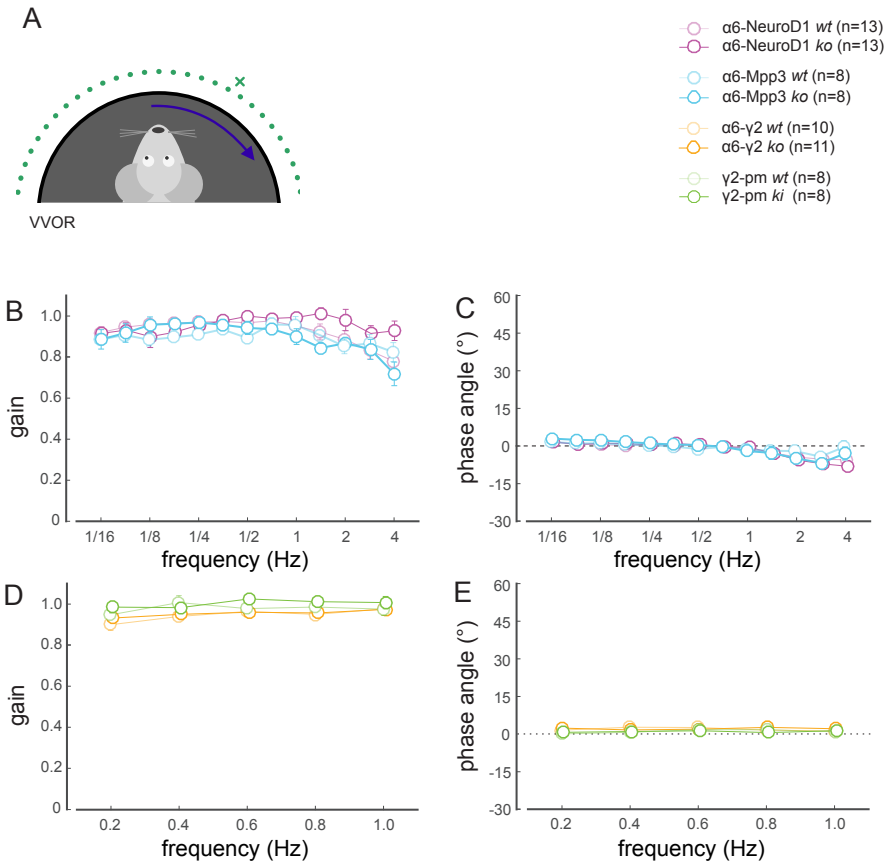

Figure 4. Visually-aided VOR eye movement behavior in 4 mouse models before VOR adaptation, phase reversal training. (A) Scheme of the setup for the visually aided vestibulo-ocular (VVOR) stimulation protocol. Panels in each row show different protocols for the VVOR stimulation: (B-C) Plots showing the eye movement gain and phase responses to the VVOR stimulation measured at frequencies ranging between 0.0625 and 4 Hz. Peak velocity of the VVOR stimulus was 18.85°/s, matching the table peak velocity of the adaptation paradigm. (B) Gain and (C) phase of the VVOR. Pink traces (α6-NeuroD1 mice), and blue traces (α6-Mpp3 mice). (D-E) Plots showing the eye movement gain and phase responses to the VVOR stimulation measured at frequencies ranging between 0.2 and 1 Hz. Peak amplitude of the optokinetic stimulus was 5°. (D) Gain and (E) phase of the VVOR. Orange traces (α6-γ2 mice), and green traces (γ2-pm mice). Colored symbols: *ko/ki* mice. Opaque symbols: *wt* mice. Error bars indicate standard error of the mean. Profiles were marginally shifted relative to each other along the abscissa to avoid overlapping error bars.

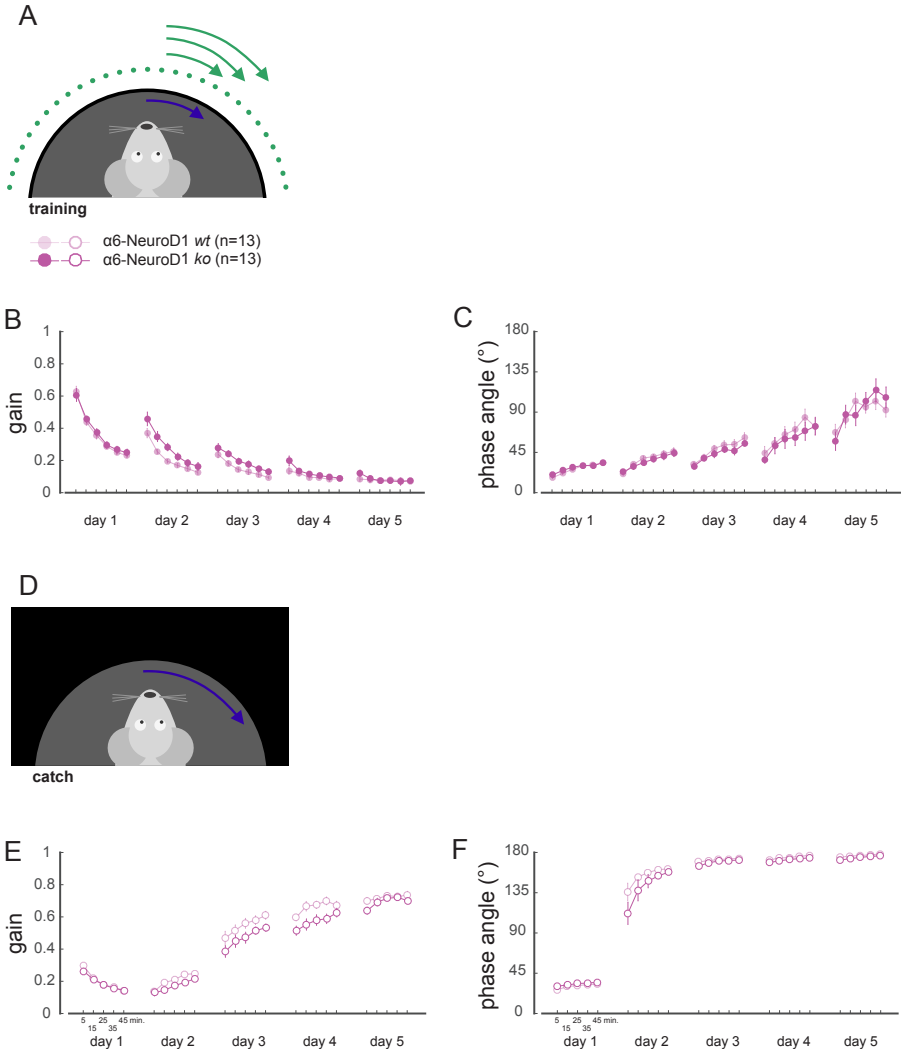

Figure 5. Adaptation of compensatory eye movements of α6-NeuroD1 mice during a visuo-vestibular conflict training paradigm, phase-reversal task. (A) Graphical depiction of the setup and stimulus conditions during training (A). (B) Gain of the eye movement response during the phase reversal paradigm. (C) Phase of the eye movement response during the phase reversal paradigm. (D) Graphical depiction of the setup and stimulus conditions during catch trials. (E-F) Changes in VOR gain (E) and phase (F) during the 5-day adaptation experiment. VOR was measured before, during, and after each daily training session. Colored symbols: *ko* mice. Opaque symbols: *wt* mice. Closed symbols: experiment in the light. Open symbols: experiment in the dark. Error bars indicate standard error of the mean. Profiles were marginally shifted relative to each other along the abscissa to avoid overlapping error bars.

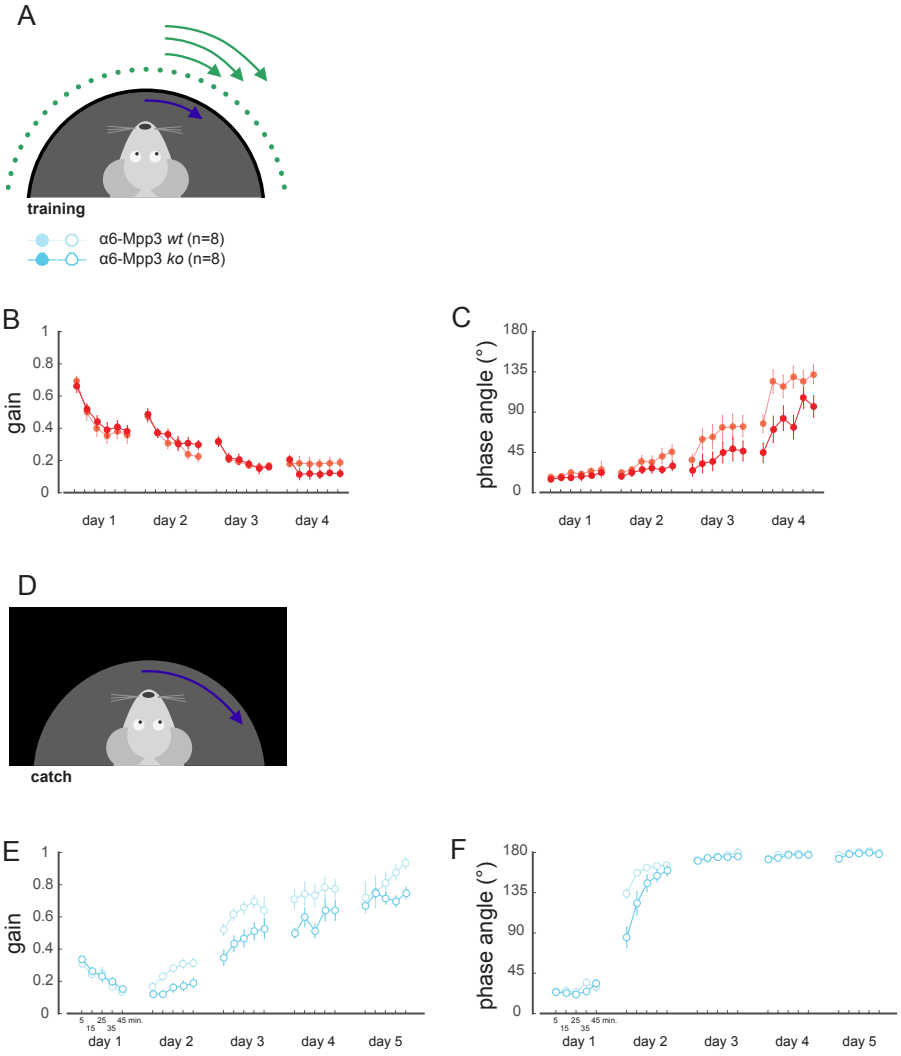

Figure 6. Adaptation of compensatory eye movements of α6-Mpp3 mice during a visuo-vestibular conflict training paradigm, phase-reversal task. (A) Graphical depiction of the setup and stimulus conditions during training (A). (B) Gain of the eye movement response during the phase reversal paradigm. (C) Phase of the eye movement response during the phase reversal paradigm. (D) Graphical depiction of the setup and stimulus conditions during catch trials. (E-F) Changes in VOR gain (E) and phase (F) during the 5-day adaptation experiment. VOR was measured before, during, and after each daily training session. Colored symbols: *ko* mice. Opaque symbols: *wt* mice. Closed symbols: experiment in the light. Open symbols: experiment in the dark. Error bars indicate standard error of the mean. Profiles were marginally shifted relative to each other along the abscissa to avoid overlapping error bars.

After 5 days of visuo-vestibular training, α6-NeuroD1 *ko* mice moved their eyes during table stimulation in the dark in the same direction as the body, rather than the opposite direction as they used to do before the training (i.e. they normally show an innate contraversive response). More specifically, the α6-NeuroD1 *ko* mice learned to shift their VOR in the dark by 180° after the training (Figures 5E and 5F). No differences were found on the learning extent, i.e., difference between the initial, 1st recording, 1st day, and final VOR performance, of the VOR adaptation displayed by the two groups (Figure 11, P=0.831).

3.3 VOR adaptation in α6-Mpp3 ko mice

The same protocol as described above was applied to the α6-Mpp3. Notwithstanding an apparent difference in phase evolution, no significant differences in VOR learning extent (scheme in Figure 6A) were observed after the 1h long training sessions (P=0.318, Figures 6B and 6C, and Figure 11). No differences were found in the initial VOR gain displayed by the *ko* mice and their *wt* littermates (P=0.943, Figure 10). Similarly, after the full phase reversal protocol, α6-Mpp3 *ko* mice learned to shift their VOR in the dark by 180° (Figures 6E and 6F). While the difference in VOR and VVOR learning extent was not significant, the learning curves suggest that α6-Mpp3 *ko* mice learn not as fast as their wildtype littermates, as can be seen in the VOR gain evolution (Fig. 6B), the phase evolution (Fig. 6C), and the gain evolution during the visuo-vestibular conflict training (Fig. 6E).

3.4 VOR adaptation in α6-γ2 ko mice

A similar protocol as used for the mouse lines described above was applied to the α6-γ2 *ko* mice and their *wt* controls. In this case, the protocol was shortened to 4 days (scheme in Figure 7A). No differences were found in the initial VOR gain displayed by the *ko* mice and their *wt* littermates (P=0.252, Figure 10). No significant difference in learning extent was observed after the 4 1h long training sessions (P=0.375, Figures 7B and 7C, and Figure 11), indicating that these mice also show normal ability to modify their VOR gain after the short-term visuo-vestibular training sessions.

Six catch trials (1 min each) were recorded in between the four training blocks of the visuovestibular training signal (8 min each; scheme in Figure 7D). After 4 days of training, α6-γ2 *ko* mice mice showed a complete phase reversal of their compensatory eye movements (Figures 7E and 7F).

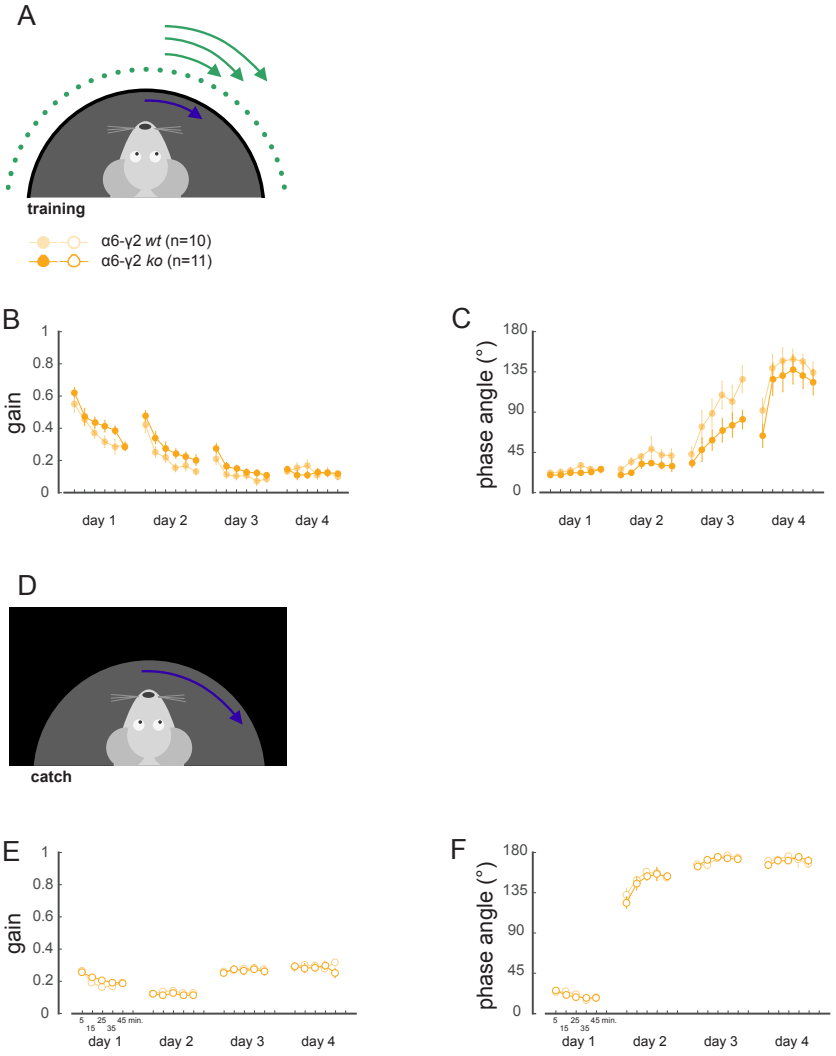

Figure 7. Adaptation of compensatory eye movements of □6-□2 mice during a visuo-vestibular conflict training paradigm, phase-reversal task. (A) Graphical depiction of the setup and stimulus conditions during training (A). (B) Gain of the eye movement response during the phase reversal paradigm. (C) Phase of the eye movement response during the phase reversal paradigm. (D) Graphical depiction of the setup and stimulus conditions during catch trials. (E-F) Changes in VOR gain (E) and phase (F) during the 4-day adaptation experiment. VOR was measured before, during, and after each daily training session. Colored symbols: *ko* mice. Opaque symbols: *wt* mice. Closed symbols: experiment in the light. Open symbols: experiment in the dark. Error bars indicate standard error of the mean. Profiles were marginally shifted relative to each other along the abscissa to avoid overlapping error bars.

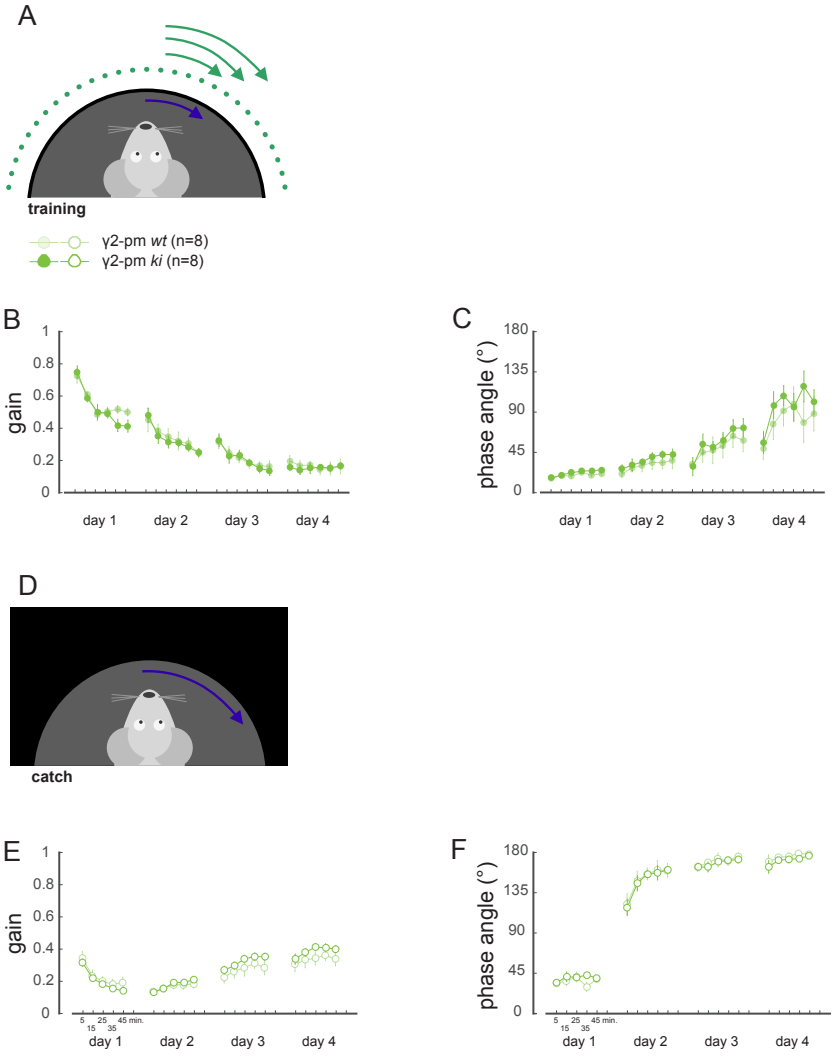

Figure 8. Adaptation of compensatory eye movements of γ2-pm mice during a visuo-vestibular conflict training paradigm, phase-reversal task. (A) Graphical depiction of the setup and stimulus conditions during training (A). (B) Gain of the eye movement response during the phase reversal paradigm. (C) Phase of the eye movement response during the phase reversal paradigm. (D) Graphical depiction of the setup and stimulus conditions during catch trials. (E-F) Changes in VOR gain (E) and phase (F) during the 4-day adaptation experiment. VOR was measured before, during, and after each daily training session. Colored symbols: *ki* mice. Opaque symbols: *wt* mice. Closed symbols: experiment in the light. Open symbols: experiment in the dark. Error bars indicate standard error of the mean. Profiles were marginally shifted relative to each other along the abscissa to avoid overlapping error bars.

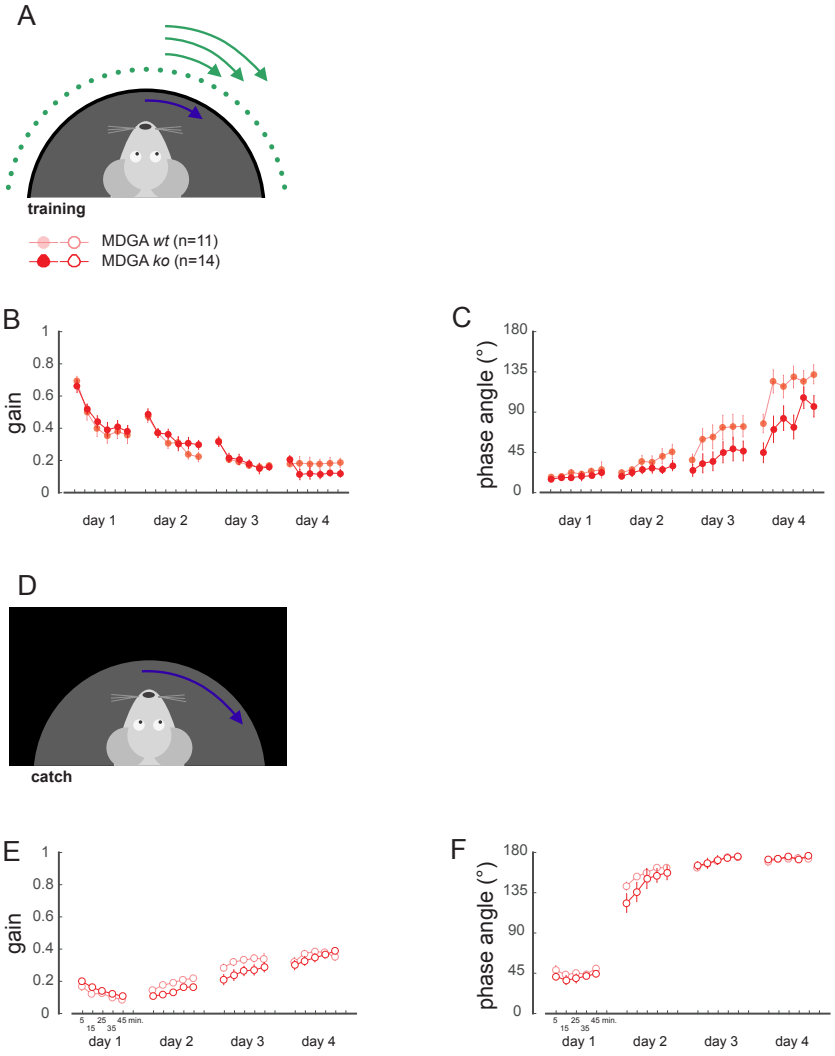

Figure 9 – Adaptation of compensatory eye movements of MDGA mice during a visuo-vestibular conflict training paradigm, phase-reversal task. (A) Graphical depiction of the setup and stimulus conditions during training (A). (B) Gain of the eye movement response during the phase reversal paradigm. (C) Phase of the eye movement response during the phase reversal paradigm. (D) Graphical depiction of the setup and stimulus conditions during catch trials. (E-F) Changes in VOR gain (E) and phase (F) during the 4-day adaptation experiment. VOR was measured before, during, and after each daily training session. Colored symbols: *ko* mice. Opaque symbols: *wt* mice. Closed symbols: experiment in the light. Open symbols: experiment in the dark. Error bars indicate standard error of the mean. Profiles were marginally shifted relative to each other along the abscissa to avoid overlapping error bars.

3.5 VOR adaptation in γ2-pm *ki* mice

The same protocol as described above was applied to the γ2-pm *ki* mice. No differences were found in the initial VOR gain displayed by the *ki* mice and their *wt* littermates (P=0.730, Figure 10). No significant difference in learning extent was observed after the 4 1h long training sessions (P=0.635, Figures 8B and 8C, and Figure 11). No significant differences in training (scheme in Figure 8A) were observed after the 1h long training sessions. Similarly, after the full phase reversal protocol, γ2-pm *ki* mice learned to shift their VOR in the dark by 180° (Figures 8E and 8F).

3.6 VOR adaptation in MDGA1 *ko* mice

The same protocol as described above was applied to the MDGA1 *ko* mice. No differences were found in the initial VOR gain displayed by the *ko* mice and their *wt* littermates (P=0.640). These mice also learned to shift their VOR in the dark by 180° (Figures 9E and 9F). There was a marginally significant difference in the learning extent of the VOR adaptation between the two groups (Figure 10, P=0.029).

4. DISCUSSION

In this study, we used long-term VOR phase reversal adaptation to assess cerebellar learning in five mouse models of cerebellar GC manipulations, to determine the effect of those manipulations in terms of cerebellar adaptation. This task presents several advantages compared with other cerebellar tasks. The modification of a reflex behavior is largely independent from other cognitive functions and depends specifically on the activity of the vestibulocerebellum (Gao et al., 2012), which makes it appropriate to measure cerebellar learning in cognitively impaired mice (Gutierrez-Castellanos, Winkelman, Tolosa-Rodriguez, Devenney, et al., 2013). The input (visual and/or vestibular) can be precisely controlled and the output (eye movement) can be monitored by video-oculography, a noninvasive technique that enables us to measure eye position virtually continuously. Therefore, this approach provides a better understanding of the input/output relation of the behavioral response than other tasks, such as the accelerating rotorod, gait analysis, or grip strength task, which can be affected by noncerebellar deficits in the musculoskeletal system or nervous system.

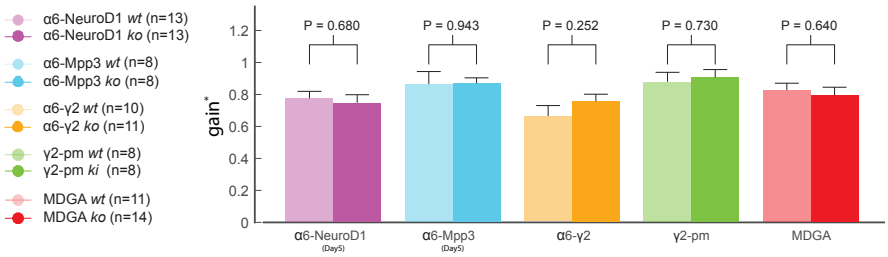

Figure 10. Summary of the initial VOR gain, given by the initial performances of VOR catch-learning trials, for all mouse models. Colored bars: *ko* mice. Opaque bars: *wt* mice. Error bars indicate standard error of the mean.

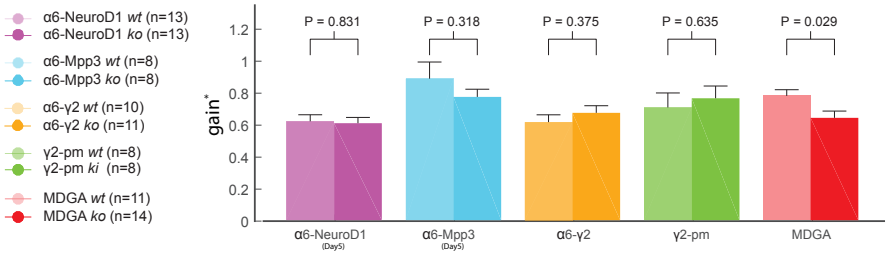

Figure 11. Summary of the learning extent. Learning extent is given by the difference between the initial (first recording, day 1) and the final VOR performance coordinate throughout the 4/5-day-spanning phase-reversal paradigm. Colored bars: *ko* mice. Opaque bars: *wt* mice. Error bars indicate standard error of the mean.

We observed that all mice showed comparable baseline performance regarding both amplitude and phase responses of the VOR and OKR (Figures 1 and 2). During vestibular stimulation in the light, the combined action of VOR and OKR resulted in near optimal CEM performance in all the groups (Figure 3).

Due to the specific genetic targeting of cerebellar elements and GC in particular (as shown in Table 1 and Figure 1), all the transgenic mouse models used in this article were expected to display VOR adaptation deficits in a challenging cerebellar task such as VOR phase reversal. However, all reported adaptation values of the transgenic mouse models were comparable to their wildtype littermate controls (Figures 5-9), with the exception of a marginally significant difference in learning extent for the MDGA1 global knockout.

While we were not able to show a positive behavioral phenotype, it goes too far to declare these are negative results, as such a statement requires a highly powered study. Two mutants are suggestive of a phenotype: MDGA1 and possibly MPP3, but these could be either spurious (false positive) or lacking power (false negative). Larger group sizes are required to establish significance for small effect sizes. However, given the pressure on reducing animal experiments, scientists must design experiments on *a priori* assumptions of the effect size, estimating sufficient sample sizes to achieve adequate power. This can compromise the power of experiments by limiting the sampling pool and leading to experiments cut too shortly. To add to this, even when the results are pointing towards a negative result, it's important to emphasize that statistically non-significant results in a study with high power contribute to the body of knowledge because power can be ruled out as a threat to internal validity.

Nonetheless, the data presented here do not show the large effect seen in other mutants, in which cerebellar GCs were affected in a cell-specific fashion using the GABA-α6 subunit promoter (Galliano et al., 2013; Seja et al., 2012). For example, α6-Cacna1a modified mice, which are missing ~75% of their GC output, show qualitatively the exact same phenotype of learning and consolidation deficits without ataxia, yet at a more severe level (Galliano et al., 2013). Regarding the γ2 subunit in particular, it has been observed before that mice lacking γ2 subunit-containing receptors in GCs learned normally to run on a rotarod and did not show obvious motor deficits (Leppä et al., 2016). This corroborates the results we observed with the a6-y2 mice. In contrast, mice lacking this subunit in PC showed a strong compromise of their ability to adapt the phase of the VOR and to consolidate gain adaptations, through disrupted inhibitory and excitatory input timing from PCs and mossy fiber collaterals (Wulff et al., 2009). We didn't observe such an effect with the γ2 point mutation.

In respect with NeuroD1, Mpp3 and MDGA1, these are models of disruption of the processes of cell migration and layering patterns of the cerebellum, with the emphasis on the GC layer. One possible explanation for the occurrence of negative findings for these models could be developmental compensation. Indeed, a common issue with any adult phenotype has to do with the (potential) confounding effect of developmental compensation. In the case of the MDGA1, there's the added factor of this being a global *ko* mutant. Plasticity of the mechanisms is quite common in the brain; when the brain lacks a particular gene, development itself is likely to be affected, so the mutant phenotype may not clearly reflect the missing gene's normal function. Thus, even though genetics

offers a degree of specificity that pharmacologists may envy, the gene knockout approach is not a replacement for pharmacology, but a complementary technique with its own interpretational problems. Indeed, because of the massive impact of a global knockout in the entire brain, it's preferable to use conditional cell-specific knockouts, that allow to overcome obstacles regarding global knocking out of a gene. However, more specific and strict approaches such as timed rescue of mutant phenotypes may pose an even better choice, though they are still to be fully established for many mutant mice. Interpreting mutant brain phenotypes requires understanding of higher-level phenomena, such as a neural circuit and the behavior it generates.

With respect to the case of NeuroD1 in particular, previous systemic or conditional NeuroD1 null mice experiments have shown that the absence of NeuroD1 leads to a lack of foliation and the complete loss of granular cells in the posterior half of the cerebellum, whereas a substantial number of granular cells survive and differentiate in the anterior lobules (Cho & Tsai, 2006; Miyata et al., 1999; Schwab et al., 2000). This is not consistent with our results, as the flocculonodular lobe, the regional area of the cerebellum responsible for eye movement reflexes, is posterior. An additional experiment here would be to check if the flocculonodular lobe is affected in these mice.

Another explanation for the absence of a phenotype in the NeuroD1 can be tied to the interplay of NeuroD1 expression with other transcription factors, which might establish a temporal window for growth regulation in the cerebellum (Butts, Hanzel, & Wingate, 2014). An example of this has been shown for the hippocampal granule cells, in which issues with maturation of these cells were only present if besides NeuroD1, other genes (i.e. bHLH gene NEX) were also knocked out. This suggests that neuronal differentiation factors are at least in part equivalent in function (Schwab et al., 2000).

Author contributions

B.H.J.W., M.S. and C.I.D.Z. designed the behavioral experiments; C.M.S.M., N.G.C., J.J.D., B.H.J.W. and M.S. performed the behavioral experiments; B.H.J.W. and C.M.S.M analyzed the data. S.G. generated the NeuroD1 conditional knockout mice; J.J.D. and J.W. generated the Mpp3 conditional knockout mice; and C.M.S.M., B.H.J.W., M.S. and C.I.D.Z. wrote the manuscript.

Funding statements

This work was supported by the Netherlands Organization for Scientific Research, the EU ERC, ERC-POC, CEREBNET and C7 programs (C.I.D.Z.). The authors declare no financial or non-financial competing interests.

Acknowledgments

We thank Leonardo Tolosa Rodriguez for his collaboration.

REFERENCES

Albus, J. S. (1971). A Theory of Cerebellar Function. *Mathematical Biosciences*, (10), 25–61.

Aller, M. I., Jones, A., Merlo, D., Paterlini, M., Meyer, A. H., Amtmann, U., … Wisden, W. (2003). Cerebellar granule cell Cre recombinase expression. *Genesis*, *36*(2), 97–103. https://doi.org/10.1002/gene.10204

Anand, B. K., Malhotra, C. L., Singh, B., & Dua, S. (2017). Cerebellar Projections to Limbic System. *Journal of Neurophysiology*, *22*(4), 451–457. https://doi.org/10.1152/jn.1959.22.4.451

Butts, T., Hanzel, M., & Wingate, R. J. T. (2014). Transit amplification in the amniote cerebellum evolved via a heterochronic shift in NeuroD1 expression. *Development*, *141*(14), 2791 LP – 2795. https://doi.org/10.1242/dev.101758

Cappello, S., Attardo, A., Wu, X., Iwasato, T., Itohara, S., Wilsch-Bräuninger, M., … Götz, M. (2006). The Rho-GTPase cdc42 regulates neural progenitor fate at the apical surface. *Nature Neuroscience*, *9*(9), 1099–1107. https://doi.org/10.1038/nn1744

Chae, J. H., Stein, G. H., & Lee, J. E. (2004). NeuroD: The Predicted and the Surprising. *Mol. Cells*, *18*(3), 271–288.

Cho, J.-H., & Tsai, M.-J. (2006). Preferential posterior cerebellum defect in BETA2/NeuroD1 knockout mice is the result of differential expression of BETA2/NeuroD1 along anterior–posterior axis. *Developmental Biology*, *290*(1), 125–138. https://doi.org/https://doi.org/10.1016/j.ydbio.2005.11.024

D'Amico, L. A., Boujard, D., & Coumailleau, P. (2013). The Neurogenic Factor NeuroD1 Is Expressed in Post-Mitotic Cells during Juvenile and Adult Xenopus Neurogenesis and Not in Progenitor or Radial Glial Cells. *PLoS ONE*, *8*(6), 1–10. https://doi.org/10.1371/journal.pone.0066487

D'Angelo, E. (2008). The critical role of Golgi cells in regulating spatio-temporal integration and plasticity at the cerebellum input stage. *Frontiers in Neuroscience*, *2*(1), 35–46. https://doi.org/10.3389/neuro.01.008.2008

de Jeu, M., & De Zeeuw, C. I. (2012). Video-oculography in mice. *Journal of Visualized Experiments : JoVE*, (65), e3971. https://doi.org/10.3791/3971

Di Cristo, G. (2007). Development of cortical GABAergic circuits and its implications for neurodevelopmental disorders. *Clinical Genetics*, *72*(1), 1–8. https://doi.org/10.1111/j.1399-0004.2007.00822.x

Dudok, J. J., Sanz, A. S., Lundvig, D. M. S., & Wijnholds, J. (2013). MPP3 Is Required for Maintenance of the Apical Junctional Complex, Neuronal Migration, and Stratification in the Developing Cortex. *Journal of Neuroscience*, *33*(19), 8518–8527. https://doi.org/10.1523/JNEUROSCI.5627-12.2013

Eccles, J. C. (1970). Neurogenesis and Morphogenesis in the Cerebellar Cortex. *Proceedings of the National Academy of Sciences*, *66*(2), 294 LP – 301. https://doi.org/10.1073/pnas.66.2.294

Farrant, M., & Nusser, Z. (2005). Variations on an inhibitory theme: phasic and tonic activation of GABAA receptors. *Nature Reviews Neuroscience*, *6*(3), 215–229. https://doi.org/10.1038/nrn1625

Fatemi, S. H., Reutiman, T. J., Folsom, T. D., Rustan, O. G., Rooney, R. J., & Thuras, P. D. (2014). Downregulation of GABAA Receptor Protein Subunits α6, β2, δ, ε, γ2, θ, and ρ2 in Superior Frontal Cortex of Subjects with Autism. *Journal of Autism and Developmental Disorders*, *44*(8), 1833–1845. https://doi.org/10.1007/s10803-014-2078-x

Fox, B. Y. C. A., & Barnard, J. W. (1957). A quantitative study of the Purkinje cell dendritic branchlets and their relationship to afferent fibres. *Journal of Anatomy*, *91*(1951), 299–313. https://doi.org/10.1039/c1rp90071d

Fünfschilling, U., & Reichardt, L. F. (2002). Cre-mediated recombination in rhombic lip derivatives. *Genesis*, *33*(4), 160–169. https://doi.org/10.1002/gene.10104

Galliano, E., Gao, Z., Schonewille, M., Todorov, B., Simons, E., Pop, A. S., … De Zeeuw, C. I. (2013). Silencing the majority of cerebellar granule cells uncovers their essential role in motor learning and consolidation. *Cell Reports*, *3*(4), 1239–1251. https://doi.org/10.1016/j.celrep.2013.03.023

Gao, Z., Todorov, B., Barrett, C. F., van Dorp, S., Ferrari, M. D., van den Maagdenberg, A. M. J. M., … Hoebeek, F. E. (2012). Cerebellar ataxia by enhanced Ca(V)2.1 currents is alleviated by Ca2+-dependent K+-channel activators in Cacna1a(S218L) mutant mice. *The Journal of Neuroscience : The Official Journal of the Society for Neuroscience*, *32*(44), 15533–15546. https://doi.org/10.1523/JNEUROSCI.2454-12.2012

Giovannucci, A., Badura, A., Deverett, B., Najafi, F., Pereira, T. D., Gao, Z., … Wang, S. S.-H. (2017). Cerebellar granule cells acquire a widespread predictive feedback signal during motor learning. *Nature Neuroscience*, *20*, 727. Retrieved from https://doi.org/10.1038/nn.4531

Goebbels, S., Bode, U., Pieper, A., Funfschilling, U., Schwab, M. H., & Nave, K.-A. (2005). Cre/loxP-mediated inactivation of the bHLH transcription factor gene NeuroD/BETA2. *Genesis*, *42*(4), 247–252. https://doi.org/10.1002/gene.20138

Goebbels, S., Bormuth, I., Bode, U., Hermanson, O., Schwab, M. H., & Nave, K.-A. (2006). Genetic targeting of principal neurons in neocortex and hippocampus of NEX-Cre mice. *Genesis*, *44*(12), 611–621. https://doi.org/10.1002/dvg.20256

Gutierrez-Castellanos, N., Winkelman, B. H. J., Tolosa-Rodriguez, L., De Gruijl, J. R., & De Zeeuw, C. I. (2013). Impact of aging on long-term ocular reflex adaptation. *Neurobiology of Aging*, *34*(12), 2784–2792. https://doi.org/10.1016/j.neurobiolaging.2013.06.012

Gutierrez-Castellanos, N., Winkelman, B. H. J., Tolosa-Rodriguez, L., Devenney, B., Reeves, R. H., & De Zeeuw, C. I. (2013). Size does not always matter: Ts65Dn Down syndrome mice show cerebellum-dependent motor learning deficits that cannot be rescued by postnatal SAG treatment. *The Journal of Neuroscience : The Official Journal of the Society for Neuroscience*, *33*(39), 15408–15413. https://doi.org/10.1523/JNEUROSCI.2198-13.2013

Hansel, C., Linden, D. J., & D'Angelo, E. (2001). Beyond parallel fiber LTD: the diversity of synaptic and non-synaptic plasticity in the cerebellum. *Nature Neuroscience*, *4*, 467. Retrieved from https://doi.org/10.1038/87419

Herrup, K., & Kuemerle, B. (1997). The compartmentalization of the cerebellum. *Annual Review of Neuroscience*, *20*(1), 61–90. https://doi.org/10.1146/annurev.neuro.20.1.61

Hirano, T., Yamazaki, Y., & Nakamura, Y. (2016). LTD, RP, and Motor Learning. *The Cerebellum*, *15*(1), 51–53. https://doi.org/10.1007/s12311-015-0698-0

Imai, F., Hirai, S., Akimoto, K., Koyama, H., Miyata, T., Ogawa, M., … Ohno, S. (2006). Inactivation of aPKCλ results in the loss of adherens junctions in neuroepithelial cells without affecting neurogenesis in mouse neocortex. *Development*, *133*(9), 1735 LP – 1744. https://doi.org/10.1242/dev.02330

Ishikawa, T., Gotoh, N., Murayama, C., Abe, T., Iwashita, M., Matsuzaki, F., … Yamamoto, T. (2011). IgSF molecule MDGA1 is involved in radial migration and positioning of a subset of cortical upper-layer neurons. *Developmental Dynamics*, *240*(1), 96–107. https://doi.org/10.1002/dvdy.22496

Ito, M. (1984). The modifiable neuronal network of the cerebellum. *The Japanese Journal of Physiology*, *34*(5), 781-92.

Ito, M. (1998). Cerebellar learning in the vestibulo–ocular reflex. *Trends in Cognitive Sciences*, *2*(9), 313–321.

Jurd, R., & Moss, S. J. (2010). Impaired GABA(A) receptor endocytosis and its correlation to spatial memory deficits. *Communicative & Integrative Biology*, *3*(2), 176–178. Retrieved from https://www.ncbi.nlm.nih.gov/pubmed/20585515

Kadowaki, M., Nakamura, S., Machon, O., Krauss, S., Radice, G. L., & Takeichi, M. (2007). N-cadherin mediates cortical organization in the mouse brain. *Developmental Biology*, *304*(1), 22–33. https://doi.org/https://doi.org/10.1016/j.ydbio.2006.12.014

Kantardzhieva, A., Alexeeva, S., Versteeg, I., & Wijnholds, J. (2006). MPP3 is recruited to the MPP5 protein scaffold at the retinal outer limiting membrane. *The FEBS Journal*, *273*(6), 1152–1165. https://doi.org/10.1111/j.1742-4658.2006.05140.x

Killian, J. E., & Baker, J. F. (2002). Horizontal Vestibuloocular Reflex (VOR) Head Velocity Estimation in Purkinje Cell Degeneration (pcd/pcd) Mutant Mice. *Journal of Neurophysiology*, *87*(2), 1159–1164.

Kim, J. A., Kim, D., Won, S. Y., Han, K. A., Park, D., Cho, E., … Kim, H. M. (2017). Structural Insights into Modulation of Neurexin-Neuroligin Trans-synaptic Adhesion by MDGA1/Neuroligin-2 Complex. *Neuron*, *94*(6), 1121-1131.e6. https://doi.org/10.1016/j.neuron.2017.05.034

Laurie, D. J., Seeburg, P. H., & Wisden, W. (1992). The distribution of 13 GABAA receptor subunit mRNAs in the rat brain. II. Olfactory bulb and cerebellum. *The Journal of Neuroscience*, *12*(3), 1063 LP – 1076. https://doi.org/10.1523/JNEUROSCI.12-03-01063.1992

Lee, H.-K. (2012). Ca2+-permeable AMPA receptors in homeostatic synaptic plasticity. *Frontiers in Molecular Neuroscience*, *5*(February), 1–11. https://doi.org/10.3389/fnmol.2012.00017

Lee, J.-K., Cho, J.-H., Hwang, W.-S., Lee, Y.-D., Reu, D.-S., & Suh-Kim, H. (2000). Expression of neuroD/BETA2 in mitotic and postmitotic neuronal cells during the development of nervous system. *Developmental Dynamics*, *217*(4), 361–367. https://doi.org/10.1002/(SICI)1097-0177(200004)217:4<361::AID-DVDY3>3.0.CO;2-8

Lein, E. S., Hawrylycz, M. J., Ao, N., Ayres, M., Bensinger, A., Bernard, A., … Jones, A. R. (2006). Genome-wide atlas of gene expression in the adult mouse brain. *Nature*, *445*, 168. Retrieved from https://doi.org/10.1038/nature05453

Leppä, E., Linden, A.-M., Aller, M. I., Wulff, P., Vekovischeva, O., Luscher, B., … Korpi, E. R. (2016). Increased Motor-Impairing Effects of the Neuroactive Steroid Pregnanolone in Mice with Targeted Inactivation of the GABA(A) Receptor γ2 Subunit in the Cerebellum. *Frontiers in Pharmacology*, *7*, 403. https://doi.org/10.3389/fphar.2016.00403

Levitt, P. (2005). Disruption of Interneuron Development. *Epilepsia*, *46*(s7), 22–28. https://doi.org/10.1111/j.1528-1167.2005.00305.x

Litwack, E. D., Babey, R., Buser, R., Gesemann, M., & O'Leary, D. D. M. (2004). Identification and characterization of two novel brain-derived immunoglobulin superfamily members with a unique structural organization. *Molecular and Cellular Neuroscience*, *25*(2), 263–274. https://doi.org/https://doi.org/10.1016/j.mcn.2003.10.016

Mapelli, J., Gandolfi, D., Vilella, A., Zoli, M., & Bigiani, A. (2016). Heterosynaptic GABAergic plasticity bidirectionally driven by the activity of pre- and postsynaptic NMDA receptors. *Proceedings of the National Academy of Sciences*, *113*(35), 9898 LP – 9903. https://doi.org/10.1073/pnas.1601194113

Marr, D. (1969). A theory of cerebellar cortex. *Journal of Physiology*, *202*, 437–470.

Miyata, T., Maeda, T., & Lee, J. E. (1999). NeuroD is required for differentiation of the granule cells in the cerebellum and hippocampus. *Genes & Development*, *13*(13), 1647–1652. Retrieved from https://www.ncbi.nlm.nih.gov/pubmed/10398678

Pettem, K. L., Yokomaku, D., Takahashi, H., Ge, Y., & Craig, A. M. (2013). Interaction between autism-linked MDGAs and neuroligins suppresses inhibitory synapse development. *Journal of Cell Biology*, *200*(3), 321–336. https://doi.org/10.1083/jcb.201206028

Ramón y Cajal, S. (1911). *Histologie du systéme nerveux de l'homme & des vertébrés*. Paris: Maloine.

Rossignol, E. (2011). Genetics and function of neocortical GABAergic interneurons in neurodevelopmental disorders. *Neural Plasticity*, *2011*, 649325. https://doi.org/10.1155/2011/649325

Sakatani, T., & Isa, T. (2004). PC-based high-speed video-oculography for measuring rapid eye movements in mice. *Neuroscience Research*, *49*(1), 123–131. https://doi.org/https://doi.org/10.1016/j.neures.2004.02.002

Schwab, M. H., Bartholomae, A., Heimrich, B., Feldmeyer, D., Druffel-Augustin, S., Goebbels, S., … Nave, K.-A. (2000). Neuronal Basic Helix-Loop-Helix Proteins (NEX and BETA2/Neuro D) Regulate Terminal Granule Cell Differentiation in the Hippocampus. *The Journal of Neuroscience*, *20*(10), 3714 LP – 3724. https://doi.org/10.1523/JNEUROSCI.20-10-03714.2000

Schweighofer, N., Doya, K., & Lay, F. (2001). Unsupervised learning of granule cell sparse codes enhances cerebellar adaptive control. *Neuroscience*, *103*(1), 35–50. https://doi.org/10.1016/S0306-4522(00)00548-0

Seja, P., Schonewille, M., Spitzmaul, G., Badura, A., Klein, I., Rudhard, Y., … Jentsch, T. J. (2012). Raising cytosolic Cl-in cerebellar granule cells affects their excitability and vestibulo-ocular learning. *EMBO Journal*, *31*(5), 1217–1230. https://doi.org/10.1038/emboj.2011.488

Sillitoe, R. V, & Joyner, A. L. (2007). Morphology, Molecular Codes, and Circuitry Produce the Three-Dimensional Complexity of the Cerebellum. *Annual Review of Cell and Developmental Biology*, *23*(1), 549–577. https://doi.org/10.1146/annurev.cellbio.23.090506.123237

Snider, R. S., & Maiti, A. (1976). Cerebellar contributions to the papez circuit. *Journal of Neuroscience Research*, *2*(2), 133–146. https://doi.org/10.1002/jnr.490020204

Song, M. Y., Kim, H. E., Kim, S., Choi, I. H., & Lee, J. K. (2012). SNP-based large-scale identification of allele-specific gene expression in human B cells. *Gene*, *493*(2), 211–218. https://doi.org/10.1016/j.gene.2011.11.058

Takeuchi, A., Hamasaki, T., Litwack, E. D., & O'Leary, D. D. M. (2007). Novel IgCAM, MDGA1, expressed in unique cortical area- and layer-specific patterns and transiently by distinct forebrain populations of cajal-retzius neurons. *Cerebral Cortex*, *17*(7), 1531–1541. https://doi.org/10.1093/cercor/bhl064

Takeuchi, A., & O'Leary, D. D. M. (2006). Radial Migration of Superficial Layer Cortical Neurons Controlled by Novel Ig Cell Adhesion Molecule MDGA1. *The Journal of Neuroscience*, *26*(17), 4460 LP – 4464. https://doi.org/10.1523/JNEUROSCI.4935-05.2006

Tretter, V., Revilla-sanchez, R., Houston, C., Terunuma, M., Havekes, R., Florian, C., … Moss, S. J. (2009). Deficits in spatial memory correlate with modified {gamma}-aminobutyric acid type A receptor tyrosine phosphorylation in the hippocampus. *Proceedings of the National Academy of Sciences of the United States of America*, *106*(47), 20039–20044. https://doi.org/10.1073/pnas.0908840106

Varecka, L., Wu, C.-H., Rotter, A., & Frostholm, A. (1994). GABAA/benzodiazepine receptor α6 subunit mRNA in granule cells of the cerebellar cortex and cochlear nuclei: Expression in developing and mutant mice. *Journal of Comparative Neurology*, *339*(3), 341–352. https://doi.org/10.1002/cne.903390304

Voogd, J., & Barmack, N. H. (2006). Oculomotor cerebellum. In J. A. B. T.-P. in B. R. Büttner-Ennever (Ed.), *Neuroanatomy of the Oculomotor System* (Vol. 151, pp. 231–268). Elsevier. https://doi.org/https://doi.org/10.1016/S0079-6123(05)51008-2

Wang, V. Y., & Zoghbi, H. Y. (2001). Genetic regulation of cerebellar development. *Nature Reviews Neuroscience*, *2*, 484. Retrieved from https://doi.org/10.1038/35081558

Wu, X., Huang, L., Wu, Z., Zhang, C., Jiang, D., Bai, Y., … Chen, G. (2013). Homeostatic competition between phasic and tonic inhibition. *The Journal of Biological Chemistry*, *288*(35), 25053–25065. https://doi.org/10.1074/jbc.M113.491464

Wulff, P., Schonewille, M., Renzi, M., Viltono, L., Sassoè-Pognetto, M., Badura, A., … De Zeeuw, C. I. (2009). Synaptic inhibition of Purkinje cells mediates consolidation of vestibulo-cerebellar motor learning. *Nature Neuroscience*, *12*(8), 1042–1049. https://doi.org/10.1038/nn.2348

Yaeger, D. B., & Trussell, L. O. (2015). Single granule cells excite Golgi cells and evoke feedback inhibition in the cochlear nucleus. *The Journal of Neuroscience : The Official Journal of the Society for Neuroscience*, *35*(11), 4741–4750. https://doi.org/10.1523/JNEUROSCI.3665-14.2015

Yeganeh-Doost, P., Gruber, O., Falkai, P., & Schmitt, A. (2011). The role of the cerebellum in schizophrenia: from cognition to molecular pathways. *Clinics (Sao Paulo)*, *66*, 71–77.

Yokoyama, M., Nishi, Y., Miyamoto, Y., Nakamura, M., Akiyama, K., Matsubara, K., & Okubo, K. (1996). Molecular cloning of a human neuroD from a neuroblastoma cell line specifically expressed in the fetal brain and adult cerebellum. *Molecular Brain Research*, *42*(1), 135–139. https://doi.org/https://doi.org/10.1016/S0169-328X(96)00154-4

Chapter 4

Motor Learning Requires Purkinje Cell Synaptic Potentiation through Activation of AMPA-Receptor subunit GluA3

Nicolas Gutierrez-Castellanos[1,2], Carla M. Da Silva-Matos[1], Kuikui Zhou[2], Cathrin B. Canto[1], Maria C. Renner[1], Linda M.C. Koene[1], Ozgecan Ozyildirim[1], Rolf Sprengel[3], Helmut W. Kessels[1,4,*] and Chris I. De Zeeuw[1,2,4,*]

[1] The Netherlands Institute for Neuroscience, Royal Netherlands Academy of Arts and Sciences, 1105 BA Amsterdam, The Netherlands
[2] Department of Neuroscience, Erasmus MC Rotterdam, NL-3015 GE Rotterdam, The Netherlands
[3] Max Planck Institute for Medical Research, D-69120 Heidelberg, Germany
[4] Co-senior author

*Correspondence: c.dezeeuw@erasmusmc.nl; h.kessels@nin.knaw.nl

Highlights

- Cerebellar learning depends on expression of GluA3, but not GluA1, in Purkinje cells.
- GluA3 is required to induce LTP, but not LTD, at PF-PC synapses.
- GluA3-dependent potentiation involves a cAMP-driven change in channel conductance.
- GluA3-mediated LTP and learning are induced via cAMP-mediated Epac activation.

eTOC

Gutierrez et al. show a novel form of synaptic LTP that requires an increase in channel conductance of GluA3-containing AMPARs and that is required for vestibulo-cerebellar motor learning.

ABSTRACT

Accumulating evidence indicates that cerebellar long-term potentiation (LTP) is necessary for procedural learning. However, little is known about its underlying molecular mechanisms. Whereas AMPA receptor (AMPAR) subunit rules for synaptic plasticity have been extensively studied in relation to declarative learning, it is unclear whether these rules apply to cerebellum-dependent motor learning. Here we show that LTP at the parallel fiber to Purkinje cell synapse and adaptation of the vestibulo-ocular reflex do not depend on GluA1-, but on GluA3-containing AMPARs. In contrast to the classic form of LTP implicated in declarative memory formation, this form of LTP does not require GluA1-AMPARs trafficking, but rather changes in open-channel probability of GluA3-AMPARs mediated by an increase of cyclic AMP and activation of the protein directly activated by cAMP (Epac). We conclude that vestibulo-cerebellar motor learning is the first form of memory acquisition shown to depend on GluA3-dependent synaptic potentiation through an increase in channel conductance.

INTRODUCTION

Plasticity mediated by synaptic trafficking of α-amino-3-hydroxy-5-methyl-4-isoxazolepropionic acid - type glutamate receptors (AMPARs) plays an important role in the acquisition of declarative memories (Kessels and Malinow, 2009). Ionotropic AMPARs drive fast excitatory neuronal activity and can consist of four different subunits named GluA1 to GluA4. In hippocampal pyramidal cells, most AMPARs are hetero-oligomers composed of either GluA1/GluA2 or GluA2/GluA3 subunits and the subunit composition dictates which role AMPARs play in synaptic plasticity (Shi et al., 2001). In the hippocampus, cortex and amygdala, both LTP and learning depend on the trafficking of GluA1-containing AMPARs to synapses (Makino and Malinow, 2011; Nedelescu et al., 2010; Rumpel et al., 2005; Mitsushima et al., 2011), whereas GluA3-containing AMPARs contribute relatively little to synaptic currents, synaptic plasticity or learning (Adamczyk et al., 2012; Meng et al., 2003; Humeau et al., 2007). To what extent GluA1-plasticity and GluA3-plasticity play a role in adaptive motor behavior, remains to be established.

Here, we sought to unravel the potential role of GluA1- and/or GluA3-containing AMPARs in cerebellar motor learning. Unlike the rich insight in the role of AMPARs in declarative memory formation in the hippocampus, relatively little is known about their role in procedural memory formation in the cerebellum. AMPAR plasticity occurs at parallel fiber to Purkinje cell (PF-PC) synapses reflecting the expression of LTP or long-term depression (LTD) (Kakegawa and Yuzaki, 2005; Steinberg et al., 2006), but the full functional significance of and the precise molecular pathways underlying this plasticity remain to be further elucidated (Gao et al., 2012). In addition, the roles of GluA1- and/or GluA3-containing AMPARs in plasticity of PCs have hardly been studied (Bats et al., 2013; Douyard et al., 2007; Kakegawa and Yuzaki, 2005).

We found that adaptation of compensatory eye movements, which is one of the most widely studied forms of cerebellar motor learning serving to stabilize gaze (Anzai et al., 2010, Nguyen-Vu et al., 2013; Schonewille et al., 2011), depends on GluA3-containing AMPARs, but not GluA1-containing AMPARs. The GluA3-containing AMPARs in PCs are critical for the induction and expression of PF-PC LTP, not by trafficking of receptors, but by a change in conductance and open probability of the channel. This form of plasticity requires activation of Epac through an increase of cyclic AMP. Together, these findings do not only show that GluA3 is crucial for cerebellar potentiation and learning, but also that it evokes its actions of plasticity through a novel mechanism.

RESULTS

Cerebellar motor learning depends on GluA3, but not on GluA1

Unlike global knock-out mice of GluA2, which suffer from severe motor performance deficits including ataxia (Gerlai et al., 1998; Jia et al., 1996), mice that lack AMPAR subunit GluA1 or GluA3 (GluA1-KO and GluA3-KO) displayed intact basic motor behavior (Figure S1). Indeed, they were able to stabilize the images on their retina and/or gaze with respect to a moving visual field (i.e. optokinetic reflex or OKR; Figure S1A), with respect to their head movements (i.e. the vestibulo-ocular reflex in the dark or VOR: Figure S1B), or with respect to a combination of both as occurs in daily life (i.e. VOR in the light or VORL; Figure S1C). None of the comparisons between GluA1-KO, GluA3-KO and their control littermates showed a significant difference in any of these paradigms (for p-values, see Figure S1 and corresponding legends). Far more challenging is the test for VOR phase-reversal adaptation, which involves cerebellum-dependent motor learning (Gutierrez-Castellanos et al., 2013). During this paradigm mice learn to shift the phase of their VOR following sinusoidal visuovestibular mismatch stimulation, in which the visual stimulus moves in the same direction as the vestibular stimulus (i.e. in-phase), yet at a greater amplitude (Figure 1A). After 5 days of visuovestibular training wild-type mice moved their eyes during table stimulation in the dark in the same direction as the body, rather than the opposite direction as they used to do before the training (i.e. they normally show an innate contraversive compensation). More specifically, the mature wild-type mice learned to shift their VOR in the dark by 159º out of the perfect 180º after the training (Figure 1B). Likewise, when we subjected littermate GluA1-deficient mice to this phase-reversal adaptation paradigm, they reached final average phase shifts of 162º (GluA1-KO vs. WT: p=0.13; Figure 1B), indicating that GluA1-containing AMPARs are dispensable for VOR adaptation. In contrast, GluA3-deficient mice showed striking deficits in shifting the phase of their VOR in the dark; they showed a final phase shift of only 35º after 5 training sessions (GluA3-KO vs. WT: p=0.001; Figure 1B). When we looked not only at the oculomotor phase but also at the learning trajectory extent (as explained in Figure S2A), we observed that, although the initial performances of VOR catch learning trials were not significantly different for any of the 3 groups tested (p=0.3 and p=0.11 for GluA1-KO and GluA3-KO, respectively), the final performances of GluA3-KO after 5 days of training were significantly different from those of both wild-type littermates (p=0.01) and GluA1-KO mice (p=0.01) (Figure 1C). Accordingly, the vector of total learning extent per mouse, which equals the distance between the initial (1st recording, 1st day) and final VOR performance coordinate throughout the 5-day spanning phase-reversal paradigm

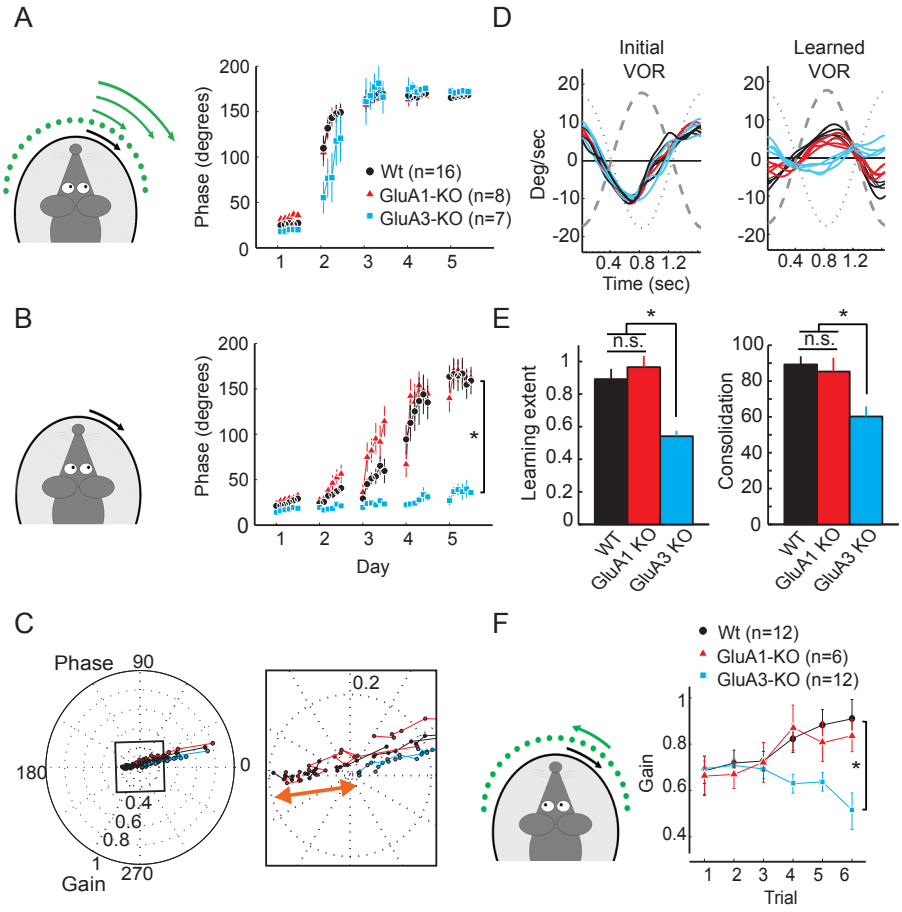

Figure 1. GluA3 is required for oculomotor learning.
(A) When adult (3-5 months of age) wild-type (black), GluA1-KO (red) and GluA3-KO mice (blue) are subjected to a visuo-vestibular mismatch training paradigm, in which the visual screen rotates sinusoidally in the same direction as the turntable, but at an increasingly greater amplitude (also referred to as phase-reversal task), they show a similar ability to follow the training signal over time as long as the light is on. Eye movement signals are expressed as phase values (in degrees) with respect to those of the turntable, which also rotates in a sinusoidal fashion (i.e., 360 degrees represents one sinusoidal cycle). (B) However, when the light is turned off, but the turntable stimulus continues (i.e. the VOR adaptation catch trials of the phase-reversal task), the phase values of the GluA3-KO mice show significantly impaired motor learning compared to those of GluA1-KO and WT mice. (C) Polar plot showing the trajectory of VOR gain and phase change during adaptation for WTs (black line), GluA3-KOs (blue), and GluA1-KOs (red). Gain (i.e. amplitude of the eye movement divided by that of the stimulus) is represented as distance from the center and phase as the angle relative to perfect compensation at 0 degrees. The data reveal a common learning trajectory and comparable initial gain, yet a difference in learning extent between the groups. Inset: the final VOR reached after 5 days of training is amplified to visualize the magnitude of the gain difference (red arrow) between the groups tested. (D) GluA3-KOs (blue line) were unable to reverse their VOR phase compared with WT (black) and GluA1-KOs (red). Four representative eye velocity traces per group compare the initial VOR before (left) and after (right) the mismatch training (left). (E) Both learning extent and consolidation during the phase-reversal task are significantly smaller in GluA3-KO mice compared to WT and GluA1-KO mice (T2-test $p < 0.05$). (F) Gain-increase learning also reveals deficits in GluA3-KO, but not in GluA1-KO, as compared to WTs.

Error bars indicate SEM, * indicates $p<0.05$.

(Figure S2), was significantly smaller for GluA3-KO mice compared to wild-type and GluA1-KO mice (p=0.001 and p=0.0002, respectively) (Figures 1D and 1E). Moreover, the consolidation rate of learning, which equals the ratio between the total learning extent and the ideal learning extent with no overnight memory loss between training days (Figure S2A), was also significantly lower in GluA3-KO compared to both GluA1-KO and wild-type littermates (p=0.0008 and p=0.001, respectively) (Figure 1E). Importantly, all groups of mice performed equally well during the visually-driven vestibular training trials over the 5 days of training (all p values >0.05; Figure 1A), indicating that the learning deficits in GluA3-KO as measured in the dark during the catch trials did not directly result from a poor response to the visuo-vestibular training signal, but rather an impaired ability to maintain this learned vestibular response in the absence of the visual cue (Figure 1B).

In addition to phase modulation, we also investigated gain modulation of vestibulo-ocular movements after either in-phase (gain-down) or out-of-phase (gain-up) visuovestibular training paradigms that aim to reduce or increase the amplitude of the eye movement response to a constant vestibular input, respectively. GluA3-KO showed severe learning deficits in both the gain-down (p=0.001 for final catch trials) and gain-up paradigms (p=0.009 for final catch trials), whereas GluA1-KO and wild-types performed again equally well in both training paradigms (p=0.11 and p=0.2 for gain-down and gain-up final catch trials, respectively) (Figure 1F and S1D). These experiments indicate that GluA3-containing AMPARs contribute to cerebellum-dependent motor learning.

GluA3 is required to induce LTP, but not LTD, at PF-PC synapses

Purkinje cells (PCs) form the sole output of the cerebellar cortex. It has previously been shown that synaptic plasticity at their parallel fiber afferents crucially contributes to motor learning (Schonewille et al., 2010). To investigate the contribution of GluA1- and GluA3-containing AMPARs to basal synaptic transmission, we recorded spontaneous miniature excitatory synaptic currents (mEPSCs) of PCs in cerebellar slices from 4-6 week old mice (Figure 2A), an age at which GluA3-KO mice showed similar motor learning deficits as during adulthood (Figure S2D). The average amplitude and frequency of mEPSCs in GluA1-deficient PCs were not significantly different (p=0.4 and p=0.2, respectively) from those in wild-type PCs (Figure 2B). In PCs of GluA3-KO mice the average amplitude (p=0.0003) and frequency (p=0.02) of mEPSCs were significantly lower than those in wild-type PCs. The low basal transmission in the GluA3-KO mice was neither reflected in structural changes at the level of spine densities of proximal

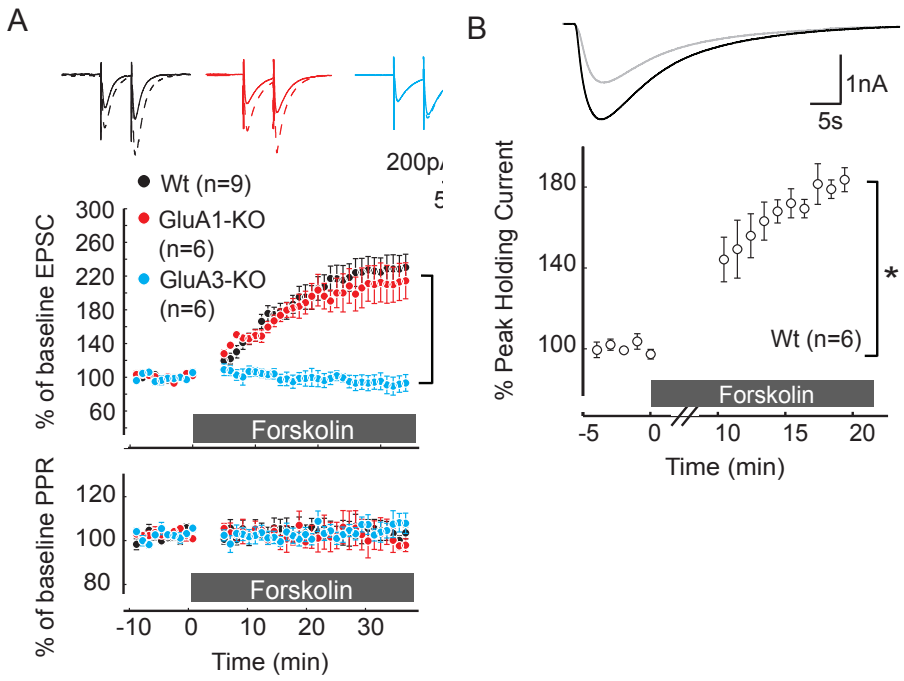

Figure 2. GluA3 is required for PF to PC LTP, but not LTD.
(A) Scheme of cerebellar cortical circuitry (Left) and representative picture of the in-vitro preparation (right) showing positions of recording electrode (yellow) at PC soma and stimulus electrode (green) at parallel fiber beam. ML, PCL and GrCL indicate molecular layer, Purkinje cell layer, and granule cell layer, respectively. (B) mEPSC amplitude (left panel) and frequency (middle panel) of both single GluA3-KO PCs (blue bar) and double GluA1/3-KO PCs (purple bar) were significantly reduced compared to those in WT PCs (black bar) (for amplitude and frequency WT vs. GluA3-KO p=0.0003 and p=0.023, respectively; for WT vs. GluA1&3-dKO p<0.0001 and p<0.0001, respectively) and single GluA1-KO PCs (red bar) (for amplitude and frequency GluA1-KO vs. GluA3-KO, p<0.0001 and p=0.0032, respectively). In contrast, GluA1-KO and WT PCs presented comparable basal transmission (for amplitude and frequency WT vs. GluA1-KO p=0.37 and p=0.16, respectively). Right panel shows corresponding raw traces of mEPSCs. (C) Both GluA1-KOs (red) and GluA3-KOs (blue) show similar cerebellar synaptic weakening after LTD induction compared to WT littermates (black) (top left panel) with unchanged PPR over time (bottom left panel). EPSC magnitude was held in a comparable range for all cases to prevent potential bias due to differential basal synaptic strength (middle panels). Representative traces of paired EPSCs before (solid lines) and after LTD induction (dashed lines) (right panels, matched genotype color code). Cj Stim indicates conjunctive stimulation (so as to induce LTD).(D) GluA3-KO PCs show severe deficits in PF to PC LTP compared with WTs and GluA1-KOs with no changes in PPR or baseline EPSC magnitude. Representative traces of paired EPSCs before (solid lines) and after LTP induction (dashed lines) (same configuration as in B). pf Stim indicates parallel fiber-only stimulation (so as to induce LTP).

Error bars indicate SEM, * indicates p<0.05.

or distal PC dendrites (p=0.7 and p=0.2 for proximal and distal, respectively) (Figure S3) nor was it compensated for by increased synaptic currents from kainate receptors (for details see Figure S4 and corresponding legends). In PCs of mice that lack both GluA1 and GluA3, mEPSC events were virtually absent (Figure 2B), suggesting that the far majority of synaptic currents in PCs are derived from either GluA1- or GluA3-containing AMPARs.

A reduced basal transmission in GluA3-deficient PC synapses can either be a cause or a consequence of impaired synaptic plasticity. We therefore investigated both LTD and LTP at the PF to PC synapse, using whole-cell recordings. LTD was induced either by pairing PF stimulation with a depolarizing voltage-clamp step, mimicking climbing fiber (CF) input (Linden, 2001; Figure 2C), or by pairing PF stimulation with CF stimulation (Schonewille et al., 2011; Figure S3C-E). The magnitudes of LTD in PCs of GluA1-KO and GluA3-KO were indistinguishable from that in the PCs of wild-type littermates with either induction protocol (with somatic depolarization, for GluA1-KO vs. wild-type p=0.4 and for GluA3-KO vs. wild-type p=0.2; with direct CF stimulation, for GluA1-KO vs. wild-type p=0.9 and for GluA3-KO vs. wild-type p=0.8). These data are in line with other studies showing that GluA2 is the key subunit for AMPAR internalization and therefore for LTD induction (Steinberg et al., 2006; Schonewille et al., 2011). Next, we induced LTP in PCs by 1 Hz tetanic stimulation of PF input alone (Lev-Ram et al., 2002) (Figure 2D). This stimulus protocol reliably produced significant LTP in both wild-type PCs (p=0.0005) and GluA1-KO PCs (p=0.0003) with a similar magnitude (p=0.5), and without significant changes in paired-pulse facilitation (PPF) of the evoked EPSCs after LTP induction (p=0.11 and p=0.6 in GluA1-KO and wild-type PCs, respectively). In contrast, with the same stimulation protocol LTP could not be induced in GluA3-KO PCs (p=0.7) (Figure 2D). These experiments demonstrate that PF to PC LTP requires GluA3-containing AMPARs.

GluA3-dependent synaptic potentiation involves a cAMP-driven change in channel conductance

What is the molecular mechanism underlying GluA3-dependent LTP of PF-PC synapses? To test whether GluA3-dependent synaptic plasticity in PCs depends on cAMP-signaling we administrated the adenylyl cyclase activator forskolin (FSK) to PCs of GluA3-KO brain slices and compared the effects to those in wild-type slices and GluA1-KO slices (Figure 3A). Whereas FSK produced on average a two-fold potentiation in PF-evoked EPSCs in both wild-type and GluA1-KO PCs (230±25% and 215±35%, respectively), it failed to induce synaptic potentiation in PCs that lack GluA3 (95±10%; p=0.005 GluA3-KO vs. wild-type). Importantly,

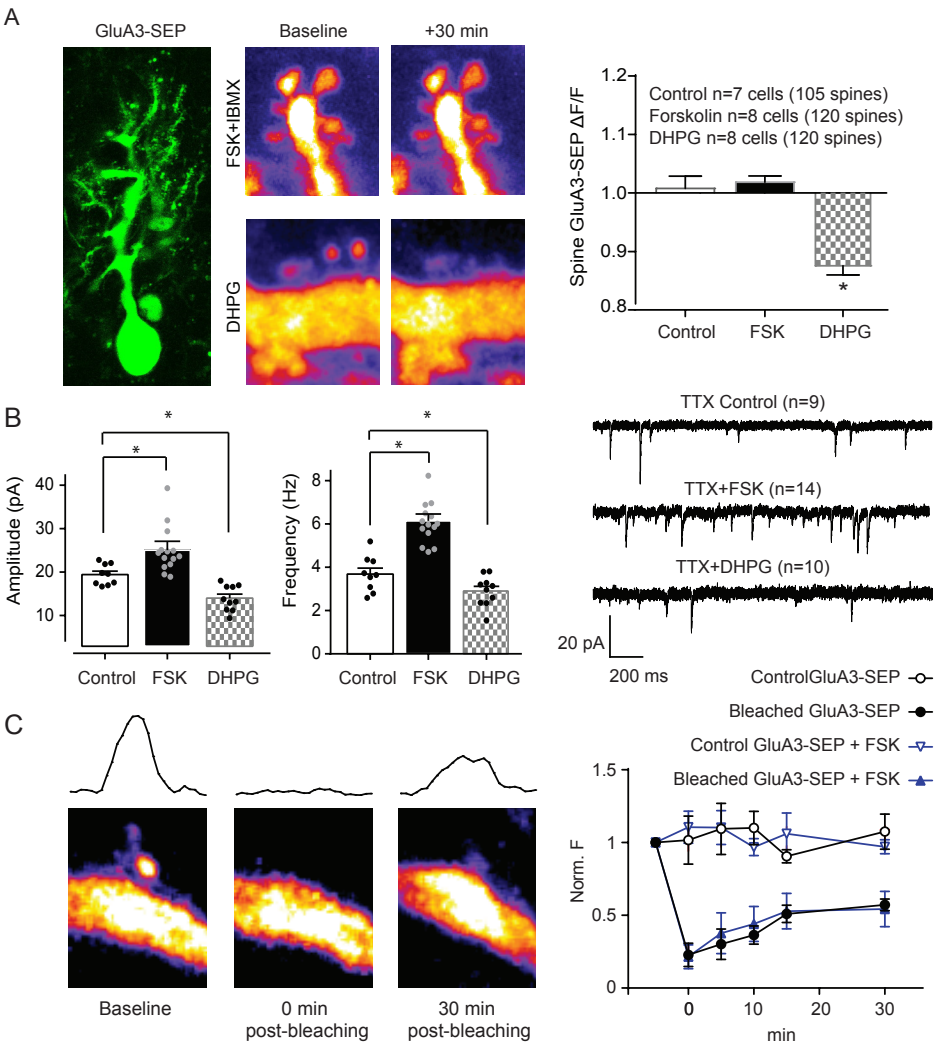

Figure 3. Rising cAMP levels produces GluA3-dependent post-synaptic potentiation.
(A) Wash-in of 50 μM FSK causes synaptic potentiation at wild-type PCs (black) and GluA1-KO PCs (red), but not at GluA3-KO PCs (blue). Top, middle and bottom panel show example traces, normalized EPSC amplitude and paired pulsed ratio (PPR), respectively.
(B) Enhancement of currents evoked by local puffs of 1 μM AMPA at the molecular layer following FSK application can also occur in the presence of TTX blocking PF input.

Error bars indicate SEM, * indicates p<0.05.

AMPAR potentiation also occurred in wild-type PCs when local stimulation with 1 μM AMPA was used, while blocking PFs with TTX (189±17%, p=0.001; Figure 3B), highlighting its postsynaptic nature (Chen and Regehr, 1997). These data indicate that a GluA3-dependent synaptic potentiation at PF-PC synapses can occur upon a rise in the cellular level of cAMP.

We next examined whether cAMP-driven synaptic potentiation is a result of synaptic trafficking of GluA3-containing AMPARs. To assess whether FSK increases GluA3 levels on the cell surface of spines, we performed time-lapse 2-photon imaging of PCs in cultured organotypic cerebellar slices infected with Sindbis virus to acutely express GluA3 subunits fused to Super Ecliptic pHluorin (SEP). SEP is a pH-sensitive variant of GFP that shows a reduction in fluorescence upon rapid application of acidic (pH 5) ACSF (Figure S4F) (Makino and Malinow, 2009). To test whether GluA3 trafficking can be detected with this method, we first triggered LTD chemically by adding the metabotropic mGluR1 receptor agonist DHPG to induce internalization of AMPARs (Linden, 2001). Indeed, application of DHPG to wild-type PCs expressing SEP-GluA3 produced a significant decrease in SEP fluorescence at spines ($p<0.0001$; Figures 4A) and in synaptic strength ($p=0.004$ for amplitude and $p=0.04$ for frequency; Figure 4B), which is in line with the endocytosis of AMPARs that occurs during the expression of LTD at the PF-PC synapse (Wang and Linden, 2000). In contrast, washing in FSK failed to induce any change in SEP-GluA3 fluorescence at PC spines (0.03±0.015% change, $p=0.4$) (Figures 4A), even though FSK significantly increased synaptic currents in the SEP-GluA3 expressing PCs ($p=0.04$ for amplitude and $p<0.0001$ for frequency) (Figure 4B). These data suggest that the cAMP-driven synaptic potentiation does not require an insertion of GluA3-containing AMPARs at the surface of spines. To assess whether FSK promotes lateral mobility of GluA3 receptors instead of an increase in receptor externalization, we performed fluorescence recovery after photobleaching (FRAP) experiments of single spines of PCs expressing SEP-GluA3 (Figure 4C). After ~80% photobleaching, the SEP signals recovered to ~50%, suggesting that a proportion of SEP-GluA3 is immobilized at synapses (Makino and Malinow 2009). The SEP fluorescence intensity recovered at a similar pace in the presence or absence of FSK ($p=0.9$), indicating that the lateral mobility of GluA3-containing AMPARs is not influenced by a rise in cAMP.

To assess whether GluA3-plasticity involves a change in channel properties, we resolved single-channel AMPA mediated currents by clamping a single AMPAR in cell-attached mode at the cell body of either GluA1-KO or GluA3-KO PCs with the recording pipette containing near-saturating concentrations of AMPA (Armstrong

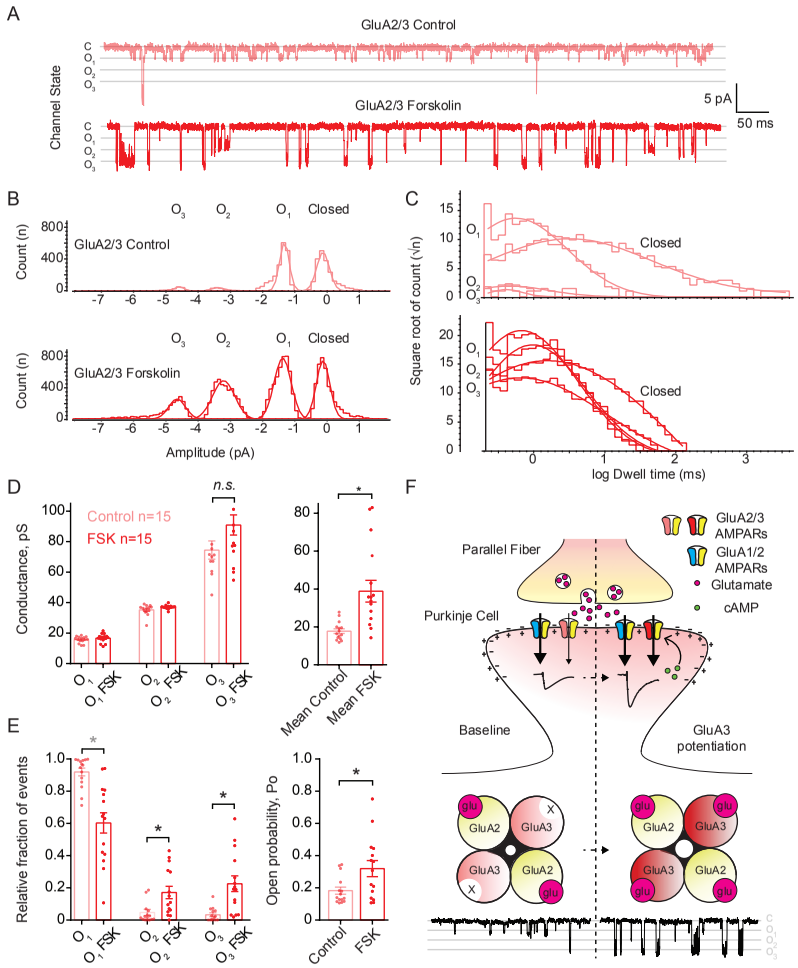

Figure 4. Rising cAMP levels produces GluA3-dependent synaptic potentiation without AMPARs trafficking.

(A) Left column: Z-max projection of a stack of pictures showing a representative GluA3-SEP transfected PC. Top row: Example pictures of a PC dendrite expressing GluA3-SEP before (middle) and after (right) FSK application were color coded according to the fluorescence intensity to improve the visualization of, in this case, the absence of changes of surface GluA3-SEP over time. Bottom row: Example pictures of a PC dendrite expressing GluA3-SEP before (middle) and after (right) DHPG application reveal a significant reduction in synaptic GluA3-SEP over time.Right column: Spine fluorescence intensity after FSK application normalized by the fluorescence before application (FSK - middle bar) showed no significant increase of GuA3-SEP compared to the spines in which the drug was not applied (Control – left bar). However, DHPG application significantly reduced GluA3-SEP in PC spines in accordance to the observed synaptic depression. (E) Lowering the extracellular pH produced a drastic reduction of GluA3-SEP fluorescence intensity corroborating its pH sensitivity. (B) Despite the lack of a detectable increase in surface GluA3-SEP, FSK produced a significant increase in mEPSCs amplitude and frequency in GluA3-SEP transfected PCs in organotypic slices. DHPG induced a significant decrease in mEPSC amplitude and frequency in these neurons. (C) Left: Example baseline max projection Z-stack (3 µm, 6 optical planes) of a dendrite transfected with GluA3-SEP obtained with two-photon microscopy before, immediately after and 30 minutes after photobleaching of the spine. The black traces above the pictures represent quantifications of SEP fluorescence across the spine and parallel to the dendrite.Right: Overall quantification of spine FRAP dynamics over time for PCs transfected with GluA3-SEP, either with (n=5) or without (n=4) 50 µM forskolin added after the moment of bleaching (0 min). SEP fluorescence intensity is normalized to baseline intensity (-5 min). No changes in SEP intensity were observed over time in spines neighboring the bleached spines.

et al., 2002). GluA1-containing AMPARs at the surface of GluA3-KO PC cell bodies stochastically reached open states 1, 2 and 3 (indicating binding of 2, 3 and 4 glutamates per receptor complex, respectively) and displayed similar conductance levels and open-channel probability in the presence or absence of FSK application (Figure S5). In contrast, GluA3-containing AMPARs on cell bodies of GluA1-KO PCs produced the vast majority of their openings in the first and lower conductance state (O1) under basal conditions (Figure 5A,B), indicating that only two out of the four ligand binding domains (LBDs) present in the AMPAR tetramer are activated by AMPA. After application of FSK the behavior of GluA3-containing AMPARs changed strikingly and produced a significantly higher amount of openings in state O2 and O3 similar to GluA1-containing AMPARs (compare Figures 5A, B and E with Figure S5B). The average duration of the openings was unchanged ($p=0.4$, $p=0.13$ and $p=0.09$ for O1, O2 and O3, respectively) (Figure 5C), but an increase of the absolute frequency of the openings caused shortening of the closed state dwell-time and thus a significant net increase in open probability ($p<0.0001$; Figure 5E). Although FSK did not significantly change the conductance level of any of the open states ($p=0.7$, $p=0.14$ and $p=0.15$ for O1, O2 and O3, respectively; Figure 5D), the higher relative fraction of events in the highly conductive open states O2 and O3 caused a significant increase ($p<0.0001$) in the overall conductance of cAMP-stimulated GluA3 channels (Figures 5B and 5D). These experiments suggest that a rise in intracellular cAMP produces synaptic potentiation by increasing the open-channel probability of the GluA3 subunit, indicating a novel mechanistic model for GluA3-dependent synaptic plasticity.

GluA3-mediated plasticity is induced via cAMP-mediated Epac activation

To further elucidate the molecular mechanism underlying GluA3-dependent plasticity, we aimed to identify the intermediary factor that translates a rise in cAMP into synaptic potentiation of GluA3-containing AMPARs. Protein kinase A (PKA) is activated by a rise in cAMP and exerts cAMP-dependent synaptic effects (Lev-Ram et al., 2002; Sokolova et al., 2006). However, incubating wild-type PCs with PKA antagonists KT5720 or H89 did not have any significant effect on synaptic potentiation induced by FSK (215±20% with KT5720 and 235±19% with H89; $p=0.7$ and $p=0.9$, respectively) (Figure 6A) indicating that PKA is not involved in mediating GluA3-plasticity. We next assessed the involvement of Epac (exchange proteins directly activated by cAMP, a.k.a. Rap guanine-nucleotide-exchange factor) as an alternative cAMP-dependent pathway that can trigger synaptic changes (Gekel and Neher, 2008; Woolfrey et al., 2009). The blockade of Epac with its selective antagonist ESI-05 (Tsalkova et al., 2012) did not reduce

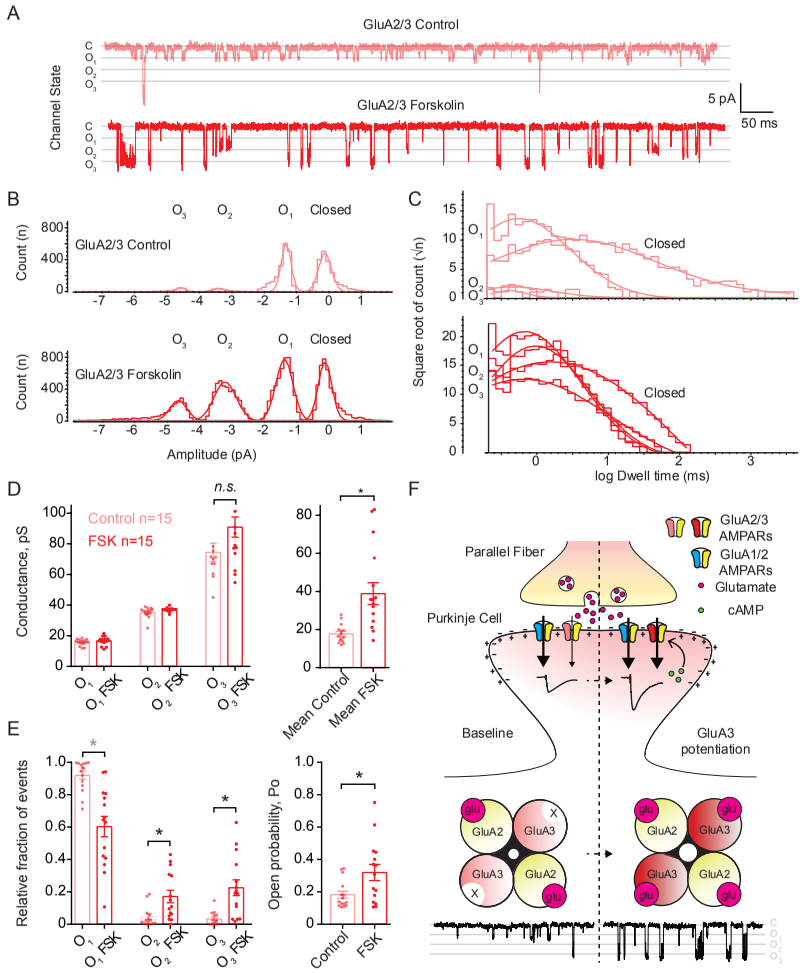

Figure 5. GluA3-plasticity occurs through cAMP-dependent changes of single channel conductance and open probability.
(A) Example traces of cell attached single channel recordings of GluA2/3 AMPARs in PCs of GluA1-KO mice. Under basal conditions (light red) the vast majority of the openings of GluA2/3 AMPARs occur at the low conductance level (O1), but in the presence of FSK the amount of openings in the higher conductance levels (O2-3) increase (red). (B) Count versus amplitude histograms of the events detected in the representative recordings shown in A illustrate the uneven distribution of events across the different conductance levels in the absence (light red) or presence (red) of FSK.(C) The opening durations (dwell time) of the same events shown in A and B were unchanged after FSK application. However, the duration of the closed state times were reduced suggesting a net increase in the total number of openings produced by GluA2/3 channels in the presence of FSK.(D) Overall quantification of GluA2/3 single channel recordings show that the conductance significantly increased in the presence of FSK, yet the conductance per open state remained unchanged. (E) FSK significantly changed the distribution of GluA2/3 AMPARs events as revealed by a significant decrease of events in O1 state and a significant increase in events at O2 and O3 states. The reduction of the closed state time shown in C was translated into a significant increase of the open channel probability.(F) The classical model of GluA1-subunit dependent LTP in pyramidal cells (see introduction) does not hold valid at PF to PC synapses. Note that the absolute numbers of subsets of both GluA1/2 and GluA2/3 AMPARs are unchanged upon LTP induction, whereas the GluA2/3 AMPARs are activated by cAMP signaling, enhancing their channel conductance and thereby increasing the current generated in potentiated synapses. This model describes for the first time a form of GluA3-dependent LTP.

Error bars indicate SEM, * indicates p<0.05.

basal transmission at PF-PC synapses (Figure 7H), but it effectively prevented the FSK-induced synaptic potentiation in wild-type PCs ($p=0.9$ vs. baseline and $p<0.0001$ vs. without ESI-05) (Figure 6A). To assess whether Epac activation is not only necessary, but also sufficient to cause GluA3-dependent synaptic potentiation, we investigated the impact of the selective Epac activator 8-CPT-2Me-cAMP (8CPT). Adding 20 µM 8CPT to the intracellular recording solution produced synaptic potentiation by 185±17% compared to baseline in wild-type PCs ($p=0.0004$; Figure 6B), but not in GluA3-deficient PCs (100±5%; $p=0.8$; Figure 6B). In addition, the postsynaptic application of 8CPT increased the amplitude and frequency of PC mEPSCs ($p=0.0005$ and $p=0.001$, respectively; Figures 6C and 6D) and did not change the PPF ratio (104±5%, Figure 5B). These experiments indicate that a rise in cAMP triggers synaptic potentiation through Epac-mediated activation of postsynaptic GluA3-containing AMPARs. This Epac-driven activation of GluA3-containing AMPARs was not limited to those located at synapses. Outside-out patches excised from wild-type PC somata produced a peak current of approximately 10 pA in response to puffs of 100 µM AMPA (Figure S4E). When the Epac activator 8CPT was added to the internal solution of the patch pipette, the peak current obtained under the same conditions was increased 2.5-fold in the absence of a presynaptic component (25±3 pA, $p<0.0001$ vs. control). This difference in peak current was largely maintained in the presence of AMPAR desensitization blockers PEPA and cyclothiazide (45±8 pA without vs. 97±10 pA with 8CPT, $p<0.0001$; Figure 6E), indicating that cAMP-driven GluA3-plasticity does not depend on a change in desensitization properties of AMPAR channels. As expected from our single channel results, non-stationary noise analysis of these non-desensitizing AMPAR responses showed a significant increase in conductance and open probability (Figures 6F-G). This analysis revealed how in a mixed pool of GluA1- and GluA3-containing AMPARs Epac-dependent GluA3 potentiation was translated into an increase in current amplitude without altering the dynamics of the response (Figure 6E), highlighting the consistent results with miniature and evoked EPSC recordings.

Epac activation is required for LTP and motor learning

We next tested whether PF-PC LTP depends on Epac activation. Incubation of slices with Epac-inhibitor ESI-05 significantly inhibited synaptic potentiation induced by tetanic PF stimulation (102±13% versus 140±8% in control conditions, $p<0.0001$ after 15 min; Figure 7A). In addition, LTP was fully occluded when brain slices were pre-incubated with the membrane-permeable analog of the Epac activator (8pCPT) (GluA3-KO vs. WT, $p=0.008$; Figure 7B). Together, these data

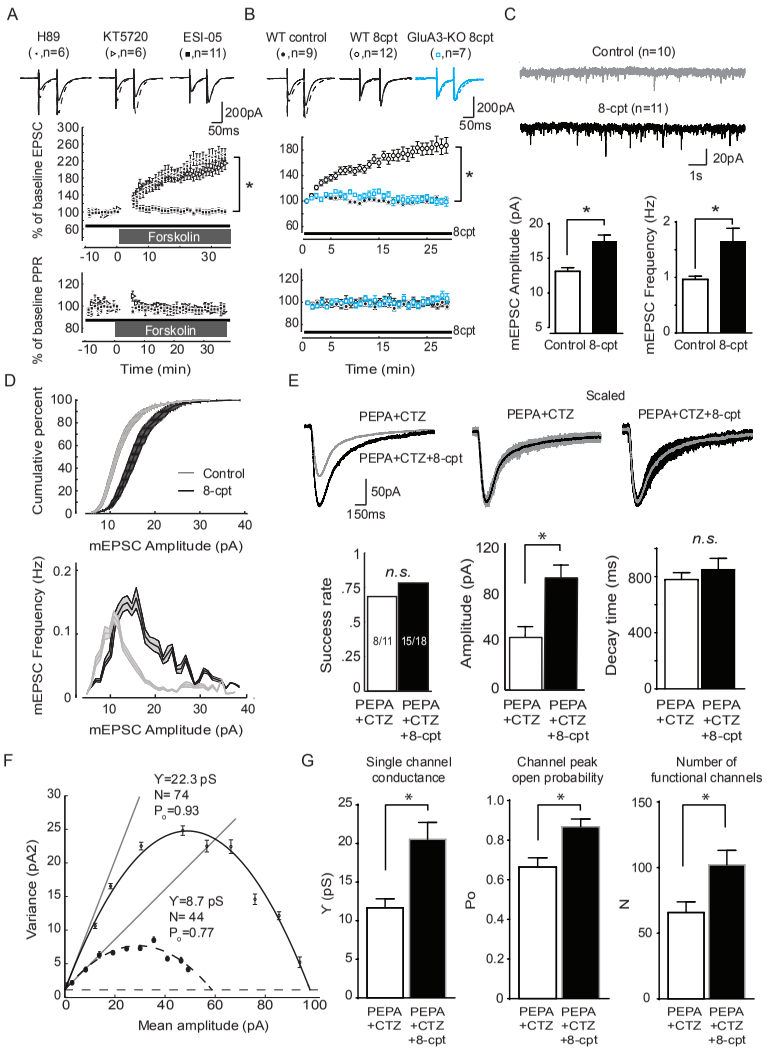

Figure 6. GluA3-plasticity requires cAMP-dependent postsynaptic activation of Epac.

(A) Epac2 antagonist ESI-05 blocks FSK-driven synaptic potentiation, whereas PKA antagonists H89 and KT5720 do not. (B) Intracellular application of membrane-impermeable Epac agonist 8CPT caused significant synaptic potentiation in WT PCs (open circles) compared with GluA3-KO PCs (blue boxes) or the no-drug condition in WT PCs (closed circles). (C) Intracellular application of 8CPT caused an increase in both mEPSC amplitude (left) and frequency (right). (D) A shift towards higher mEPSC amplitudes was visualized both in the cumulative distribution and in the mEPSC frequency versus amplitude distribution plots, once again suggesting postsynaptic effects of EPAC activation.(E) Outside-out patches excised from PC somata recorded in the presence of AMPARs desensitization blockers (PEPA and CTZ) had a similar success rate of containing AMPA events (left panel), but generated significantly larger currents (middle panel) with similar decay time kinetics (right panel) when 8CPT was present in the internal solution.(F) Example parabolic distribution of the variance versus amplitude relationship obtained from bins of the current decay profile. Non-stationary noise analysis (NSNA) was done by fitting a parabolic equation to this distribution in order to estimate conductance, open probability and number of active receptors.(G) NSNA performed on the PC recordings in E revealed a significantly increased single channel conductance (left panel) and peak open channel probability upon 8CPT application (middle panel), which in turn led to an increased number of functional channels responding to the local AMPA application (right panel).

Error bars indicate SEM, * indicates p<0.05.

indicate that Epac2 activation is responsible for postsynaptic LTP at the PF to PC synapse through activation of GluA3-containing AMPARs.

To investigate the involvement of Epac activation in cerebellar synaptic plasticity in-vivo, we performed phase-reversal adaptation in wild-type mice that received daily IP injections with either Epac antagonist ESI-05 (0.2-0.3 ml at 10 mg/kg) or with vehicle alone 30 minutes prior to the training protocol. Mice administrated with ESI-05 were not affected in basal eye reflex behavior, but performed significantly worse in the phase-reversal task compared to vehicle injected animals (Figure 7D). Although both groups eventually reached a reversal of the VOR phase (Veh: 157±2%, ESI-05: 148±15°; Figure 7D), its magnitude was significantly lower in the ESI-05 injected mice compared to vehicle controls ($p=0.01$; Figure 7E-F). This difference reached after training could not be explained by a poor basic response to the training stimuli (Figure 7C), but only by a significantly reduced learning extent ($p=0.01$) and consolidation rate ($p=0.03$). Importantly, systemic ESI-05 injections produced learning deficits without a change in basal synaptic transmission compared to vehicle-injected mice ($p=0.5$ and $p=0.9$ for mEPSCs amplitude and frequency, respectively) (Figure 7H), suggesting that absence of Epac-dependent synaptic potentiation without any change in basal transmission is sufficient to impair learning capabilities.

GluA3 expression in Purkinje cells is required for VOR learning

We showed that VOR learning depends on global expression of GluA3 and that LTP at PF-PC synapses requires GluA3-plasticity, but does VOR learning depend on GluA3 specifically in PCs? To address this question, we generated and tested a PC-specific GluA3-KO mouse (referred to as L7/GluA3-KO; Figure S6) by crossbreeding mice expressing Cre-recombinase under the PC-specific promotor L7-pcp2 with mice in which the GluA3 gene is flanked by loxP sites (Barski et al., 2000; Sanchis-Segura et al., 2006). After establishing the single-unit identity of floccular vertical-axis Purkinje cells in adult L7/GluA3-KO mice by demonstrating a climbing fiber pause in their simple spike activity as well as a preferred modulation tuning-curve during extracellular recordings in-vivo (Figure 8A) (Hoebeek et al., 2005), we investigated the action potential generation of their simple spike activity in the awake state. In the absence of visual stimulation, both the firing frequency and regularity (i.e. coefficient of variation of adjacent interspike intervals or CV2) of the simple spike activity of the L7/GluA3-KO mice did not differ significantly from those of wild-types (Figure S7A), which is consistent with the similar I-V relationships recorded in-vitro for wild-type and GluA3-lacking PCs (Figure S7B). Next, we provided visual stimulation at the frequency that was used for the training

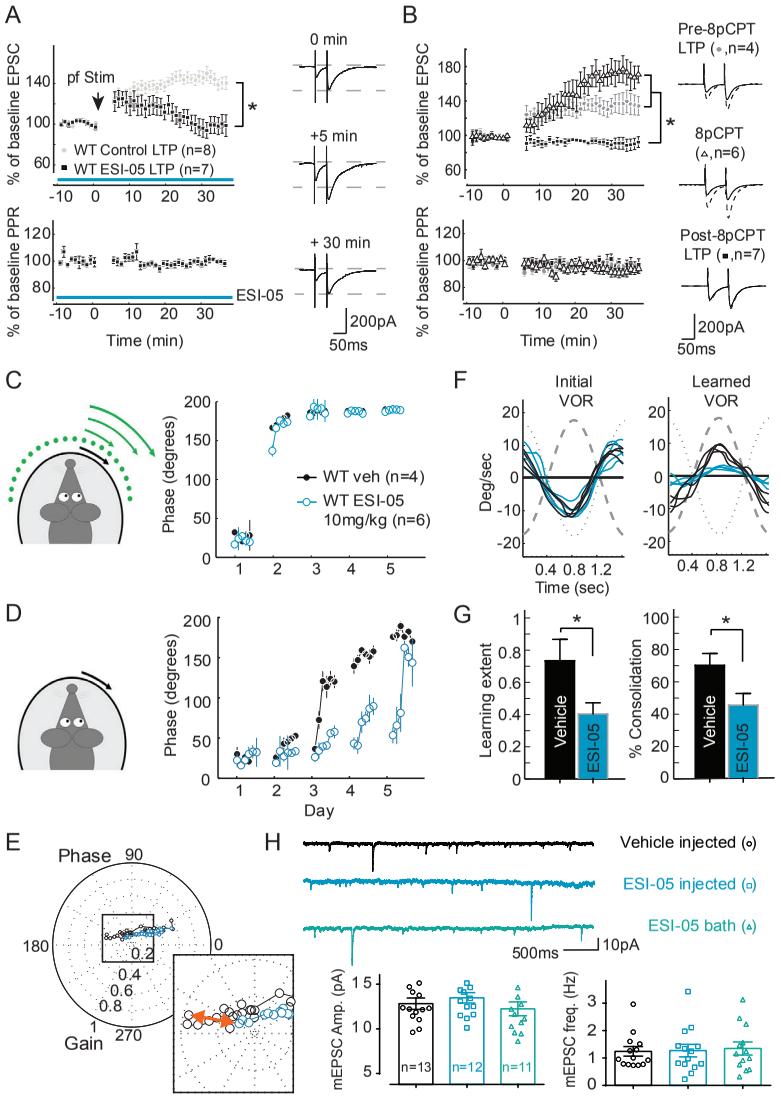

Figure 7. Pharmacological manipulation of Epac activity impairs LTP in-vitro and motor learning in-vivo without affecting synaptic transmission.

(A) Epac antagonist ESI-05 prevents PF to PC LTP induced by tetanic PF stimuli.(B) Epac activation through incubation with 8pCPT potentiates AMPAR currents (open triangles). As a consequence, a minimal 30 minute incubation with 8cCPT fully occludes LTP induction (black squares) compared with LTP induction in the absence of 8cCPT (gray circles).

(C) Eye movement phase values in wild-type mice that are injected with ESI-05 10 mg/kg (open blue circles) or injected with vehicle only (black circles) are virtually identical during the visuo-vestibular mismatch training when the light is on.(D) During the catch trials in the dark, the phase shift of VOR adaptation in the mice injected with ESI-05 10 mg/kg is significantly delayed compared with those in their littermates injected with vehicle only.(E) Polar plot of the combined gain and phase data shows a common learning trajectory and comparable initial gain, yet different final outcome, for both groups. Inset: the final VOR reached after 5 days of training is amplified to visualize the magnitude of the gain difference (red arrow) between ESI-05 and vehicle-injected mice. (F) Four representative eye velocity traces of the VOR before (left) and after (right) phase-reversal training show that, whereas both ESI-05 and vehicle-injected mice show equal baseline performance and that both are able to flip the phase of the VOR, the magnitude of the VOR reached after the training is substantially different.(G) Both learning extent and consolidation during the phase-reversal task are significantly smaller in the mice injected with ESI-05 compared to those injected with vehicle only (T2-test $p < 0.05$).(H) Impaired motor learning after ESI-05 injections does not correlate with a decreased transmission at PF to PC synapse. The PC mEPSC amplitude and frequency of WT mice injected with ESI-05 are similar compared with those in vehicle-injected mice.

Error bars indicate SEM, * indicates $p<0.05$.

paradigm (0.6 Hz). Again the firing frequency and regularity (i.e. CV2) of the simple spike activity of the L7/GluA3-KO mice did not differ from those of wild-types (p=0.7 and p=0.8 respectively) (Figure 8A). Moreover and most importantly, the amplitude of the simple spike modulation during visual stimulation did not differ (p=0.8; Figure 8A), suggesting that the PF output is in effect sufficient to mediate the visual training signals in the L7/GluA3-KO mice despite the reduced PF to PC synaptic transmission (Figure S7C). Finally, the firing frequency and modulation amplitude of the complex spikes did not show any significant difference either (p=0.7 and p=0.9, respectively; Figure 8A). Together, these data indicate that the in-vivo excitability and spike generation of PCs are intact in L7/GluA3-KO mice.

We then tested 3 to 5 month-old L7/GluA3-KO and control littermates for their ability to adapt eye reflexes. The baseline OKR and VOR performances of these L7/GluA3-KO mice were indistinguishable from those in controls (Figure S1). Similarly to global GluA3-KOs, VOR motor learning was prominently affected in L7-GluA3-KO mice (Figure 8C-G). The absence of GluA3 in PCs showed significant deficits throughout the phase-reversal paradigm (all p values < 0.01 after day 2), including a significantly different learning extent at the end of it (p=0.0005; Figure 8B-F). Moreover, consolidation during the phase-reversal paradigm was significantly lower (p=0.0006, Figure 7F). Gain modulation was also impaired as shown by a significant difference between the final eye movement gain of L7/GluA3-KO mice compared to control littermates after either gain-down or gain-up training sessions (p=0.04 and p=0.006 for gain-down and gain-up, respectively) (Figure 8G).

In contrast to the single L7/GluA3-KO as well as single global GluA1-KO and GluA3-KO mice, mice that lack both GluA1 and GluA3 receptor subunits specifically in Purkinje cells (L7-GluA1/3-KO) showed significant aberrations in baseline eye movement performance (p=0.0001 for OKR and p=0.03 for VORD) (Figures S1A and S1B). Together with the findings presented above (see also Figure 1), these data suggest that the presence of GluA3 in the GluA1-KO can compensate for their lack of GluA1 during both baseline and learning behavior, but that the presence of GluA1 in the global GluA3-KO and single L7-GluA3-KO is not sufficient to fully compensate for the lack of GluA3 during adaptation of compensatory eye movements, highlighting the putative impact of GluA3-dependent synaptic plasticity in PCs.

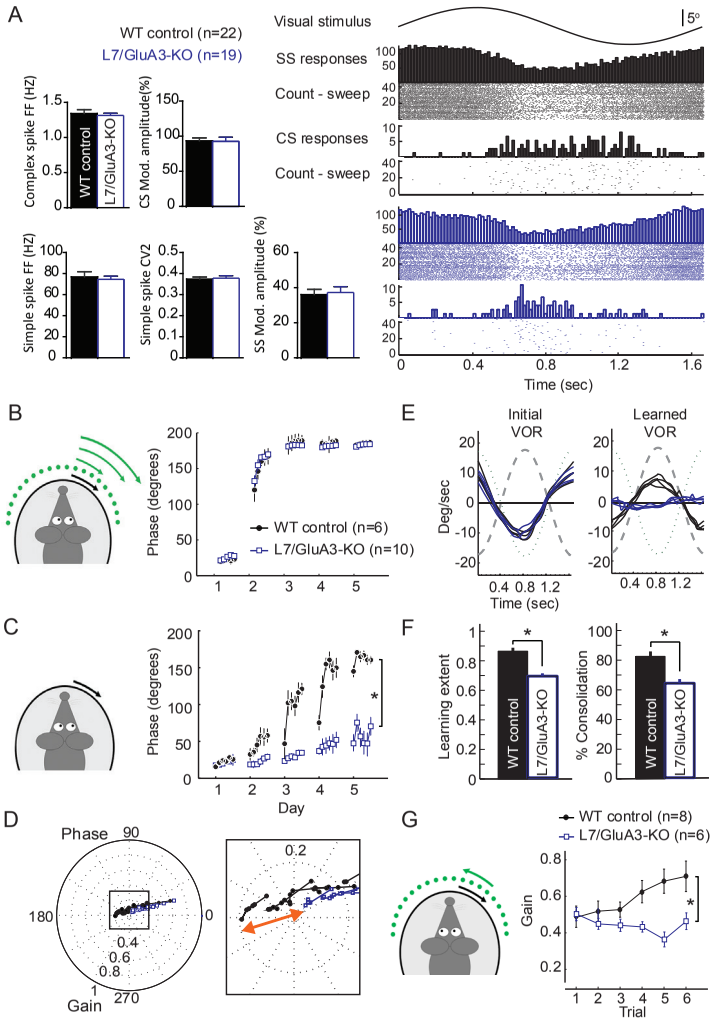

Figure 8. Lack of GluA3 in PCs causes motor learning deficits.
(A) Representative activity of vertical-axis Purkinje cells recorded in the flocculus of wild-type and L7/GluA3-KO mice during visual stimulation (5°, 0.6 Hz). Bar graphs show that averages of firing frequency (FF), the coefficient of variation in adjacent intervals (CV2) and modulation amplitude of simple spikes, as well as frequency and modulation amplitude of complex spike during OKR stimulation were similar in control (n = 22) and L7/GluA3-KO mice (n = 19). The visual stimulus is shown together with histograms of simple spike and complex spike frequencies and corresponding raster plots in the right panels. (B) Eye movement phase values in L7/GluA3-KO mice (open square) and WT mice (closed circle) during visuo-vestibular mismatch training are comparable, highlighting that the strength of the visual signals was in principle sufficient to induce learning. (C) Phase values of VOR adaptation catch trials in L7/GluA3-KOs show a significantly impaired shift over 5 days compared with those in their WT littermates, illustrating that motor learning is affected despite normal visual signaling as demonstrated in A and B. (D) Polar plot of the gain and phase data shows a common learning trajectory and comparable initial gain for both groups. Inset: the final VOR reached after 5 days of training is amplified to visualize the magnitude (red arrow) of the gain difference between L7/GluA3 KO and WT mice. (E) L7/GluA3-KOs (blue line) show equal baseline performance compared with WTs (black line), but are unable to reverse the phase of their VOR. Data show four representative eye velocity traces of the VOR before (left) and after (right) phase-reversal training. (F) Both learning extent and consolidation during the phase-reversal task are significantly smaller in L7-GluA3 KO mice compared to those in WT littermates (T2-test $p < 0.05$). (G) Gain-increase learning reveals deficits for L7/GluA3-KO mice compared to WT mice.

Error bars indicate SEM, * indicates $p<0.05$.

DISCUSSION

It is widely believed that LTP- and LTD-type synaptic plasticity mechanisms act in concert to mediate several types of learning in brain regions such as the hippocampus, amygdala and cerebral cortex (Malinow and Malenka, 2002; Makino and Malinow, 2011; Nabavi et al., 2014; Nedelescu et al., 2010; Rumpel et al., 2005; Takahashi et al., 2003). For cerebellar learning, LTD at the PF to PC synapse has historically been considered the dominant plasticity mechanism (Ito, 2002; Linden and Connor, 1995). Although the simple spike suppression observed at early stages of some forms of motor learning in-vivo may suggest LTD occurrence (ten Brinke et al., 2015; Yang and Lisberger, 2014), an increasing amount of studies suggest that LTD is not a strict requisite for motor learning (Hesslow et al., 2013; Schonewille et al., 2011). In the present study we show that LTP at PF to PC synapses is a required mechanism for cerebellar motor learning. We show that LTP, but not LTD, at the PF to PC synapse requires plasticity of GluA3-containing AMPARs and that both the selective removal of GluA3 in PCs and the pharmacological blockade of the pathway leading to GluA3 plasticity in-vivo severely impair the ability to adapt the vestibulo-ocular reflex. Combined, these findings provide the first correlative link between GluA3-dependent LTP and behavioral learning in general.

Previous studies proposed a role for cerebellar LTP in the context of bidirectional gain modulation (Boyden et al., 2006). This work suggested that gain-down modulation of the eye movements might require PF to PC LTP, and conversely, gain-up modulation would require LTD. According to this hypothesis one would expect that GluA3-KO mice show impaired gain-down modulation with intact gain-up adaptation. However, our data show that the specific absence of GluA3 in Purkinje cells most prominently impairs gain-up and phase modulation, supporting an opposite kind of role for GluA3-dependent LTP in oculomotor learning. Whereas the role of GluA3 in PC plasticity and cerebellar motor learning is becoming more clear now, that of GluA1 is still largely obscure. The presence of GluA1 in PCs was neither essential for the induction of LTD or LTP nor were there overt signs of deficits in motor performance or motor learning in the GluA1-KO. Its possible role became only indirectly apparent, when we observed that, in contrast to the single GluA1-KO, the double GluA1/GluA3-KO virtually completely lacked glutamatergic currents in PCs and that the double L7-GluA1/A3-KO showed significant signs of ataxia and deficits in motor learning. Given that the single GluA3-KO did not show any sign of motor performance deficit, these findings indicate that GluA1-

containing AMPARs in PCs do contribute to cerebellar motor performance, but that their absence can be compensated for by GluA3-containing AMPARs.

The possible role of LTP at the PF to PC synapse in cerebellar motor learning has been suggested before by various other cell-specific mouse mutant studies (Andreescu et al., 2007; Schonewille et al., 2010; Peter et al., 2016). However, these studies tackled more upstream PC processes, which involved the nuclear estrogen receptor, cytosolic protein phosphatase calcineurin and subsynaptic protein shank2, and as a consequence they suffered from various side-effects that prevented definitive conclusions (Gao et al., 2012). In the current study, in which we tackled PF to PC LTP more downstream by targeting GluA3-containing AMPARs at the level of the synapse itself, we did not find any evidence for structural changes or firing differences in PCs of awake behaving mice. We did find that the basal transmission was reduced in PCs lacking GluA3 (both in the global and the cell-specific KO mice), but this deficit was probably not the reason for the impairment of LTP or of motor learning, because acutely inhibiting GluA3-plasticity through blockade of Epac prevented both LTP and motor learning without affecting basal transmission. We therefore propose that the reduced basal transmission in GluA3-KO mice is the consequence of a prolonged deficit in LTP.

GluA1-dependent synaptic plasticity is mediated by active trafficking (Makino and Malinow, 2011; Shi et al., 2001) as well as by changes in conductance and open probability at the single receptor level (Benke et al., 1998; Derkach et al., 1999). Here, we present evidence that, at least at the short-term scale of tens of minutes, synaptic potentiation through activation of GluA3-plasticity does not involve trafficking but mainly a prominent increase in open-channel probability of GluA3-containing receptors, suggesting that in the case of GluA3, changes in receptor properties is the predominant mechanism to produce synaptic potentiation. These findings imply that PF to PC LTP is mechanistically not just the reverse of LTD at this synapse (Jorntell and Hansel, 2006). Linden and colleagues have shown that PF to PC LTD is largely expressed by endocytosis of GluA2-containing AMPARs (Linden, 2001; Schonewille et al., 2011), thus mainly dependent on AMPAR trafficking. Given the current findings on GluA3-mediated LTP, it may be worthwhile to find out whether changes in AMPAR unitary conductance or glutamate affinity also play a minor role in early LTD expression at the PF to PC synapse, as interference with clathrin-mediated endocytosis did not produce a total attenuation of LTD expression (Wang and Linden, 2000).

Full genetic ablation of GluA2 subunits produces, in contrast to that of GluA3, an ataxic, hardly viable phenotype (Gerlai et al., 1998). Interestingly, the remaining, mainly GluA1- and GluA3-containing, AMPARs in these knock-out mice have an unusual subunit composition and are abnormally distributed at the synapse (Sans et al., 2003). In this respect, it should be noted that GluA3 is an obligatory heteromeric subunit: GluA3 homomers are energetically unfavorable (Rossman et al., 2011) and form intracellular aggregates that don't reach the cellular surface efficiently (Coleman et al., 2016). Genetic mouse models in which GluA2 trafficking is blocked reveal an impairment in LTD induction at their PF to PC synapses, whereas LTP is normal (Schonewille et al., 2011; Steinberg et al., 2006), which is in line with our finding that LTP can be induced without trafficking of GluA2/A3-containing AMPARs. Differently from these GluA2 mutants, GluA3-KO mice prominently express surface GluA2-containing AMPARs (heteromerized with GluA1), but lack a cAMP-dependent synaptic LTP. These data highlight the differential roles of GluA2 and GluA3 in the structural dynamics and localization of AMPARs and the related forms of synaptic plasticity. In contrast to GluA3, GluA2 is unlikely to be directly involved in cAMP-dependent plasticity, since its expression coupled to GluA1 does not compensate for the absence of GluA3 subunits. We propose that GluA2 expression is a structural requisite for GluA3 plasticity, as it appears necessary for proper expression and location of GluA3-containing AMPARs. GluA1/2 heteromers in PCs may then serve to maintain basal synaptic currents when cAMP levels are low.

The finding that an Epac-mediated change in single channel conductance and open probability of GluA2/3-containing AMPARs may underlie LTP at the PF to PC synapse raises the question how this change in configuration comes about. Interestingly, the distribution of GluA3-containing AMPARs openings does not seem to respond to a stochastic probability distribution of four ligand binding domains (LBDs) "catching" glutamate with equal probability. Instead it is biased towards the lowest conductance state opening, in which only two out of four LBDs bind glutamate. Since GluA3-containing AMPARs predominantly consist of two GluA3 and two GluA2 subunits, only the GluA2 LBDs effectively may bind glutamate under basal conditions. Our observation that enhancing cAMP levels exerts GluA3-containing receptors to produce higher conductance openings (resembling the behavior of GluA1-containing receptors) may suggest that Epac activation triggers a conformational change in the two GluA3 subunits present in each tetramer, such that they become responsive to glutamate binding at the LBD (Figure 5F).

It is widely accepted that intracellular calcium signaling is a key mechanism for LTP induction in PCs (Coesmans et al., 2004; van Woerden et al., 2009). In the present study we show that postsynaptic LTP depends on cAMP-dependent activation of GluA3-containing receptors. How low calcium signals in PCs are transduced into activation of adenylyl cyclase to raise cAMP levels remains to be elucidated. Interestingly, it has been shown that the tetanic activity of PFs required for LTP induction produces local calcium increases dependent on low-threshold CaV3.1 T-type calcium channels (Hildebrand et al., 2009) and that global deletion or blockage of these channels prevents LTP induction and motor learning (Ly et al., 2013). In this respect, the calcium/calmodulin-dependent adenylyl cyclase Adcy1 (Masada et al., 2012) could be an interesting candidate to convert local calcium activity in a rise in cAMP.

We have shown here that postsynaptic GluA3-dependent synaptic potentiation depends on a rise in cAMP. Therefore, this study expands the repertoire of forms of PC plasticity already known to depend on cAMP, such as presynaptic plasticity (Chen and Regehr, 1997; Kaneko and Takahashi, 2004; Lev-Ram et al., 2002), intrinsic plasticity (Belmeguenai et al., 2010) or plasticity at inhibitory synapses (Mitoma and Konishi, 1996). Epac2 has recently been reported to also have a role in presynaptic plasticity in that it may modify glutamate release probability (Gekel and Neher, 2008). This raises the interesting possibility that Epac2 and/or cAMP in their pre- and postsynaptic domains operate in a synergistic fashion to control synaptic plasticity (Le Guen and De Zeeuw, 2010; (Wang et al., 2014). Likewise, the induction protocol of LTP produces an increase in intrinsic excitability in PCs, via cAMP-mediated PKA modulation of SK potassium channels (Belmeguenai et al., 2010). Thus, since this change in intrinsic excitability occurs at least partly as a secondary process following tetanic PF stimulation, LTP at the PF to PC synapse may act as a feed-forward amplifier of synaptic inputs to modulate firing rate in PCs via cAMP production. Finally, it should be noted that rebound potentiation at the molecular layer interneuron to PC synapse, which occurs following PC depolarization, is also mediated by cAMP-mediated PKA modulation (Hirano and Kawaguchi, 2012). Together, these findings point towards a central role of cAMP following induction of PF to PC LTP, regulating multiple forms of plasticity with different identities and natures in a synergistic fashion (Gao et al., 2012).

Synapses are highly dynamic structures and early removal of synaptic proteins can lead to compensatory mechanisms to occur in order to overcome unbalanced synaptic function. However, no compensatory mechanism is able to overcome the declarative memory deficits observed in GluA1 KO mice (Feyder et al., 2007;

Humeau et al., 2007). In contrast, GluA1-KO learned to adapt their vestibulo-ocular reflexes virtually identically to wild-type littermates. This finding suggests two possible scenarios: either PCs synapse are capable to compensate for the absence of GluA1 through a mechanism that is not present in hippocampal pyramidal or amygdalar cells, or GluA1 is not involved in this form of learning at all. With the evidence presented here, none of these possibilities can be unequivocally discarded. Yet, these findings in the GluA1-KO emphasize the insufficiency of compensation in the GluA3-KO; the fact that their PCs could not compensate for the absence of GluA3 to overcome the lack of LTP and the learning deficits, highlights the importance of GluA3 for PC synaptic plasticity and motor learning. Taken together, the picture emerges that the learning rules for AMPAR-mediated plasticity in PCs are inverted compared with those in the hippocampus: cerebellar LTP and learning do not require GluA1, but depend on plasticity of GluA3-containing AMPARs.

Experimental procedures

For extended experimental procedures, which have all been done in a blinded fashion, please see supplementary material.

Author contributions

N.G.C., C.M.D.S., H.W.K. and C.I.D.Z. designed, performed and analyzed the behavioral and histological experiments; N.G.C., L.M.C.K., K.Z., C.B.C., M.C.R., H.W.K., and C.I.D.Z. designed, performed and analyzed the electrophysiological and pharmacological experiments; R.S. generated conditional AMPAR-knockout mice; and N.G., C.B.C., H.W.K. and C.I.D.Z. wrote the manuscript.

Acknowledgments

This work was supported by the Dutch Organization for Medical Sciences (C.I.D.Z.), Life Sciences (C.I.D.Z.), and Social and Behavioral Sciences (C.I.D.Z.), and ERC-adv, ERC-POC, CEREBNET, C7 programs of the EU (C.I.D.Z.), and the Netherlands Organization for Scientific Research (H.W.K.). The authors declare no financial or non-financial competing interests.

REFERENCES

Adamczyk, A., Mejias, R., Takamiya, K., Yocum, J., Krasnova, I.N., Calderon, J., Cadet, J.L., Huganir, R.L., Pletnikov, M.V., and Wang, T. (2012). GluA3-deficiency in mice is associated with increased social and aggressive behavior and elevated dopamine in striatum. Behav. Brain Res. *229*, 265-272.

Anzai, M., Kitazawa, H., and Nagao, S. (2010). Effects of reversible pharmacological shutdown of cerebellar flocculus on the memory of long-term horizontal vestibulo-ocular reflex adaptation in monkeys. Neurosci. Res. *68*, 191-198.

Barski, J.J., Dethleffsen, K., and Meyer, M. (2000). Cre recombinase expression in cerebellar Purkinje cells. Genesis. *28*, 93-98.

Bats, C., Farrant, M., and Cull-Candy, S.G. (2013). A role of TARPs in the expression and plasticity of calcium-permeable AMPARs: evidence from cerebellar neurons and glia. Neuropharmacology *74*, 76-85.

Belmeguenai, A., Hosy, E., Bengtsson, F., Pedroarena, C.M., Piochon, C., Teuling, E., He, Q., Ohtsuki, G., de Jeu, M.T., Elgersma, Y., De Zeeuw, C.I., Jorntell, H., and Hansel, C. (2010). Intrinsic plasticity complements long-term potentiation in parallel fiber input gain control in cerebellar Purkinje cells. J. Neurosci. *30*, 13630-13643.

Benke, T.A., Luthi, A., Isaac, J.T., and Collingridge, G.L. (1998). Modulation of AMPA receptor unitary conductance by synaptic activity. Nature *393*, 793-797.

Boyden, E.S., Katoh, A., Pyle, J.L., Chatila, T.A., Tsien, R.W., and Raymond, J.L. (2006). Selective engagement of plasticity mechanisms for motor memory storage. Neuron *51*, 823-834.

Chen, C., and Regehr, W.G. (1997). The mechanism of cAMP-mediated enhancement at a cerebellar synapse. J. Neurosci. *17*, 8687-8694.

Coesmans, M., Weber, J.T., De Zeeuw, C.I., and Hansel, C. (2004). Bidirectional parallel fiber plasticity in the cerebellum under climbing fiber control. Neuron *44*, 691-700.

Coleman, S.K., Hou, Y., Willibald, M., Semenov, A., Moykkynen, T., and Keinanen, K. (2016). Aggregation Limits Surface Expression of Homomeric GluA3 Receptors. J. Biol. Chem. *291*, 8784-8794.

Derkach, V., Barria, A., and Soderling, T.R. (1999). Ca2+/calmodulin-kinase II enhances channel conductance of alpha-amino-3-hydroxy-5-methyl-4-isoxazolepropionate type glutamate receptors. Proc. Natl. Acad. Sci. U. S. A *96*, 3269-3274.

Douyard, J., Shen, L., Huganir, R.L., and Rubio, M.E. (2007). Differential neuronal and glial expression of GluR1 AMPA receptor subunit and the scaffolding proteins SAP97 and 4.1N during rat cerebellar development. J. Comp Neurol. *502*, 141-156.

Feyder M, Wiedholz L, Sprengel R, Holmes A. Impaired associative fear learning in mice with complete loss or haploinsufficiency of AMPA GluR1 receptors. Front Behav Neurosci. 2007 Dec 30;1:4.

Frey, M.C., Sprengel, R., and Nevian, T. (2009). Activity pattern-dependent long-term potentiation in neocortex and hippocampus of GluA1 (GluR-A) subunit-deficient mice. J. Neurosci. *29*, 5587-5596.

Gao, Z., van Beugen, B.J., and De Zeeuw, C.I. (2012). Distributed synergistic plasticity and cerebellar learning. Nat. Rev. Neurosci. *13*, 619-635.

Gekel, I., and Neher, E. (2008). Application of an Epac activator enhances neurotransmitter release at excitatory central synapses. J. Neurosci. *28*, 7991-8002.

Gerlai, R., Henderson, J.T., Roder, J.C., and Jia, Z. (1998). Multiple behavioral anomalies in GluR2 mutant mice exhibiting enhanced LTP. Behav. Brain Res. *95*, 37-45.

Granger, A.J., Shi, Y., Lu, W., Cerpas, M., and Nicoll, R.A. (2013). LTP requires a reserve pool of glutamate receptors independent of subunit type. Nature *493*, 495-500.

Gutierrez-Castellanos, N., Winkelman, B.H., Tolosa-Rodriguez, L., De Gruijl, J.R., and De Zeeuw, C.I. (2013). Impact of aging on long-term ocular reflex adaptation. Neurobiol. Aging *34*, 2784-2792.

Hildebrand, M.E., Isope, P., Miyazaki, T., Nakaya, T., Garcia, E., Feltz, A., Schneider, T., Hescheler, J., Kano, M., Sakimura, K., Watanabe, M., Dieudonne, S., and Snutch, T.P. (2009). Functional coupling between mGluR1 and Cav3.1 T-type calcium channels contributes to parallel fiber-induced fast calcium signaling within Purkinje cell dendritic spines. J. Neurosci. *29*, 9668-9682.

Hirano, T., and Kawaguchi, S.Y. (2012). Regulation of inhibitory synaptic plasticity in a Purkinje neuron. Cerebellum. *11*, 453-454.

Humeau, Y., Reisel, D., Johnson, A.W., Borchardt, T., Jensen, V., Gebhardt, C., Bosch, V., Gass, P., Bannerman, D.M., Good, M.A., Hvalby, O., Sprengel, R., and Luthi, A. (2007). A pathway-specific function for different AMPA receptor subunits in amygdala long-term potentiation and fear conditioning. J. Neurosci. *27*, 10947-10956.

Ito, M. (2002). Historical review of the significance of the cerebellum and the role of Purkinje cells in motor learning. Ann. N. Y. Acad. Sci. *978*, 273-288.

Jia, Z., Agopyan, N., Miu, P., Xiong, Z., Henderson, J., Gerlai, R., Taverna, F.A., Velumian, A., MacDonald, J., Carlen, P., Abramow-Newerly, W., and Roder, J. (1996). Enhanced LTP in mice deficient in the AMPA receptor GluR2. Neuron *17*, 945-956.

Jorntell, H., and Hansel, C. (2006). Synaptic memories upside down: bidirectional plasticity at cerebellar parallel fiber-Purkinje cell synapses. Neuron *52*, 227-238.

Kakegawa, W., and Yuzaki, M. (2005). A mechanism underlying AMPA receptor trafficking during cerebellar long-term potentiation. Proc. Natl. Acad. Sci. U. S. A *102*, 17846-17851.

Kaneko, M., and Takahashi, T. (2004). Presynaptic mechanism underlying cAMP-dependent synaptic potentiation. J. Neurosci. *24*, 5202-5208.

Kessels, H.W., and Malinow, R. (2009). Synaptic AMPA receptor plasticity and behavior. Neuron *61*, 340-350.

Le Guen, M.C., and De Zeeuw, C.I. (2010) Presynaptic plasticity at cerebellar parallel fiber terminals. Funct Neurol. *25*, 141-51.

Lev-Ram, V., Wong, S.T., Storm, D.R., and Tsien, R.Y. (2002). A new form of cerebellar long-term potentiation is postsynaptic and depends on nitric oxide but not cAMP. Proc. Natl. Acad. Sci. U. S. A *99*, 8389-8393.

Linden, D.J. (2001). The expression of cerebellar LTD in culture is not associated with changes in AMPA-receptor kinetics, agonist affinity, or unitary conductance. Proc. Natl. Acad. Sci. U. S. A *98*, 14066-14071.

Linden, D.J., and Connor, J.A. (1995). Long-term synaptic depression. Annu. Rev. Neurosci. *18*, 319-357.

Makino, H., and Malinow, R. (2009). AMPA receptor incorporation into synapses during LTP: the role of lateral movement and exocytosis. Neuron *64*, 381-390.

Malinow, R., and Malenka, R.C. (2002). AMPA receptor trafficking and synaptic plasticity. Annu. Rev. Neurosci. *25*, 103-126.

Masada, N., Schaks, S., Jackson, S.E., Sinz, A., and Cooper, D.M. (2012). Distinct mechanisms of calmodulin binding and regulation of adenylyl cyclases 1 and 8. Biochemistry *51*, 7917-7929.

Mead, A.N., and Stephens, D.N. (2003). Selective disruption of stimulus-reward learning in glutamate receptor gria1 knock-out mice. J. Neurosci. *23*, 1041-1048.

Meng, Y., Zhang, Y., and Jia, Z. (2003). Synaptic transmission and plasticity in the absence of AMPA glutamate receptor GluR2 and GluR3. Neuron *39*, 163-176.

Mitoma, H., and Konishi, S. (1996). Long-lasting facilitation of inhibitory transmission by monoaminergic and cAMP-dependent mechanism in rat cerebellar GABAergic synapses. Neurosci. Lett. 217, 141-144.

Nedelescu, H., Kelso, C.M., Lazaro-Munoz, G., Purpura, M., Cain, C.K., Ledoux, J.E., and Aoki, C. (2010). Endogenous GluR1-containing AMPA receptors translocate to asymmetric synapses in the lateral amygdala during the early phase of fear memory formation. J. Comp Neurol. *518*, 4723-4739.

Nguyen-Vu, T.D., Kimpo, R.R., Rinaldi, J.M., Kohli, A., Zeng, H., Deisseroth, K., and Raymond, J.L. (2013). Cerebellar Purkinje cell activity drives motor learning. Nat. Neurosci. *16*, 1734-1736.

Peter, S., Ten Brinke M.M., Stedehouder J., Reinelt C.M., Wu B., Zhou H., Zhou K., Boele H.J., Kushner S.A., Lee M.G., Schmeisser M.J., Boeckers T.M., Schonewille M., Hoebeek F.E., and De Zeeuw C.I. (2016) **Dysfunctional cerebellar Purkinje cells contribute to autism-like behaviour in Shank2-deficient mice.** Nat Commun. *7*:12627.

Poon, K., Ahmed, A.H., Nowak, L.M., and Oswald, R.E. (2011). Mechanisms of modal activation of GluA3 receptors. Mol. Pharmacol. *80*, 49-59.

Poon, K., Nowak, L.M., and Oswald, R.E. (2010). Characterizing single-channel behavior of GluA3 receptors. Biophys. J. *99*, 1437-1446.

Rossmann, M., Sukumaran, M., Penn, A.C., Veprintsev, D.B., Babu, M.M., and Greger, I.H. (2011). Subunit-selective N-terminal domain associations organize the formation of AMPA receptor heteromers. EMBO J. *30*, 959-971.

Rumpel, S., Ledoux, J., Zador, A., and Malinow, R. (2005). Postsynaptic receptor trafficking underlying a form of associative learning. Science *308*, 83-88.

Salin, P.A., Malenka, R.C., and Nicoll, R.A. (1996). Cyclic AMP mediates a presynaptic form of LTP at cerebellar parallel fiber synapses. Neuron *16*, 797-803.

Sanchis-Segura, C., Borchardt, T., Vengeliene, V., Zghoul, T., Bachteler, D., Gass, P., Sprengel, R., and Spanagel, R. (2006). Involvement of the AMPA receptor GluR-C subunit in alcohol-seeking behavior and relapse. J. Neurosci. *26*, 1231-1238.

Sans, N., Vissel, B., Petralia, R.S., Wang, Y.X., Chang, K., Royle, G.A., Wang, C.Y., O'Gorman, S., Heinemann, S.F., and Wenthold, R.J. (2003). Aberrant formation of glutamate receptor complexes in hippocampal neurons of mice lacking the GluR2 AMPA receptor subunit. J. Neurosci. *23*, 9367-9373.

Schonewille, M., Gao, Z., Boele, H.J., Veloz, M.F., Amerika, W.E., Simek, A.A., de Jeu, M.T., Steinberg, J.P., Takamiya, K., Hoebeek, F.E., Linden, D.J., Huganir, R.L., and De Zeeuw, C.I. (2011). Reevaluating the role of LTD in cerebellar motor learning. Neuron *70*, 43-50.

Shi, S., Hayashi, Y., Esteban, J.A., and Malinow, R. (2001). Subunit-specific rules governing AMPA receptor trafficking to synapses in hippocampal pyramidal neurons. Cell *105*, 331-343.

Sokolova, I.V., Lester, H.A., and Davidson, N. (2006). Postsynaptic mechanisms are essential for FSK-induced potentiation of synaptic transmission. J. Neurophysiol. *95*, 2570-2579.

Steinberg, J.P., Takamiya, K., Shen, Y., Xia, J., Rubio, M.E., Yu, S., Jin, W., Thomas,G.M., Linden, D.J., and Huganir, R.L. (2006). Targeted in vivo mutations of the AMPA receptor subunit GluR2 and its interacting protein PICK1 eliminate cerebellar long-term depression. Neuron *49*, 845-860.

Sukumaran, M., Rossmann, M., Shrivastava, I., Dutta, A., Bahar, I., and Greger, I.H. (2011). Dynamics and allosteric potential of the AMPA receptor N-terminal domain. EMBO J. *30*, 972-982.

Takahashi, T., Svoboda, K., and Malinow, R. (2003). Experience strengthening transmission by driving AMPA receptors into synapses. Science *299*, 1585-1588.

Tsalkova, T., Mei, F.C., Li, S., Chepurny, O.G., Leech, C.A., Liu, T., Holz, G.G., Woods, V.L., Jr., and Cheng, X. (2012). Isoform-specific antagonists of exchange proteins directly activated by cAMP. Proc. Natl. Acad. Sci. U. S. A 109, 18613-18618.

Ten Brinke MM, Boele HJ, Spanke JK, Potters JW, Kornysheva K, Wulff P, IJpelaar AC, Koekkoek SK, and De Zeeuw CI. (2015) Evolving Models of Pavlovian Conditioning: Cerebellar Cortical Dynamics in Awake Behaving Mice. Cell Rep. *13*, 1977-88.

van Woerden, G.M., Hoebeek, F.E., Gao, Z., Nagaraja, R.Y., Hoogenraad, C.C., Kushner, S.A., Hansel, C., De Zeeuw, C.I., and Elgersma, Y. (2009). betaCaMKII controls the direction of plasticity at parallel fiber-Purkinje cell synapses. Nat. Neurosci. *12*, 823-825.

Wang, D.J., Su, L.D., Wang, Y.N., Yang, D., Sun, C.L., Zhou, L., Wang, X.X., and Shen, Y. (2014). Long-term potentiation at cerebellar parallel fiber-Purkinje cell synapses requires presynaptic and postsynaptic signaling cascades. J. Neurosci. *34*, 2355-2364.

Wang, Y.T., and Linden, D.J. (2000). Expression of cerebellar long-term depression requires postsynaptic clathrin-mediated endocytosis. Neuron *25*, 635-647.

Woolfrey, K.M., Srivastava, D.P., Photowala, H., Yamashita, M., Barbolina, M.V., Cahill, M.E., Xie, Z., Jones, K.A., Quilliam, L.A., Prakriya, M., and Penzes, P. (2009). Epac2 induces synapse remodeling and depression and its disease-associated forms alter spines. Nat. Neurosci. *12*, 1275-1284.

4

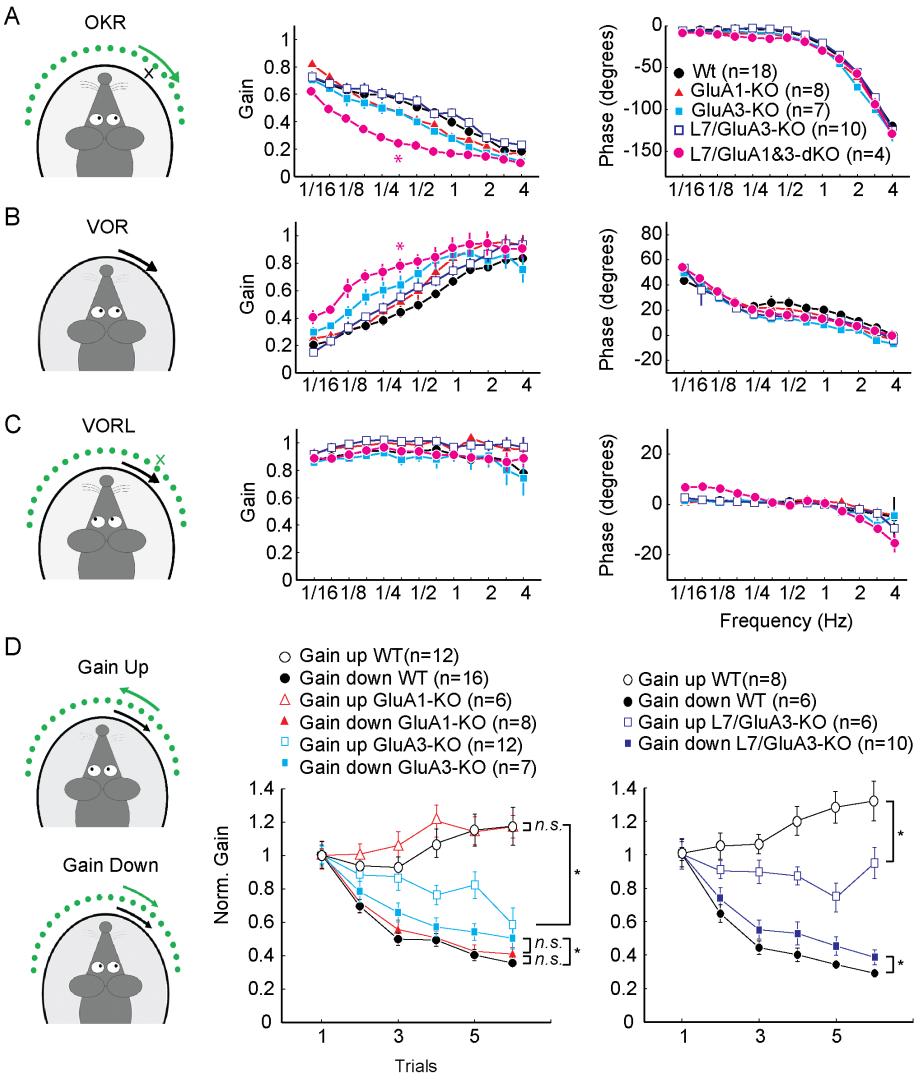
A
OKR
Gain
Phase (degrees)
Wt (n=18)
GluA1-KO (n=8)
GluA3-KO (n=7)
L7/GluA3-KO (n=10)
L7/GluA1&3-dKO (n=4)
1/16 1/8 1/4 1/2 1 2 4
B
VOR
C
VORL
Frequency (Hz)
D
Gain Up
Gain Down
Gain up WT(n=12)
Gain down WT (n=16)
Gain up GluA1-KO (n=6)
Gain down GluA1-KO (n=8)
Gain up GluA3-KO (n=12)
Gain down GluA3-KO (n=7)
Gain up WT(n=8)
Gain down WT (n=6)
Gain up L7/GluA3-KO (n=6)
Gain down L7/GluA3-KO (n=10)
Norm. Gain
n.s.
Trials

Figure S1. Related to Figures 1 and 8, Basic compensatory eye movements in the single global KO mice for GluA1 or GluA3 as well as in PC-specific KO for GluA3 are relatively normal, whereas those in the double PC-specific KO for GluA1 and GluA3 show pronounced gain deficits.

(A) The optokinetic reflex (OKR), which stabilizes gaze with respect to a moving visual field (Stahl et al., 2000), showed a normal baseline gain in GluA1-KO and GluA3-KO mice ($F(2,29)=2.361$, $p = 0.11$; Repeated measures ANOVA and Tukey post hoc analysis), whereas phase values in both mutants presented a small, but consistent, delay across the entire frequency range tested ($F(2,29)=14.86$, $p < 0.01$, Tukey's multiple comparisons test revealed differences for the 95% confidence intervals of both mutants with respect to wild-type controls, but not between them). L7/GluA3-KO mice presented intact gain and phase values compared to controls ($F(1,26) = 0.21$, $p = 0.64$ and $F(1,26) = 1.24$, $p = 0.27$, respectively). In contrast, PC-specific double GluA1 and GluA3 KO mice (L7/GluA1&3-dKO) showed a highly significantly impaired OKR response ($F(1,20) = 21.30$, $p = 0.0001$)

(B) During VOR compensation GluA1-KO and GluA3-KO showed both a normal gain ($F(2,29)=1.745$, $p = 0.17$) and normal phase ($F(2,29)=1.382$, $p = 0.26$). In addition, L7/GluA3-KO mice also showed a normal basic eye movement performance ($F(1,26) = 1.65$, $p = 0.21$ and $F(1,26) = 1.53$, $p = 0.22$, for gain and phase, respectively). Interestingly, L7/GluA1&3-dKO showed significantly improved VOR performance when compared to control mice ($F(1,20) = 5.245$, $p= 0.033$), most likely as a compensation for their impaired OKR.

(C) When we combined optokinetic stimulation with vestibular stimulation (i.e. VOR in the light or VORL) as occurs in daily life, all mutants also showed normal performances for both gain and phase compared to those in wild-type littermates ($F(2,29) = 1.33$, $p = 0.29$ for GluA1-KO, GluA3-KO and their WT littermates and $F(1,26) = 1.51$, $p = 0.23$ for L7/GluA3-KO vs. control littermates gain values).

(D) Oculomotor adaptation was assessed through paradigms aiming to either increase (i.e. gain-up paradigm, in which the visual stimulus moves with the same amplitude as the vestibular stimulus, but with opposite direction, resulting in improved VOR compensation) or decrease (i.e. gain-down paradigm, in which both visual and vestibular stimuli move with the same amplitude in the same direction, resulting in cancelation of compensatory eye movements) the amplitude of the VOR. Schematic drawings of the training stimuli are shown in the left column. Our results show that whereas GluA1-KO mice show a comparable increase ($p=0.23$ for final catch trials) and decrease ($p=0.11$) of gains compared to those in WT mice, GluA3-KO mice show significantly impaired gain-up ($p=0.009$) as well as gain-down ($p=0.001$) paradigms. The deficits observed in the global GluA3-KO mice were also present in the PC-cell specific KO (L7/GluA3-KO compared to WT littermates, $p = 0.006$ and $p = 0.04$ for gain-up and gain-down, respectively).

Error bars indicate SEM, * indicates $p<0.05$.

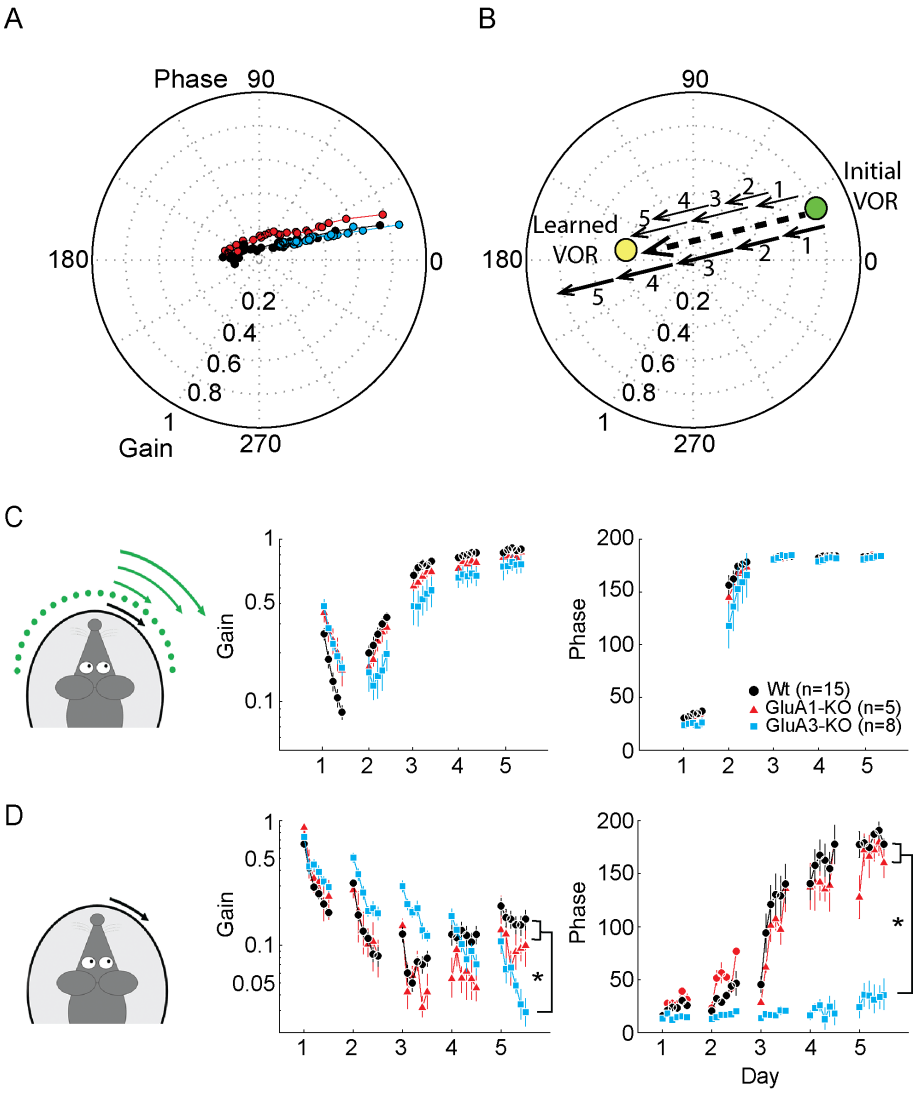
A
Phase
90
180
0
270
0.2
0.4
0.6
0.8
1
Gain
B
90
180
0
270
Initial
VOR
Learned
VOR
1
2
3
4
5
0.2
0.4
0.6
0.8
1
C
Gain
Phase
Wt (n=15)
GluA1-KO (n=5)
GluA3-KO (n=8)
D
Gain
Phase
Day
*
*

Figure S2. Related to Figure 1, (A) The full range of the 2 variables that explain ocular movements (0 to 1 for the gain and 0 to 360 for the phase) determine a circular bi-dimensional Cartesian plane (shown as a polar plot), in which every eye movement can be defined. Given that phase-reversal learning takes place through a defined common learning trajectory over several days during which phase covariates with gain (left polar plot), we performed statistics on the Cartesian coordinates defining gain and phase using the paired Hotteling's T2-Test.
(B) Polar plots of gain and phase vectorial representation during phase-reversal VOR learning data to illustrate the data analysis procedure. The data are composed of 5 individual learning vectors (one per day) moving across a constant learning trajectory towards the target set by the training paradigm (Phase of 180 degrees; Gain of 1). Based on the raw gain and phase data (A), we first calculate the learning extent for each mouse as the vectorial difference between the final performance and the initial performance (recording 6 of day 5 – recording 1 of day 1) and subsequently average these values per group. Between days of training there is partial retention of motor memories; to calculate the overall consolidation we calculate the ratio between the learning extent and the absolute summed extent of the learning vectors as if there was no memory loss overnight (100% consolidation). This ratio calculated per mouse is then also averaged across the mice, generating consolidation values for each group.
(C) Eye movement behavior of 4-6 week old GluA3-KO mice is virtually identical to that of 3-5 month old mice. Scatter plots of gain and phase values of 4-6 week old mice during the visuo-vestibular training for VOR phase-reversal shows no significant differences in the ability to follow the training signal ($p>0.05$ for last training recording on day 5 for comparison of GluA1-KO vs GluA3-KO and of WT vs GluA3-KO).
(D) Scatter plots of gain and phase values of the VOR catch trials show that WT and GluA1-KO mice, but not GluA3-KO mice, are able to reverse the phase of the VOR after training ($p<0.01$ for last catch recording on day 5 for comparison of GluA1-KO vs GluA3-KO and of WT vs GluA3-KO). For comparison with data in 3-5 month old animals see also Figure 1.
Error bars indicate SEM, * indicates $p<0.05$.

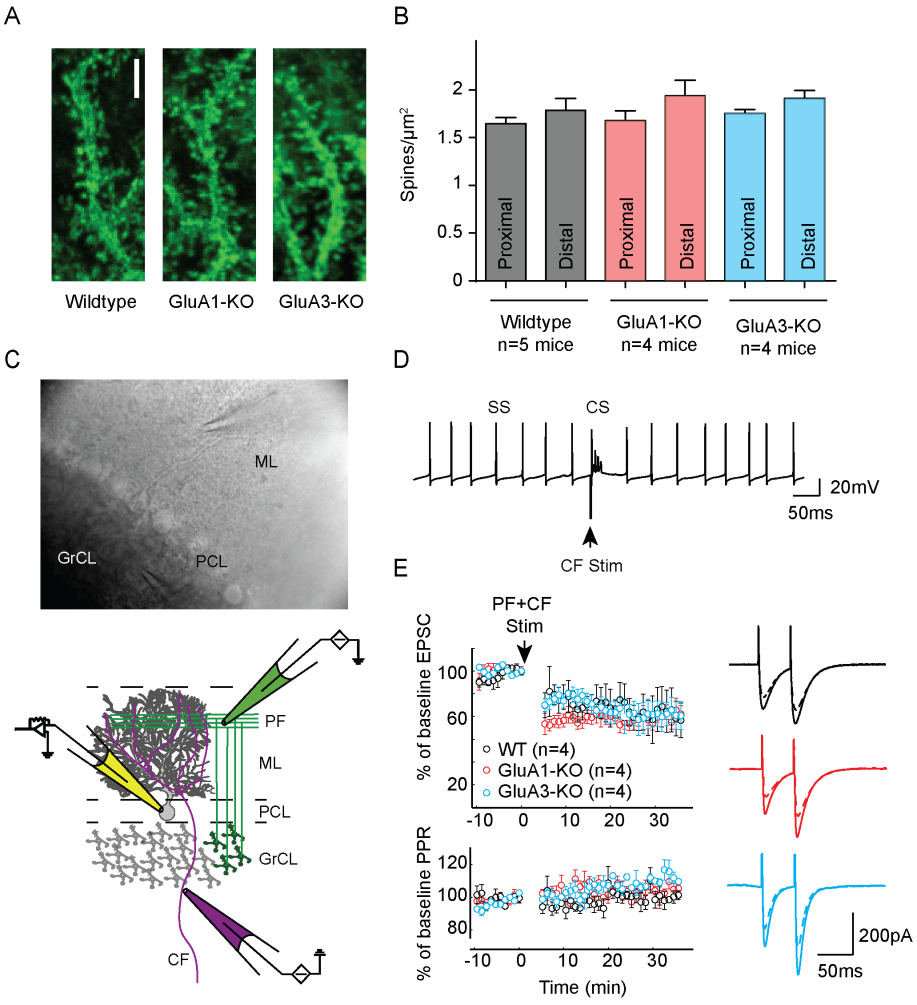
A
Wildtype
GluA1-KO
GluA3-KO
B
Spines/µm²
2
1.5
1
0.5
0
Proximal
Distal
Proximal
Distal
Proximal
Distal
Wildtype
n=5 mice
GluA1-KO
n=4 mice
GluA3-KO
n=4 mice
C
ML
GrCL
PCL
PF
ML
PCL
GrCL
CF
D
SS
CS
20mV
50ms
CF Stim
E
PF+CF
Stim
% of baseline EPSC
100
60
20
WT (n=4)
GluA1-KO (n=4)
GluA3-KO (n=4)
-10
0
10
20
30
% of baseline PPR
120
100
80
-10
0
10
20
30
Time (min)
200pA
50ms

Figure S3. Related to Figure 2, PCs lacking GluA1 or GluA3 have comparable spine density and show comparable levels of LTD induction compared to those in wild type (WT) PCs.
(A) Representative confocal optical planes (0.5 µm thick) of PC distal dendrites used to quantify spine densities of WT, GluA1-KO or GluA3-KO PCs.
(B) Densities plotted for each genotype correspond to the average spine density of at least 20 dendritic branches of PCs in lobules V to X per animal. Scale bar = 5 µm. The results show that neither the lack of GluA1 nor that of GluA3 yielded differences in spine densities of proximal or distal dendrites of PCs.
(C) Scheme of cerebellar cortical circuitry (bottom panel) and representative picture of the in-vitro preparation (top panel) showing positions of recording electrode (yellow) at PC soma and stimulus electrodes (green and purple) at parallel fiber (PF) beam and climbing fiber (CF), respectively. ML, PCL and GrCL indicate molecular layer, Purkinje cell layer, and granule cell layer, respectively.
(D) PCs were recorded in current clamp mode and the location of the stimulus pipettes were determined functionally by evoking responses to electrical stimulation at resting potential. Once the proper locations were identified, cells were kept in hyperpolarized state (-80 mV approx.) and a conjunctive CF and PF stimulation protocol was applied to the cell for 5 minutes (see Suppl. Methods for details).
(E) Both GluA1-KOs (red) and GluA3-KOs (blue) show similar cerebellar synaptic weakening after LTD induction (top panel) compared to WT littermates (black) with unchanged PPR over time (bottom panel). Representative traces of paired EPSCs before (solid lines) and after LTD induction (dashed lines) (right panels; genotypes match the color codes in B).

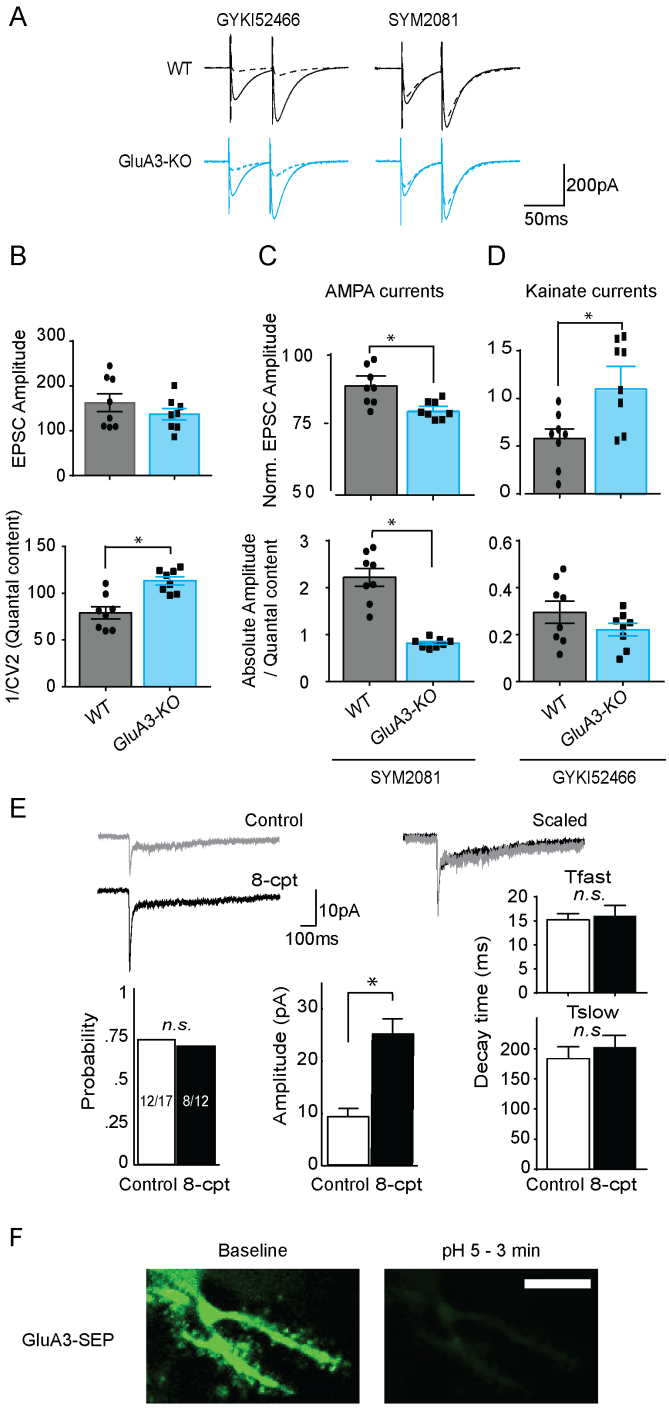
A
GYKI52466
SYM2081
WT
GluA3-KO
200pA
50ms
B
C
D
AMPA currents
Kainate currents
EPSC Amplitude
Norm. EPSC Amplitude
1/CV2 (Quantal content)
Absolute Amplitude / Quantal content
WT
GluA3-KO
SYM2081
GYKI52466
E
Control
8-cpt
10pA
100ms
Scaled
Tfast
Tslow
n.s.
Probability
12/17
8/12
Amplitude (pA)
Decay time (ms)
Control 8-cpt
F
Baseline
pH 5 - 3 min
GluA3-SEP

Figure S4. Related to Figures 2, 4 and 6. Kainate receptors do not compensate for weakening of glutamatergic transmission at PF to PC synapses in the absence of GluA3.
(A) To assess possible compensatory components in the glutamatergic transmission of PCs in GluA3-KO mice we investigated the impact of blocking either AMPA-receptors with 30 μM of GYKI-52466 (Cossart et al., 2002) or kainate receptors with 5 μM of SYM2081 (Yan et al., 2013) after establishing a stable baseline of eEPSCs in WT and GluA3-KO PCs.
(B) PF stimulation intensity was manually adjusted to obtain comparable EPSC amplitudes between 100-200 pA in WT and GluA3-KO PCs ($p = 0.3$, GluA3-KO vs. WT). The average quantal content released to produce events of comparable amplitude (estimated as the inverse of the square coefficient of variation; Kerchner and Nicoll, 2008), was significantly higher in the GluA3-KO ($p < 0.001$), indicating post-synaptic weakening.
(C) Blocking AMPARs reduced the total glutamatergic transmission in GluA3-KO PCs by 89±2%, which was significantly less than that in wild-type PCs (94±2%; $p = 0.01$ for GluA3-KO vs. WT, top panel). However, this difference was exacerbated after normalizing the amplitude to the quantal content, revealing that in the absence of GluA3, PCs have about half the normal magnitude of AMPA-mediated current ($p < 0.001$, bottom panel).
(D) To investigate to what extent kainate receptors can compensate for an impairment in GluA3-dependent transmission in PCs (Yan et al., 2013), we investigated the impact of a blockage of kainate-receptors in both WT and GluA3-KO PCs. The contribution of kainate-receptor mediated events to EPSC amplitude normalized to baseline magnitude was significantly higher in PCs of GluA3-KO (21±1.5%) than that in WT PCs (16±3%; $p = 0.024$ for GluA3-KO vs. WT, top panel). However, when normalized to the quantal content, the absolute contribution of kainate receptors was comparable among genotypes ($p=0.19$, bottom panel). Together, these data indicate that glutamatergic transmission in GluA3-KO mice can be largely explained by GluA1/GluA2-mediated AMPA-currents and to a lesser extent by kainate-currents, none of which is able to compensate for the synaptic weakening caused by the absence of GluA3.
(E) Excised patches of PC somata that received puffs of 100 μm AMPA generated significantly larger currents when 8-CPT-2Me-cAMP (8-CPT) was present in the internal solution. Note that the control patches showed the same probability of presenting AMPA events (left). Fast desensitizing and slow decay time kinetics were also unchanged (right panels).
(F) Super-ecliptic pHluorin (SEP) fused to GluA3 AMPARs showed the expected pH sensitivity. Washing in of acidic ACSF (pH 5) produced a dramatic reduction in the fluorescence intensity of externalized GluA3-SEP receptors. This is in line with the fact that GluA3-SEP AMPARs internalized in acidic vesicles contribute marginally to the fluorescent signal imaged. Scale bar, 200 μm.

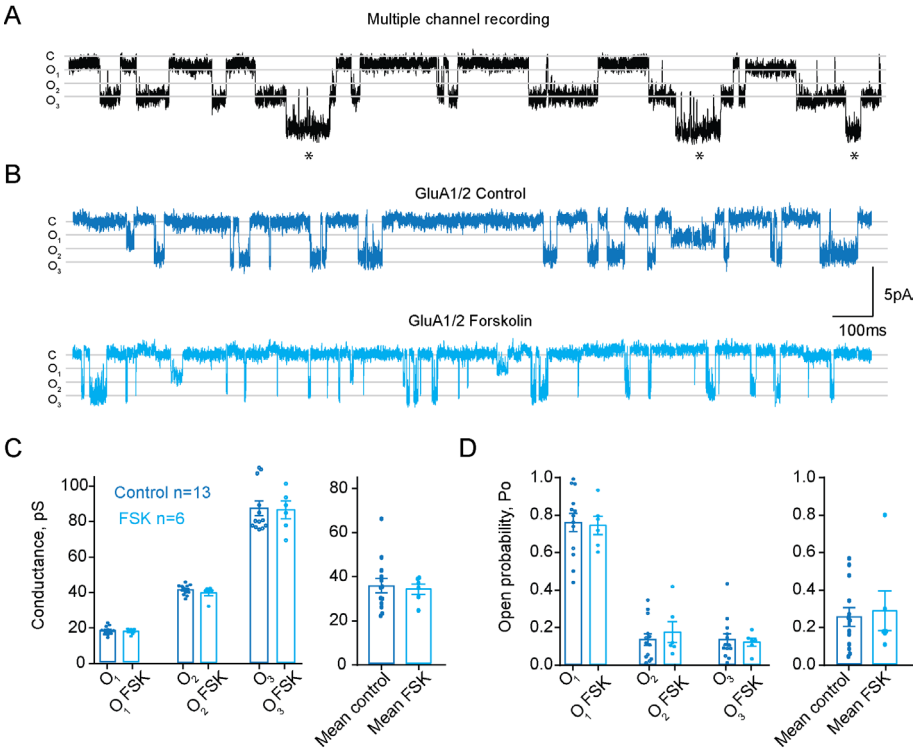

Figure S5. Related to figure 5, GluA1-containing AMPARs single channel properties are unchanged after forskolin application. (A) Example of multichannel activity recording. The presence of "escalated" openings that produced multiple conductance levels (asterisks) before reaching baseline was used as a criterion to discard recordings with multiple channels. (B) Single channels of GluA1-containing AMPARs showed comparable behavior in the presence and absence of forskolin. Note that under baseline conditions (top panel) the conductance level was higher than that of GluA3 channels as presented in main Figure 4A (top panel). (C) Conductance of the 3 different open levels of these channels was unchanged in the presence of forskolin and also comparable to that of GluA3 channels. (D) The relative fraction of openings and overall open probability of GluA1 channels was also unchanged after forskolin application and it resembled that of cAMP-activated GluA3 channels.

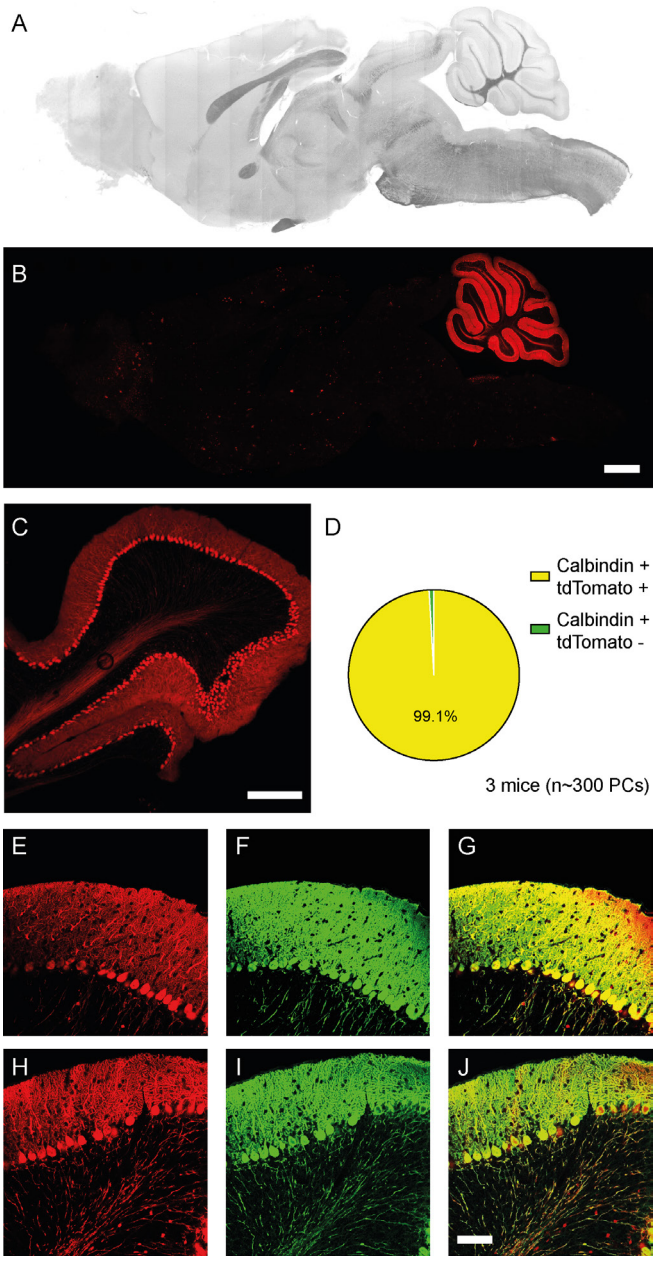

Figure S6. Related to Figure 8, Cre-dependent tdTomato expression under the L7 promotor confirms its Purkinje cells specificity. (A) Example of a L7Cre/floxedGluA3-KO mouse sagittal brain slice in bright field. (B) Same brain slice imaged with an epifluorescence microscope reveals how tdTomato expression is restricted to cerebellar PCs. (C) PCs in the vestibulocerebellum (flocculus and paraflocculus) also express the reporter under the L7 promotor. (D) Quantification of the population of PCs expressing tdTomato under the L7 promotor. Nearly all PC's with tdTomato (E, H) express calbindin (F, I with single labeling in green; G, J with double labeling in yellow) and vice versa, proving that the L7 promotor can be effectively used to genetically manipulate virtually the entire population of PCs. Scale bars 1 mm (A,B), 250 µm (C) and 100 µm (E-J).

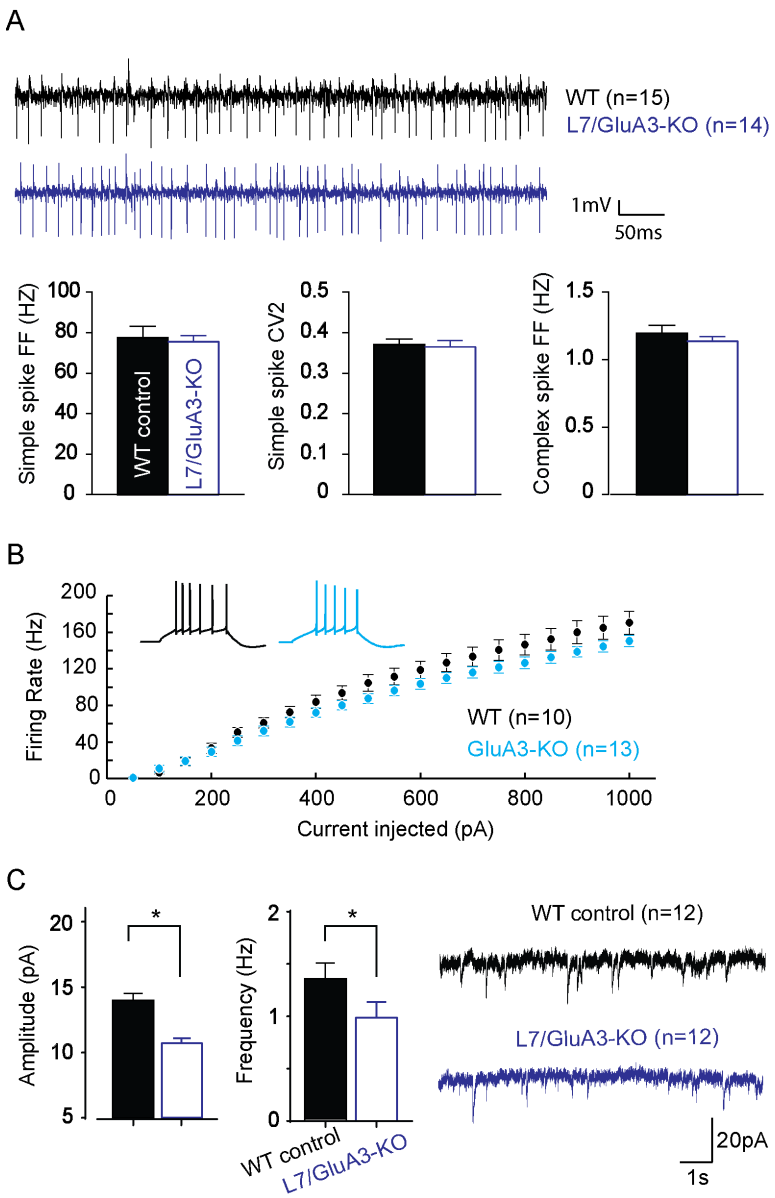

Figure S7. Related to Figure 8, GluA3 lacking PCs show intact excitability in-vitro and in-vivo despite their reduced synaptic transmission. (A) In-vivo spontaneous firing of L7/GluA3-KO PCs show comparable firing frequency and regularity of simple spikes as well as comparable amount of complex spikes, suggesting once more that, despite weaker PF to PC synapses, PC excitability is unaffected. (B) Short square steps of increasing current injected into PCs of both wild-types and GluA3-KOs showed no differences in the I/V relationships between genotypes ($F(1,21)=2.3$, $p = 0.14$, Repeated Measures ANOVA), showing that despite the weaker synaptic transmission in the absence of GluA3, PCs have unchanged excitability in vitro. (C) Synaptic transmission is also reduced in the PC specific KO for GluA3 (L7/GluA3-KO) tested in-vitro. Error bars indicate SEM, * indicates $p<0.05$.

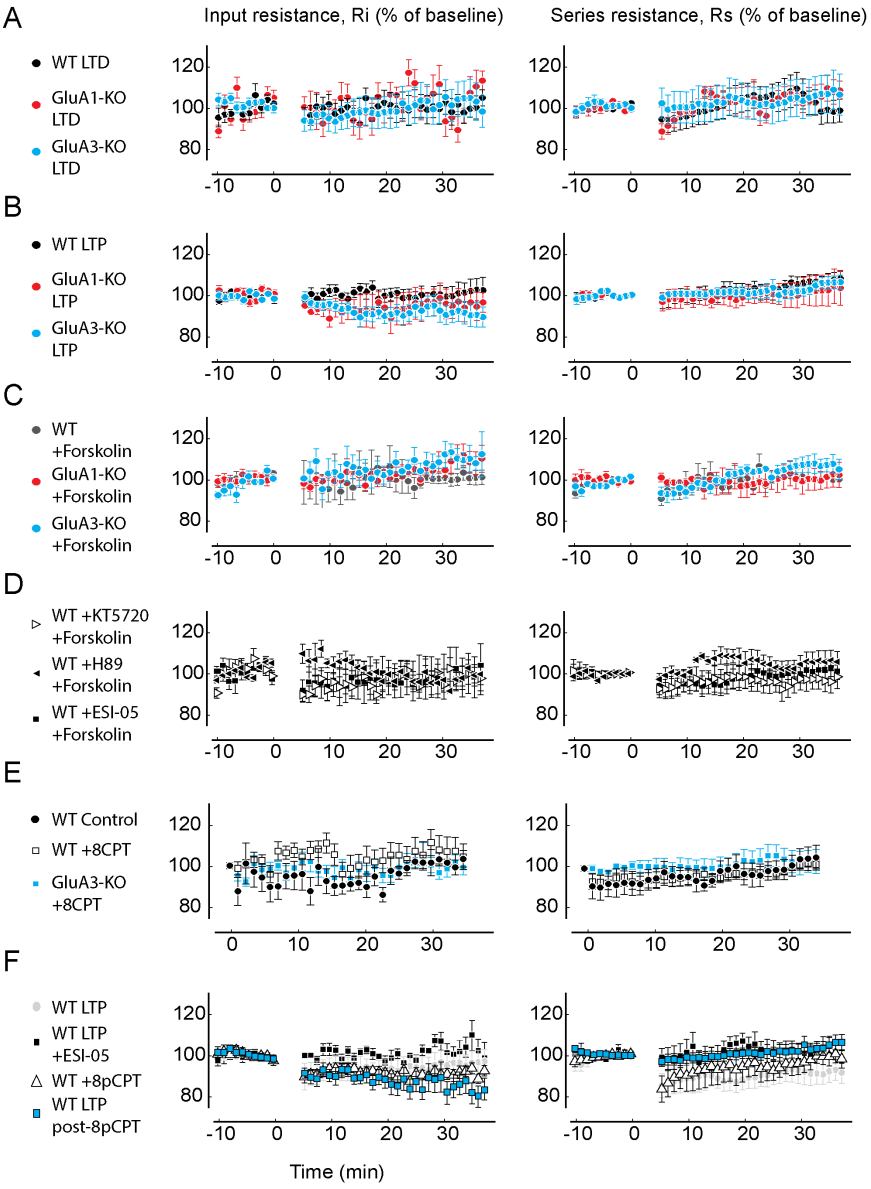

Figure S8. Related to Figures 2, 3, 6 and 7. Overview of membrane resistance (Rm) and series resistance (Rs) of every group of PCs used to generate the experimental figures of the current study. Data are plotted with the same color code as in main figures. All PCs that had a change in resistance bigger than 20% over a period longer than 2 minutes were discarded for further analysis. Rs and Rm for data shown in figure 2C (A), figure 2D (B), figure 3A (C), figure 6A (D), figure 6B (E) and figure 7A-B (F). Error bars indicate SEM.

EXTENDED EXPERIMENTAL PROCEDURES

Mice

Inbred breeding colonies were used to obtain the experimental knockout mice. GluA1-KO mice, kindly provided by Dr. R. Huganir (Kim et al., 2005), were generated by mating heterozygous c57bl6/129 mice; GluA3-KO and wild-type littermates were bred from c57bl6x129P2-Gria3tm1Dgen/Mmnc mutant ancestors (MMRRC, Davis, CA) at least 6 times backcrossed to c57bl6 mice; and Purkinje cell specific GluA3 knockout mice were generated by crossing floxed GluA3 mice (Sanchis-Segura et al., 2006) with L7-Cre mice (Barski et al., 2000). All experiments were conducted in line with the European guidelines for care and use of laboratory animals (Council Directive 86/6009/EEC). The experimental protocol was approved by the Animal Experiment Committee (DEC) of the Royal Netherlands Academy of Arts and Sciences (KNAW). All data of the experiments described below were acquired and analyzed in a blinded fashion with respect to the genotype.

Eye movement recordings and oculomotor learning tasks

Baseline performance of compensatory eye movements and VOR adaptation were first tested in three groups of male mice at the age of 4-6 weeks and 3-5 months. These included wild-type littermate mice (WT, n = 15 + 14, for both age categories, respectively), GluA1 knockout mice (n = 5 + 6) and GluA3 knockout mice (n = 8 + 6). Mice were surgically prepared for chronic head restrained experiments (de Jeu and De Zeeuw, 2012). During the experiment the mouse was placed head-fixed in a holder tube on a vestibular motion platform (R2000 'Rotopod', Parallel Robotic Systems Corporation, Hampton, USA). Left eye orientation was measured using video pupil tracking with a table-fixed CCD camera (Pulnix TM-6710CL, 120 frames/s) and IR illumination (850 nm LED, 6.5 cm distance from the eye). Pilocarpine (2%) eye drops were applied before the experiment to limit pupil dilatation in darkness. Online image analysis was performed to extract the location of pupil edges and corneal light reflections using custom built software for Labview (National Instruments, Austin, TX, USA). Angular eye velocity was computed offline using custom software written for Matlab (The Mathworks Inc., Natick, MA) using the algorithm outlined elsewhere (Stahl et al., 2000). Saccadic eye movements and quick-phases of the vestibular nystagmus were removed using a 50°/s velocity threshold and 200 ms margins at each threshold crossing. Each mouse was accustomed to the setup for a period of three training days before the experimental data were collected. The horizontal VOR was characterized in both darkness and light using sinusoidal rotation about the vertical axis, using

frequencies ranging between 1/16th to 4 Hz, presented in a sequence of increasing order, holding constant peak velocity of 18.8°/s. The number of cycles ranged between 5 at 1/16Hz to 60 at 4 Hz. Mice were subjected to a VOR cancellation stimulus on the first day (in-phase sinusoidal movement at 0.6 Hz, 5° amplitude of both the table and the visual surround) and a VOR reversal stimulus on subsequent days (2-5), where the amplitude of the visual surround was increased to 7.5° (day 2) and 10° (days 3, 4, and 5). The amplitude of the turntable remained constant at 5° amplitude (18.8°/s peak velocity). Training sessions consisted of 6 VOR measurements (30 cycles, 50 seconds, in darkness) that were alternated with 5 periods of visuo-vestibular mismatch training (300 cycles, 500 seconds). Apart from the training sessions, animals were kept in total darkness during the consecutive training days. The eye movement response was expressed as gain and phase relative to head movement, which was calculated using multiple linear regression of eye velocity to in-phase and quadrature components of the turntable velocity trace. Gain of the eye movement response was defined as the ratio between the eye velocity and the table velocity magnitudes. Phase was expressed in degrees and offset by 180°, so that a phase of 0° indicates an eye movement that is in-phase with contraversive head movement; positive phase values indicate phase leads. Consolidation of the adapted VOR was assessed by computing the ratio between the long-term change in VOR and the cumulative sum of short-term changes in VOR of preceding training sessions. The long-term change was defined as the absolute difference between the ending VOR on day 5 and the naive VOR on day 1. The short-term change was defined as the absolute difference between the VOR at the beginning and end of a training session. For a period of at least 10 days animals were allowed to rest between different VOR adaptation protocols. Bivariate 2-sample Hotelling's T2-test was used to compare gain and phase values between groups, and One Way ANOVA/ Tukey post-hoc test was used for cumulative consolidation values.

Spine density quantification in Purkinje neurons

In order to calculate the spine density in PCs, 5 WT, 4 GluA1-KO and 4 GluA3-ko mice received an overdose of sodium pentobarbital via IP injection and were perfused intracardially with 10 ml of PB 0.1M (pH 7.6) followed by 60 ml of fixative (4% paraformaldehyde in 0.1 M PB, pH7.6) at a rate of 5.5 ml/min. Brains were carefully removed from the skull, post-fixed for a maximum of 2 hours in the same fixative solution at 4°C, immersed in 30% sucrose in PB at 4°C until they sank, and subsequently cut into 40µm thick frontal sections, which were collected as four matching series. For calbindin detection, the slices were incubated in blocking solution containing 10% horse serum in 0.1 M PB to minimize non-specific binding

of the antibodies. After 1 hour, blocking solution was replaced by the primary antibody solution containing 5% horse serum in 0.1M PB, rabbit anti-Calbindin antibody (Chemicon, Millipore) at a concentration of 1:1000 for 12 hours at 4°C. After several rinses with 0.1 M PB slices were incubated for 4 hours in a solution containing 5% horse serum in 0.1 M PB and horse anti-rabbit combined with Alexa 488 secondary antibody at a concentration of 1:200. After several rinses, slices were mounted and covered with Dako mounting medium (Dako), and imaged under a confocal microscope (Leica SP5). All images were acquired with the same settings and the analysis was performed with ImageJ. Stacks of pictures across the Z-axis (10-30 µm) were made to count total spine number in proximal (max 30 µm away from the PC soma) and distal dendrites of PCs. The spine density was calculated for each dendrite dividing the dendrite's spine count by its length; all images were processed using ImageJ. All proximal and distal dendrites counted were averaged for each mouse and mice of the same genotype were averaged to obtain the final spine densities (Figure S3A-B).

In-vitro electrophysiology

Sagittal slices of the cerebellar vermis (250 to 400 µm thick) from 4 to 6 weeks old mice were obtained in ice-cold oxygenated "slicing" solution containing (in mM) 2.5 KCl, 1 CaCl2, 3 MgCl2, 25 NaHCO3, 1.25 NaH2PO4, 240 sucrose, 25 D-glucose and 0.01 kyneurenic acid. Slices were transferred to the same slicing solution at 34°C for 5-10 minutes and then transferred to oxygenated ACSF at 34°C containing (in mM) 124 NaCl, 5 KCl, 1.25 Na2HPO4, 1 MgSO4, 2 CaCl2, 26 NaHCO3, 20 D-glucose. Subsequently, the slices were allowed to recover for at least 30 minutes until they were moved to the recording chamber containing the same oxygenated ACSF with 100 µM picrotoxin to prevent GABAergic transmission at near physiological temperature of 30±2°C. Whole-cell patch-clamp recordings of Purkinje cells located in lobules VI to X were performed using an EPC-10 amplifier (HEKA, Lambrecht). 3-5 MΩ resistance patch pipettes were filled with (in mM) K-Gluconate 122.5 mM, NaATP 4, NaGTP 0.4, HEPES 10, NaCl, KCl 9 and 0.6 mM EGTA (Sigma) at pH 7.25 for all the recordings that required current clamp mode (including LTP) or with (in mM) 115 mM cesium methanesulfonate, 20 mM CsCl, 10 mM Hepes, 2.5 mM MgCl2, 4 mM Na2ATP, 0.4 mM Na3GTP, 10 mM sodium phosphocreatine (Sigma), and 0.6 mM EGTA (Sigma), at pH 7.25 for the experiments that were exclusively done in voltage clamp mode. For both voltage-clamp and current-clamp recordings, PC membrane potential was held at -70mV to prevent spontaneous firing. Series resistance (5-10 MΩ) was measured before the experiment and compensated with standard procedures. During the experiment series and membrane resistances were monitored by applying a 100

ms hyperpolarizing pulse (-10 mV). Only cells with stable membrane and series resistance (change < 20% of the last 5 minutes of recordings compared to the last 5 minutes of baseline) were included in the analysis (Figure S8). Whole-cell recordings were digitized at 40 kHz and filtered with a Bessel filter at 4 kHz for voltage clamp recordings (8 kHz for current clamp mode). PF to PC LTD was induced by pairing PF stimulation at 1Hz for 1 minute with a 100 ms somatic depolarization from 70 mV to 0 mV, mimicking climbing fiber input (Linden, 2001; Saab et al., 2012), or by pairing PF stimulation at 1Hz for 5 minutes with real climbing fiber stimulation at 1Hz (Schonewille et al., 2011). Instead, PF to PC LTP was induced by PF stimulation alone at 1 Hz for 5 min. To monitor EPSC amplitude over time, two test responses to a PF pulse (with 50 ms interval) were evoked every 20s in voltage-clamp mode. In LTP experiments, cells were switched to current-clamp mode for tetanization. Paired-pulse ratio (PPR) was calculated as the ratio of the amplitude of the second evoked excitatory postsynaptic current (eEPSC) to that of the first. eEPSC amplitudes and PPR were averaged per minute and normalized for final representation. For the experiments on intrinsic excitability recordings were performed in current-clamp mode, again using an EPC-10 amplifier (HEKA Electronics). Intrinsic excitability was monitored through injection of brief steps (550 ms) of increasing depolarizing current (20 steps from 50 to 1000pA). The spike count was taken as a measure of excitability. Input resistance (Ri) was measured by injection of hyperpolarizing test currents (200 pA; 100 ms) and was calculated from the voltage transient toward the end of current injection. Recordings were excluded if the input resistance varied by > 20%.

Single channel activity was measured in cell attached configuration with pipettes between 6-8 MΩ of resistance, containing the same intracellular solution used for whole cell recordings but containing 100 µM of S-AMPA (Tocris). After reaching a patch resistance above 2 GΩ, the patch voltage clamp was decreased from close to resting potential (-60 mV approx.) to twice as negative (-120 mV approx.). In this configuration the ionic driving force across the channel was reversed and therefore the openings produced depolarizing events in the patch pipette. To determine the actual driving force across the AMPAR we broke into whole cell mode after the single channel recording was acquired and measured the cell resting potential. The driving potential, resulting from subtraction of the resting potential and clamped voltage, was used to calculate the receptor conductance. To further corroborate that the openings observed were caused by AMPARs, a subset of channels was also recorded close to resting potential voltages (-60 mV) and at 0 mV. When clamped close to cell resting potential, the driving force across the channel was minimal and the openings were no longer visible. When clamped

at 0 mV the events detected by the pipette were of similar size, but the driving force was reversed, consistent with AMPARs behavior.

For the outside-out patches of AMPA responses, pipettes with 4-6 MΩ resistance were use to establish a Giga-seal (1 GΩ resistance) with PC somata. After compensating the capacitance artifact, we let the seal rest until it reached a resistance above 2 GΩ. After breaking into whole cell mode, the pipette was slowly retracted until both the cell and the outside-out patch were re-sealed again. Every 20 seconds a 100 ms puff of 100 μM AMPA was delivered with a Picospritzer III (Parker, Hollis, USA) to generate an AMPA-dependent response. In each sweep, a 100 ms depolarizing test pulse (-10 mV) was applied in order to test series resistance and membrane capacitance. Only patches with a constant resistance over 1 GΩ were considered for analysis. Membrane capacitance was used to control for outside-out patch size, assuming a specific membrane capacitance of 0.01 pF per 1 μm2 (Schmidt-Hieber and Bischofberger, 2010). Our patches presented comparable estimated areas of 12.1±0.9 and 11.8±0.8 μm2 in control and 8-CPT containing patches, respectively (p=0.42).

Drugs and pharmacology

For mEPSC recordings, tetrodotoxin (TTX, 1 μM, Sigma) was added to the bath solution to block network activity in order to only measure excitatory spontaneous release. In order to isolate the specific contribution of AMPA and kainate receptors to glutamatergic transmission in WT and KO mice, the AMPA specific blocker GYKI52466 (30 μM, Sigma) or the kainate specific blocker SYM2081 (5 μM, Sigma) were added to the extracellular bath solution. For pharmacological investigation of the cAMP-GluA3 dependent pathway the following membrane permeable drugs were added to the bath of ACSF: 50 μM Forskolin (adenylyl cyclase activator, Sigma), 20 μM H89 (PKA antagonist, Tocris), 5 μM KT5720 (PKA antagonist, Sigma), and 10 μM ESI-05 (EPAC antagonist, BioLog). In addition, we applied the membrane non-permeable agonist for EPAC, 8-CPT-2Me-cAMP (20 μM, Tocris Bioscience) to the intracellular whole cell recording solution to investigate the postsynaptic impact of EPAC. In order to obtain a monophasic time decay of the AMPA-evoked responses in outside-out patches we added a final mixture of 80 μM PEPA (AMPAR flop splice variant desensitization blocker, Tocris bioscience) and 100 μM cyclothiazide (CTZ, AMPAR flip splice variant desensitization blocker, Tocris bioscience) to the bath solution.

Analysis of cell physiological data

Spontaneous mEPSC and evoked EPSC recordings were analyzed with MiniAnalysis software (Synaptosoft) and ClampFit (Molecular Devices), respectively. To calculate τ_{fast} (fast desensitizing component) and τ_{slow} (slow non-desensitizing component) of AMPA evoked currents in outside-out patches a double exponential function was fitted using ClamPFit with DC offset set at 0. The decay of the averaged current was fitted to the following equation:

In this equation $\tau 1$ represents τ_{fast}. The percentage of the decay represented by the slow component ($\%_{slow}$) was calculated by the function A1/(A1+A2), as described elsewhere (Christian et al., 2013). The weighted decay time constant for AMPA evoked currents in outside-out patches in the presence of desensitization blockers was calculated by dividing the total charge transfer (in fC) by the peak amplitude (in pA). Non-stationary fluctuation analysis of outside-out patches traces was carried out following previously described methods (Alvarez et al., 2002; Benke et al., 2001; Hartveit and Veruki, 2007). In short, peak aligned AMPA evoked currents recorded over 10-15 sweeps per outside-out patch were binned in 10 equally sized bins of 150 ms each and for each bin the mean amplitude and variance were calculated. The data distribution resulting after plotting amplitude versus variance was fitted with the following equation:

Where the variance (σ^2) of the amplitude of the current (I) obtained at each time point is explained as a function of the single unitary current (i) and the number of functional conducting channels (N) with an offset given by the variance of the baseline noise (σ^2_b). The number of funtional channels was extracted from the derivative at I = 0, and the single channel conductance was calculated by dividing the unitary current by the applied voltage with respect to the reversal potential ($V_{holding}$-$E_{reversal}$, -70 mV and 0 mV, respectively). The peak open probability (P_o), which corresponds to the fraction of available functional channels open at the time of the peak current (I_{peak}), was calculated from the following equation:

In this equation N_{max} represents the theoretical maximum of available channels opened at the point where the theoretical maximum amplitude reaches the minimum variability (σ^2_b) in the given parabola fit.

Single channel activity was analyzed using ClampFit (Molecular Devices). Three detection thresholds were used to detect O1 (1.5 pA), O2 (3 pA) and O3 (4.5 pA) openings in single channel AMPA receptors in steady baseline recordings (no holding current fluctuations). Events with a latency shorter than 0.3 ms were ignored to prevent noise to be recognized as openings.

Statistics

For statistical analysis of behavioral and in-vitro electrophysiological data we used either Matlab statistical toolbox (The MathWorks Inc., Natick, MA, 2000) or GraphPad Prism 6 (La Jolla, California, USA). Although Matlab always reports exact p-values, GraphPad Prism 6 does not report exact values when $p < 0.0001$. Thus we have reported exact p-values when possible, taken into consideration the limitation explained above.

In-vitro two-photon imaging

Organotypic cerebellar slices were made from P7-9 mice using a protocol adapted from previous studies (Hurtado de et al., 2011; Stoppini et al., 1991) and kept in culture 4-7 days prior to the experiments. Slices were then transfected with sindbis virus expressing rat flip GluA3 AMPAR fused to the pH sensitive version of GFP Super Eccliptic pHluorophor (GluA3-SEP) for a period of 24-48 hours prior to the imaging session. Electrophysiological recordings of PC mEPSCs were performed in this preparation. In our hands, mEPSC amplitudes and frequencies were consistently higher in organotypic cultured PCs than in acute (e.g. Fig 2B and 4B, WT-Acute vs. WT-Organotypic $p = 0.0002$ and $p < 0.0001$ for amplitude and frequency, respectively), using the same concentration of TTX and PTX. For imaging, slices were transferred from the incubation solution to the recording chamber containing ACSF (same composition as mentioned before but with 4 µM calcium and 4 µM magnesium). Three-dimensional images were collected on a custom-built two-photon microscope based on a Fluoview laser-scanning microscope (Olympus). The light source was a mode-locked Ti:sapphire laser (Chameleon, Coherent) tuned at 850 nm using a 60x objective. Optical sections were captured every 0.5 µm from transfected PC dendrites. Fluorescence intensity was quantified from projections of stacked sections using ImageJ software (NIH). For single spine bleaching in the FRAP experiments, a ROI was selected covering the surface of a single spine, which was used to target the laser for 20-30 seconds (with the same intensity as for regular imaging).

In-vivo electrophysiology

Mice (males, 4-6 month old) were prepared for chronic experiments as described previously (Wulff et al., 2009). In short, under general anesthesia a pedestal with a magnet was placed on the frontal and parietal bones of the animal, and a recording chamber was constructed around a small craniotomy in the left occipital bone. After 2 days of recovery, animals were habituated in the setup for 20 min for two days. During the experiments, the animals were alert and immobilized in a custom restrainer. Extracellular activities were recorded with glass micropipettes filled with 2M NaCl solution and advanced into the cerebellar cortex from the surface of Crus I and II. Electrode signals were filtered, amplified and stored for off-line analyses (Spike2, CED, and Cambridge, UK). PCs were identified by the occurrence of both simple spikes and complex spikes, and single-unit activity was confirmed by a brief pause in simple-spike firing following each complex spike (i.e. climbing fiber pause; see De Zeeuw et al., 2011). The whole field visual stimulation was presented by rotating a cylindrical screen (diameter 63 cm) with a random-dotted pattern (each element 2°) at 0.6 Hz with an amplitude of 5°. Offline analysis was conducted in Matlab (Mathworks, Natick, MA, USA). CV2 of simple spikes was calculated as the mean value of (2 × (ISIn+1 - ISIn))/ (ISIn+1 + ISIn) (Wulff et al., 2009). Modulation of simple spikes and complex spikes was calculated as the amplitude of the sine wave fitted to the histogram of spike rate. Statistical analysis was done using Student's t-test with SPSS (IBM Corporation, Armonk, NY, USA).

REFERENCES

Alvarez, O., Gonzalez, C., and Latorre, R. (2002). Counting channels: a tutorial guide on ion channel fluctuation analysis. Adv. Physiol Educ. *26*, 327-341.

Benke, T.A., Luthi, A., Palmer, M.J., Wikstrom, M.A., Anderson, W.W., Isaac, J.T., and Collingridge, G.L. (2001). Mathematical modelling of non-stationary fluctuation analysis for studying channel properties of synaptic AMPA receptors. J. Physiol *537*, 407-420.

Christian, C.A., Herbert, A.G., Holt, R.L., Peng, K., Sherwood, K.D., Pangratz-Fuehrer, S., Rudolph, U., and Huguenard, J.R. (2013). Endogenous positive allosteric modulation of GABA(A) receptors by diazepam binding inhibitor. Neuron *78*, 1063-1074.

Cossart, R., Epsztein, J., Tyzio, R., Becq, H., Hirsch, J., Ben-Ari, Y., and Crepel, V. (2002). Quantal release of glutamate generates pure kainate and mixed AMPA/kainate EPSCs in hippocampal neurons. Neuron *35*, 147-159.

de Jeu, M., and De Zeeuw, C.I. (2012). Video-oculography in mice. J. Vis. Exp. e3971.

Hartveit, E., and Veruki, M.L. (2007). Studying properties of neurotransmitter receptors by non-stationary noise analysis of spontaneous postsynaptic currents and agonist-evoked responses in outside-out patches. Nat. Protoc. *2*, 434-448.

Hurtado de, M.T., Balana, B., Slesinger, P.A., and Verma,I.M. (2011). Organotypic cerebellar cultures: apoptotic challenges and detection. J. Vis. Exp.

Kerchner, G.A., and Nicoll, R.A. (2008). Silent synapses and the emergence of a postsynaptic mechanism for LTP. Nat. Rev. Neurosci. *9*, 813-825.

Linden, D.J. (2001). The expression of cerebellar LTD in culture is not associated with changes in AMPA-receptor kinetics, agonist affinity, or unitary conductance. Proc. Natl. Acad. Sci. U. S. A *98*, 14066-14071.

Saab, A.S., Neumeyer, A., Jahn, H.M., Cupido, A., Simek, A.A., Boele, H.J., Scheller, A., Le, M.K., Gotz, M., Monyer, H., Sprengel, R., Rubio, M.E., Deitmer, J.W., De Zeeuw, C.I., and Kirchhoff, F. (2012). Bergmann glial AMPA receptors are required for fine motor coordination. Science *337*, 749-753.

Schmidt-Hieber, C., and Bischofberger, J. (2010). Fast sodium channel gating supports localized and efficient axonal action potential initiation. J. Neurosci. *30*, 10233-10242.

Stahl, J.S., van Alphen, A.M., and De Zeeuw,C.I. (2000). A comparison of video and magnetic search coil recordings of mouse eye movements. J. Neurosci. Methods *99*, 101-110.

Stoppini, L., Buchs, P.A., and Muller, D. (1991). A simple method for organotypic cultures of nervous tissue. J. Neurosci. Methods *37*, 173-182.

Yan, D., Yamasaki, M., Straub, C., Watanabe, M., and Tomita, S. (2013). Homeostatic control of synaptic transmission by distinct glutamate receptors. Neuron *78*, 687-699.

4

Chapter 5

Noradrenergic Signalling Triggers the Activation of GluA3-Plasticity in the Hippocampus

Maria C. Renner[1,3], Eva H.H. Albers[1,3], Carla M. da Silva-Matos[1,2], Daniel Amado-Ruiz[1], Niels R. Reinders, Aile N. van Huijstee[1], Tessa R. Lodder[1], and Helmut W. Kessels[1,*]

[1] The Netherlands Institute for Neuroscience, Royal Netherlands Academy of Arts and Sciences, 1105 BA, Amsterdam, The Netherlands.

[2] Erasmus University Medical Center, Dept. of Neuroscience, Rotterdam, The Netherlands

[3] Co-first author

*Correspondence: h.kessels@nin.knaw.nl

SUMMARY

AMPA receptors are responsible for fast excitatory synaptic transmission in the brain. In CA1 pyramidal neurons of the hippocampus two types of AMPA receptors predominate: those that contain subunits GluA1 and GluA2, and those that contain subunits GluA2 and GluA3. GluA1-containing AMPA receptors have been extensively studied and are known to play a key role in several forms of synaptic plasticity and memory formation. In contrast, the contribution of GluA3 to synapse physiology in the hippocampus has remained elusive. Here we show that during fear, the activation of beta-adrenergic receptors triggers a massive and transient synaptic potentiation of GluA3-mediated currents. Our results further indicate that the beta-adrenergic activation of GluA3-containing AMPA receptors promotes the retrieval of fear memories.

INTRODUCTION

Memory formation involves the selective strengthening of groups of synapses within neuronal circuits that are activated during an experience. The encoding of memories is thought to depend on the long-term potentiation (LTP) and long-term depression (LTD) of synaptic strength (Nabavi et al., 2014; Whitlock, Heynen, Shuler, & Bear, 2006). LTP and LTD can be expressed by a change in the number of postsynaptic AMPA-type glutamate receptors (AMPARs) (Huganir & Nicoll, 2013; Malinow & Malenka, 2002). AMPAR channels are formed through the assembly of four AMPAR subunits. In excitatory neurons of the mature hippocampus, the majority of AMPARs consist of subunits GluA1 and GluA2 (GluA1/2 heteromers) or GluA2 and GluA3 (GluA2/3 heteromers) (Wenthold, Petralia, & Niedzielski, 1996).

GluA1-containing AMPARs play an essential role in several forms of experience-dependent plasticity (Kessels & Malinow, 2009). GluA1 is inserted into synapses upon the induction of LTP or the formation of fear memories; a selective blockade of GluA1 trafficking impairs LTP and memory formation (Mitsushima, Ishihara, Sano, Kessels, & Takahashi, 2011; Rumpel, LeDoux, Zador, & Malinow, 2005). In line with this, LTP and the formation of fear memories are severely impaired in GluA1-deficient mice (Humeau et al., 2007). In contrast to the short cytoplasmic tails (C-tails) of GluA2 or GluA3, the GluA1 subunit has a long C-tail that contains several unique phosphorylation sites by which the trafficking of GluA1 to synapses can be regulated. For instance, the C-tail of GluA1 can be phosphorylated by protein kinase A (PKA), which lowers the threshold for LTP and facilitates the formation of memories (Crombag et al., 2008; Hu et al., 2007; Qian et al., 2012). Such activation by PKA can occur following activation of beta-adrenergic receptors (β-ARs) by norepinephrine (NE), which leads to activation of adenylyl cyclases, producing a rise in intracellular cyclic AMP (cAMP) (Hall, 2004; Vanhoose & Winder, 2003). Whereas the role of GluA1 in synaptic plasticity and learning is well established, the role of GluA3-containing AMPARs has remained unclear. In hippocampal neurons that lack GluA3, LTP and LTD are intact (Meng, Zhang, & Jia, 2003) and the capacity of GluA3-deficient mice to acquire fear memories is comparable to wild-type congenics (Adamczyk et al., 2012; Humeau et al., 2007). Although GluA3-deficient mice show few apparent physiological and behavioral abnormalities, they do show altered electroencephalographic and respiratory patterns during sleep (Steenland, Kim, & Zhuo, 2008) and reduced alcohol-seeking behaviour (Sanchis-Segura et al., 2006). Interestingly, the presence of GluA3 is required for amyloid-β, the prime suspect to cause Alzheimer's disease (AD), to mediate synaptic and memory deficits (Reinders et al., 2016).

There are currently two theories on the relevance of having two different types of AMPARs in excitatory neurons. One model dictates that LTP and learning involve synaptic trafficking of GluA1-containing AMPARs, whereas GluA3-containing AMPARs are constitutively replacing AMPARs at synapses independently of neuronal activity (McCormack, Stornetta, & Zhu, 2006; Shi, Hayashi, Esteban, & Malinow, 2001). In this model GluA3-containing AMPARs are implicated to participate in homeostatic scaling of synaptic strength (Makino & Malinow, 2011; Rial Verde, Lee-Osbourne, Worley, Malinow, & Cline, 2006). The second model states that in essence any type of AMPAR can be inserted into synapses upon LTP induction (Granger, Shi, Lu, Cerpas, & Nicoll, 2013) and therefore AMPARs can contribute to learning in a manner independent of subunit composition. In this model, the observation that GluA1-containing AMPARs dominate in mediating synaptic strengthening is explained by the notion that GluA3-containing AMPARs contribute little to synaptic and extrasynaptic AMPAR currents in hippocampal pyramidal cells (Lu et al., 2009).

A recent paper by our lab (Renner et al., 2017) essentially combined these two models, showing that, in mice, GluA3-containing AMPARs are present at CA1 synapses in hippocampal slices, but transmit no or low currents upon glutamate binding under basal conditions; when intracellular cyclic AMP (cAMP) levels rise, GluA2/3 channels shift to a high-conductance state, leading to synaptic potentiation. This cAMP-driven synaptic potentiation requires the activation of both protein kinase A (PKA) and the GTPase Ras. In addition, β-AR activation was shown to be able to evoke GluA3-dependent plasticity upon a robust increase in cAMP levels and NE-release induces potentiation of GluA2/3-currents at CA1 pyramidal synapses in the hippocampus. However, how exactly GluA3-plasticity contributes to memory processing in the hippocampus remains unknown.

In this study, we elaborate on these previous findings. We show that GluA3-plasticity is activated under physiological conditions in a β-AR dependent fashion, leading to synaptic potentiation. Additionally, we show that this NE-driven plasticity of GluA3-containing AMPARs does not contribute to the formation of a fear memory, but instead facilitates the retrieval of a fear memory.

MATERIALS AND METHODS

Mice

GluA3-deficient (GluA3-KO) and wild-type littermate colony was established from c57bl6x129P2-Gria3tm1Dgen/Mmnc mutant ancestors (MMRRC, Davis, CA), which were at least 6 times backcrossed to c57bl6 mice. GluA1-deficient (GluA1-KO) mice were a kind gift from Dr. R. Huganir (Kim et al., 2005), and a colony was generated by mating heterozygous c57bl6/129 mice. For spine density experiments, mice were crossed to Thy1-eYFP transgenic mice (Porrero, Rubio-Garrido, Avendaño, & Clascá, 2010). GluA1xGluA3 double deficient colony was established by crossing homozygote GluA1-deficient males with heterozygote GluA3 females. Floxed GluA3 mice were a kind gift from Dr. R. Sprengel (Sanchis-Segura et al., 2006) and maintained in a homozygous colony. Mice were kept on a 12-hours day-night cycle (light onset 7 am) and had ***ad libitum*** access to food and water. All experiments were conducted in line with the European guidelines for the care and use of laboratory animals (Council Directive 86/6009/EEC). The experimental protocol was approved by the Animal Experiment Committee of the Royal Netherlands Academy of Arts and Sciences (KNAW).

Electrophysiology

Acute hippocampal slices were prepared from 6 to 8 week-old mice when used for experiments involving fear conditioning and/or IP injections, or from 3 to 5 week-old mice when used for purely in vitro experiments. Dissection was done in ice-cold sucrose cutting solution containing (in mM): 2.5 KCl, 1.25 NaH_2PO_4, 26 $NaHCO_3$, 10 D-glucose, 230 Sucrose, 0.5 $CaCl_2$, 10 $MgSO_4$, bubbled with 95%O_2/5%CO_2. Brain slices (400 µm) were cut using a vibratome (Thermo Scientific) and placed in a holding chamber containing ACSF supplemented with (in mM) 1 $MgCl_2$, 2 $CaCl_2$, 20 glucose and bubbled with 95%O_2/5%CO_2. They were allowed to recover at 34°C for 40 min then at room temperature for at least 40 min. Whole-cell recordings (3-5 MΩ pipettes, R_{access} < 26 MΩ, and R_{input} > 10 x R_{access}) were made in ACSF containing TTX (1 µM) and picrotoxin (50 µM) at 28°C. IBMX (50 µM; Tocris) and isoproterenol (10 µM; Sigma) were added to the perfusion solution where indicated. Data was acquired using a Multiclamp 700B amplifier (Molecular Devices). mEPSC recordings were analyzed with MiniAnalysis (Synaptosoft). Individual events were manually selected, and an amplitude threshold of 5 pA was used. Evoked recordings were analyzed using pClamp 10 software (Molecular Devices). During evoked recordings, a cut was made between CA1 and CA3, and picrotoxin (50 µM) and 2-chloroadenosine (4 µM; Tocris) were added to the bath. Two stimulating electrodes, two-contact Pt/Ir cluster electrode

(Frederick Haer), were placed between 100 and 300 µm down the apical dendrite, 100 µm apart, and 200 µm laterally in opposite directions. AMPAR-mediated EPSCs were measured as the peak inward current at -60 mV. Paired pulse ratios were achieved by an interpulse interval of 50 ms. NMDAR-mediated EPSC were measured as the mean outward current between 40 and 90 ms after the stimulation at +40 mV, and corrected by the current at 0 mV. Rectification was calculated as the ratio of the peak AMPAR current at -60 and +40 mV, corrected by the current at 0 mV, in the presence of D-APV (100 µM; Tocris) in the bath and Spermine (0.1 mM; Sigma) inside the pipette. EPSC amplitudes were obtained from an average of at least 50 sweeps at each holding potential. The quantal content $1/CV^2$ was calculated as M^2/σ^2, where M and σ^2 are the mean amplitude and the variance of the EPSCs respectively, and is determined by the probability of presynaptic release (P_r) and the number of active synapses (N), but is independent of postsynaptic strength (I_{ps}), which has been experimentally validated in the CA1 region of the hippocampus (Manabe, Wyllie, Perkel, & Nicoll, 1993). Assuming a binomial model of transmitter release, $1/CV^2$ can be described using the following formula:

$$\frac{1}{CV_2} = N * \frac{n * P_r - P_r}{n - n * P_r}$$

Contextual Fear Conditioning Protocol and E-injection

For fear conditioning experiments, a box (29 cm high, 31.5 cm wide, 23 cm deep) with two metal walls, two transparent Plexiglas walls and grid floor with stainless steel bars through which the foot shock was delivered was used. The box was placed inside a sound-attenuating chamber (Med Associates Inc., Georgia, VT). The box was cleaned with 70% ethanol before each trial. During the training session, 6 to 8 weeks old mice were placed in the box. After 2 min, they were given 3 consecutive shocks (0.80 mA for most of the experiments except Figure 5F and Figure 6: 0.65 mA,1 sec duration, 1 min interval). They remained in the box 2 min after the last shock. For in vitro experiments either 10 minutes or 2 hours after the session the mice were decapitated and brain slices were obtained. For behavioral experiments mice were re-exposed to the fearful context at the specific time of testing. Freezing and motion were quantified using Matlab-based custom-made software (Kopec, Real, Kessels, & Malinow, 2007). To test generalization of fear memories the mice were put in two different contexts. The shock context was the regular fear conditioning box, cleaned with 70% ethanol. The neutral context was a modified version of the fear conditioning box. The walls consisted of circle-shaped white Plexiglas surrounding the walls, a white Plexiglas plate on the

floor and the cage was cleaned with citric acid. For E injections (±)-Epinephrine hydrochloride (0.5mg/kg, Sigma-Aldrich) was dissolved in saline (0.9%, NaCl) and injected intraperitoneally (5ml/kg).

Stereotactic hippocampal viral injections

Adeno-associated virus (AAV) with a titer between 1012-1013 particles/ml were produced from AAV5-pSynapsin1-GFP and AAV5-pSynapsin1-CreGFP, AAV1-pCaMKII-GFP and AAV1-pCaMKII-SEP-GluA1, or AAV5-pCaMKII-GFP and AAV5-pCaMKII-SEP-GluA3. The AAV1-pCaMKII-SEP-GluA1 and AAV5-pCaMKII-SEP-GluA3 were constructed without a WPRE element due to packaging-size restrictions. Three to four week-old mice were anesthetized with isofluorane (induction 5%, maintenance 2%) and positioned in a stereotaxic apparatus, kept on a heating pad. Bilateral hippocampal injections of viral solutions (3 injection sites per side; 400 nl per site; AP: -1.5, -1.7, -1.9; L: ±1.5; DV: 1.2 mm) were delivered with a glass micropipette through a hole drilled in the skull by pressure application (Nanoject II, Auto-Nanoliter Injector, Drummond Scientific). Experiments were performed at least 3 weeks after viral injections.

Two-photon Laser Scanning Microscopy

Organotypic GluA3-deficient slices were sparsely infected with Sindbis virus expressing rat GluA3(flip) tagged with SEP, and were allowed to express for 20–28 hours. Threedimensional images were collected on a custom-built two-photon microscope based on a Fluoview laser-scanning microscope (Femtonics). The light source was a mode-locked Ti:sapphire laser (Chameleon, Coherent) tuned at 910 nm using a 60x objective. Optical sections were captured every 1 µm from infected CA1 pyramidal cell bodies or apical dendrites past the point of bifurcation of primary to secondary dendrites, approximately 300 µm from the cell body. Fluorescence intensity was quantified from projections of stacked sections using ImageJ software (NIH).

Spine Analysis

For spine density measurement Thy1-eYFP positive wild-type, GluA1-deficient or GluA3-deficient mice were anesthetized with pentobarbital and perfused with 20 ml 0.1 M PBS followed by 80 ml of fixative (4% paraformaldehyde in 0.1 M PBS, pH 7.2). Brains were removed, post-fixed for 1 hour in fixative, washed and stored in PBS at 4°C. Coronal 50 µm-thick slices were prepared with a vibratome (Leica). They were mounted and covered with Vectashield mounting medium (Vector Labs). Z-stack images were made using a confocal microscope (Leica SP5) and analyzed with ImageJ software. Spine density was manually quantified and

spine size (i.e. spinehead diameter) was measured from reconstructed dendrites (Neurolucida, MBF Bioscience) made by an experimenter blind to experimental conditions and genotype.

Statistics

Data sets were Log-transformed and normal distributions were obtained. These were analyzed using two-tailed Student t tests to compare 2 conditions or ANOVAs with post-hoc Tukey comparisons for comparing more than 2 conditions. ***P*** values below 0.05 were considered statistically significant.

RESULTS

GluA3-plasticity is induced by a fear conditioning experience

Fear induced in mice by foot shocks in an unfamiliar context triggers the acute release of NE in the hippocampus, which peaks approximately 10 minutes after delivery of the shocks (Bremner, Krystal, Southwick, & Charney, 1996; McIntyre, Hatfield, & McGaugh, 2002), leading to synaptic strengthening in the CA1 region of the hippocampus (Whitlock et al., 2006; Zhou, Conboy, Sandi, Joëls, & Krugers, 2009). To assess whether such fear elicits GluA3-plasticity at CA1 neurons, brain slices were prepared 10 minutes after mice received three electric shocks as an aversive stimulus. Fear conditioning was not accompanied by changes in spine density or average spine size at apical dendrites (Figure 1). Whole-cell recordings on CA1 pyramidal neurons revealed that fear conditioning induced a significant increase in AMPA/NMDA ratio at CA1 synapses that receive Schaffer collateral input (Sc-CA1; Figure 2A), but not at those receiving perforant path input (pp-CA1; Figure 2B). No decrease in paired-pulse ratio was measured (Figure 2A,B), suggesting that predominantly postsynaptic strengthening at Sc-CA1 synapses can be detected in slices. We analyzed the variance-to-mean ratio (VMR) and the coefficient of variation (CV) to further dissect the contributions of presynaptic release probability (***P***r), post-synaptic currents (***I***ps) and number of active synapses (***N***) to synaptic changes. The VMR is independent of ***N*** and relates to the average synapse strength as: (1-***P***r)×***I***ps. The VMR of AMPAR currents increased without a change in VMR of NMDAR currents (Figure 2C), suggesting postsynaptic strengthening of AMPAR currents. The quantal content ($1/CV^2$) ratio of AMPAR to NMDAR components did not change (Figure 2D), indicating that the synaptic potentiation occurred without unsilencing synapses. In mEPSC analysis the post-synaptic strengthening was reflected as a significant increase in mEPSC frequency ($p<0.0001$; Figure 2E) in the majority of CA1 pyramidal

neurons (Figure 3), but not in average mEPSC amplitude (p=0.6; Figure 2E). When wild-type mice were injected with β-AR antagonist propranolol 30 minutes prior to fear conditioning, the increase in mEPSC frequency in slices prepared 10 minutes after administering foot shocks was significantly reduced compared to saline-injected control mice (p=0.02; Figure 2F), indicating that fear-induced plasticity relies in part on β-AR activation. The synaptic potentiation of CA1 neurons elicited by the fearful experience was transient: in acute slices prepared 2 hours after fear conditioning mEPSC frequencies had returned to baseline levels (Figure 2E).

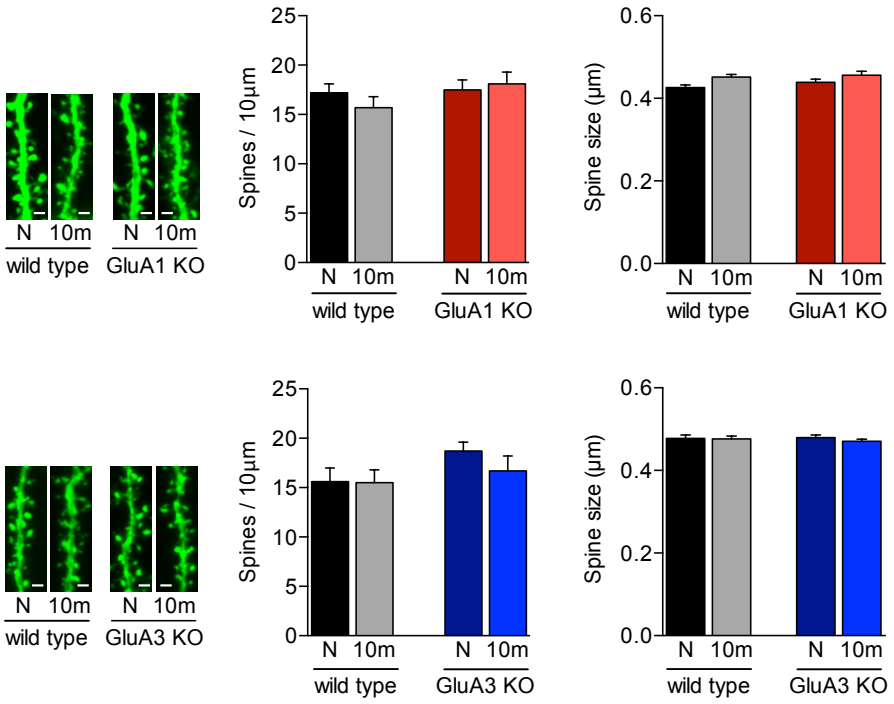

Figure 1. Fear conditioning didn't cause changes in spine density or average spine size at apical dendrites of CA1 neurons

No significant changes in spine density or average spine size at Sc-CA1 synapses 10 minutes after fear conditioning. Spine densities were counted on apical dendrites of Thy1-eYFP-expressing CA1 pyramidal neurons from GluA1-KO (N: n=44 neurons (3 mice), 10m: n=29(2)) and WT littermates (N: n=57(4), 10m: n=38(3)), and from GluA3-KO (N: n=55 dendrites (5 mice), 10m: n=43(4)) and WT littermates (N: n=32(3), 10m: n=43(4)) sacrificed naïve (N) or 10 minutes after fear conditioning. Scale bars indicate 1 µm. Error bars indicate SEM.

Fear conditioning was shown to induce synaptic trafficking of GluA1-containing AMPARs to Sc-CA1 synapses (Mitsushima et al., 2011). To study whether also GluA1-independent forms of synaptic plasticity are elicited, GluA1-deficient mice were fear conditioned. Although AMPA/NMDA ratios and paired pulse ratios remained unchanged in the absence of GluA1 (Figure 2A,B), synaptic changes did take place at Sc-CA1 synapses. Firstly, the VMR of AMPAR currents decreased in GluA1-deficient neurons after fear conditioning (Figure 2C). Since the VMR of NMDAR currents did not change (Figure 2C), these data suggest that fear conditioning leads to postsynaptic weakening at Sc-CA1 synapses in the absence of GluA1. Secondly, the quantal content ($1/CV^2$) AMPAR to NMDAR ratio shows that a substantial proportion of Sc-CA1 synapses were AMPAR silent in GluA1-deficient mice and became unsilenced after fear conditioning (Figure 2D). These data suggest two separate events took place at Sc-CA1 synapses of GluA1-deficient mice: synaptic weakening and unsilencing of synapses.

Figure 2. Fear conditioning triggers GluA3-plasticity at CA1 synapses
(A-H) Acute brain slices were prepared from naïve mice (N) or from littermate mice 10 min or 2 h after they received a fear conditioning session consisting of three electric shocks of 0.80mA. (A) Schaffer collateral (Sc) stimulation onto CA1 synapses depicted as AMPA/NMDA ratios of WT (N: black, n=11; 10m: grey, n=14) and GluA1-KO neurons (N: dark red; n=9, 10m: light red, n=10) and paired pulse ratios of WT (N: n=11, 10m: n=13) and GluA1-KO neurons (N: n=9, 10m: n=10). (B) Perforant path (Pp) stimulation onto CA1 synapses depicted as AMPA/NMDA ratios of WT (N: n=7, 10m: n=16) and GluA1-KO neurons (N: n=21, 10m: n=19) and paired pulse ratios of WT (N: n=6, 10m: n=15) and GluA1-KO neurons (N: n=10, 10m: n=10). (C) Variance-to-mean ratio (VMR) at Sc-CA1 synapses of AMPAR currents from WT (N: n=11, 10m: n=11) or GluA1-KO neurons (N: n=9, 10m: n=9), and of NMDAR currents from WT (N: n=9, 10m: n=9) or GluA1-KO neurons (N: n=9, 10m: n=9). (D) 1/CV2 AMPAR to 1/CV2 NMDAR ratios shows unsilencing of Sc-CA1 synapses at GluA1-KO neurons (N: n=8, 10m: n=9), but not at WT neurons (N: n=9, 10m: n=6). (E) mEPSC frequency and amplitude recorded from WT (N: n=29, 10m: n=12, 2h: n=21) and GluA1-KO (N: n=29, 10m: n=19, 2h: n=30) CA1 neurons. (F) WT and GluA1-KO mice were injected with propranolol or vehicle 30 min prior to fear conditioning and brain slices were prepared 10 min after conditioning. mEPSC frequencies and amplitudes were recorded from WT (Veh: n=22, Prop: n=16) and GluA1-KO (Veh: n=10, Prop: n=9) CA1 neurons. (G) mEPSC frequency and amplitude recorded from WT (N: n=15, 10m: n=18, 2h: n=16) and GluA3-KO (N: n=22, 10m: n=22, 2h: n=10) CA1 neurons. (H) flGluA3 mice stereotactically injected with AAV virus were subjected to fear conditioning, and 10 min later brain slices were prepared. Average mEPSC frequencies and amplitudes of CA1 neurons expressing Cre-GFP (n=11) or GFP (n=15). Error bars indicate SEM, * indicates $p<0.05$.

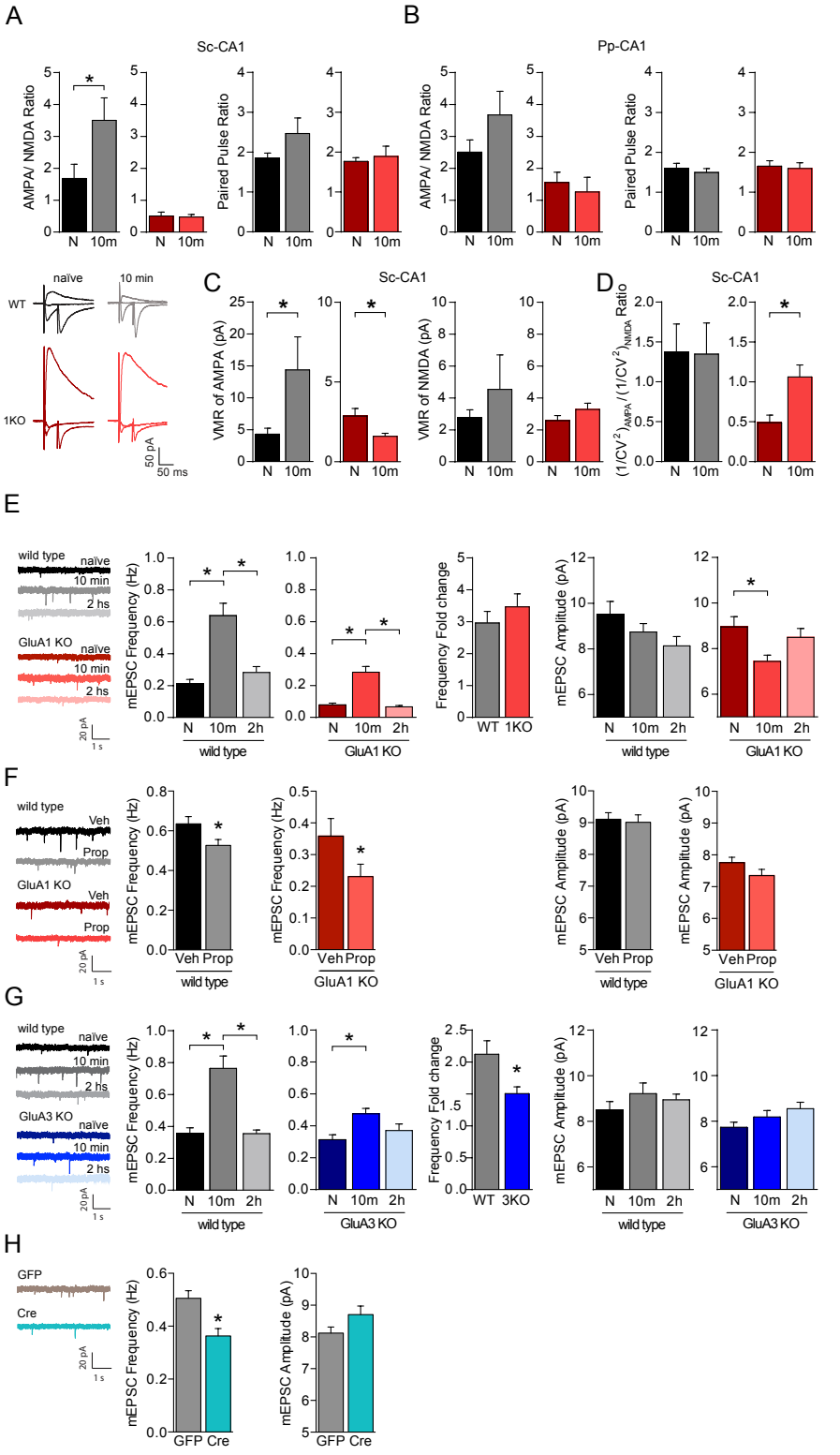
A
Sc-CA1
AMPA/ NMDA Ratio
Paired Pulse Ratio
N 10m
B
Pp-CA1
naïve
10 min
WT
1KO
50 pA
50 ms
C
Sc-CA1
VMR of AMPA (pA)
VMR of NMDA (pA)
D
Sc-CA1
(1/CV²)AMPA / (1/CV²)NMDA Ratio
E
wild type
naïve
10 min
2 hs
GluA1 KO
mEPSC Frequency (Hz)
Frequency Fold change
WT 1KO
mEPSC Amplitude (pA)
N 10m 2h
wild type
GluA1 KO
F
Veh
Prop
Veh Prop
G
GluA3 KO
GluA3 KO
WT 3KO
H
GFP
Cre
GFP Cre

In accordance with this, fear conditioning induced both a decrease in average mEPSC amplitude and an increase in mEPSC frequency at the majority of CA1 neurons from GluA1-deficient mice (Figure 2E and Figure 3). The increase in mEPSC frequency in GluA1-KO was smaller in absolute size compared with that in slices from wild-type littermates, but similar in relative magnitude, and required β-AR activation (Figure 2F and Figure 3). These experiments suggest that in the absence of GluA1 fear conditioning causes both an activation GluA2/3 channels and the removal of GluA2/3s from synapses. To further examine whether fear conditioning induced GluA3-plasticity in the hippocampus, we also recorded mEPSCs in brain slices isolated from GluA3-deficient and wild-type littermates. In CA1 neurons of GluA3-deficient mice an increase in mEPSC frequency was observed in slices isolated 10 minutes after fear conditioning that was substantially smaller in magnitude than that in CA1 neurons of wild-type littermates (p=0.005; Figure 2G; also Figure 3), indicating that GluA3-plasticity was induced in the CA1 region of the hippocampus of the wild-type mice. When looking at the distribution of the mEPSC frequency, it is visible a population shift 10 minutes after fear conditioning in wild-type neurons and GluA1-KO neurons, but not in GluA3-KO neurons, indicating that the majority of neurons show an increase in mEPSC frequency after fear conditioning (Figure 3).

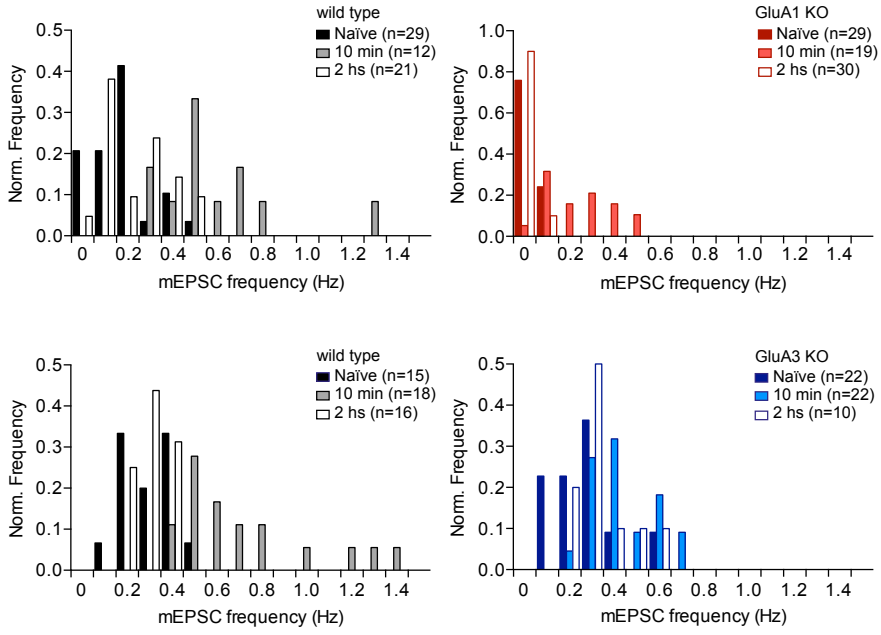

Figure 3. NE release increases mEPSC frequency in the majority of CA1 neurons
GluA3 plasticity is induced in the majority of CA1 neurons in acute slices prepared from mice 10 min after fear conditioning. Histograms of mEPSC show a population shift 10 min after fear conditioning in WT neurons (left) and GluA1-KO neurons (right top), but not in GluA3-KO neurons (right bottom).

Similarly, when GluA3 was knocked out by Cre-expression selectively in the CA1 region of flGluA3 mice after development, the increase in mEPSC frequency from Cre-positive cells of slices isolated 10 minutes after fear conditioning was significantly smaller compared with neurons expressing GFP as a control ($p=0.001$; Figure 2H).

In summary, we conclude that three different types of plasticity take place at Sc-CA1 synapses upon fear conditioning: 1) GluA1-dependent LTP-like synaptic strengthening, 2) LTD-like synaptic weakening, and 3) GluA3-plasticity through the activation of β-ARs.

GluA3-plasticity does not contribute contextual fear conditioning

We next aimed to assess whether GluA3-plasticity contributes to the formation of contextual fear memories. Mice were allowed to explore a novel environment whereupon they received three electric shocks. In wild-type mice the fear conditioning protocol led a similar freezing response either immediately after receiving the shocks (Figure 4A) or when re-exposed to the shock cage at varying time-points after conditioning (Figure 4B), indicating that contextual fear memories were formed that remained stable over time. Note that each group of littermate mice was tested only once to avoid effects of extinction or habituation in the fear response (see methods). GluA1-deficient mice did not show a freezing response immediately following the shocks ($p<0.0001$; Figure 4A) or following re-exposure to the shock-cage 10 minutes after conditioning ($p<0.0001$; Figure 4B). Injecting GluA1-deficient mice with epinephrine (or saline as a control) shortly before conditioning did not increase freezing levels (Figure 4C), indicating that the inability of GluA1-deficient mice to form short-term contextual fear memories is not improved by promoting GluA3-plasticity during learning. Interestingly, GluA1-deficient mice were able to gradually develop long-term contextual fear memories, although they never reached the freezing levels of wild-type littermates (Figure 4B). A similar time-course of slowly developing fear responses was observed in mice that lack both GluA1 and GluA3 (Figure 4D), indicating that these delayed memories relied on plasticity mechanisms that did not involve GluA1 or GluA3. To assess whether the memory impairment of GluA1-deficient mice originates from disrupted plasticity during development, AAV virus expressing SEP-GluA1 or GFP under control of the CaMKII-promoter was injected in the hippocampi of 3-4 week old mice (Figure 5). When tested at the age of 2 months, the ability to freeze when exposed to the fearful context was rescued for mice that expressed SEP-GluA1 selectively in excitatory hippocampal neurons (Figure 4E), indicating that GluA1-plasticity in the mature hippocampus is sufficient for creating contextual fear

memories. These data infer that GluA2/3s cannot compensate for the absence of GluA1-containing AMPARs to generate short-term contextual memories.

The behavior of GluA3-deficient mice during the fear conditioning protocol was normal: their locomotor activity was similar to wild-type littermates when placed in a novel environment (p=0.9) and their startle response to the shocks did not differ (p=0.8, Figure 4F). Their freezing levels were similar to those of wild-type littermates when re-exposed to the shock-cage either 10 minutes (p>0.9) or 2 hours (p=0.4) after fear conditioning (Figure 4G). GluA3-plasticity did not contribute to the formation or stability of long-term fear memories; if anything, long-term memories tended to be improved in GluA3-deficient mice compared to wild-type littermates (Figure 4G). The fear responses were equally context-specific for wild-type and GluA3-deficient mice (p=0.6; Figure 4H), indicating that the absence of GluA3 did not cause a generalization of conditioned fear. These data indicate that in contrast to GluA1-dependent plasticity, GluA3-plasticity does not directly contribute to hippocampal learning, underscoring the functional relevance of AMPAR-subunit composition.

Figure 4. GluA3-plasticity does not contribute to contextual fear memory formation
Mice received a fear conditioning session consisting of three electric shocks of 0.80mA (A-E) or 0.65mA (F-H). (A) Locomotion was quantified during fear conditioning in WT (n=17) and GluA1-KO (n=16) littermates. (B) Different groups of WT (10 min: n=8; 2h: n=9; 24h: n=8; 1 week: n=12; 1 month: n=5) and GluA1-KO (10 min: n=8; 2h: n=8; 24h: n=7; 1 week: n=12; 1 month: n=10) littermate mice were re-exposed to the shock cage and freezing levels were quantified. (C) Freezing levels of GluA1-KO mice injected with saline (n=8) or epinephrine (n=11) 10 min before contextual fear conditioning and re-exposed to the context two hours after conditioning. (D) Different groups of GluA1-KO (2h: n=7; 24h: n=9) and GluA1/3-KO (2h: n=6; 24h: n=8) littermates were re-exposed to the shock cage and freezing levels were quantified. (E) Freezing levels of GluA1-KO mice injected with AAV expressing SEP-GluA1 (n=8) or GFP (n=6) in the hippocampus, re-exposed 10m and 24h after fear conditioning. (F) Locomotion was quantified during fear conditioning in WT (n=22) and GluA3-KO (n=22) littermates. (G) Different groups of WT (10 min: n=11; 2h: n=11; 24h: n=10; 1 week: n=10; 1 month: n=5) and GluA3-KO (10 min: n=11; 2h: n=11; 24h: n=8; 1 week: n=6; 1 month: n=7) littermates were re-exposed to the shock cage and freezing levels were quantified. (H) Fear memories in WT and GluA3-KO mice are context specific. WT (n=13) and GluA3-KO (n=12) are exposed to context A and context B but only receive shocks in A. 2h after conditioning the mice are re-exposed to both context A and B and freezing levels are scored. Error bars indicate SEM, * indicates p<0.05.

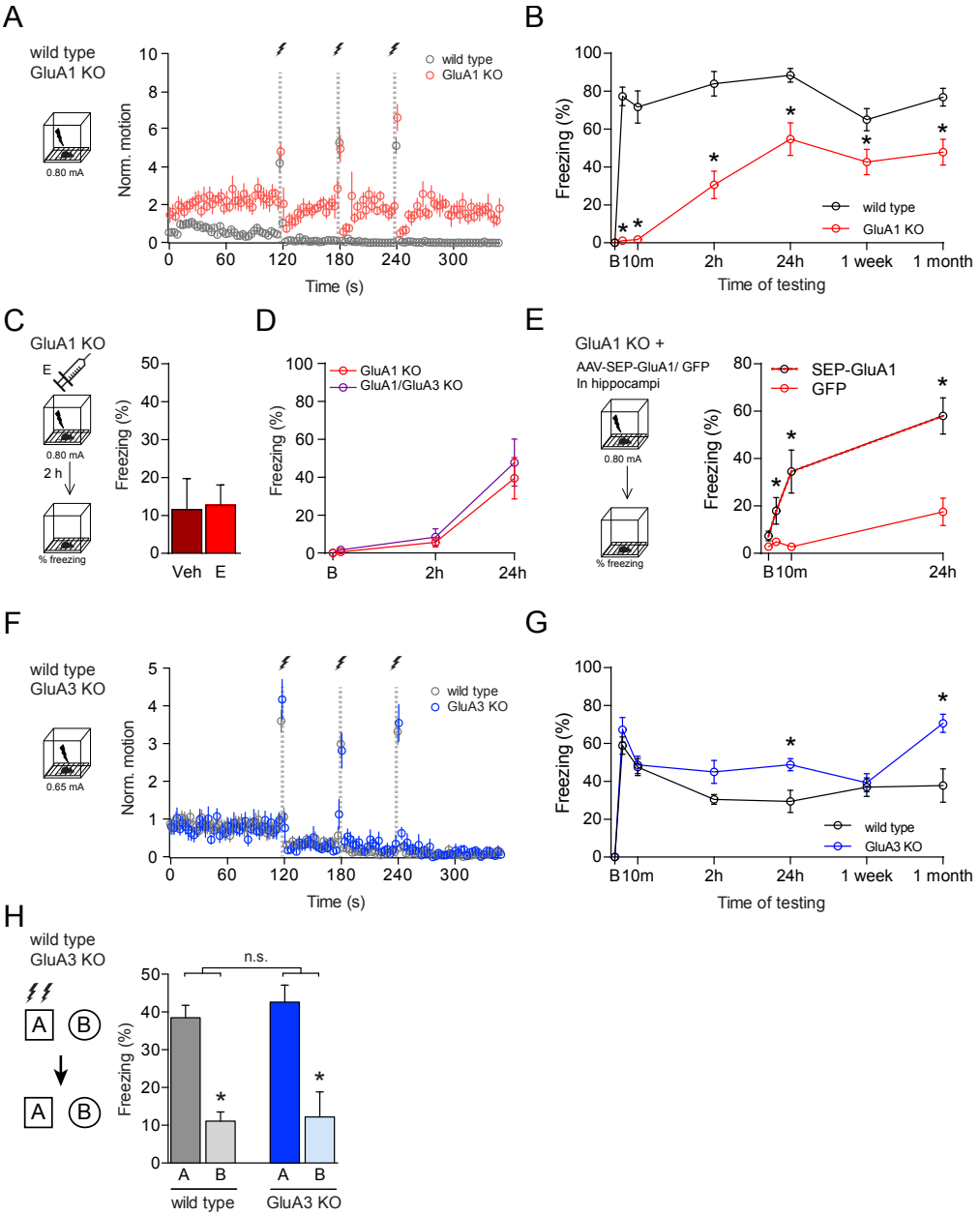
A
wild type
GluA1 KO
0.80 mA
Norm. motion
wild type
GluA1 KO
Time (s)
B
Freezing (%)
wild type
GluA1 KO
B
10m
2h
24h
1 week
1 month
Time of testing
C
GluA1 KO
E
0.80 mA
2 h
% freezing
Freezing (%)
Veh
E
D
Freezing (%)
GluA1 KO
GluA1/GluA3 KO
B
2h
24h
E
GluA1 KO +
AAV-SEP-GluA1/ GFP
In hippocampi
0.80 mA
% freezing
Freezing (%)
SEP-GluA1
GFP
B
10m
24h
F
wild type
GluA3 KO
0.65 mA
Norm. motion
wild type
GluA3 KO
Time (s)
G
Freezing (%)
wild type
GluA3 KO
B
10m
2h
24h
1 week
1 month
Time of testing
H
wild type
GluA3 KO
A
B
A
B
Freezing (%)
n.s.
A
B
A
B
wild type
GluA3 KO

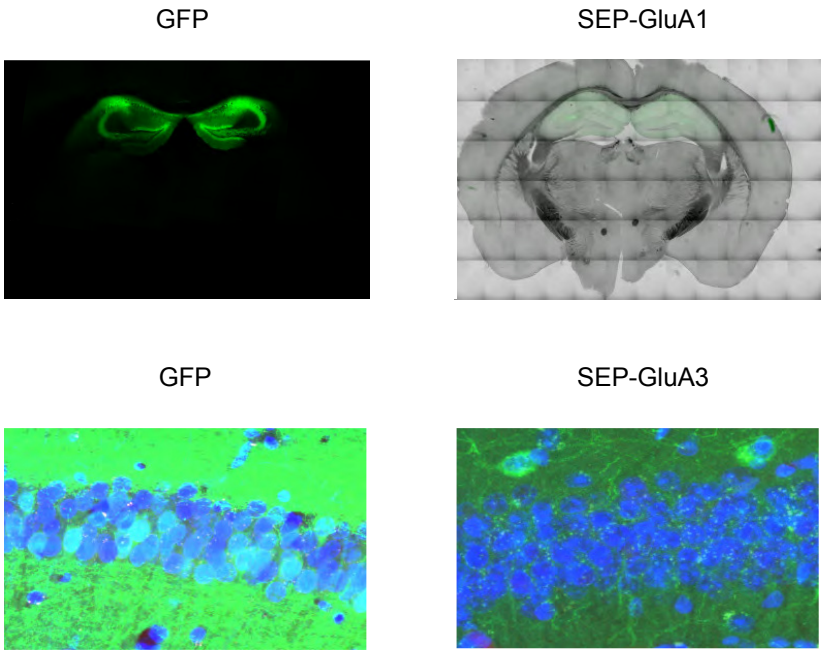

Figure 5. Bilateral AAV-infection selectively in the hippocampi of 3-4 week old mice
(Top) Representative images of brain slices infected with AAV1-pCaMKII-GFP (left) and AAV1-pCaMKII-SEP-GluA1 (right) indicate the selective targeting of hippocampal regions. (Bottom) Representative images of CA1 region infected with AAV5-pCaMKII-GFP (left) and AAV5-pCaMKII-SEP-GluA3 (right) and stained with DAPI (blue) indicate that a large proportion of CA1 neurons expressed the fluorescent transgene. The expression levels of SEP-GluA1 and SEP-GluA3 were held low, due to the absence of the woodchuck hepatitis post-transcriptional regulatory element (WPRE) in these constructs.

Hippocampal GluA3-plasticity influences fear memory retrieval

As a possible explanation for enhanced long-term memories in GluA3-deficient mice, we reasoned that after learning GluA2/3s may gradually replace GluA1-containing AMPARs (McCormack et al., 2006). After such AMPAR replacement process, the memory would only be vivid when cAMP levels are high and GluA2/3s are active, and would be veiled when GluA2/3s become inactive due to low levels of cAMP. To test whether GluA3-plasticity affects memory retrieval, mice were fear conditioned and prior to a memory test GluA3-plasticity was either inhibited or promoted, by injecting propranolol or epinephrine respectively (Figure 6A). For WT mice, propranolol injection suppressed the freezing response ($p=0.02$), while epinephrine injection led to enhanced freezing upon re-exposure the fearful context ($p=0.01$). For GluA3-deficient littermates the difference in freezing levels after propranolol and epinephrine injection were significantly smaller ($p=0.008$), indicating that GluA3 contributes to the facilitation of memory retrieval upon NE release in the brain. To examine whether memory retrieval was dependent on

GluA3-plasticity in excitatory neurons of the hippocampus, we used AAV viral transfer to introduce SEP-GluA3 (or GFP as a control) under control of the CaMKII promoter selectively into the hippocampi of 3-4 week old GluA3-deficient littermates (Figure 5), and tested the mice in contextual fear conditioning when 2 months old (Figure 6B). Viral expression of SEP-GluA3, but not GFP, significantly reinforced the dependence of memory retrieval on β-AR activation (p=0.04). These experiments demonstrate that GluA3-plasticity in the hippocampus regulates the ability to retrieve a contextual fear memory.

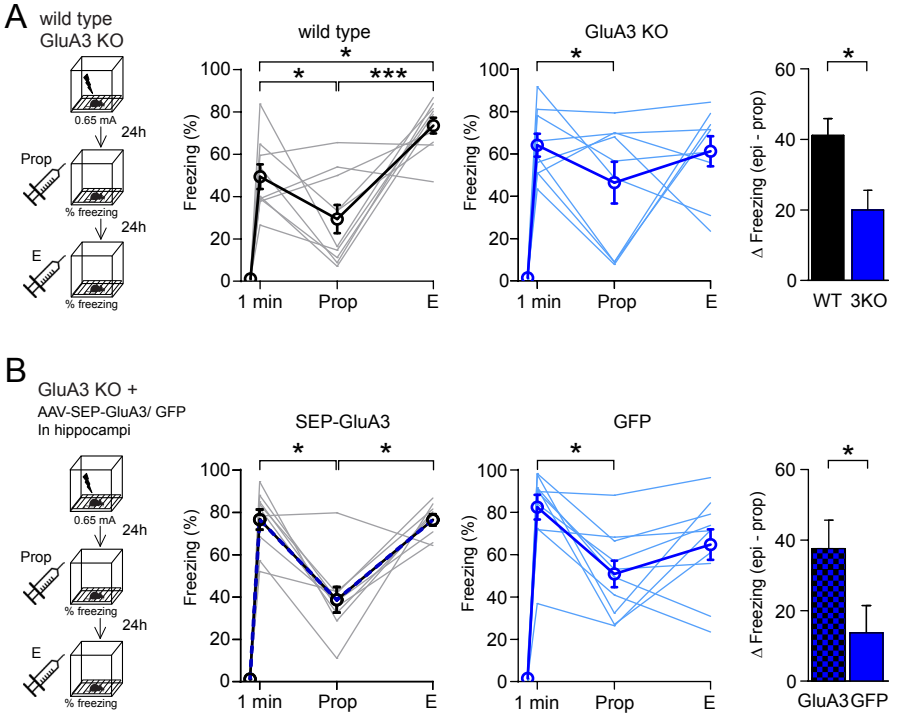

Figure 6. GluA3-plasticity facilitates the retrieval of contextual fear memories
(A,B) Mice were fear conditioned with three 0.65mA shocks. 24h after conditioning mice were injected with propranolol 30 min prior to re-exposure to the shock cage. 48h after conditioning mice were injected with epinephrine 10 min before re-exposure to the shock cage. (A) Freezing levels of WT (n=10) and GluA3-KO (n=9) mice immediately following the shocks, after propranolol injection and after epinephrine injection were quantified. The difference in freezing between epinephrine and propranolol is depicted in the bar graph. (B) Same as for GluA3-KO littermate mice bilaterally injected with AAV expressing either SEP-GluA3 (n=9) or GFP (n=10). Error bars indicate SEM, * indicates p<0.05.

DISCUSSION

We previously demonstrated that GluA3-containing AMPARs are present at synapses and on the cell surface, and that, though electrically quiet under basal conditions, GluA3-mediated currents become visible when intracellular cAMP levels are increased in CA1 neurons of the hippocampus upon the activation of β-ARs (Renner et al., 2017).

Here we elaborate on these previous findings and show that GluA3-plasticity is activated in the hippocampus under physiological conditions. Our experiments indicate that, when mice receive mild electric shocks, β-ARs are activated and evoke two independent forms of cAMP-dependent AMPAR plasticity in parallel. In the first form, PKA phosphorylation of GluA1-containing AMPARs facilitates their trafficking to synapses (Man, Sekine-Aizawa, & Huganir, 2007), thereby facilitating memory formation (Hu et al., 2007; Renner et al., 2017). And in the second one, GluA3-containining AMPARs present at synapses increase their conductance in a Ras/PKA-dependent manner, thereby facilitating memory retrieval.

Fear learning is known to depend on GluA1-dependent long-term potentiation of a subset of synapses on a fraction of neurons in the hippocampus and the lateral amygdala (Mitsushima et al., 2011; Rumpel et al., 2005). We show that GluA3-plasticity also plays a part and it's transiently activated at the majority of CA1 neurons. This was visible as an increase in mEPSC frequency after fear conditioning in GluA3-containing neurons, which was not observed in neurons lacking GluA3.

When considering that fear memories require sparse coding and remain present long-term, it may not be surprising that GluA3-plasticity does not contribute to hippocampus-dependent memory formation. GluA3-plasticity also did not mask a memory by selectively potentiating synapses that took no part in the memory engram, since GluA3-deficient mice displayed fear responses indistinguishable from wild-type littermates shortly after fear conditioning when GluA3s are largely active.

It was previously suggested that GluA2/3s gradually replace GluA1-containing AMPARs at synapses after experience-dependent plasticity (McCormack et al., 2006; Takahashi, Svoboda, & Malinow, 2003). This AMPAR-subunit replacement process does not appear to be necessary to stabilize a memory, since we observed that fear memories remained stable in GluA3-deficient mice for up to one month

after fear conditioning. Our results are also consistent with the view that the replacement of GluA1- by GluA3-containing AMPARs may have an adverse effect on the retrieval of memories when GluA3 channels would become inactive after replacement, and explain why β-AR signalling promotes the retrieval of contextual fear memories (Murchison et al., 2004). It will be interesting to assess whether GluA3-plasticity can be attributed to other cognitive functions that depend on β-AR signalling such as attention and perception.

One could speculate that, after AMPAR replacement, the memory would only be vivid when cAMP levels are high and GluA2/3s are active; the memory would be concealed when GluA2/3s become inactive due to low levels of cAMP. This would mean that GluA3-deficient mice, that have GluA1, can learn. Additionally, these mice could potentially retrieve a memory better than a wildtype mouse, almost as if they can't hide a memory and all their memories are always switched on, always online. The role of GluA3 would be to store a memory offline, and GluA3-plasticity to bring a memory back to attention.

Other signalling pathways that influence intracellular cAMP levels, for instance those activated by dopamine, serotonin or acetylcholine release, may theoretically influence GluA3-containing AMPARs as well. It will be interesting to assess under which other conditions GluA3-containing AMPARs in the hippocampus are activated, besides β-AR activation.

We previously found that Purkinje cells of the cerebellum also express both GluA1- and GluA3-containing AMPARs, but in these neurons GluA3-plasticity, and not GluA1-plasticity, was crucial for long-term synaptic strengthening and motor learning (Gutierrez-Castellanos et al., 2017). Thus, even though the AMPAR subunit rules for synaptic plasticity are inverted in Purkinje neurons with respect to those in CA1 hippocampal neurons (motor learning and the expression of LTP did not require GluA1, but critically depended on GluA3), synaptic potentiation was accomplished in both upon a rise in cAMP.

We also previously showed that the presence of GluA3-containing AMPARs is critical for Aβ-mediated synaptic and cognitive deficits, where Aβ is a crucial suspect for causing those deficits during the early phases of AD (Reinders et al., 2016). A recent paper by the Tonegawa lab has demonstrated that the memory problems in AD-mice are not due to an inability to make memories but, instead, to retrieve them (Roy et al., 2016). One could speculate that, if the presence of GluA3 renders the synapses susceptible to Aβ and Aβ removes GluA3 from said

synapses, the memory retrieval issues in AD-mice are a direct consequence of the disappearance of GluA3-containing receptors from the synapses, impairing this way the capacity of AD patients of retrieving a memory.

Author contributions

M.C.R., E.H.H.A., and H.W.K. designed the study. M.C.R., E.H.H.A., C.M.d.S.-M., D.A.R., A.N.v.H., T.R.L. and H.W.K. performed experiments and analyzed data. M.C.R., E.H.H.A., C.M.d.S.-M., and H.W.K. wrote the manuscript.

Acknowledgments

We thank Wobbie van den Hurk, Karlijn van Aerde and Rianne Wetzels for technical assistance, Rolf Sprengel for providing flGluA3-KO mice. This work was supported by ZonMw – The Netherlands Organisation for Health Research and Development, grant nr. 733050106, dementia research and innovation programme 'Memorabel' as a part of the 'Deltaplan for Dementia'. The authors declare no financial or non-financial competing interests.

REFERENCES

Adamczyk, A., Mejias, R., Takamiya, K., Yocum, J., Krasnova, I. N., Calderon, J., … Wang, T. (2012). GluA3-deficiency in mice is associated with increased social and aggressive behavior and elevated dopamine in striatum. ***Behavioural Brain Research***, ***229***(1), 265–272. https://doi.org/https://doi.org/10.1016/j.bbr.2012.01.007

Bremner, J. D., Krystal, J. H., Southwick, S. M., & Charney, D. S. (1996). Noradrenergic mechanisms in stress and anxiety: I. preclinical studies. ***Synapse***, ***23***(1), 28–38. https://doi.org/10.1002/(SICI)1098-2396(199605)23:1<28::AID-SYN4>3.0.CO;2-J

Crombag, H. S., Sutton, J. M., Takamiya, K., Lee, H.-K., Holland, P. C., Gallagher, M., & Huganir, R. L. (2008). A necessary role for GluR1 serine 831 phosphorylation in appetitive incentive learning. ***Behavioural Brain Research***, ***191***(2), 178–183. https://doi.org/https://doi.org/10.1016/j.bbr.2008.03.026

Granger, A. J., Shi, Y., Lu, W., Cerpas, M., & Nicoll, R. a. (2013). LTP requires a reserve pool of glutamate receptors independent of subunit type. ***Nature***, ***493***(7433), 495–500. https://doi.org/10.1038/nature11775

Gutierrez-Castellanos, N., Da Silva-Matos, C. M., Zhou, K., Canto, C. B., Renner, M. C., Koene, L. M. C., … De Zeeuw, C. I. (2017). Motor Learning Requires Purkinje Cell Synaptic Potentiation through Activation of AMPA-Receptor Subunit GluA3. ***Neuron***, ***93***(2), 409–424. https://doi.org/10.1016/j.neuron.2016.11.046

Hall, R. A. (2004). β-Adrenergic receptors and their interacting proteins. ***Seminars in Cell & Developmental Biology***, ***15***(3), 281–288. https://doi.org/https://doi.org/10.1016/j.semcdb.2003.12.017

Hu, H., Real, E., Takamiya, K., Kang, M. G., Ledoux, J., Huganir, R. L., & Malinow, R. (2007). Emotion Enhances Learning via Norepinephrine Regulation of AMPA-Receptor Trafficking. ***Cell***, ***131***(1), 160–173. https://doi.org/10.1016/j.cell.2007.09.017

Huganir, R. L., & Nicoll, R. A. (2013). AMPARs and synaptic plasticity: The last 25 years. ***Neuron***, ***80***(3), 704–717. https://doi.org/10.1016/j.neuron.2013.10.025

Humeau, Y., Reisel, D., Johnson, A. W., Borchardt, T., Jensen, V., Gebhardt, C., … Lüthi, A. (2007). A pathway-specific function for different AMPA receptor subunits in amygdala long-term potentiation and fear conditioning. ***The Journal of Neuroscience : The Official Journal of the Society for Neuroscience***, ***27***(41), 10947–10956. https://doi.org/10.1523/JNEUROSCI.2603-07.2007

Kessels, H. W., & Malinow, R. (2009). Synaptic AMPA receptor plasticity and behavior. ***Neuron***, ***61***(3), 340–350. https://doi.org/10.1016/j.neuron.2009.01.015

Kim, C.-H., Takamiya, K., Petralia, R. S., Sattler, R., Yu, S., Zhou, W., … Huganir, R. (2005). Persistent hippocampal CA1 LTP in mice lacking the C-terminal PDZ ligand of GluR1. ***Nature Neuroscience***, ***8***(8), 985–987. https://doi.org/10.1038/nn1432

Kopec, C. D., Real, E., Kessels, H. W., & Malinow, R. (2007). GluR1 links structural and functional plasticity at excitatory synapses. ***The Journal of Neuroscience : The Official Journal of the Society for Neuroscience***, ***27***(50), 13706–13718. https://doi.org/10.1523/JNEUROSCI.3503-07.2007

Lu, W., Shi, Y., Jackson, A. C., Bjorgan, K., During, M. J., Sprengel, R., … Nicoll, R. A. (2009). Subunit Composition of Synaptic AMPA Receptors Revealed by a Single-Cell Genetic Approach. ***Neuron***, ***62***(2), 254–268. https://doi.org/10.1016/j.neuron.2009.02.027

Makino, H., & Malinow, R. (2011). Compartmentalized versus Global Synaptic Plasticity on Dendrites Controlled by Experience. ***Neuron***, ***72***(6), 1001–1011. https://doi.org/10.1016/j.neuron.2011.09.036

Malinow, R., & Malenka, R. C. (2002). AMPA Receptor Trafficking and Synaptic Plasticity. ***Annual Review of Neuroscience***, ***25***(1), 103–126. https://doi.org/10.1146/annurev.neuro.25.112701.142758

Man, H.-Y., Sekine-Aizawa, Y., & Huganir, R. L. (2007). Regulation of α-amino-3-hydroxy-5-methyl-4-isoxazolepropionic acid receptor trafficking through PKA phosphorylation of the Glu receptor 1 subunit. ***Proceedings of the National Academy of Sciences***, ***104***(9), 3579 LP – 3584. https://doi.org/10.1073/pnas.0611698104

Manabe, T., Wyllie, D. J., Perkel, D. J., & Nicoll, R. A. (1993). Modulation of synaptic transmission and long-term potentiation: effects on paired pulse facilitation and EPSC variance in the CA1 region of the hippocampus. ***Journal of Neurophysiology***, ***70***(4), 1451–1459. https://doi.org/10.1152/jn.1993.70.4.1451

McCormack, S. G., Stornetta, R. L., & Zhu, J. J. (2006). Synaptic AMPA receptor exchange maintains bidirectional plasticity. ***Neuron***, ***50***(1), 75–88. https://doi.org/10.1016/j.neuron.2006.02.027

McIntyre, C. K., Hatfield, T., & McGaugh, J. L. (2002). Amygdala norepinephrine levels after training predict inhibitory avoidance retention performance in rats. ***European Journal of Neuroscience***, ***16***(7), 1223–1226. https://doi.org/10.1046/j.1460-9568.2002.02188.x

Meng, Y., Zhang, Y., & Jia, Z. (2003). Synaptic transmission and plasticity in the absence of AMPA glutamate receptor GluR2 and GluR3. ***Neuron***, ***39***(1), 163–176. Retrieved from http://www.ncbi.nlm.nih.gov/pubmed/12848940

Mitsushima, D., Ishihara, K., Sano, A., Kessels, H. W., & Takahashi, T. (2011). Contextual learning requires synaptic AMPA receptor delivery in the hippocampus. ***Proceedings of the National Academy of Sciences of the United States of America***, ***108***(30), 12503–12508. https://doi.org/10.1073/pnas.1104558108

Murchison, C. F., Zhang, X.-Y., Zhang, W.-P., Ouyang, M., Lee, A., & Thomas, S. A. (2004). A Distinct Role for Norepinephrine in Memory Retrieval. ***Cell***, ***117***(1), 131–143. https://doi.org/10.1016/S0092-8674(04)00259-4

Nabavi, S., Fox, R., Proulx, C. D., Lin, J. Y., Tsien, R. Y., & Malinow, R. (2014). Engineering a memory with LTD and LTP. ***Nature***, ***511***(7509), 348–352. https://doi.org/10.1038/nature13294

Porrero, C., Rubio-Garrido, P., Avendaño, C., & Clascá, F. (2010). Mapping of fluorescent protein-expressing neurons and axon pathways in adult and developing Thy1-eYFP-H transgenic mice. ***Brain Research***, ***1345***, 59–72. https://doi.org/https://doi.org/10.1016/j.brainres.2010.05.061

Qian, H., Matt, L., Zhang, M., Nguyen, M., Patriarchi, T., Koval, O. M., … Hell, J. W. (2012). β2-Adrenergic receptor supports prolonged theta tetanus-induced LTP. ***Journal of Neurophysiology***, ***107***(10), 2703–2712. https://doi.org/10.1152/jn.00374.2011

Reinders, N. R., Pao, Y., Renner, M. C., da Silva-Matos, C. M., Lodder, T. R., Malinow, R., & Kessels, H. W. (2016). Amyloid-β effects on synapses and memory require AMPA receptor subunit GluA3. ***Proceedings of the National Academy of Sciences***, ***113***(42), E6526 LP-E6534. https://doi.org/10.1073/pnas.1614249113

Renner, M. C., Albers, E. H., Gutierrez-Castellanos, N., Reinders, N. R., van Huijstee, A. N., Xiong, H., … Kessels, H. W. (2017). Synaptic plasticity through activation of GluA3-containing AMPA-receptors. ***ELife***, ***6***, e25462. https://doi.org/10.7554/eLife.25462

Rial Verde, E. M., Lee-Osbourne, J., Worley, P. F., Malinow, R., & Cline, H. T. (2006). Increased Expression of the Immediate-Early Gene Arc/Arg3.1 Reduces AMPA Receptor-Mediated Synaptic Transmission. ***Neuron***, ***52***(3), 461–474. https://doi.org/10.1016/j.neuron.2006.09.031

Roy, D. S., Arons, A., Mitchell, T. I., Pignatelli, M., Ryan, T. J., & Tonegawa, S. (2016). Memory retrieval by activating engram cells in mouse models of early Alzheimer's disease. ***Nature***, ***531***(7595), 508–512. https://doi.org/10.1038/nature17172

Rumpel, S., LeDoux, J., Zador, A., & Malinow, R. (2005). Postsynaptic receptor trafficking underlying a form of associative learning. ***Science (New York, N.Y.)***, ***308***(5718), 83–88. https://doi.org/10.1126/science.1103944

Sanchis-Segura, C., Borchardt, T., Vengeliene, V., Zghoul, T., Bachteler, D., Gass, P., … Spanagel, R. (2006). Involvement of the AMPA receptor GluR-C subunit in alcohol-seeking behavior and relapse. ***The Journal of Neuroscience : The Official Journal of the Society for Neuroscience***, ***26***(4), 1231–1238. https://doi.org/10.1523/JNEUROSCI.4237-05.2006

Shi, S., Hayashi, Y., Esteban, J. A., & Malinow, R. (2001). Subunit-specific rules governing AMPA receptor trafficking to synapses in hippocampal pyramidal neurons. ***Cell***, ***105***(3), 331–343. https://doi.org/10.1016/S0092-8674(01)00321-X

Steenland, H. W., Kim, S. S., & Zhuo, M. (2008). GluR3 subunit regulates sleep, breathing and seizure generation. ***The European Journal of Neuroscience***, ***27***(5), 1166–1173. https://doi.org/10.1111/j.1460-9568.2008.06078.x

Takahashi, T., Svoboda, K., & Malinow, R. (2003). Experience Strengthening Transmission by Driving AMPA Receptors into Synapses. ***Science***, ***299***(5612), 1585 LP – 1588. https://doi.org/10.1126/science.1079886

Vanhoose, A. M., & Winder, D. G. (2003). NMDA and β₁-Adrenergic Receptors Differentially Signal Phosphorylation of Glutamate Receptor Type 1 in Area CA1 of Hippocampus. ***The Journal of Neuroscience***, ***23***(13), 5827 LP – 5834. https://doi.org/10.1523/JNEUROSCI.23-13-05827.2003

Wenthold, J., Petralia, S., & Niedzielski, S. (1996). Evidence for Multiple Neurons Complexes in Hippocampal, ***76***(6), 1982–1989.

Whitlock, J. R., Heynen, A. J., Shuler, M. G., & Bear, M. F. (2006). Learning Induces Long-Term Potentiation in the Hippocampus. ***Science***, ***313***(5790), 1093 LP – 1097. https://doi.org/10.1126/science.1128134

Zhou, M., Conboy, L., Sandi, C., Joëls, M., & Krugers, H. J. (2009). Fear conditioning enhances spontaneous AMPA receptor-mediated synaptic transmission in mouse hippocampal CA1 area. ***European Journal of Neuroscience***, ***30***(8), 1559–1564. https://doi.org/10.1111/j.1460-9568.2009.06951.x

Chapter 6

Amyloid-β Effects on Synapses and Memory Require AMPA-Receptor Subunit GluA3

Niels R. Reinders[a,1], Yvonne Pao[b,1], Maria C. Renner[a], Carla M. da Silva-Matos[a], Tessa R. Lodder[a], Roberto Malinow[b] and Helmut W. Kessels[a,2]

[a] Netherlands Institute for Neuroscience, Royal Netherlands Academy of Arts and Sciences, Amsterdam, 1105BA, The Netherlands.

[b] Center for Neural Circuits and Behavior, Department of Neuroscience and Section of Neurobiology, Division of Biology, University of California at San Diego, San Diego, CA 92093, USA.

[1] NRR and YP contributed equally to this work

[2] To whom correspondence should be addressed.

Author contributions: N.R.R., Y.P., M.C.R., C.M.d.S.-M., T.R.L. and H.W.K. performed experiments and analyzed data. N.R.R., Y.P., R.M. and H.W.K. wrote the manuscript.

The authors declare no conflict of interest.

To whom correspondence may be addressed. Email: h.kessels@nin.knaw.nl or rmalinow@ ucsd.edu.

ABSTRACT

Amyloid-β (Aβ) is a prime suspect to cause cognitive deficits during the early phases of Alzheimer's disease (AD). Experiments in AD-mouse models have shown that soluble oligomeric clusters of Aβ degrade synapses and impair memory formation. We show that all Aβ-driven effects measured in these mice depend on AMPA-receptor subunit GluA3. Hippocampal neurons that lack GluA3 were resistant against Aβ-mediated synaptic depression and spine loss. In addition, Aβ oligomers only blocked long-term synaptic potentiation in neurons that expressed GluA3. Furthermore, whereas Aβ-overproducing mice showed significant memory impairment, memories in GluA3-deficient congenics remained unaffected. These experiments indicate that the presence of GluA3-containing AMPA-receptors is critical for Aβ-mediated synaptic and cognitive deficits.

Significance

In Alzheimer's disease, soluble clusters of amyloid-β (Aβ) are believed to degrade synapses and impair memory formation. The removal of AMPA-receptors from synapses was previously shown to be a critical step in Aβ-driven synapse loss. In this report, we establish that AMPA-receptors that contain subunit GluA3 play a central role in Aβ-driven synaptic and memory deficits. Neurons that lack GluA3 are resistant to synaptic weakening and inhibition of synaptic plasticity, and mice that lack GluA3 were resistant to memory impairment and premature mortality. Our experiments suggest that Aβ initiates synaptic and memory deficits by removing GluA3-containing AMPA-receptors from synapses.

INTRODUCTION

At the early stages of Alzheimer's disease (AD), synaptic perturbations are strongly linked to cognitive decline and memory impairment in AD patients (Brown et al., 1998; Scheff et al., 2006). The accumulation of soluble oligomeric clusters of amyloid-β (Aβ), a secreted proteolytic derivative of the amyloid precursor protein (APP), may be important for the early synaptic failure that is seen in AD pathogenesis (Lambert et al., 1998; Lesne et al., 2006; McLean et al., 1999; Shankar et al., 2008). Neurons that overexpress APP or are exposed to Aβ-oligomers show synaptic depression, a loss of dendritic spines and a reduced capacity for synaptic plasticity (Kamenetz et al., 2003; Lacor et al., 2007; Walsh et al., 2002; Mucke & Selkoe, 2012). For all these effects to occur NMDA-receptor (NMDAR) activity is required (Kamenetz et al., 2003; Kessels, Nabavi & Malinow, 2013; Shankar et al., 2007; Wei et al., 2010). Aβ-oligomers trigger an NMDAR-dependent signaling pathway that leads to synaptic depression through the removal of AMPA-receptors (AMPARs) and NMDARs from synapses (Kamenetz et al., 2003; Kessels, Nabavi & Malinow, 2013; Snyder et al., 2005). Interestingly, a blockade of AMPAR endocytosis prevents the depletion of NMDARs and a loss of spines (Hsieh et al., 2006; Miyamoto et al., 2016), suggesting that the removal of AMPARs from synapses is critical for this pathway to induce synaptic failure.

Excitatory neurons of the mature hippocampus predominantly contain two types of AMPARs in approximately equivalent amounts (Kessels et al., 2009): those consisting of subunits GluA1 and GluA2 (GluA1/2s), and those consisting of GluA2 and GluA3 (GluA2/3s) (Wenthold et al., 1996). GluA1-containing AMPARs are inserted into synapses upon the induction of long-term potentiation (LTP) in brain slices (Hayashi et al., 2000) and play a prominent role in memory formation (Mitsushima et al., 2011; Rumpel et al., 2005). In contrast, GluA2/3s contribute relatively little to synaptic currents, LTP or memory formation (Adamczyk et al., 2012; Humeau et al., 2007; Lu et al., 2009; Meng, Zhang & Jia, 2003) and have been implicated to participate in homeostatic scaling of synapse strength (Makino & Malinow, 2011; Rial Verde et al., 2006). We here demonstrate that the AMPAR subunit GluA3 plays a major role in AD pathology by showing that mice lacking GluA3 are protected against Aβ-driven synaptic deficits, spine loss and memory impairment.

RESULTS

GluA3-deficient neurons are resistant against Aβ-mediated synaptic depression. To assess whether the removal of AMPARs from synapses by Aβ depends on AMPAR subunit composition, organotypic hippocampal slice cultures were prepared from GluA1-deficient or GluA3-deficient mice and their wild-type littermates. CA1 neurons were sparsely (<10%) infected with Sindbis virus expressing APP_{CT100}, the β-secretase product of APP and precursor to Aβ, together with tdTomato under control of a second subgenomic promoter. 20-30 hrs after viral infection, synaptic currents evoked by electrical stimulation of Schaffer collateral inputs were measured on tdTomato-expressing and neighboring uninfected pyramidal CA1 neurons simultaneously. We ascertained that the majority of tdTomato expressing neurons produced APP_{CT100} without affecting their membrane resistance (Fig. S1), supporting previous demonstrations that in these conditions the health of the neurons is not affected by Sindbis infection (Hayashi et al., 2000; Kamenetz et al., 2003; Kessels, Nabavi & Malinow, 2013). Wild-type neurons that expressed APP_{CT100} showed decreased AMPAR currents ($p<0.01$; Fig. 1*A*) and reduced AMPA/NMDA ratios ($p=0.03$; Fig. 1*C*), which has been shown to be caused by increased neuronal production of Aβ (Kamenetz et al., 2003; Kessels, Nabavi & Malinow, 2013). In CA1 neurons of GluA3-deficient organotypic slices the AMPA/NMDA ratios were on average 35% reduced compared with wild-type neurons CA1 neurons ($p=0.05$; Fig. 1*C*) and APP_{CT100} expression failed to decrease synaptic AMPAR currents ($p=0.6$; Fig. 1*A* and *B*) or AMPA/NMDA ratios ($p=0.6$; Fig. 1*C* and *D*). However, GluA1-deficient neurons had a more reduced AMPA/NMDA ratio (55%; Fig. 1*C*), yet still show APP_{CT100}-induced synaptic AMPAR depression ($p=0.01$; Fig. 1*A*) that was a similar depression as in wild-type neurons ($p=0.2$; Fig. 1*B*). These data indicate that the presence of GluA3-containing AMPARs, but not of those containing GluA1, is crucial for Aβ to trigger synaptic AMPAR depression.

To assess the effect of Aβ on NMDARs, we compared synaptic NMDAR currents between pairs of APP_{CT100} infected and nearby uninfected neurons (Fig. 2). APP_{CT100} expression led to a significant decrease in synaptic NMDAR currents in wild-type CA1 neurons ($p<0.01$; Fig. 2*A*) and in GluA1-deficient CA1 neurons ($p=0.02$), but not in those lacking GluA3 ($p>0.9$; Fig. 2*A* and *C*). These data indicate that neurons are only susceptible to Aβ-mediated NMDAR depression when they express AMPAR subunit GluA3. Digital subtraction of currents before and after wash-in of the specific GluN2B blocker Ro 25-6981 permitted measurement of the relative contribution of GluN2A and GluN2B to the NMDAR currents. The

relative contribution of GluN2A and GluN2B to total NMDAR currents was not altered by the absence of GluA1 or GluA3 (Fig. 2*B*). As previously shown (Kessels, Nabavi & Malinow, 2013), APP_{CT100} expression in wild-type neurons selectively affected NMDAR currents mediated by GluN2B (p=0.01; Fig. 2*B* and *E*) and not those mediated by GluN2A (p=0.4; Fig. 2*B* and *D*). APP_{CT100} expression in GluA3-deficient neurons failed to reduce NMDAR currents independently of whether they contained GluN2A (p=0.6; Fig. 2*B* and *D*) or GluN2B (p=0.3; Fig. 2*B* and *E*). In GluA1-deficient neurons both GluN2A (p=0.02) and GluN2B (p=0.03) NMDAR currents were significantly reduced upon APP_{CT100}-expression (Fig. 2*B* to *E*), suggesting that the presence of GluA1 protects synapses from an Aβ-mediated

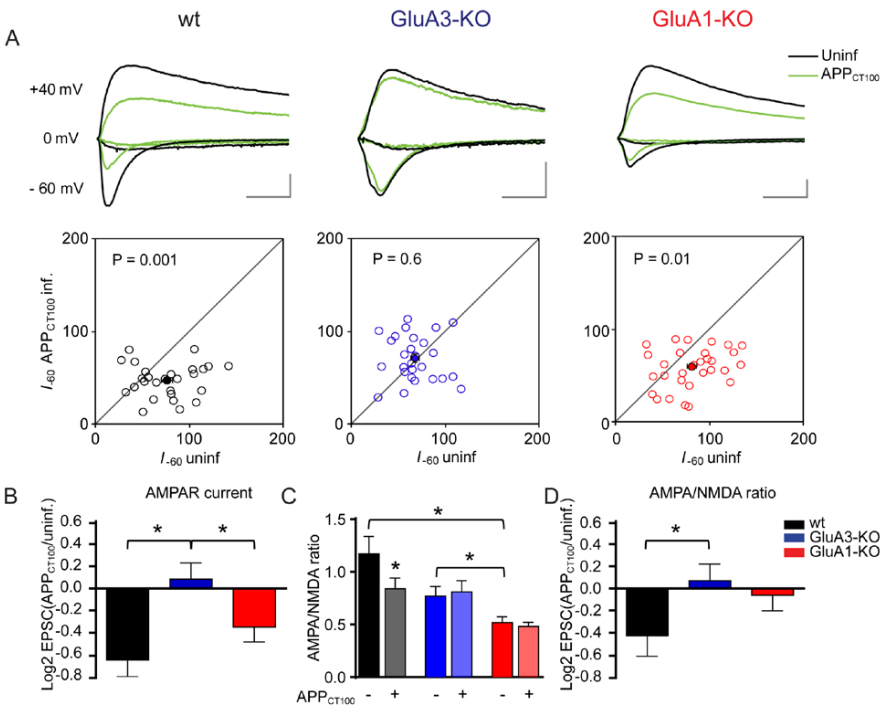

Fig. 1. GluA3-deficient neurons are resistant against Aβ-mediated synaptic AMPAR depression. (***A-D***) Dual whole-cell recordings of APP_{CT100} infected and neighboring uninfected CA1 neurons from organotypic slices of wt mice (black), GluA3-KO littermate mice (blue), or GluA1-KO littermate mice (red). (***A***) Example traces (top) and dot plots (bottom) of paired EPSC recordings (open dots) with averages denoted as filled dots (wt: n=27; GluA3-KO: n=27; GluA1-KO: n=31). Genotype x APP_{CT100}: p<0.01 (two-way ANOVA). Scale bars: 20 ms and 50pA. (***B***) Fold change in AMPAR currents upon APP_{CT100} expression, calculated as the average log2-transformed ratio of EPSC recorded from APP_{CT100}-infected over EPSC from neighboring uninfected neuron. (***C***) AMPA/NMDA ratios of uninfected and APP_{CT100} infected neurons (wt: n=18; GluA3-KO: n=18; GluA1-KO: n=20); Genotype x APP_{CT100}: p=0.3 (two-way ANOVA). (***D***) Fold change in AMPA/NMDA ratios upon APP_{CT100} expression, calculated as in (***B***). Data are mean ±SEM. Statistics: 2-tailed paired (***A,C***) or unpaired (***B-D***) ***t*** test. * indicates p<0.05.

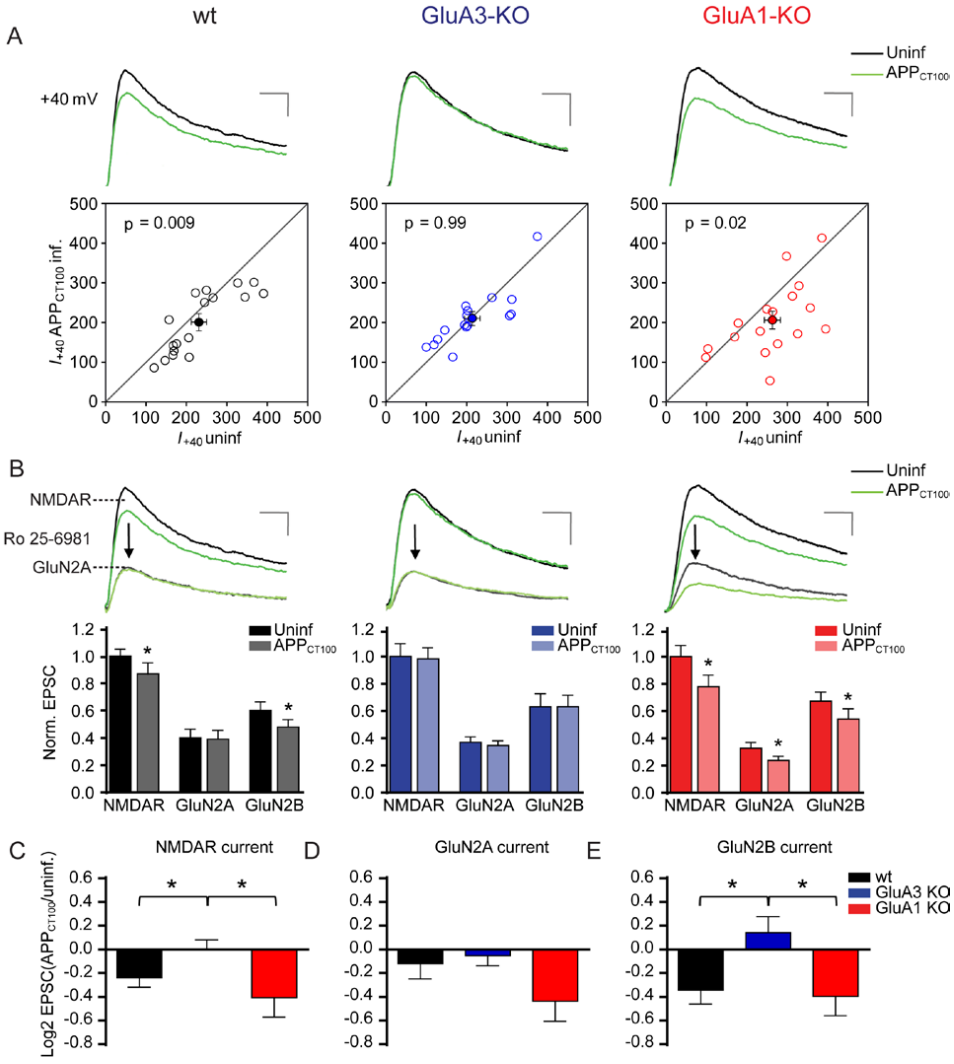

Fig. 2. GluA3-deficient neurons are resistant against Aβ-mediated synaptic NMDAR depression. (*A-E*) Dual whole-cell recordings of APP_{CT100} infected and neighboring uninfected CA1 neurons from organotypic slices of wt mice (black), GluA3-KO littermate mice (blue), or GluA1-KO littermate mice (red). (*A*) Example traces (top) and dot plots (bottom) of paired NMDAR EPSC recordings (open dots) with average denoted as filled dot (wt: n=17; GluA3-KO: n=16; GluA1-KO: n=17). Genotype x APP_{CT100}: p=0.05 (two-way ANOVA). Scale bars: 20 ms and 50pA. (*B*) Example traces (top) and average EPSC currents normalized to the average of the uninfected neurons (bottom) before and after Ro 25-6981 wash-in to reveal GluN2A and GluN2B contributing NMDAR currents. Scale bars: 20 ms and 50pA. (*C*) Fold change in total NMDAR, (*D*) GluN2A and (*E*) GluN2B currents upon APP_{CT100} expression, calculated as the average log2-transformed ratio of EPSC recorded from APP_{CT100}-infected over EPSC from neighboring uninfected neuron. Data are mean ±SEM. Statistics: 2-tailed paired (*A,B*) or unpaired (*C-E*) *t* test. * indicates p<0.05.

reduction in synaptic GluN2A currents. A proportional decrease in AMPAR (Fig. 1*B*) and NMDAR (Fig. 2*C*) currents in APP_{CT100}-expressing GluA1-deficient neurons corresponds with their unchanged AMPA/NMDA ratio (Fig. 1*D*).

Aβ-mediated synapse loss depends on the presence of GluA3. The number of AMPARs at a synapse correlates well with the synapse size and the spine size (Matsuzaki et al., 2001). To examine whether Aβ selectively targets a specific subtype of synapses harboring GluA3-containing AMPARs, we analyzed spine densities, spine size and miniature EPSC (mEPSC) events in Aβ-overproducing neurons. We assessed Aβ-induced spine loss by expressing APP_{CT100} together with the cytosolic marker tdTomato in CA1 neurons of organotypic slices. As a control

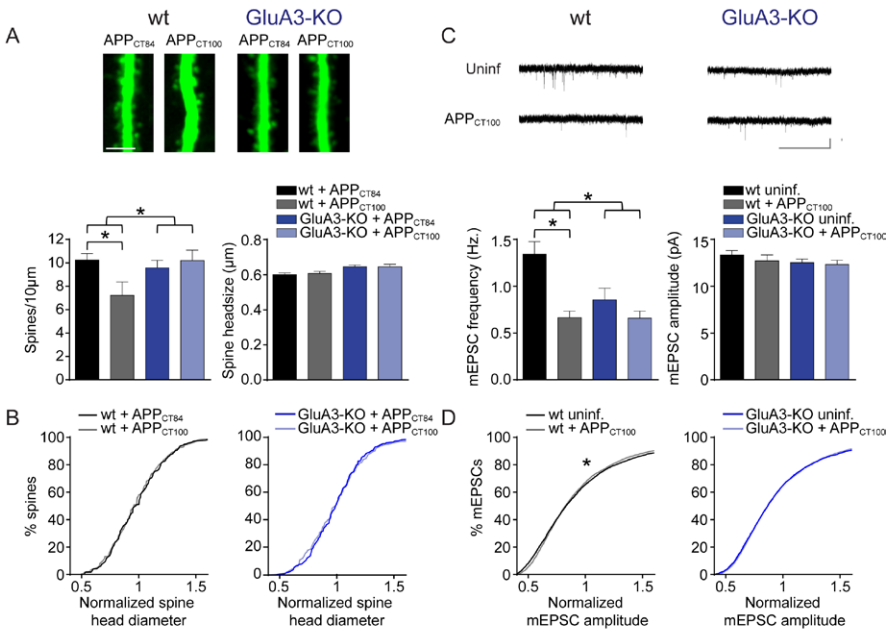

Fig. 3. GluA3-deficient neurons are resistant against Aβ-mediated spine loss. (***A-D***) Spine and mEPSC analysis of CA1 neurons in organotypic slices from wild-type (black) or GluA3-KO mice (blue). (***A, top***) Example images of wt and GluA3-KO dendrites expressing APP_{CT84} or APP_{CT100}. Scale bar: 5 µm. (***A, bottom***) APP_{CT100} expression reduced spine density in wild-type but not GluA3-KO neurons without changing the average spine head diameter. (wt, APP_{CT84}: n=20 and APP_{CT100}: n=13; GluA3-KO, APP_{CT84}: n=26; APP_{CT100}: n=19). (***B***) Distribution of spine head diameters in APP_{CT100} versus APP_{CT84} expressing wt or GluA3-KO neurons. (***C, top***) Example mEPSC traces of wt and GluA3-KO neurons with or without APP_{CT100}-expression. Scale bar: 3 sec, 10 pA. (***C, bottom***) APP_{CT100} expression reduced mEPSC frequency in wild-type but not GluA3-KO neurons without changing average mEPSC amplitude. (wt, APP_{CT100}: n=24 and uninf: n=25; GluA3-KO, APP_{CT100}: n=21 and uninf: n=22). (***D***) APP_{CT100} changed the normalized distribution of mEPSC amplitudes of wt but not of GluA3-KO neurons. Data are mean ±SEM. Statistics: two-way ANOVA with post-hoc Sidak (***A,C***) or K-S test (***B,D***). * indicates p<0.05.

we expressed APP_{CT84}, the α-secretase product of APP, which does not produce Aβ, and did not affect spine density, mEPSC frequency or mEPSC amplitude (Fig. S2). The spine density at apical dendrites was significantly lower in APP_{CT100}-expressing wild-type CA1 neurons compared to APP_{CT84} infected ones (p=0.01; Fig. 3*A*). The loss of spines in APP_{CT100}-expressing CA1 neurons occurred without a change in the average spine head diameter (p=0.6; Fig. 3*A*) or in the distribution of spine head sizes (Fig. 3*B*). Correspondingly, CA1 neurons expressing APP_{CT100} showed a decrease in mEPSC frequency (p<0.01; Fig. 3*C*) but not in average mEPSC amplitude (p=0.9; Fig. 3*C*). A minor change in the distribution of mEPSC amplitudes (p=0.02; Fig. 3*D*) indicates that APP_{CT100}-expressing neurons have a slightly smaller proportion of synapses with large AMPAR current amplitudes.

GluA3-deficient CA1 neurons have a similar spine density as wild-type neurons (p=0.6) with on average slightly larger spine heads (p=0.02; Fig. 3*A*). APP_{CT100} expression in these GluA3-deficient neurons did not lead to a reduced spine density (p>0.9) or spine head size (p>0.9; Fig. 3*A*). The average mEPSC amplitude and was also similar between GluA3-deficient neurons and wild-type neurons (p=0.2), and was not altered upon APP_{CT100}-expression in GluA3-deficient neurons (p=0.7; Fig. 3*C,* p=0.6; Fig. 3*D*). Notably, the mEPSC frequency was significantly lower in GluA3-deficient neurons (p<0.01; Fig. 3*C*) to a size similar to APP_{CT100}-expressing wild-type neurons (p=0.2), and did not change upon APP_{CT100} expression (p=0.2; Fig. 3*C*). These findings indicate that Aβ triggers a reduction in synaptic AMPAR currents and a loss of spines, only when GluA3 is present. Combined with previous reports that show that AMPAR endocytosis is required for the synaptotoxic effects of Aβ (Hsieh et al., 2006; Miyamoto et al., 2016), our data imply that the active removal of GluA3-containing AMPARs by Aβ (but not the genetic deficiency of GluA3) leads to a loss of spines.

GluA3-deficient neurons are insensitive to the Aβ-mediated blockade of LTP. Aβ-oligomers are capable of blocking NMDAR-dependent LTP (Walsh et al., 2002). To assess whether GluA3-deficient neurons are susceptible to the Aβ-mediated blockade of LTP, we performed extracellular local field potential recordings in brain slices acutely isolated from wild-type mice and GluA3-deficient littermates. Previous studies have shown that LTP induction in GluA3-deficient brain slices produces a level of potentiation that is similar (Humeau et al., 2007) or larger (Meng, Zhang & Jia, 2003) than in wild-type neurons. We observed that a theta-burst stimulation onto CA3-CA1 synapses produced stable, pathway-specific LTP of similar magnitude in wild-type and GluA3-deficient slices (Fig. S3). This experiment was repeated in slices incubated with cell culture medium from a

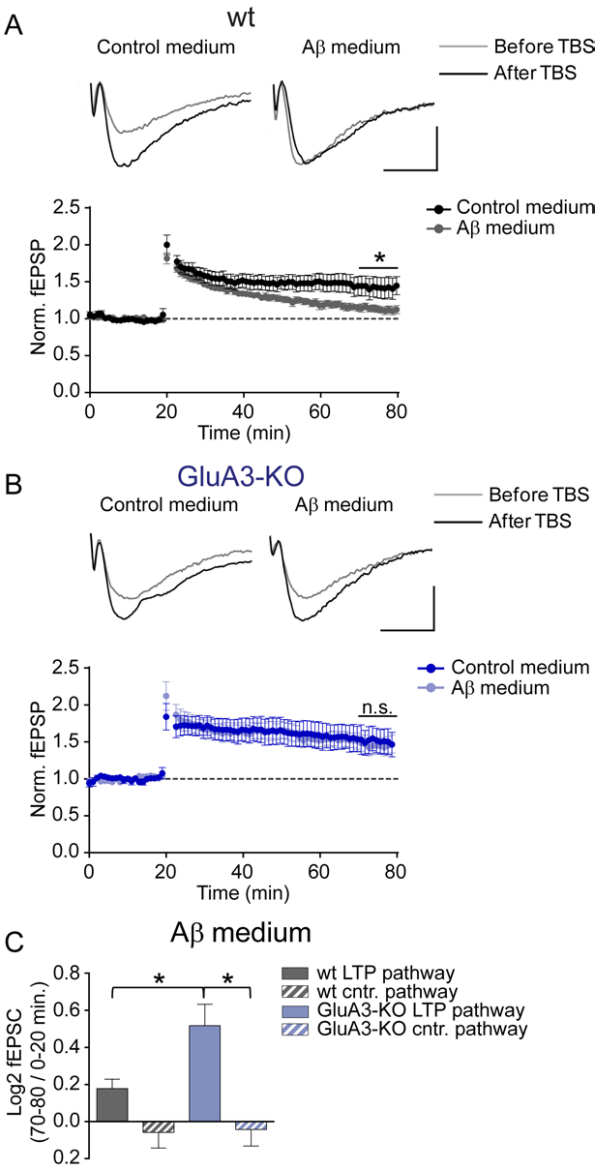

Fig. 4. GluA3-deficient neurons are resistant against the Aβ-mediated block in LTP. (*A,B*) Example traces (top) and average peak field potential responses recorded at the CA1 stratum radiatum before and after theta burst stimulation (TBS). Scale bars: 10 ms, 0.2 mV. (*A*) LTP was inhibited in wild-type neurons by Aβ-containing medium (gray: n=11) compared with control medium (black; n=6). (*B*) In GluA3-KO slices LTP was not inhibited by Aβ-medium (light blue; n=8) in comparison to control medium (dark blue; n=8). (*C*) In the presence of Aβ-medium, the fold change in AMPAR currents upon TBS, calculated as log2-transformed ratio of the fEPSP 50-60 min after TBS (70-80 min) over the fEPSP during baseline (0-20 min), was larger in LTP pathway of GluA3-KO slices compared to wt slices and control pathways (plots of control pathways shown in Fig.S3). Data are mean ±SEM. Statistics: 2-tailed unpaired *t* test over the last 10 minutes of the recording (*A,B*) and two-way ANOVA with post-hoc Sidak (*C*). * indicates p<0.05.

cell line that produces Aβ in oligomeric form, or with control medium (Podlisny et al., 1995). The incubation of slices with 1 nM of oligomeric Aβ blocked LTP in wild-type slices (p=0.03; Fig. 4*A*), but failed to block LTP in GluA3-deficient slices (p=0.8; Fig. 4*B*). In the presence of Aβ-oligomers LTP was significantly smaller in wild-type slices compared to GluA3-deficient slices (p=0.04; Fig. 4*C*). Thus, GluA3-expression was critical for Aβ-oligomers to block LTP.

GluA3-deficient APP/PS1 transgenic mice do not display spine loss or memory impairment. Mice that express human APP (APPswe) and mutant presenilin 1 (PS1dE9) transgenes produce high levels of $A\beta_{42}$ and are used as a mouse model for familial AD (Savonenko et al., 2005). An immunostaining for Aβ shows that these APP/PS1-transgenic mice started to develop plaques in the CA1 region of the hippocampus at the age of 6 months, with more plaques situated in the stratum lacunosum-moleculare (SLM) than in the stratum radiatum (SR) (Fig. 5*A* and Fig. S4*A*). To assess whether these local differences in Aβ-load correspond with location-specific patterns of spine loss (Siskova et al., 2014), spine analysis was performed on oblique CA1 dendrites in both SR and SLM. Indeed, whereas the spine density remained unaffected in the SR (p=0.6; Fig. 5*C* and *D* and Fig. S4*B*), we did observe a reduced spine density in the SLM (p<0.01; Fig. 5*E* and *F*). Although in 12-month old mice the plaque load had approximately quadrupled in both the SR and the SLM (Fig. 5*B*), the spine loss in the CA1 had not aggravated (Fig. 5*D* and *F*). The observed spine loss in the SLM of APP/PS1-transgenic mice was not accompanied by a change in the average diameter of spine heads (Fig. 5*G* and *J*) or the distribution of spine head sizes (Fig. 5*I* and *J*). In APP/PS1 mice that were GluA3-deficient the development of plaque formation was similar compared to GluA3-expressing APP/PS1 littermates (p>0.9; Fig. 5*A* and *B*), suggesting that the level of Aβ accumulation was unaffected in the absence of GluA3. As we observed in organotypic slice cultures, GluA3-deficient CA1 neurons

Fig. 5. APP/PS1 mice that lack GluA3 develop Aβ plaques but do not show spine loss. (***A,B***) Examples of 6E10 staining (left) and average mean plaque load of 6 month (***A***) and 12 month (***B***) APP/PS1 mice (n=4 mice for all groups) demonstrate that more Aβ plaques were formed in the stratum lacunosum-moleculare (SLM) than in the stratum radiatum (SR). PCL, pyramidal cell layer; MO, molecular layer of the dendate gyrus. (***C,D***) Example images (left) and average spine density (right) of CA1 dendrites in the SR was similar in dendrites of 6 month (***C***, wt=18; APP/PS1=24; GluA3-KO=18; APP/PS1/GluA3-KO=18) and 12 month old APP/PS1 mice (***D***, wt=24; APP/PS1=24; GluA3-KO=12; APP/PS1/GluA3-KO=18) Scale bar: 2 µm. (***E,F***) Example images (left) and average spine density (right) was lower in APP/PS1-expressing SLM dendrites provided that they expressed GluA3 for both 6 month (***E***, wt=18; APP/PS1=24; GluA3-KO=18; APP/PS1/GluA3-KO=18) and 12 month (***F***, wt=24; APP/PS1=24; GluA3-KO=12; APP/PS1/GluA3-KO=18) old mice. Scale bar: 2 µm. (***G,H***) Mean spine head diameter was unaffected in 6 month (***G***) and 12 month (***H***) old APP/PS1 mice. (***I,J***) Spine head size normalized distribution was unaffected in 6 month (***I***) and 12 month (***J***) old APP/PS1 mice. Data are mean ±SEM. Statistics: two-way ANOVA with post-hoc Sidak test (***A-H***), or K-S test (***I,J***). * indicates p<0.05.

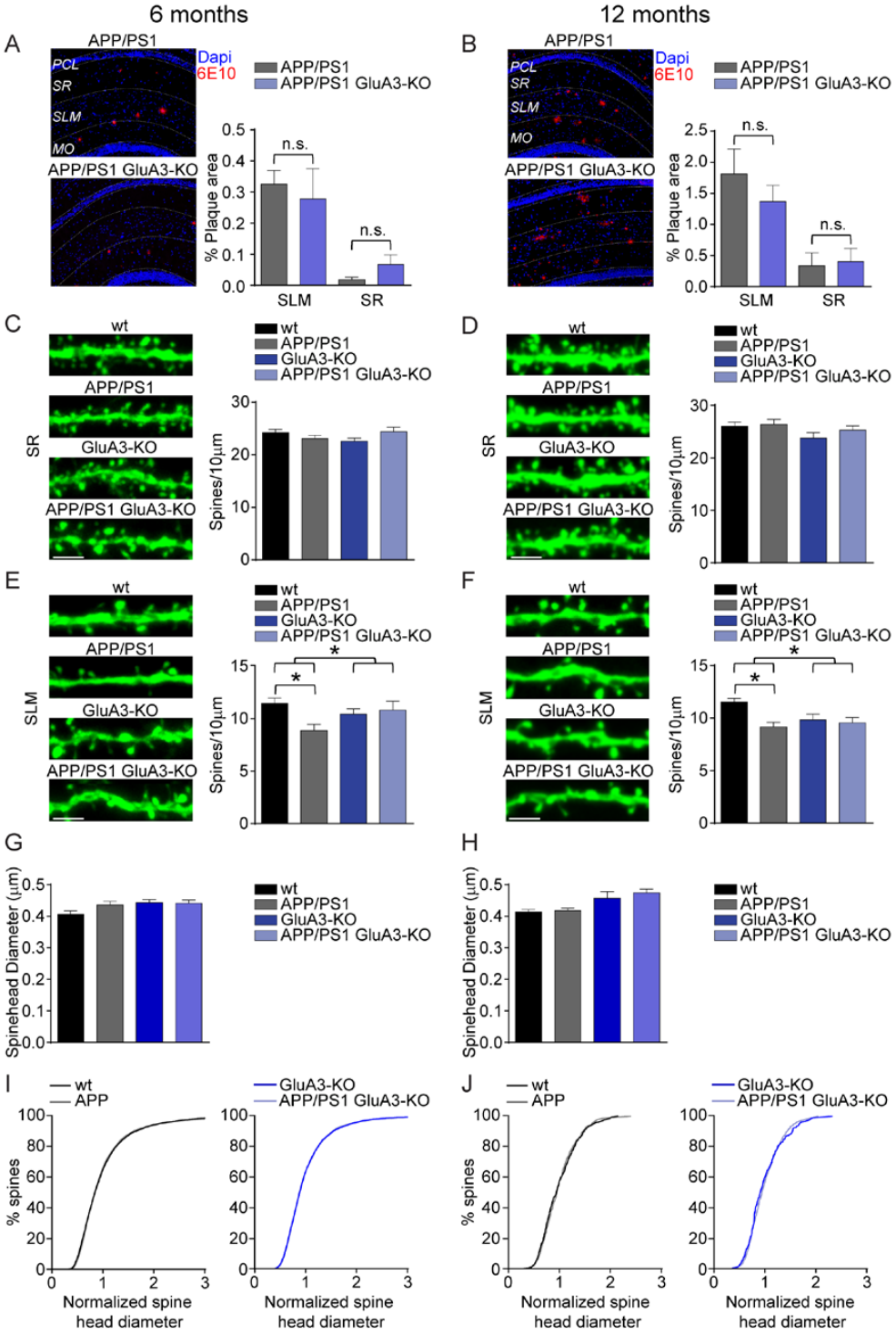
6 months
12 months
A
B
APP/PS1
Dapi
6E10
PCL
SR
SLM
MO
APP/PS1 GluA3-KO
% Plaque area
n.s.
SLM
SR
C
D
E
F
wt
APP/PS1
GluA3-KO
Spines/10µm
*
G
H
Spinehead Diameter (µm)
I
J
wt
APP
GluA3-KO
% spines
Normalized spine head diameter

have on average a similar spine density (Fig. 5*C* to *F*) and larger spine heads (Fig. 5*G* and *H*; and Fig. S5) compared with age-matched wild-type littermates. Notably, in GluA3-deficient mice the APP/PS1 transgenes did not cause a reduced spine density in the SLM at both 6 and 12 months of age (Fig. 5*E* and *F*), indicating that APP/PS1 mice are only susceptible to spine loss when they express AMPAR subunit GluA3.

In addition to Aβ plaque and spine pathology, APP/PS1 mice show cognitive deficits and premature mortality. In our colony the survival rate of APP/PS1 mice was reduced compared with wild-type littermates ($p<0.01$). APP/PS1 mice did not show premature mortality when they were GluA3-deficient ($p=0.2$, Fig. 6*A*). We tested the ability to form hippocampus- and amygdala-dependent memories by submitting either 6 or 12-month old mice to a contextual fear-conditioning paradigm. Upon exposure to the shock cage, the mice with different genotypes displayed a similar locomotor activity in a novel environment and a similar startle response to a mild foot shock (Fig. 6*B* and *C*). When re-exposed to the shock cage 24 hours after conditioning, APP/PS1 mice showed impaired fear memories as expressed by a lower level of freezing behavior compared with wild-type littermates ($p=0.01$; Fig. 6*D* and $p=0.03$; Fig. 6*E*). For GluA3-deficient mice, the freezing response to the fearful context were equal irrespectively of having APP/PS1 transgenes ($p>0.9$; Fig. 6*D* and $p>0.9$; Fig. 6*E*). Similar results were obtained when another group of 6-month old mice was tested 7 days after conditioning (Fig. 6*F* and *G*), indicating that also the long-term stability of contextual fear memories remained unaffected by APP/PS1 transgenes in the absence of GluA3. GluA3-deficient mice consistently displayed a lower (non-significant) memory performance compared to their wild-type littermate controls at both 6 ($p=0.7$; Fig. 7*D*) and 12 months of age ($p=0.6$; Fig. 7*E*). In 3-month old mice this was not observed (Fig. S6). Combined, these findings indicate that GluA3 renders APP/PS1 mice susceptible to memory impairment.

DISCUSSION

We studied the influence of AMPAR subunit composition on Aβ-mediated synapto-toxicity in three different model systems. Firstly we showed that synaptic depression and spine loss in APP_{CT100}-overexpressing CA1 neurons of organotypic slices require GluA3 expression. Secondly, exogenously added Aβ-oligomers block LTP in acutely isolated brain slices of wild-type mice, but not of GluA3-deficient mice. Finally, increased mortality, contextual fear memory deficits and

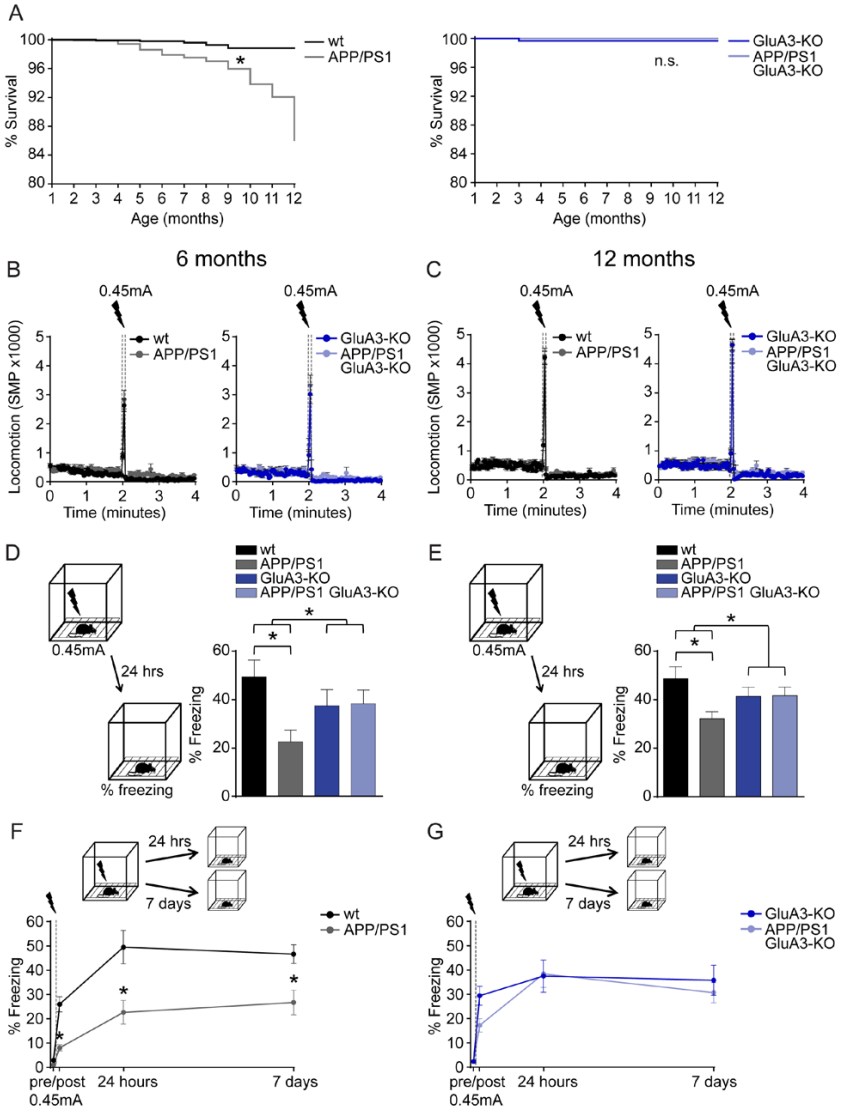

Fig. 6. APP/PS1 mice do not show increased mortality or memory deficits when they lack GluA3. (*A*) Kaplan Meier curves demonstrating that APP/PS1 but not APP/PS1/GluA3-KO mice have increased mortality rates (n=780 at 1 month, n=127 at 12 months). (*B,C*) Locomotion is similar before and during (startle response) the foot-shock in the conditioning trial, in both 6 month old (*B*) and 12 month old (*C*) mice. Automated quantification of motion as the number of Significant Motion Pixels (SMP) as described previously (Kopec et al., 2007). (*D,E*) Freezing levels during fear-memory retrieval 24 hrs after conditioning in 6-month old littermates (*D*, wt n=13; APP/PS1 n=13; GluA3-KO n=11; APP/PS1/GluA3-KO n=15) and 12-month old littermates (*E*, wt n=13; APP/PS1 n=20; GluA3-KO n=12; APP/PS1/GluA3-KO n=19). (*F*) Freezing responses to the fear context at 24 hrs (same as in *D*) and a different group of mice tested 7 days after conditioning (wt n=14; APP/PS1 n=13; GluA3-KO n=16; APP/PS1/GluA3-KO n=19) showed that long-term stability of contextual fear memories is unaffected in APP/PS1/GluA3-KO mice. Data are mean ±SEM. Statistics: Mantel-Cox test with Bonferroni correction (*A*), two-way ANOVA with post-hoc Sidak test (*D,E*), and unpaired *t* test (*F,G*). * indicates p<0.05.

spine loss in APP/PS1-transgenic mice are absent when they lack GluA3. Our data indicate that GluA3-containing AMPARs play a central role in these Aβ-mediated deficits. The increased mortality of APP/PS1 transgenic mice appears related to the occurrence of epileptic seizures and not to neurodegeneration (Scharfman, 2012). It will be interesting to assess whether GluA3 is also required for seizure generation in APP/PS1 mice.

How Aβ-oligomers initiate synaptic deficits remains largely unclear. Aβ-oligomers have a broad range of binding partners at the surface of neurons (Rahman et al., 2015), and a number of these partners have been proposed to be necessary for inducing pathological effects (Benilova, Karran & De, 2012; Mucke & Selkoe, 2012). Although GluA3 may be another candidate Aβ receptor, we consider the possibility that GluA3 is not so much responsible for the induction, but rather for the expression of Aβ-driven synaptic deficits. We propose a model where Aβ-oligomers bind one (or a combination) of surface receptors, thereby hijacking or facilitating an endogenous NMDAR-dependent signaling cascade that ultimately leads to the selective removal of GluA3-containing AMPAR from synapses. A factor that potentially mediates the depletion of GluA2/3 AMPARs from synapses is PICK1, an adaptor protein that selectively interacts with GluA2 and GluA3. The phosphorylation of the GluA2 or GluA3 c-tail by protein kinase Cα (PKCα) permits PICK1 to bind, leading to AMPAR endocytosis (Kim et al., 2001; Terashima et al., 2008). Notably, PICK1 as well as PKCα are necessary for Aβ-mediated synaptic depression to take place (Alfonso et al., 2014; Alfonso et al., 2016). The PICK1-dependent removal of AMPARs from the surface by Aβ was shown to be more prominent for GluA2 than for GluA1 (Alfonso et al., 2014), suggesting that Aβ-oligomers particularly trigger the endocytosis of GluA2/3s. The removal of GluA3-containing receptors by Aβ as a mechanism of action is supported by our finding that AMPAR currents are similarly reduced in neurons lacking GluA3 as in wild-type neurons expressing APP_{CT100}. (i.e. similar mini EPSC frequency and AMPAR/NMDAR ratio). Other effects of Aβ, including synaptic NMDAR depression, spine loss, LTP blockade, memory impairment and premature mortality did not fully mimic the lack of GluA3, possibly because these effects require the active removal of GluA3-containing AMPARs and/or because GluA3-deficiency is chronic and could allow compensatory mechanisms to ameliorate some of the deficits. Regardless of the mechanisms underlying the partial mimicry, our experiments indicate that the presence of GluA3 is required for these effects to occur.

GluA3-containing AMPARs have been proposed to be involved in the homeostatic scaling of synapse strength (Makino & Malinow, 2011; Rial Verde et al., 2006). In such a scenario, neurons that are deprived of synaptic input increase their synaptic GluA2/3 levels, and conversely neurons that are hyperactive counteract by lowering the number of GluA2/3s at synapses. It has recently been suggested that AD-related synaptic and memory deficits may arise from defects in homeostatic plasticity (Megill et al., 2015; Jang & Chung, 2016). Possibly Aβ-oligomers mediate a persistent synaptic downscaling by reducing the levels of GluA2/3s at synapses irrespective of the history of neuronal activity. Alternatively, Aβ-oligomers may trigger an increased neuronal network activity (Verret et al., 2012) to which neurons respond by lowering synaptic GluA2/3 levels. However, the consequences of an excess deposition of Aβ are not limited to the loss of synaptic AMPAR levels. Our observation that other Aβ-driven effects are not observed in GluA3-deficient mice is consistent with the notion that the removal of AMPARs from synapses is one of the first critical steps in Aβ pathogenesis (Hsieh et al., 2006; Miyamoto et al., 2016), followed or accompanied by the collateral removal of GluA1/2s and GluN2B-containing NMDARs and the disintegration of the synapse. Possibly GluA2/3s play a role in the stabilization of spine structures, for instance through their interaction with N-cadherins at synapses (Saglietti et al., 2007; Silverman et al., 2007). Alternatively, the endocytosis of GluA3-containing AMPARs may trigger a cellular signal that leads to the dismantling of spine structures. We propose that an intervention in the signaling pathway that is used by Aβ to remove GluA2/3s from synapses may be an attractive approach to prevent all Aβ-driven synaptic and memory deficits.

Lowering the neuronal or synaptic levels of GluA3-containing AMPARs may reduce the vulnerability of neurons for the detrimental effects of oligomeric Aβ. Interestingly, a recent study that screened for gene expression profiles associated with mild cognitive impairment (MCI), a clinical transition stage between aging and AD dementia (Boyle et al., 2006), found that among the genes that showed a strong negative correlation with cognitive performance were genes encoding glutamate receptors GluA3 and GluN2B (Berchtold et al., 2014). It is tempting to speculate that people with relatively low levels of GluA3 and GluN2B expression are less likely to develop MCI despite the presence of Aβ-oligomers. Along these lines, a mentally active brain would theoretically provide a reduced susceptibility for MCI, since learning behavior and sensory experiences trigger the delivery of GluA1-containing AMPARs to synapses (Mitsushima et al., 2011; Rumpel et al., 2005) and the subsequent homeostatic removal of synaptic GluA2/3s (Makino

& Malinow, 2011; Rial Verde et al., 2006). Future experiments may reveal under which physiological conditions the levels of GluA3 change in neurons, and whether differences in the expression levels of GluA3 determine the severity of AD-symptoms.

ACKNOWLEDGEMENTS

We thank Prof. Dr. Ed Koo for providing Aβ-oligomer samples, and Prof. Elly Hol and Dr. Willem Kamphuis for their expert advice. This work was supported by the Netherlands Organization for Scientific Research (NWO-ALW), the Netherlands Organization for Health Research and Development (ZonMW), the Alzheimer's association and the Internationale Stichting Alzheimer Onderzoek. The authors declare no financial or non-financial competing interests.

EXPERIMENTAL PROCEDURES

Mice. GluA3-deficient (Gria3tm1Dgen/Mmnc; MMRRC, Davis, CA), APPswe/PS1dE9 mice (Savonenko et al., 2005) (kindly provided by Dr. Elly Hol), and Thy1-eYFP mice (B6.Cg-Tg(Thy1-YFP)HJrs/J; Jackson, Bar Harbor, USA) were at least 6 times backcrossed to c57bl6 mice. GluA1-deficient mice were in a c57bl6/129 hybrid background and were a kind gift from Dr. R. Huganir (Kim et al., 2005). GluA3 is an X-linked gene; for behavioral experiments only male GluA3$^{-/Y}$ and littermate GluA3$^{+/Y}$ were used. For electrophysiology both male GluA3$^{-/Y}$ and GluA3$^{+/Y}$ and female GluA3$^{-/-}$ and GluA3$^{+/+}$ littermates were used; female GluA3$^{+/-}$ were excluded from this study. Mice were kept on a 12-hours day-night cycle and had ad libitum access to food and water. All experiments were were approved by the Institutional Animal Care and Use Committee of the Royal Netherlands Academy of Arts and Sciences (KNAW) or the University of San Diego, California.

Organotypic and acute hippocampal slices. Organotypic hippocampal slices were prepared from P7-8 mice as described previously (Stoppini, Buchs & Muller, 1991) and used after 7-12 days in culture for electrophysiology or after 13-15 days in culture for spine analysis. Constructs of APP-CT100+tdTomato, APP-CT84+tdTomato, GFP-GluA3(i) and GFP-GluA3(i)+APP-CT100 were cloned into a pSinRep5 shuttle vector and infective Sindbis pseudo viruses were produced according to the manufacturer's protocol (Invitrogen BV, Leek, Netherlands). Acute hippocampal slices were prepared from 3- to 4-week-old mice. Slices were cut coronally in cold sucrose cutting buffer (72 mM sucrose, 22 mM glucose, 2.6 mM $NaHCO_3$, 83 mM NaCl, 2.5 mM KCl, 3.3 mM $MgSO_4$, and 0.5 mM $CaCl_2$)

at a thickness of 350 µm and transferred to a recovery chamber containing oxygenated artificial cerebrospinal fluid (ACSF) containing 11 mM glucose, 1 mM $MgCl_2$, and 2 mM $CaCl_2$. Slices were maintained at 34°C for 45 min and then at room temperature for 45 min.

Preparation of Aβ oligomers. Chinese hamster ovary (CHO) cells stably transfected with APP751(V717F) mutation, referred to as 7PA2 cells (Podlisny et al., 1995), were a gift from Dr. Edward Koo. 7PA2 cells or control CHO cells were cultured in Dulbecco's modified Eagle's medium (DMEM) containing 10% bovine fetal calf serum and grown to near confluence, then cultured in plain DMEM for 16 hr. The Aβ medium is collected, centrifuged at 200 *g* for 10 min and concentrated 10 fold using an Amicon Ultra 3k filtration device at 4000 x g for 30 min at 4°C. Levels of $Aβ_{40}$ and $Aβ_{42}$ oligomers were measured by enzyme-linked immunosorbent assay (ELISA). 7PA2 conditioned medium was diluted to 1 nM total Abeta, and CHO conditioned medium from the same batch was diluted similarly. Western Blots were used to confirm the presence of Aβ oligomers.

Electrophysiology. Organotypic hippocampal slices were perfused with artificial CSF (ACSF, in mM: 118 NaCl, 2.5 KCl, 26 $NaHCO_3$, 1 NaH_2PO_4, 4 $MgCl_2$, 4 $CaCl_2$, 20 glucose) gassed with 95%O_2/5%CO_2). Whole-cell recordings were made with 3 - 5 MΩ pipettes, (R_{access} < 20 MΩ, and R_{input} > 10 x R_{access}) filled with internal solution containing (in mM): 115 $CsMeSO_3$, 20 CsCl, 10 HEPES, 2.5 $MgCl_2$, 4 Na_2-ATP, 0.4 Na-GTP, 10 Na-Phosphocreatine, 0.6 EGTA. Miniature EPSCs were recorded at -60 mV with TTX (1 µM) and picrotoxin (50 µM) added to the bath. For evoked recordings, a cut was made between CA1 and CA3, and picrotoxin (50 µM) and 2-chloroadenosine (4 µM; Tocris) were added to the bath. Two stimulating electrodes, two-contact Pt/Ir cluster electrode (Frederick Haer, Bowdoin, USA), were placed between 100 and 300 µm down the apical dendrite, 100 µm apart, and 200 µm laterally in opposite directions. AMPAR-mediated EPSCs were measured as the peak inward current at -60 mV. NMDAR-mediated EPSCs were measured as the mean outward current between 40 and 90 ms after the stimulation at +40 mV, corrected by the current at 0 mV. EPSC amplitudes were obtained from an average of at least 40 sweeps at each holding potential. Data was acquired using a Multiclamp 700B amplifier (Molecular Devices, Sunnyvale, USA). Evoked recording were analyzed using custom software written in Igor Pro (Wavemetrics, Tigard, USA). Miniature EPSC recordings were analyzed with MiniAnalysis (Synaptosoft, Decatur, USA) with an amplitude threshold of 5 pA. For LTP recordings, acute slices were transferred to a recording chamber, where it was submerged and received a continuous flow of ACSF supplemented with 11 mM glucose, 1 mM

$MgCl_2$, 2 mM $CaCl_2$, and 100 µM picrotoxin (pH 7.4). Extracellular field potentials were recorded in the SR with glass electrodes (1.5-2.5 MΩ) containing ACSF. Field excitatory postsynaptic potentials (fEPSPs) were evoked by stimulating independent afferents by placing bipolar stimulation electrodes 150 µm down the apical dendrites, and 150-200 µm laterally in opposite directions. Aβ or control medium was added to the perfusion for 20 minutes during the acquisition of a stable baseline prior to LTP induction. LTP was induced by applying 4 trains of electrical stimulation at 100 Hz, lasting 100 ms each, every 20 s. After LTP induction, fEPSPs were recorded for an additional 60 min. Averaged normalized fEPSP for the last 10 minutes (50-60 minutes after LTP induction) of each recording was used to quantify the potentiation value. Experiments were conducted blind to experimental conditions.

Dendritic spine analysis in organotypic hippocampal slices. Three-dimensional images were collected by two-photon laser scanning microscopy (Femtonics Ltd. Hungary) with a Ti:sapphire laser (Chameleon, Coherent, Santa Clara, USA) tuned at 910 nm. Optical z-sections were captured every 0.75 µm of apical dendrites approximately 180 µm from the cell body. The density and diameter of spines protruding in the horizontal (x/y) plane were manually quantified from projections of stacked 3D images by an experimenter blind to experimental conditions and genotype using ImageJ software (http://fiji.sc).

Aβ plaque load and spine analysis in APP/PS1 mice. Mice were anesthetized with pentobarbital and perfused with 20 ml 0.1 M PBS followed by 80 ml of fixative (4% paraformaldehyde in 0.1 M PBS pH 7.2). Brains were removed, post-fixed for 1 hour in fixative, and washed in PBS.

For plaque load analysis: brains were kept in 20% sucrose overnight, snap-frozen in dry-ice and stored at -80°C. The brains were sliced into 10 µm sections on a Leica CM3050S cryostat and thaw-mounted onto microscope slides. Epitope retrieval was achieved by incubating the slides in a sodium citrate buffer (10mM sodium citrate, 0.05% Tween-20, pH 6.0) at 95 °C. The sections were washed in PBS, incubated in blocking solution (10% normal donkey serum, 0.4% Triton X-100 in PBS) for 1 hour and subsequently incubated with the 6E10 antibody (1:15000 dilution, SIG-39320, Covance, Princeton, NJ, USA) overnight at room temperature in blocking solution, washed in PBS and incubated with Cy3-conjugated donkey anti-mouse IgG (1:1400, in PBS; Jackson ImmunoResearch, West Grove, PA, USA) for 2 hours at room temperature. Sections were washed in PBS and covered with VectaShield mounting medium with DAPI (Vector Labs, Burlingame, CA, USA).

Images of the CA1 (10x magnified, 1392x1040, pixel size 0.65μm^2) were obtained using a fluorescence microscope (Leica DM-RE, Wetzlar, Germany). Eight images per animals were acquired blind to experimental conditions, and analyzed with Image-Pro Plus software script (Media Cybernetics, Rockville, MD, USA). The level of plaque area was expressed as the percentage of positive pixels. Slices from wt and GluA3-KO littermates were included as negative controls (Fig. S4*A*).

For spine analysis: coronal 50 μm-thick slices were prepared from the fixed brains of Thy1-eYFP with a vibratome (Leica, Rijswijk, Netherlands) and mounted with Vectashield medium (Vector Labs, Peterborough UK). Z-stack images of oblique apical dendrites were obtained with a Leica SP5 II confocal microscope. Laser power was adjusted to achieve similar fluorescence levels across images. Spine density and spine size was manually quantified by an experimenter blind to experimental conditions and genotype using ImageJ software ('http://fiji.sc'). Spine size was determined by measuring spine head diameters, since diameter measurements were largely independent on fluorescence intensity levels (Fig. S4*C*).

Contextual Fear Conditioning Behavioral Essay

Male mice (GluA3$^{-/Y}$) were placed in a box (29 cm high, 31.5 cm wide, 23 cm deep; Med Associates Inc., Georgia, VT) inside a sound-attenuating chamber for 4 min, in which a shock (0.45 mA, 2 s) was delivered after 2 min through a grid floor with stainless steel bars. Each trial took place between 1:00 and 4:00 pm during the light cycle. Freezing behavior and locomotion were quantified using custom-made Matlab script (Kopec et al., 2007). Absence of movement for at least 1 second was considered as freezing. Experiments were conducted blind to the genotype of the mice.

Statistical analysis

The Kolmogorov-Smirnov test (K-S) was used to test whether data sets were normally distributed. The F-test was used to test equal variance. Where necessary, data were log- or square root-transformed to obtain normal distributions and homogeneity of variance. Significance was determined using two-tailed Student *t* tests to compare 2 groups. Two-way ANOVA followed by post-hoc Sidak comparisons were used when two independent variables (i.e. genotype and the expression/presence of Aβ) were measured. The K-S tests on the cumulative distributions were done on data normalized to its group mean. This allowed a comparison of distributions independent of a difference in mean. Mantel-Cox test with Bonferroni correction was used to compare mortality rates. *P* values below 0.05 were considered statistically significant.

REFERENCES

Brown, D. F. *et al.* (1998) Neocortical synapse density and Braak stage in the Lewy body variant of Alzheimer disease: a comparison with classic Alzheimer disease and normal aging. *J. Neuropathol. Exp. Neurol.* **57**(10): 955-960.

Scheff, S. W., Price, D. A., Schmitt, F. A., & Mufson, E. J. (2006) Hippocampal synaptic loss in early Alzheimer's disease and mild cognitive impairment. *Neurobiol. Aging* **27**(10): 1372-1384.

Lambert, M. P. *et al.* (1998) Diffusible, nonfibrillar ligands derived from Abeta1-42 are potent central nervous system neurotoxins. *Proc. Natl. Acad. Sci. U. S. A* **95**(11): 6448-6453.

Lesne, S. *et al.* (2006) A specific amyloid-beta protein assembly in the brain impairs memory. *Nature* **440**(7082): 352-357.

McLean, C. A. *et al.* (1999) Soluble pool of Abeta amyloid as a determinant of severity of neurodegeneration in Alzheimer's disease. *Ann. Neurol.* **46**(6): 860-866.

Shankar, G. M. *et al.* (2008) Amyloid-beta protein dimers isolated directly from Alzheimer's brains impair synaptic plasticity and memory. *Nat. Med.* **14**(8): 837-842.

Kamenetz, F. *et al.* (2003) APP processing and synaptic function. *Neuron* **37**(6): 925-937.

Lacor, P. N. *et al.* (2007) Abeta oligomer-induced aberrations in synapse composition, shape, and density provide a molecular basis for loss of connectivity in Alzheimer's disease. *J. Neurosci.* **27**(4): 796-807.

Walsh, D. M. *et al.* (2002) Naturally secreted oligomers of amyloid beta protein potently inhibit hippocampal long-term potentiation in vivo. *Nature* **416**(6880): 535-539.

Mucke, L. & Selkoe, D. J. (2012) Neurotoxicity of amyloid beta-protein: synaptic and network dysfunction. *Cold Spring Harb. Perspect. Med.* **2**(7): a006338.

Kessels, H. W., Nabavi, S., & Malinow, R. (2013) Metabotropic NMDA receptor function is required for beta-amyloid-induced synaptic depression. *Proc. Natl. Acad. Sci. U. S. A* **110**(10): 4033-4038.

Shankar, G. M. *et al.* (2007) Natural oligomers of the Alzheimer amyloid-beta protein induce reversible synapse loss by modulating an NMDA-type glutamate receptor-dependent signaling pathway. *J. Neurosci.* **27**(11): 2866-2875.

Wei, W. *et al.* (2010) Amyloid beta from axons and dendrites reduces local spine number and plasticity. *Nat. Neurosci.* **13**(2): 190-196.

Snyder, E. M. *et al.* (2005) Regulation of NMDA receptor trafficking by amyloid-beta. *Nat. Neurosci.* **8**(8): 1051-1058.

Hsieh, H. *et al.* (2006) AMPAR removal underlies Abeta-induced synaptic depression and dendritic spine loss. *Neuron* **52**(5): 831-843.

Miyamoto, T., Kim, D., Knox, J. A., Johnson, E., & Mucke, L. (2016) Increasing the Receptor Tyrosine Kinase EphB2 Prevents Amyloid-beta-induced Depletion of Cell Surface Glutamate Receptors by a Mechanism That Requires the PDZ-binding Motif of EphB2 and Neuronal Activity. *J. Biol. Chem.* **291**(4): 1719-1734.

Kessels, H. W., Kopec, C. D., Klein, M. E., & Malinow, R. (2009) Roles of stargazin and phosphorylation in the control of AMPA receptor subcellular distribution. *Nat. Neurosci.* **12**(7): 888-896.

Wenthold, R. J., Petralia, R. S., Blahos, J., II, & Niedzielski, A. S. (1996) Evidence for multiple AMPA receptor complexes in hippocampal CA1/CA2 neurons. *J. Neurosci.* **16**(6): 1982-1989.

Hayashi, Y. *et al.* (2000) Driving AMPA receptors into synapses by LTP and CaMKII: requirement for GluR1 and PDZ domain interaction. *Science* **287**(5461): 2262-2267.

Mitsushima, D., Ishihara, K., Sano, A., Kessels, H. W., & Takahashi, T. (2011) Contextual learning requires synaptic AMPA receptor delivery in the hippocampus. *Proc. Natl. Acad. Sci. U. S. A* **108**(30): 12503-12508.

Rumpel, S., LeDoux, J., Zador, A., & Malinow, R. (2005) Postsynaptic receptor trafficking underlying a form of associative learning. *Science* **308**(5718): 83-88.

Adamczyk, A. *et al.* (2012) GluA3-deficiency in mice is associated with increased social and aggressive behavior and elevated dopamine in striatum. *Behav. Brain Res.* **229**(1): 265-272.

Humeau, Y. *et al.* (2007) A pathway-specific function for different AMPA receptor subunits in amygdala long-term potentiation and fear conditioning. *J. Neurosci.* **27**(41): 10947-10956.

Lu, W. *et al.* (2009) Subunit composition of synaptic AMPA receptors revealed by a single-cell genetic approach. *Neuron* **62**(2): 254-268.

Meng, Y., Zhang, Y., & Jia, Z. (2003) Synaptic transmission and plasticity in the absence of AMPA glutamate receptor GluR2 and GluR3. *Neuron* **39**(1): 163-176.

Makino, H. & Malinow, R. (2011) Compartmentalized versus global synaptic plasticity on dendrites controlled by experience. *Neuron* **72**(6): 1001-1011.

Rial Verde, E. M., Lee-Osbourne, J., Worley, P. F., Malinow, R., & Cline, H. T. (2006) Increased expression of the immediate-early gene arc/arg3.1 reduces AMPA receptor-mediated synaptic transmission. *Neuron* **52**(3): 461-474.

Hayashi, Y. *et al.* (2000) Driving AMPA receptors into synapses by LTP and CaMKII: requirement for GluR1 and PDZ domain interaction. *Science* **287**(5461): 2262-2267.

Matsuzaki, M. *et al.* (2001) Dendritic spine geometry is critical for AMPA receptor expression in hippocampal CA1 pyramidal neurons. *Nat. Neurosci.* **4**(11): 1086-1092.

Podlisny, M. B. *et al.* (1995) Aggregation of secreted amyloid beta-protein into sodium dodecyl sulfate-stable oligomers in cell culture. *J. Biol. Chem.* **270**(16): 9564-9570.

Savonenko, A. *et al.* (2005) Episodic-like memory deficits in the APPswe/PS1dE9 mouse model of Alzheimer's disease: relationships to beta-amyloid deposition and neurotransmitter abnormalities. *Neurobiol. Dis.* **18**(3): 602-617.

Siskova, Z. *et al.* (2014) Dendritic structural degeneration is functionally linked to cellular hyperexcitability in a mouse model of Alzheimer's disease. *Neuron* **84**(5): 1023-1033.

Scharfman, H. E. (2012) "Untangling" Alzheimer's disease and epilepsy. *Epilepsy Curr.* **12**(5): 178-183.

Rahman, M. M., Zetterberg, H., Lendel, C., & Hard, T. (2015) Binding of human proteins to amyloid-beta protofibrils. *ACS Chem. Biol.* **10**(3): 766-774.

Benilova, I., Karran, E., & De, S. B. (2012) The toxic Abeta oligomer and Alzheimer's disease: an emperor in need of clothes. *Nat. Neurosci.* **15**(3): 349-357.

Kim, C. H., Chung, H. J., Lee, H. K., & Huganir, R. L. (2001) Interaction of the AMPA receptor subunit GluR2/3 with PDZ domains regulates hippocampal long-term depression. *Proc. Natl. Acad. Sci. U. S. A* **98**(20): 11725-11730.

Terashima, A. *et al.* (2008) An essential role for PICK1 in NMDA receptor-dependent bidirectional synaptic plasticity. *Neuron* **57**(6): 872-882.

Alfonso, S. *et al.* (2014) Synapto-depressive effects of amyloid beta require PICK1. *Eur. J. Neurosci.* **39**(7): 1225-1233.

Alfonso, S. I. *et al.* (2016) Gain-of-function mutations in protein kinase Calpha (PKCalpha) may promote synaptic defects in Alzheimer's disease. *Sci. Signal.* **9**(427): ra47.

Megill, A. *et al.* (2015) Defective Age-Dependent Metaplasticity in a Mouse Model of Alzheimer's Disease. *J. Neurosci.* **35**(32): 11346-11357.

Jang & Chung (2016) Emerging Link between Alzheimer's Disease and Homeostatic Synaptic Plasticity. *Neural Plast.* **2016**(2016): 1-19.

Verret, L. *et al.* (2012) Inhibitory interneuron deficit links altered network activity and cognitive dysfunction in Alzheimer model. *Cell* **149**(3): 708-721.

Saglietti, L. *et al.* (2007) Extracellular interactions between GluR2 and N-cadherin in spine regulation. *Neuron* **54**(3): 461-477.

Silverman, J. B. *et al.* (2007) Synaptic anchorage of AMPA receptors by cadherins through neural plakophilin-related arm protein AMPA receptor-binding protein complexes. *J. Neurosci.* **27**(32): 8505-8516.

Boyle, P. A., Wilson, R. S., Aggarwal, N. T., Tang, Y., & Bennett, D. A. (2006) Mild cognitive impairment: risk of Alzheimer disease and rate of cognitive decline. *Neurology* **67**(3): 441-445.

Berchtold, N. C. *et al.* (2014) Brain gene expression patterns differentiate mild cognitive impairment from normal aged and Alzheimer's disease. *Neurobiol. Aging* **35**(9): 1961-1972.

Kim, C. H. *et al.* (2005) Persistent hippocampal CA1 LTP in mice lacking the C-terminal PDZ ligand of GluR1. *Nat. Neurosci.* **8**(8): 985-987.

Stoppini, L., Buchs, P. A., & Muller, D. (1991) A simple method for organotypic cultures of nervous tissue. *J. Neurosci. Methods* **37**(2): 173-182.

Kopec, C. D. *et al.* (2007) A robust automated method to analyze rodent motion during fear conditioning. *Neuropharmacology* **52**(1): 228-233.

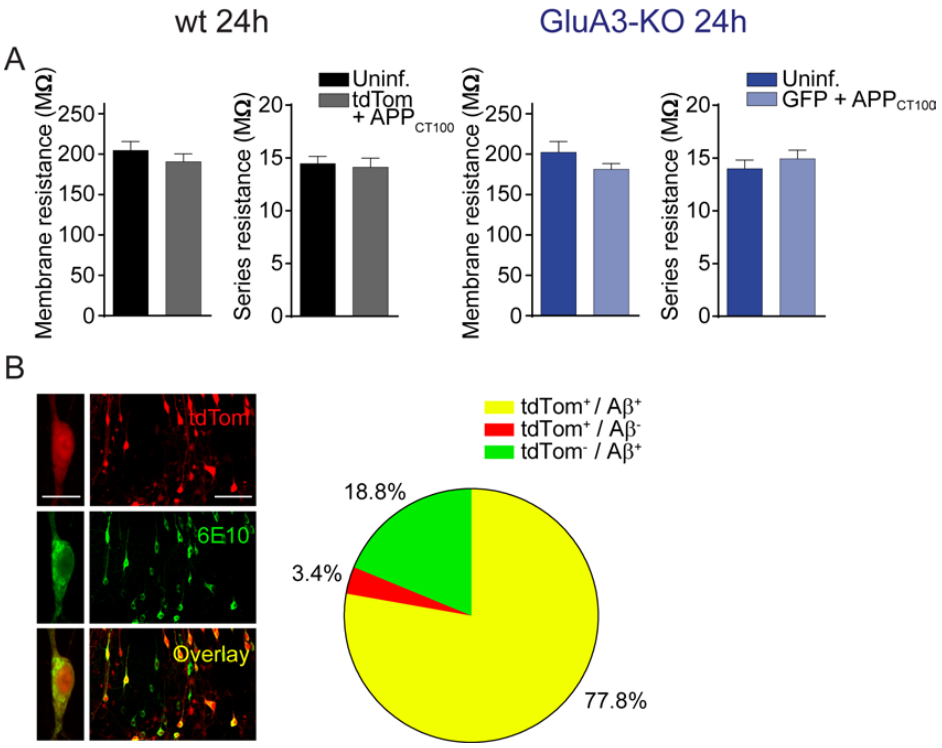

Figure S1. Sindbis virus expression does not affect membrane resistance of neurons and allows dual APP_{CT100}/tdTomato expression. (A) Average membrane and series resistance of whole-cell patch-clamped CA1 neurons expressing tdTomato+APP_{CT100}(gray; n = 24) and uninfected WT neurons (black; n = 24) 24 h after infection, GFP+APP_{CT100}-expressing (light blue; n = 13) and uninfected (dark blue; n = 15) GluA3-KO neurons 24 h after infection. The mean membrane resistance indicates that Sindbis-driven APP_{CT100} expression did not compromise neuronal health. Data are mean ± SEM. Statistics: two-tailed unpaired t test. (B, Left) Sample images of an individual neuron and a population of CA1 neurons in an organotypic slice infected with Sindbis virus expressing APP_{CT100}/tdTomato and immunostained for Aβ (6E10 antibody). [Scale bars: 20 µm (Left) and 100 µm (Right).] (Right) The majority of tdTomato-expressing CA1 neurons (total: n = 144) showed positive staining for Aβ.

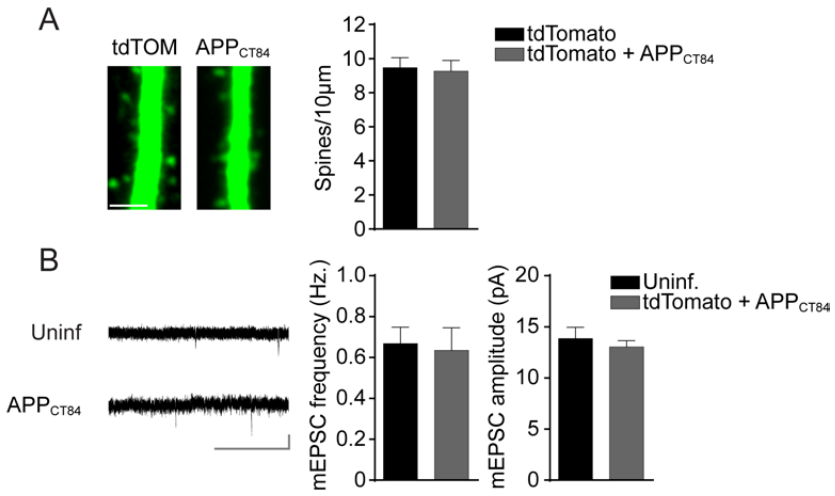

Figure S2. Expression of APP_{CT84} does not affect spine density or mEPSCs. (A, *Left*) Sample two-photon images of apical CA1 dendrites expressing tdTomato or tdTomato+APP_{CT84}. (Scale bar: 3 µm.) (*Right*) The average spine density was not different in CA1 pyramidal neurons expressing tdTomato (n = 11) or tdTomato+APP_{CT84} (n = 11). (B, *Left*) Sample mEPSC traces of WT neurons with or without APP_{CT84} expression. (Scale bar: 3 s, 10 pA.) (*Right*) APP_{CT84} expression did not affect mean mEPSC frequency or amplitude in WT neurons (uninfected, n = 17; CT84, n = 14). Data are mean ± SEM. Statistics: two-tailed unpaired t test.

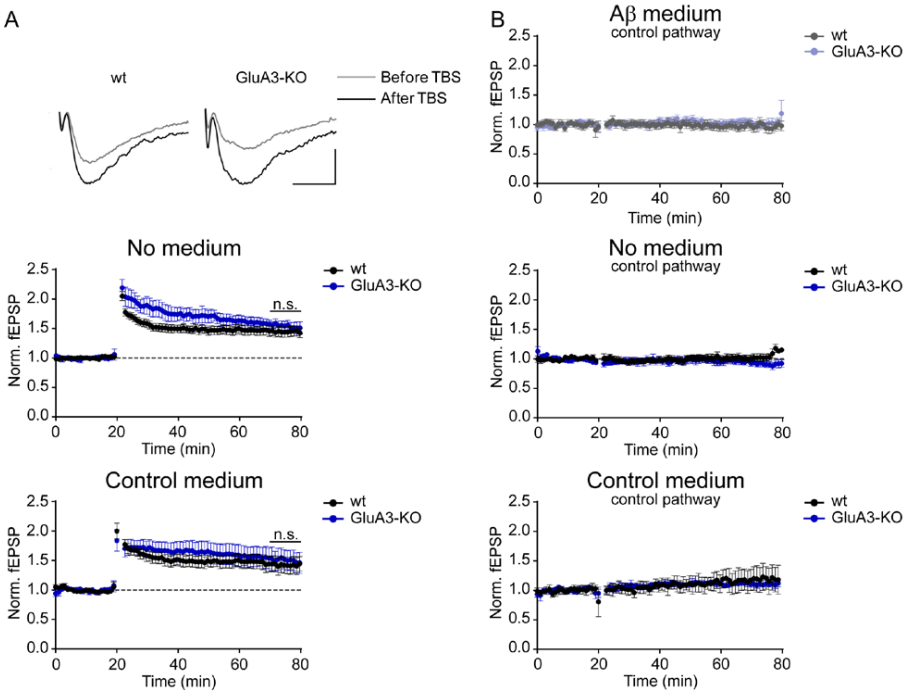

Figure S3. GluA3–deficient CA1 neurons have increased spine head size in the SLM. Shown are the average spine head diameter (Upper) and the normalized distribution of spine head sizes (Lower) of CA1 pyramidal neurons in WT (black) and GluA3-KO (blue) littermate mice. (A) SR dendrites expressing APP_{CT84} + tdTomato in organotypic hippocampal slices as in Fig. 3A. (B and C) SLM dendrites in 6-mo-old mice as in Fig. 6G (B) and in 12-mo-old mice as in Fig. 5H (C). Data are mean ± SEM. Statistics: two-tailed unpaired t tests for spine diameter and K–S test for spine size distributions. *P < 0.05.

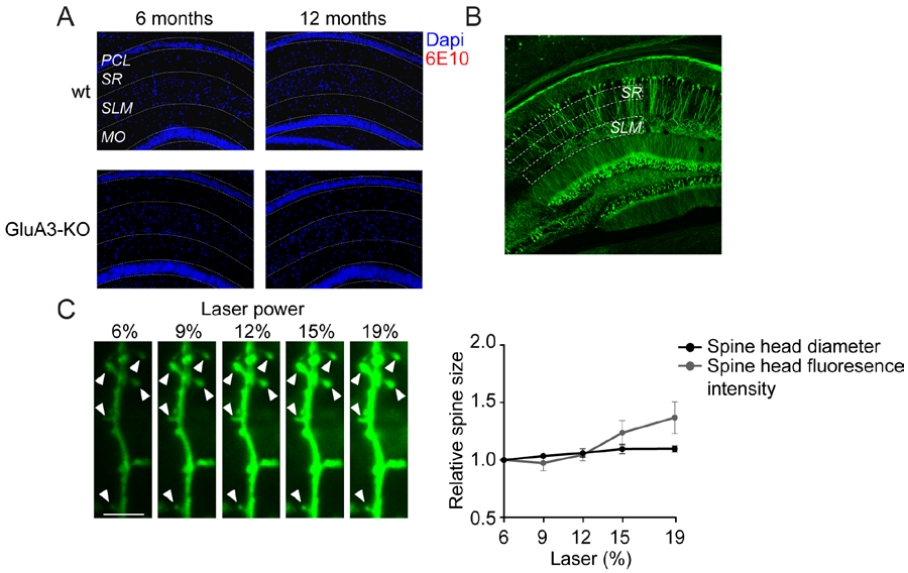

Figure S4. GluA3-KO slices show normal pathway-specific LTP. (A) Sample LTP traces (Top; scale bar: 10 ms, 0.2 mV) and peak LTP responses (Middle and Bottom) show LTP with similar magnitude in the absence of medium (WT, n = 11; GluA3-KO, n = 6) and in the presence of control medium (WT, n = 6; GluA3-KO, n = 8) in WT and GluA3-KO slices. (B) The control pathways of the LTP experiments shown in Fig. 4 remained stable over time in Aβ medium (WT, n = 5; GluA3-KO n = 8) (Top), in the absence of medium (WT, n = 6; GluA3-KO, n = 6) (Middle), and in control medium (WT, n = 3; GluA3-KO, n = 3) (Bottom), demonstrating that the LTP was specific for the stimulated pathway. Data are mean ± SEM. Statistics: two-tailed unpaired t test over the last 10 min of the recording.

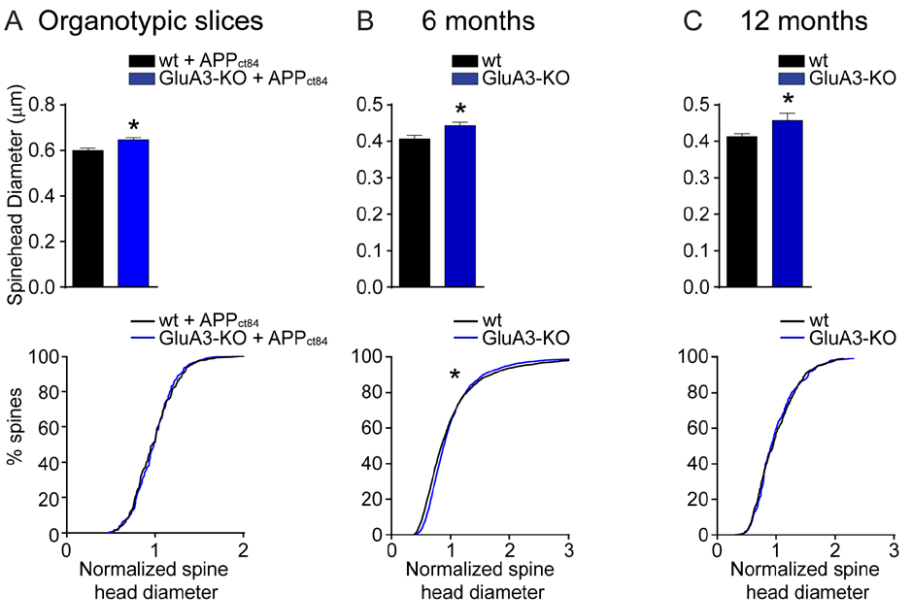

Figure S5. Control experiments for plaque load analysis and spine size analysis in the CA1 of aged mice. (A) 6E10 staining in 6-mo-old (Left) and 12-mo-old (Right) WT and GluA3-KO mice without the APP/PS1 transgenes confirmed an absence of plaque formation. (Scale bar: 250 µm.) (B) Confocal image of a hippocampal slice of a Thy1-eYFP mouse depicting the regions where spine density was quantified. (Scale bar: 250 µm.) (C) Comparison of two different spine-size analyses showed that the average spine head diameter was less sensitive than spine volume to variation in fluorescence intensity reflected as the spine brightness (background-subtracted and corrected for fluorescence levels in the dendritic shaft). (Left) Confocal images of a CA1 dendrite obtained with different levels of laser intensity. Arrowheads indicate the spines analyzed. (Scale bar: 2 µm.) (Right) Spine head diameter and spine fluorescence (after background fluorescence subtraction) normalized to the value at 6% laser intensity plotted against laser intensity (n = 5 spines). Data are mean ± SEM.

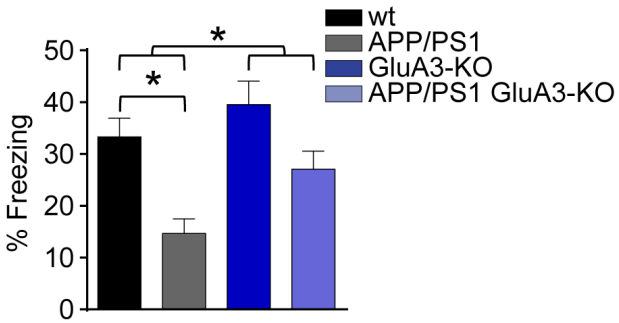

Figure S6. Freezing levels during fear-memory retrieval 24 h after conditioning in 3-mo-old littermates (WT, n = 11; APP/PS1, n = 10; GluA3-KO, n = 7; APP/PS1/GluA3-KO, n = 11) show memory impairment in APP/PS1 mice that is not seen in APP/PS1 GluA3-KO mice. Statistics: Two-way ANOVA with post hoc Sidak comparisons. *P < 0.05.

Chapter 7

Amyloid-β Causes Synaptic Depression via Phosphorylation of AMPA-Receptor subunit GluA3 at Serine 885

Niels R. Reinders[a,b], Sophie van der Spek[c], Carla M. da Silva-Matos[a], Ka Wan Li[c], August B. Smit[c], Helmut W. Kessels[a,b].

In preparation

[a] Netherlands Institute for Neuroscience, Royal Netherlands Academy of Arts and Sciences, Amsterdam, 1105BA, The Netherlands.
[b] Swammerdam Institute of Life Sciences, dept. of Cellular and Computational Neuroscience, University of Amsterdam, Amsterdam, 1098XH, The Netherlands.
[c] Department of Molecular and Cellular Neurobiology, Center for Neurogenomics and Cognitive Research, Amsterdam Neuroscience, VU University Amsterdam, Amsterdam, the Netherlands

Author contributions: N.R.R., S.vd.S and C.M.d.S.-M. performed experiments and analyzed data. K.W.L and A.B.S helped design experiments. N.R.R., S.vd.S and H.W.K. wrote the manuscript.

To whom correspondence may be addressed. Email: h.w.h.g.kessels@uva.nl

ABSTRACT

Amyloid-β (Aβ) is a prime suspect to cause cognitive deficits in Alzheimer's disease (AD) patients. Experiments in AD-mouse models have shown that soluble oligomeric clusters of Aβ (oAβ) degrade synapses and impair memory formation. A key initial step in oAβ-driven synaptic dysfunction is the suppression of AMPA-type glutamate receptor (AMPAR) mediated synaptic transmission. We here show that oAβ initiates synaptotoxicity by selectively targeting synapses that contain AMPAR subunit GluA3. Through mutagenesis of recombinant GluA3 we demonstrate that the PDZ-binding motif at the carboxy terminal end of GluA3 is critically involved in oAβ-driven synaptic depression. This PDZ-binding domain regulates the cycling of AMPARs in and out of synapses. When GRIP binds this domain, AMPARs are allowed to accumulate in intracellular vesicles and to enter synapses. Upon serine phosphorylation of this PDZ-binding motif by PKCα, GRIP binding is lost and PICK1 binds, which triggers the endocytosis of AMPARs. We could prevent oAβ-induced synaptic depression and spine loss by blocking either the binding of GRIP to GluA3, or phosphorylation at serine 885 of GluA3. Our data indicate that oAβ induces the removal of AMPARs from synapses and that this requires PKCα phosphorylation of the GluA3 subunit at serine 885. We propose that oAβ cause synaptic deficits by corrupting the constitutive cycling of GluA3-containing AMPA-receptors at synapses.

INTRODUCTION

Synaptopathology is emerging as a cause of cognitive impairment in Alzheimer's disease (AD) (de Wilde et al. 2016). In AD patients, a loss of synapses is associated with AD-related symptoms (DeKosky et al. 1996, McLean et al. 1999, Scheff et al. 2006, Scheff et al. 2003, Coleman et al. 2003). Progressing synaptopathology in AD patients is most likely caused by the accumulation of soluble oligomeric amyloid-beta (oAβ). Studies using AD animal models demonstrate that oAβ is toxic to synapses and sufficient to compromise memory retrieval in mice (Kamenetz et al. 2003, Lesne et al. 2006, Shankar et al. 2008, Muller-Schiffmann et al. 2016). Importantly, preventing the effects of oAβ on synaptic function averts AD-like symptoms in AD mouse models (Knafo et al. 2016, Reinders et al. 2016, Kim. et al. 2013, Cisse et al. 2011). These findings suggest that protecting synapses against the accumulation of oAβ can be a valid strategy to prevent AD symptoms.

For oAβ-mediated synapse loss to occur, AMPA-type glutamate receptors (AMPARs) play a central role. AMPARs, which are responsible for fast synaptic transmission, are composed of four different subunits: glutamate receptor subunits GluA1 to 4 (Diering et al. 2018). In excitatory neurons of the hippocampus, the majority of AMPARs consist of either GluA1/2 or GluA2/3 dimers (Wenthold et al. 1996). GluA1/2s and GluA2/3s have distinct functional properties, which are regulated by protein interactions at their intracellular carboxy-terminal tails (c-tails) (Shi et al. 2001, Zhou et al. 2018). The GluA1 subunit has a long intracellular c-tail that controls activity-dependent synaptic targeting of AMPARs (Kopec et al. 2007). In contrast, GluA2/3s enter synapses independent of synaptic activity and constitutively cycle into synapses to replace GluA1/2s (McCormack et al. 2006, Shi et al. 2001). GluA1/2s play an important role in several learning and memory processes (Kessels, Malinow 2009), but the role of GluA2/3s in synapse physiology has remained an enigma. GluA1/2 levels are lowered and GluA2/3s are enriched at synapses of neurons that are devoid of experience-dependent input, suggesting that GluA2/3 AMPARs are involved in homeostatic scaling of synapse strength (Makino, Malinow 2011). We recently discovered that GluA2/3s have a unique type of plasticity: they are in an electrically inactive state under basal conditions, and become activated in a cyclic AMP (cAMP) dependent manner (Renner et al. 2017, Gutierrez-Castellanos et al. 2017). GluA2/3s therefore only substantially contribute to synaptic currents upon a rise in intracellular cAMP.

GluA2 and GluA3 have short and similarly structured c-tails that contain identical PDZ binding motifs, which interact with glutamate receptor interacting protein (GRIP) and protein interacting with C-kinase-1 (PICK1). GRIP and PICK1 each play important roles in the cycling of AMPARs between the synaptic surface and intracellular endosomal compartments (Moretto, E. et al. 2018). While PICK1 promotes AMPAR endocytosis, GRIP is involved in transportation of AMPAR to synapses and retaining them in (recycling) endosomal vesicles (Kim, C. H. et al. 2001, Perez et al. 2001, Seidenman et al. 2003, Osten et al. 2000, Setou et al. 2002). Whether PICK1 or GRIP bind to the PDZ binding motif at the GluA2 or GluA3 c-tail is determined by protein kinase C-alpha (PKCα) phosphorylation of a serine residue within the PDZ-binding motif (Daw et al. 2000, Chung et al. 2000, Lin et al. 2007). Interestingly, PICK1 and GRIP regulate AMPAR trafficking during NMDA-receptor (NMDAR) dependent LTD. Upon the induction of NMDAR-dependent LTD, PKCα phosphorylation of the GluA2 and GluA3 c-tails releases their interaction with GRIP and allows PICK1 to bind and internalize AMPARs (Seidenman et al. 2003, Kim, C. H. et al. 2001, Iwakura et al. 2001, Terashima et al. 2008). Several recent observations suggest that oAβ corrupts PICK1/GRIP mediated trafficking of AMPARs. Firstly, the oAβ-driven synaptic depression critically depends on PICK1 (Alfonso, S. et al. 2014). Secondly, PKCα activation is required for the synaptotoxic effects of oAβ to occur (Alfonso, S. I. et al. 2016). Third, expression of GluA2-homomeric AMPARs with a mutation within their PDZ domain that prevents PICK1 mediated AMPAR endocytosis, is sufficient to block oAβ-driven spine loss (Hsieh et al. 2006, Fiuza et al. 2017).

We previously demonstrated that all oAβ-driven effects on synapses and memories are dependent on GluA3. CA1 neurons that lack GluA3, and only express GluA1/2s, are fully resistant to oAβ-driven synaptic depression and spine loss, and APP/PS1-transgenic mice were insensitive to memory impairment and premature mortality when they are GluA3-deficient (Reinders et al. 2016). However, why GluA3-lacking neurons are resistant to the effects of oAβ remains unclear. In this study we show that oAβ-driven synaptic depression and spine loss critically depends on protein interactions at the PDZ-binding domain in the GluA3 c-tail. Our experiments implicate PKCα-dependent removal of synaptic GluA3-containing AMPARs from synapses as a key event in oAβ-induced synaptotoxicity. We conclude that oAβ causes cognitive decline by corrupting the trafficking of synaptic GluA3-containing AMPARs.

RESULTS

oAβ suppresses cAMP-driven potentiation of synapses

To examine the effects of oAβ on synapses, we use Sindbis viral vectors express APP_{CT100}, the β-secretase product of APP and precursor to Aβ, in ~10% of CA1 pyramidal neurons of organotypic hippocampal slice cultures. In this model system, APP_{CT100} expression causes reliable synaptic depression as a consequence of the formation of oAβs (Kamenetz et al. 2003, Kessels et al. 2013). 20-52 hrs after infection with viral vectors expressing APP_{CT100} together with GFP, synaptic currents, evoked by electrical stimulation of Schaffer collateral inputs, were recorded simultaneously from neighboring infected and uninfected CA1 neurons. In line with previous studies (Reinders et al. 2016, Kessels et al. 2013, Kamenetz et al. 2003), APP_{CT100} expression caused synaptic depression of AMPAR currents (figure 1A). We previously showed that APP_{CT100}-expression failed to produce synaptic depression in slice cultures from GluA3-deficient mice (Reinders et al. 2016), suggesting GluA3-containing AMPARs play a central role. Under basal conditions GluA3-containing AMPARs are largely in an inactive state and contribute little to synaptic transmission until they convert to an active state upon a rise in cAMP (Renner et al. 2017, Gutierrez-Castellanos et al. 2017). To test whether oAβ-driven synaptic depression is more evident when GluA3 has switched to its active state, synaptic currents were recorded in the presence of adenylyl cyclase activator forskolin. The degree of synaptic depression through APP_{CT100} expression was similar in the presence of forskolin (figure 1A,B). APP_{CT100} expression did not change AMPA/NMDA ratio's (figure 1C,D), which is consistent with previous observations that oAβ reduces both synaptic AMPAR and NMDAR (Kamenetz et al. 2003, Kessels et al. 2013). Notably, forskolin significantly increased AMPA/NMDA ratios in uninfected neurons, but not in neighboring APP_{CT100} expressing neurons (Figure 1C,D). These data indicate that a rise in cAMP fails to potentiate AMPAR currents when neurons overproduce oAβ. Since the effect of cAMP on AMPAR currents is largely dependent on GluA3 (Gutierrez-Castellanos et al. 2017, Renner et al. 2017), these data support the notion that oAβ preferentially acts on GluA3-containing AMPARs. These results suggest that APP_{CT100}-expression either removes GluA3-containing AMPARs from synapses or prevents the activation of channel function of GluA3-containing AMPARs.

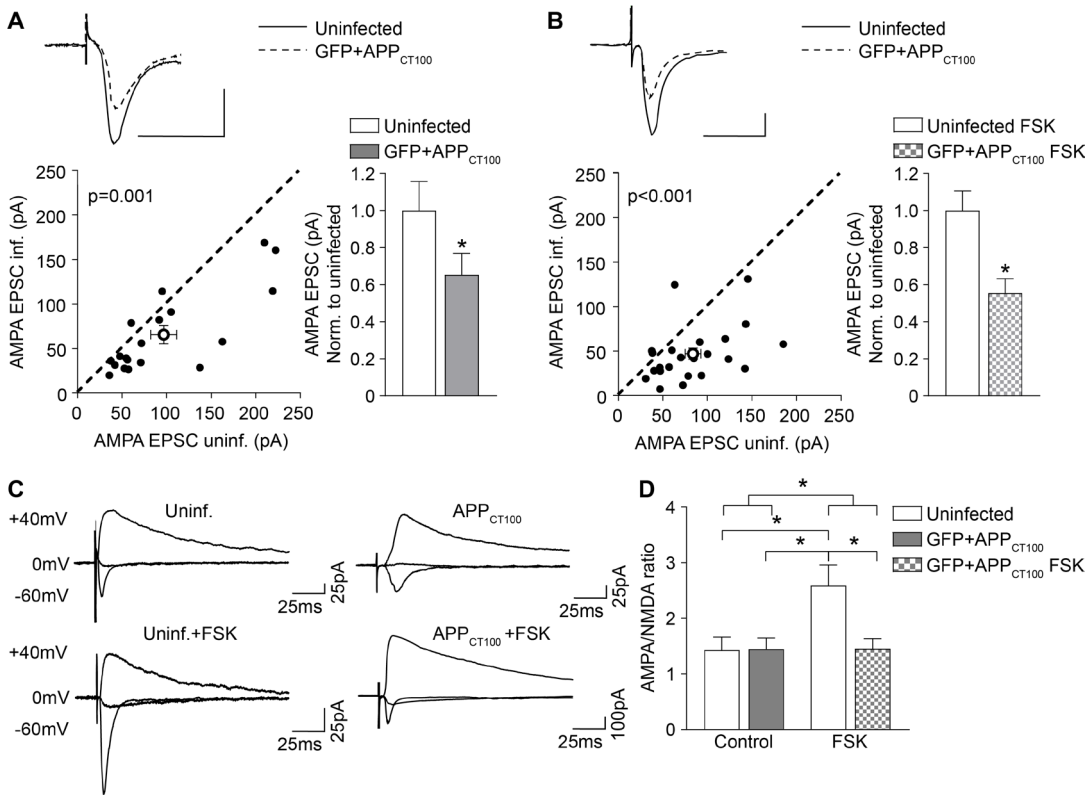

Figure 1. Neuronal expression of APP$_{CT100}$ suppresses cAMP-driven potentiation of synapses. (A) Example trace (top, scale bar: 25 ms, 50 pA), dot plots (open dots denote averages, filled dots represents a paired EPSC responses) and bar graphs (bottom, n = 19) of paired EPSC recordings from APP$_{CT100}$ expressing neurons (grey) and neighboring uninfected neurons (white). (A) Example trace (top, scale bar: 25 ms, 50 pA), dot plots and bar graphs (bottom, n = 23) of paired EPSC recordings from APP$_{CT100}$ expressing neurons (blocked) and neighboring uninfected neurons (white) in the presence FSK. (C) Sample traces of AMPA (-60mV) and NMDAR (+40mV) EPSCs of APP$_{CT100}$ expressing neurons in the presence or absence of FSK. (D) AMPAR/NMDA ratio was unaffected by APP$_{CT100}$. APP$_{CT100}$ expression prevented the FSK-induced increased AMPA/NMDA ratio (uninf. n=10, APP$_{CT100}$ n=15, uninf.+FSK n=17, APP$_{CT100}$+FSK n=18). Data are mean ± SEM. *P < 0.05.

GluA3 expression sensitizes neurons to effects of oAβ on synapses

To assess whether the oAβ-driven synaptic depression requires GluA3 expression in CA1 neurons, we infected CA1 neurons with sindbis virus expressing GFP-GluA3 with or without APP$_{CT100}$ in organotypic slices isolated from GluA3-deficient mice. 44-52 hrs after viral infection, synaptic currents evoked by electrical stimulation of Schaffer collateral inputs (eEPSC) were recorded from GFP-GluA3 infected and neighboring uninfected GluA3-deficient neurons. We note that GluA3-containing AMPARs obligatorily exist as heteromers (Coleman, S. K. et al. 2016), and that viral

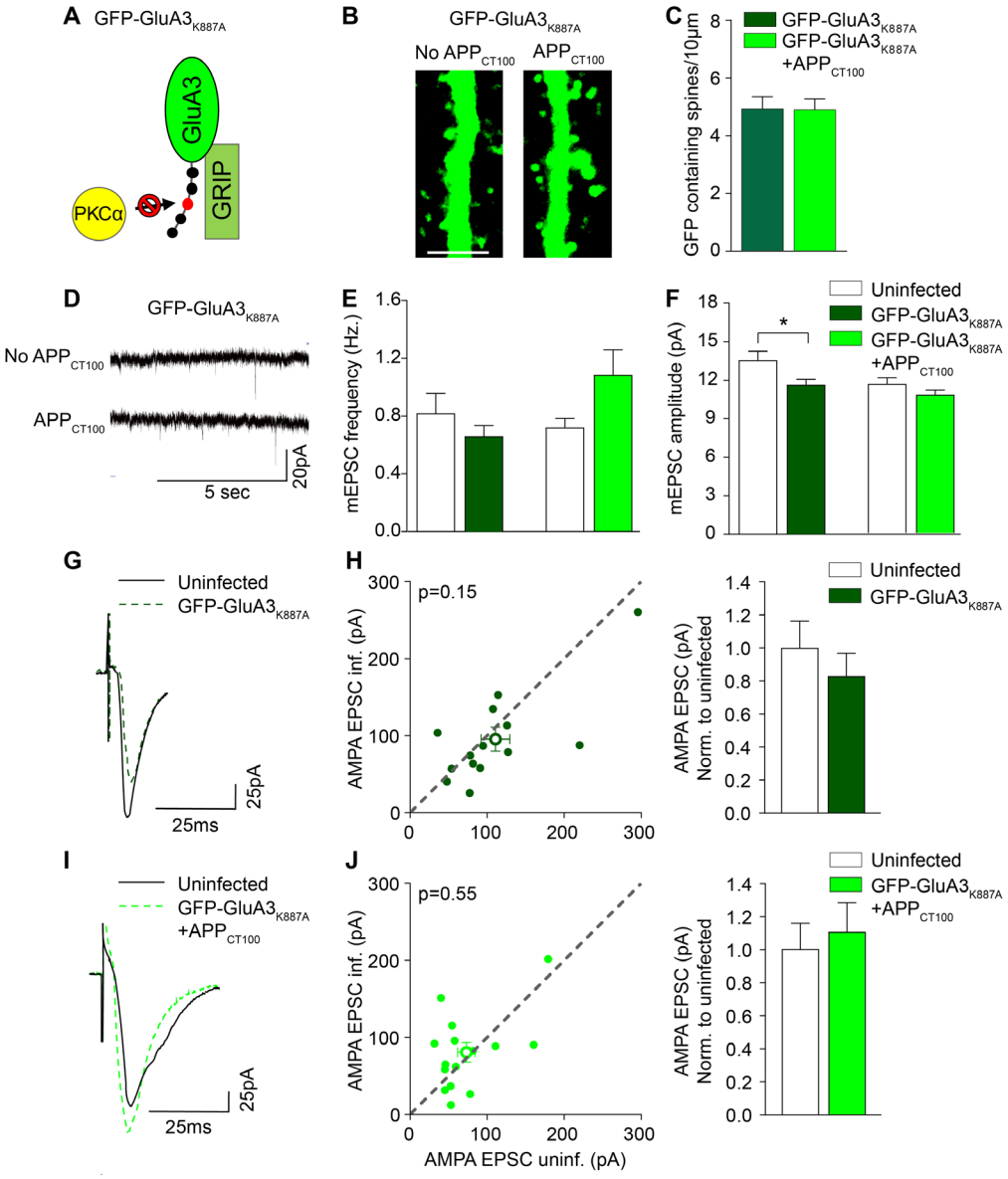

Figure 2. Neuronal expression of GluA3 is sufficient for oAβ to affect synaptic function.
(A-D) Example traces (A,C), dot plots (filled dots represents individual paired recording, open dots denote averages) and normalized mean amplitude of paired EPSC recordings (B,D). (A,B) GFP-GluA3 expressing GluA3-KO neurons showed no significant synaptic depression (n=18). (C,D) GFP-GluA3+APP$_{CT100}$ expressing GluA3-KO neurons did show significant synaptic depression (n=19). (E) Example mEPSC traces of GluA3-KO neurons with or without APP$_{CT100}$ and/or GFP-GluA3 expression. (F) Only the combined expression of GFP-GluA3 with APP$_{CT100}$ lowered mEPSC frequency, (G) but not mEPSC amplitude (GFP+APP$_{CT100}$ n=29 , uninf. n=24; GFP-GluA3 n=30 , uninf. n=29; GFP-GluA3+APP$_{CT100}$ n= 27, uninf. n= 29). (H) Example images of GluA3-KO apical dendrites expressing GFP (left) or GFP-GluA3 (right) with or without APP$_{CT100}$ (scale bar: 5 µm). (I) APP$_{CT100}$ lowered GFP-containing spine density only when GFP-GluA3 was co-expressed (GFP n=19, GFP+APP$_{CT100}$ n=15, GFP-GluA3 n=25, GFP-GluA3+APP$_{CT100}$ n=29). (F,G,I) Data are mean ± SEM. *P < 0.01.

overexpression of GFP-GluA3 in GluA3-deficient neurons results in the presence of GluA2/3 heteromers at synapses (Renner et al. 2017). GFP-GluA3 expression by itself did not significantly change eEPSC amplitudes (Figure 2 A,B), indicating that increasing GluA3 levels does not affect synaptic currents. When we co-expressed APP_{CT100} a significant reduction in eEPSC amplitude was observed compared with uninfected neighbors (Figure 2 C,D), although this synaptic depression was not significantly larger compared with expression of GFP-GluA3 alone. A clearer picture emerged when we recorded miniature excitatory post-synaptic currents (mEPSCs) from uninfected and nearby infected GluA3-knockout neurons expressing GFP-GluA3 with or without APP_{CT100}. As previously shown (Reinders et al. 2016), GluA3-deficient CA1 neurons are fully resistant to APP_{CT100}-driven reductions in mEPSCs (Fig. 2 E,F,G). Whereas GFP-GluA3 expression had no effect on average mEPSC amplitude or mEPSC frequency, co-expression of APP_{CT100} resulted in a reduction in mEPSC frequency (Fig. 2 E,F,G). These data indicate that GFP-GluA3 expression renders CA1 neurons sensitive for APP_{CT100}-driven synaptic depression. The decrease in mEPSC frequency without a change in mEPSC amplitude may be partly explained by a loss of synapses (Reinders et al. 2016). As we demonstrated previously (Reinders et al. 2016), spine density is lowered in APP_{CT100} expressing wild-type, but not GluA3-deficient CA1 neurons (chapter 1; figure 3 and S2), indicating GluA3-deficient neurons are resistant to oAβ-mediated spine loss. We next assessed whether neuronal GluA3 expression is required for oAβ to induce a loss of spines. Spines on apical dendrites were visualized by expressing GFP as a cytosolic or GluA3-fused marker and were imaged by 2-photon laser scanning microscopy. We measured GFP levels at spines of CA1 neurons expressing GFP-GluA3 and observed that the majority of spines contained detectable levels of GFP (figure 1H,I), indicating that recombinantly expressed GluA3 was present at most spines of apical CA1 dendrites. Co-expression of APP_{CT100} and GFP-GluA3 significantly decreased the number of GFP-containing spines (figure 1H,I). These data suggest that neuronal expression of GluA3 is sufficient for oAβ to cause a loss of GluA3-containing synapses.

Interaction between GRIP and GluA3 is required for oAβ effects on synapses.

Having established that expressing recombinant GluA3 sensitizes GluA3-deficient CA1 neurons for oAβ-driven synapse loss, we used this model system to investigate whether GRIP interaction with the PDZ binding domain of the GluA3 c-tail is necessary for this sensitization. We repeated the experiments with a recombinant GFP-GluA3 in which a serine at position 885 in its c-terminal PDZ-binding domain is substituted by an alanine (GFP-$GluA3_{S885A}$). Similarly as

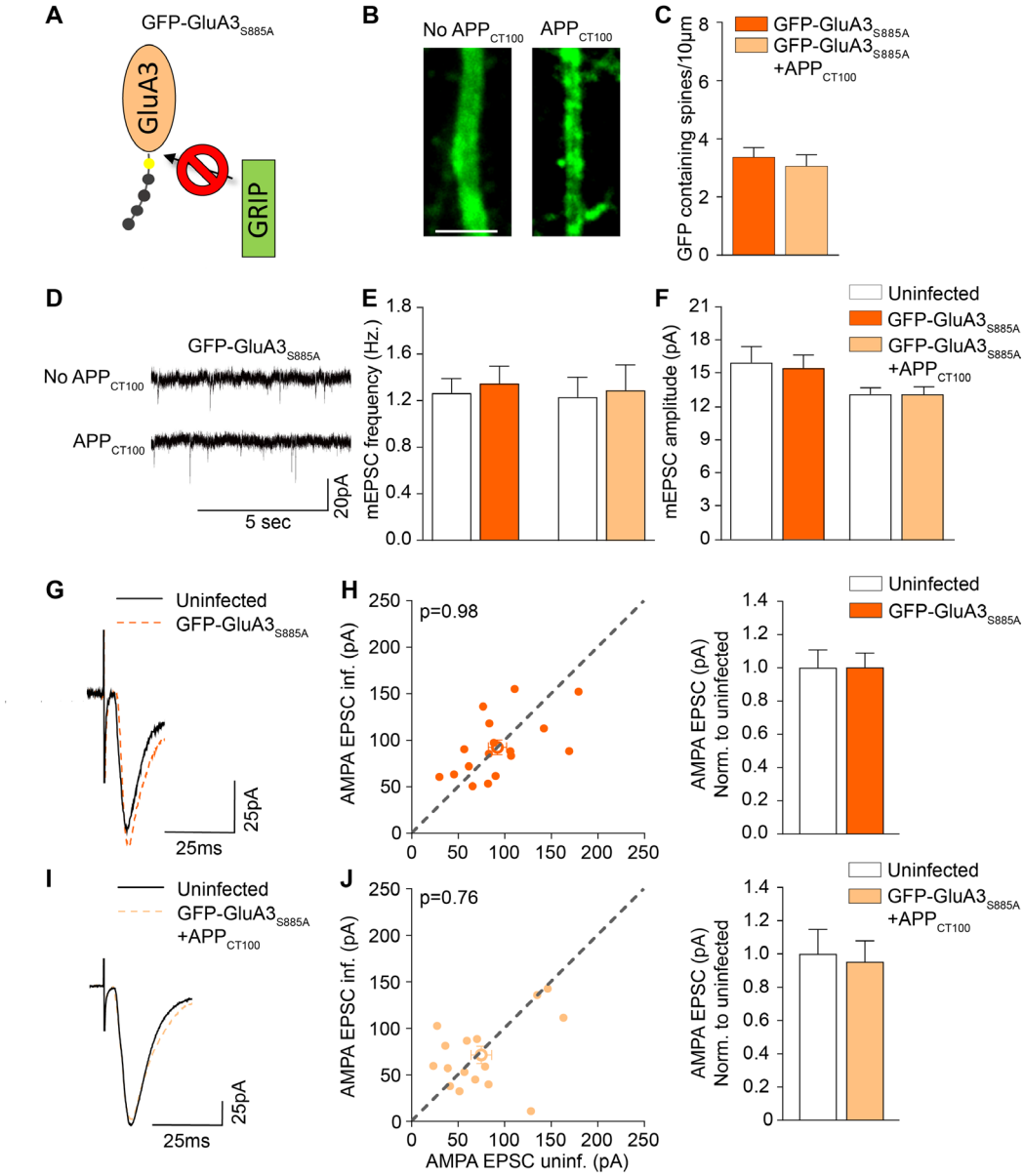

Figure 3. Neuronal expression of GluA3$_{S885A}$ does not sensitize GluA3-KO neurons to oAβ.
(A) Schematic of recombinant GFP-GluA3$_{S885A}$ and its inability to interact with GRIP (figure S1A). (B) Example images of GluA3-KO dendrites expressing GFP-GluA3$_{S885A}$ without (left) or with APP$_{CT100}$ (right) (scale bar: 5 µm). (C) GFP-GluA3$_{S885A}$ expressing GluA3-KO dendrites showed a low density of GFP-containing spines which was unchanged by APP$_{CT100}$ co-expression (GFP-GluA3$_{S885A}$ n=19, GFP-GluA3$_{S885A}$+APP$_{CT100}$ n=17). (D) Example mEPSC traces of GluA3-KO neurons expressing GFP-GluA3$_{S885A}$ with or without APP$_{CT100}$ (scale bar: 5 s, 20 pA). (E) GFP-GluA3$_{S885A}$ with or without APP$_{CT100}$ did not affect mEPSC frequency or (F) amplitude (uninf. n=22, GFP-GluA3$_{S885A}$ n=23; uninf. n=25, GFP-GluA3$_{S885A}$ +APP$_{CT100}$ n=29). (G) Example traces (H left) dot plots and (H right) normalized mean amplitude of paired EPSC recordings (scale bar: 25 ms, 25 pA). EPSC amplitude was unchanged in GFP-GluA3$_{S885A}$ expressing GluA3-KO neurons compared to uninfected controls. Open dots denote averages, filled dots represent pairs of EPSC responses (n=17). (I,J) same as G,H for GFP-GluA3$_{S885A}$+APP$_{CT100}$ (n=16). Data are mean ± SEM.

observed for GluA2 (Dong et al. 1997, Osten et al. 2000), this mutation prevented interaction between GRIP and GFP-GluA3$_{S885A}$ (figure 3A and S1A). A lack of GRIP binding prevents the accumulation of AMPARs on the surface and in recycling endosomes, redirecting them into the lysosomal degradation pathway (Setou et al. 2002, Osten et al. 2000, Lin et al. 2007). As a result, GFP levels in apical dendrites were 3-fold reduced in GFP-GluA3$_{S885A}$ expressing CA1 neurons compared with those expressing unmutated GFP-GluA3 (figure S1B), and the signal of GFP-GluA3$_{S885A}$ could only be detected in ~half the proportion of spines (figure 3B,C). Upon expression of GFP-GluA3$_{S885A}$ in GluA3-deficient neurons the average mEPSCs frequency and amplitude (figure 3 D-F), and eEPSC amplitude (figure 3 G-J) remained unchanged, indicating synaptic currents were unaffected. Co-expression of APP$_{CT100}$ with GFP-GluA3$_{S885A}$ did not sensitize these neurons for spine loss (figure 3 B,C) or synaptic depression upon co-expression of APP$_{CT100}$ (figure 3 D-J). These results indicate that GRIP-GluA3 interaction is required for oAβ to cause a loss of synapses. Most likely, GRIP dependent stable insertion of GluA2/3s into synapses is required to sensitize a neuron for oAβ.

Preventing S885 phosphorylation of GluA3 completely blocks oAβ-induced synapse loss.

We next determined the effect of disabling GluA3 S885 phosphorylation on oAβ-mediated synaptic depression. The S885 residue lies within the ESVKI sequence, in which the basic residue (K887) is critical to recognition by PKC (Kreegipuu et al. 1998). As was previously shown for GluA2 (Seidenman et al. 2003), substituting this lysine to an alanine (GluA3$_{K887A}$) prevents phosphorylation of this site, while the ability of GRIP to interact with GFP-GluA3$_{K887A}$ is maintained (Figure S1A). The GFP levels in GFP-GluA3$_{K887A}$ expressing CA1 apical dendrites and spines were similar to those in GFP-GluA3 expressing ones (figure S1 B). The expression of GFP-GluA3$_{K887A}$ in GluA3 deficient neurons had no effect on GFP-containing spine density (figure 4 B,C), mEPSC frequency (figure 4 D,E) or eEPSC amplitude (figure 4 G,H), although mEPSC amplitude was on average decreased (figure 4F). Co-expression of APP$_{CT100}$ did not affect the density of GFP-containing spines at CA1 neurons (figure 4 B,C), mEPSC frequency (figure 4 D,E), mEPSC amplitude (figure 4 D,F) or eEPSC amplitude (figure 4I,J). These data indicate that oAβ is unable to induce synaptic depression or spine loss in neurons when they express GFP-GluA3$_{K887A}$, suggesting oAβ corrupts synapses through phosphorylation of the GluA3 c-tail at S885.

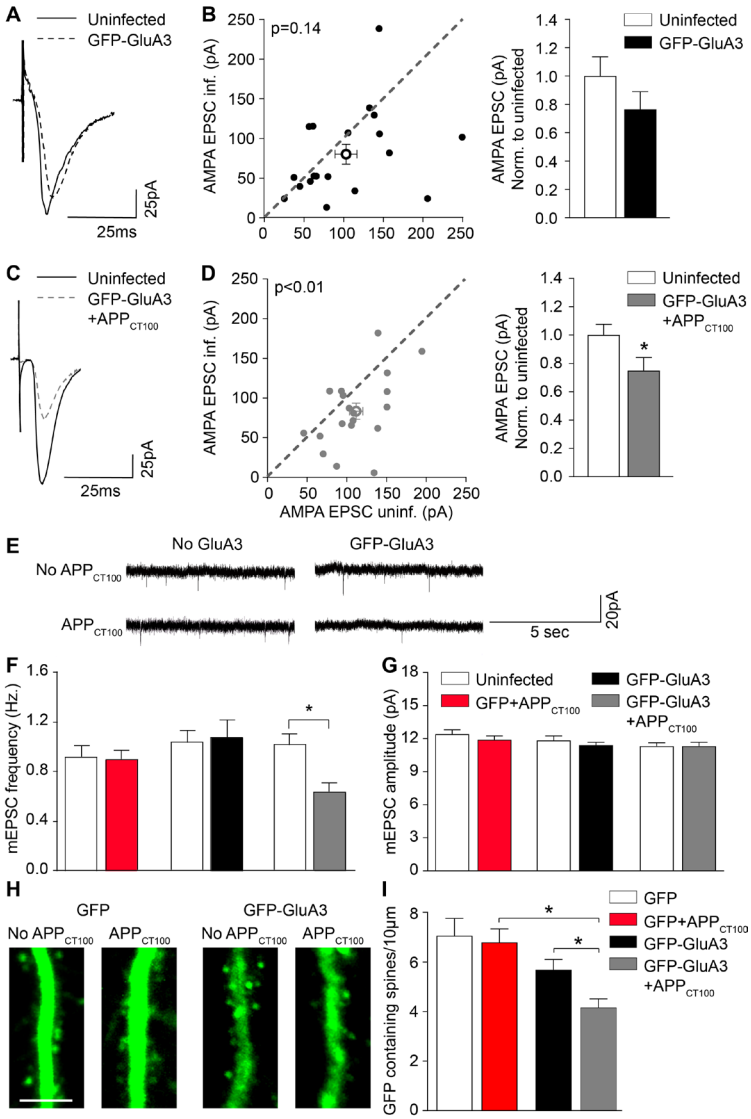

Figure 4. Neuronal expression of GluA3$_{K887A}$ does not sensitize GluA3-KO neurons to oAβ.
(A) Schematic of recombinant GFP-GluA3$_{K887A}$ and its disrupted PKCα interacting domain. (B) Example images of GluA3-KO dendrites expressing GFP-GluA3$_{K887A}$ without (left) and with APP$_{CT100}$ (right) (scale bar: 5 µm). (C) Density of GFP-containing spines on GFP-GluA3$_{K887A}$ expressing GluA3-KO dendrites was unchanged by APP$_{CT100}$ co-expression (GFP-GluA3$_{K887A}$ n=31, GFP-GluA3$_{K887A}$+APP$_{CT100}$ n=27). (D) Example mEPSC traces of GluA3-KO neurons expressing GFP-GluA3$_{K887A}$ with or without APP$_{CT100}$ (scale bar: 5 s, 20 pA). (E) Expression of GFP-GluA3$_{K887A}$ with or without APP$_{CT100}$ did not affect mEPSC frequency. (F) GFP-GluA3$_{K887A}$ expression lowered mEPSC amplitude but not when APP$_{CT100}$ was co-expressed (uninf n=23, GFP-GluA3$_{K887A}$ n=28; uninfected n=27, GFP-GluA3$_{K887A}$ + APP$_{CT100}$ n=31). (G) Example traces (H left) dot plots and (H right) normalized mean amplitude of paired EPSC recordings (scale bar: 25 ms, 25 pA). GFP-GluA3$_{K887A}$ expression in GluA3-KO neurons did not show significantly lower EPSC amplitude (n=15). Open dots denote averages, filled dots represent pairs of EPSC responses. (I,J) same as G,H for GFP- GluA3$_{K887A}$+APP$_{CT100}$ (n=14). Data are mean ± SEM. *P < 0.05.

OAβ removes synaptic GluA3-AMPARs

We next aimed to directly assess whether oAβ removes GluA3-containing AMPARs from synapses. Single-particle tracking experiments demonstrate that extra-synaptic AMPARs freely diffuse across the surface of dendritic spines, while synaptic AMPARs are largely immobile (Triller, Choquet 2005, Ehlers et al. 2007). These AMPAR properties allow an estimation of the relative fraction of synaptic versus extra-synaptic recombinant AMPARs on the surface of a spine using fluorescence recovery after photobleaching (FRAP) (Makino, Malinow 2009). If for instance APP_{CT100} expression would lower the levels of synaptic GluA3, this would decrease the fraction of immobile surface GluA3 on dendritic spines. GluA3 was tagged with a pH-sensitive form of GFP (Super Ecliptic pHluorin, SEP), enabling to distinguish between surface receptors, which display green fluorescence, and intracellular receptors, which show no fluorescence (Kopec et al. 2006). GluA3-deficient CA1 neurons of organotypic hippocampal slices were infected with sindbis expressing SEP-GluA3 and ~48 hours later fluorescent signals were analyzed using 2-photon laser scanning microscopy. During the FRAP experiment, the SEP-GluA3 signal at single dendritic spines was fully bleached, whereupon the fluorescence gradually recovered as a result of the lateral diffusion of bleached extra-synaptic SEP-GluA3 which interchanged with non-bleached SEP-GluA3 from the dendritic surface (figure 5 A and S2 A,B). The fraction of fluorescence that remained bleached (i.e. did not recover) was used to estimate the immobile fraction of SEP-GluA3 as a proxy for the level of synaptically incorporated SEP-GluA3. 30 minutes after bleaching, the recovery of SEP-GluA3 signal reached 45%, indicating that on average ~55% of recombinant GluA3 at the spine surface was immobilized at synapses (figure 5 A). Co-expression of SEP-GluA3 with APP_{CT100} did not alter the speed of FRAP, indicating no effect of oAβ-production on lateral diffusion of SEP-GluA3 across the membrane surface (figure 5 C). However, APP_{CT100}-expression significantly increased the level of SEP-GluA3 recovery to ~60% measured 30 min after bleaching (figure 5 B), consistent with 40% immobile SEP-GluA3 at spines. These results indicate that APP_{CT100} expression reduces the amount of synaptic GluA3 by ~27%, suggesting oAβ triggers the removal of GluA2/3s from synapses.

To examine whether the removal of GluA3 from synapses depends on its phosphorylation at S885, we analyzed FRAP on spines of GluA3-deficient neurons expressing SEP-$GluA3_{K887A}$. The FRAP of SEP-$GluA3_{K887A}$ was similar to that of SEP-GluA3, both in speed and in levels of recovery, indicating that the K887A mutation did not affect lateral diffusion and incorporation into synapses of the AMPAR (figure 5 D,E and S2 C). Co-expression of APP_{CT100} with SEP-$GluA3_{K887A}$ did

not alter the speed of recovery, indicating no effect on lateral movement speed of SEP-GluA3$_{K887A}$ across the membrane surface (figure 5 E). In sharp contrast to unmutated SEP-GluA3, APP$_{CT100}$ did not effectively lower the level of immobilized SEP-GluA3$_{K887A}$ signal (figure 5 D and S2 C). These experiments demonstrate that oAβ removes GluA3-containing AMPARs from synapses through PKCα phosphorylation of GluA3 at S885.

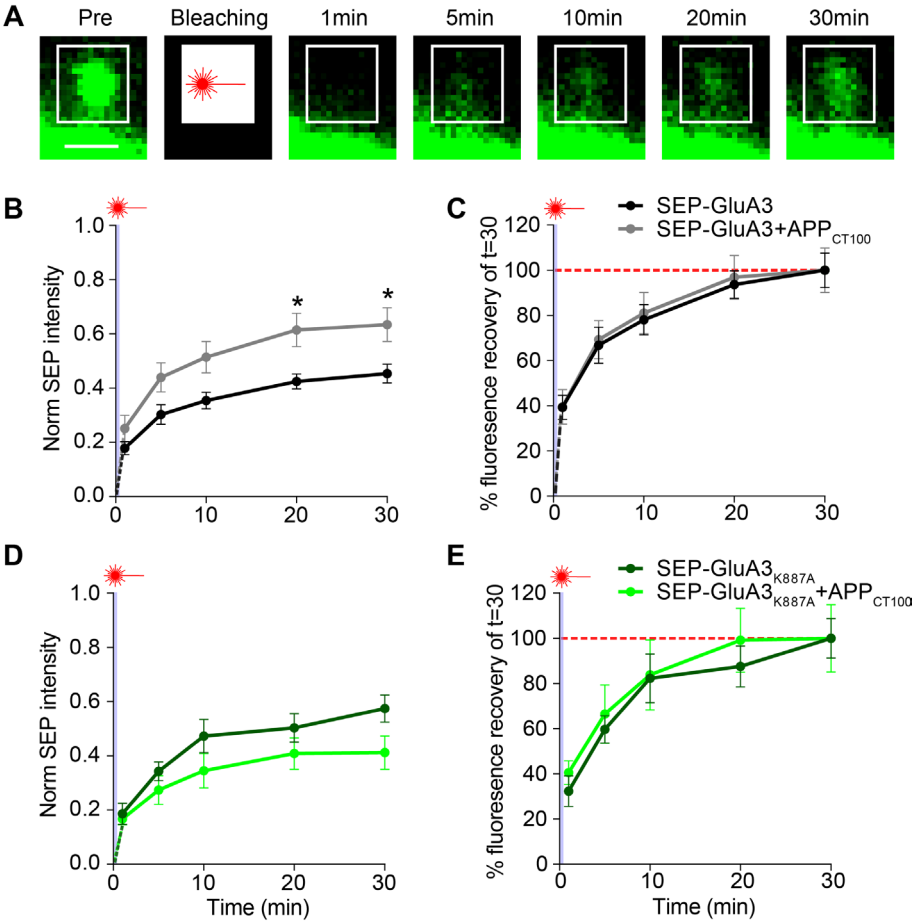

Figure 5. GluA3$_{K887A}$ prevents APP$_{CT100}$ induced GluA3 mobilization on spines. (A) Time series of an SEP-GluA3 expressing dendritic spine before and after fluorescence bleaching (scale bar: 1 µm). (B) FRAP of dendritic spines expressing SEP-GluA3 (black, n=22) was lower but (C) equally fast as those expressing SEP-GluA3+APP$_{CT100}$ (grey, n=22). (D) FRAP and its speed (E) in dendritic GluA3-KO spines expressing SEP-GluA3$_{K887A}$ (dark green, n=12) was similar to that of SEP-GluA3 (green, n=13 (figure S2 C) and unaffected by APP$_{CT100}$ co-expression. Data are mean ± SEM. *P < 0.05.

DISCUSSION

We investigated the role of AMPAR subunit GluA3 in the effects of oAβ on synapses. We found that GluA3-deficient neurons, which are resistant against the effect of oAβ (Reinders et al. 2016), were re-sensitized to oAβ after viral expression of GFP-GluA3. Since this Sindbis mediated expression is relatively fast (<48 hrs), it is unlikely that GluA3-deficient neurons became resistant to oAβ as a consequence of compensatory adjustments during early development. These experiments also indicate that oAβ-mediated synaptic depression requires GluA3 to be expressed at the post-synaptic membrane, and not, for instance, at presynaptic compartments or in glial cells. The excessive pruning of spines in neurons overproducing oAβ appears therefore fully dictated by the presence of GluA3 at these spines. Our results are therefore in line with a model in which oAβ-mediated effects originate at synapses rather than at the glia-mediated pruning machinery [review (Hong et al. 2016)].

Virally expressed GFP-GluA3 was inserted into synapses of CA1 neurons from GluA3-knockout mice but did not increase synaptic currents. It is possible that the newly produced GluA2/3s are added to synapses but remain in an inactive, nonconductive state, therefore contributing little to synaptic transmission (Renner et al. 2017). Alternatively, the GluA1/2s at synapses of GluA3-deficient neurons were replaced by newly formed active GluA2/3s, negating the increase in synapse strength (Shi et al. 2001, McCormack et al. 2006). The replacement of conductive GluA1/2s by inactive GluA2/3s may theoretically result in synaptic depression. Indeed, overexpression of GFP-GluA3 in CA1 neurons of wild-type rats resulted in synaptic depression (Shi et al. 2001) and also in our experiments GFP-GluA3 overexpression in GluA3-ko neurons resulted in a small, albeit non-significant, synaptic weakening.

We found that for oAβ to cause synaptic depression, GluA3 needs to be present at synapses. GluA3-deficient neurons were not re-sensitized to oAβ when reconstituted with a mutant GluA3 that fails to reach synapses because of its inability to interact with GRIP (GFP-$GluA3_{S885A}$). We tested another mutant, which cannot be phosphorylated by PKCα but interacted with GRIP and was incorporated into synapses at similar levels as unmutated GluA3 ($GluA3_{K887A}$). These properties of $GluA3_{K887A}$ are in line with studies showing that a homologous mutation in GluA2 ($GluA2_{K882A}$) prevents PKCα-induced c-tail phosphorylation without disrupting GluA2-GRIP interactions (Chung et al. 2000, Seidenman et al. 2003). The $GluA3_{K887A}$ mutant completely alleviated APP_{CT100}-induced removal of GluA3 from synapses,

implying that oAβ triggers PICK1-mediated endocytosis of synaptic GluA3. Our results are in line with a model in which oAβ triggers increased PKCα catalytic activity at synapses (Alfonso, S. I. et al. 2016), thereby promoting PICK1-mediated AMPAR endocytosis. Increased PKCα activity at synapses would unbalance the constitutive AMPAR cycling that replaces synaptic GluA1/2s with GluA2/3 (Shi et al. 2001, McCormack et al. 2006). It may also disrupt the homeostatic scaling of synaptic strength as observed in the barrel cortex: Levels of GluA2/3 increase while GluA1/2s levels decrease in synapses of neurons deprived of sensory input (Makino, Malinow 2011). In GluA2/3 enriched synapses oAβ triggers excessive GluA2/3 endocytosis resulting in synaptic weakening and ultimately loss of spines. This spine loss may account for the observed oAβ-driven reduction in NMDARs and GluA1-containing AMPARs (Reinders et al. 2016). It is also possible that GluA1-containing AMPARs are removed from synapses through a different oAβ-driven mechanism (Guntupalli et al. 2017, Zhang et al. 2017).

The oAβ mediated effects on synapses through the removal of synaptic GluA2/3 AMPARs, may involve an endogenous signaling cascade that is similar to the signaling cascade involved in NMDAR-dependent long-term depression (LTD). The mechanisms of synaptic depression mediated either by low-frequency stimulation (LFS) or by oAβ show striking similarities. To induce synaptic depression, LFS and oAβ both require metabotropic NMDAR activation (Nabavi et al. 2013, Kessels et al. 2013), synaptic recruitment of PTEN (Jurado et al. 2010, Knafo et al. 2016), PICK1-AMPAR interaction (Seidenman et al. 2003, Terashima et al. 2008, Daw et al. 2000, Kim, C. H. et al. 2001), endocytosis of AMPARs (Alfonso, S. et al. 2014, Hsieh et al. 2006), GSK-3 activity (Bradley et al. 2012, Kirouac et al. 2017) and hyper phosphorylation of tau (Takashima et al. 1993, Bloom 2014, Regan et al. 2015). In this scenario, oAβ could act on the removal of GluA3-AMPAR as a trigger for synapse weakening and/or removal during NMDAR-induced LTD.

How removal of synaptic GluA3-containing AMPARs can lead to spine breakdown is unclear. Possibly the response of neurons to oAβ is similar to their response to oxygen/glucose deprivation (Koszegi et al. 2017, Dixon et al. 2009). In these studies, cell-death after oxygen/glucose deprivation was facilitated by PICK1-mediated lysosomal targeting of GluA2/3s. In an oAβ-rich context, excessive metabotropic NMDAR activation could cause local PICK1-mediated lysosomal targeting of synaptic GluA2/3s, initiating the elimination of synapse and spines. Further study on lysosomal targeting of GluA2/3s may offer more insight on how oAβ induces the depletion of synapses.

Our results imply that not all synapses have equal susceptibility for oAβ-mediated synaptic depression; while synapses having GluA3-containing AMPARs are susceptible, those lacking GluA3, only containing GluA1-containing AMPARs, are resistant. The selective targeting of GluA3-enriched synapses could fit a scenario where PICK1-mediated endocytosis specifically targets GluA2/3 and not so much GluA1/2s. Several studies that manipulate PICK1 function observed that GluA2 levels were decreased, while GluA1 levels remained unaffected (Koszegi et al. 2017, Daw et al. 2000). In line with these studies, our data suggest that for taking part in GRIP/PICK1-driven AMPAR trafficking, a PDZ-binding motif is required at all four AMPAR subunits. Expression of recombinant GluA3 in our model system leads to the formation of non-rectifying AMPARs, i.e. GluA2/3 heteromers (Renner et al. 2017), and we show that mutating its phosphorylation sites at the two GluA3s was sufficient to fully prevent its endocytosis. Similarly, despite having two GluA2 subunits that allow interaction with GRIP and PICK1, GluA1/2s appear to not play a part in the in the constitutive homeostatic AMPAR cycling pathway; they are only inserted into synapses upon the induction of LTP-like activity (Shi et al. 2001, Makino, Malinow 2009, Makino, Malinow 2011).

We present evidence that oAβ can disrupt constitutive AMPAR cycling by inducing excessive removal of GluA3-containing AMPARs from synapses. Our data indicate that the removal of synaptic GluA3 is a key event in the mechanism by which oAβ causes synaptic deficits. Further study on synaptic GluA3-AMPAR removal as a trigger for synapse and spine breakdown has the potential to reveal therapeutical targets against the detrimental effects of oAβ.

METHODS

Mice

The *Gria3*-deficient (GluA3-KO) and wild-type littermate colony was established from C57Bl/6 × 129P2-Gria3tm1Dgen/Mmnc mutant ancestors (RRID:MMRRC_030969-UNC) (MMRRC, Davis, CA), which were at least 20 times backcrossed to C57Bl/6 mice. Mice were kept on a 12 hr day-night cycle (light onset 8 or 7am) and had *ad libitum* access to food and water. All experiments were conducted in line with the European guidelines for the care and use of laboratory animals (Council Directive 86/6009/EEC). The experimental protocol was approved by the Animal Experiment Committee of the Royal Netherlands Academy of Arts and Sciences (KNAW)

Organotypic hippocampal slice preparation and exogenous protein expression

Organotypic hippocampal slices were prepared from P6-8 mice as described previously (Stoppini et al. 1991) and used at 7–12 days in vitro for electrophysiology and 14-21 days in vitro for imaging. For the expression of exogenous GFP, APP_{CT100} and GFP- or SEP-tagged rat GluA3 (flip), $GluA3_{S885A}$ and $GluA3_{K887A}$, the respective constructs were cloned into a pSinRep5 shuttle vector. The resulting pSinRep5 plasmids were used to produce infective Sindbis pseudo viruses according to the manufacturer's protocol (Invitrogen BV). Sindbis virus infection was achieved by injecting diluted virus into slices 20-52 hours prior to the experiments.

Electrophysiology

During recordings, slices were perfused with artificial cerebrospinal fluid (ACSF): (in mM) 118 NaCl, 2.5 KCl, 26 $NaHCO_3$, 1 NaH_2PO_4, supplemented with 4 $MgCl_2$, 4 $CaCl_2$, 20 glucose at 27°C, gassed with 95%O_2/5%CO_2. Patch recording pipettes were filled with internal solution containing (in mM): 115 $CsMeSO_3$, 20 CsCl, 10 HEPES, 2.5 $MgCl_2$, 4 Na_2-ATP, 0.4 Na-GTP, 10 Na-Phosphocreatine, 0.6 EGTA. Whole-cell recordings in were made with 2.5–4.5 MΩ pipettes (R_{access} < 20 MΩ, and R_{input} > 10× R_{access}). Where indicated, forskolin (50 µM; Sigma) was added to the perfusion solution and during mEPSC recordings, TTX (1 µM; Tocris) and picrotoxin (100 µM; Sigma) were added. During evoked recordings, a cut was made between CA1 and CA3, and picrotoxin (50 µM) was added to the bath. 2-chloroadenosine was purposefully omitted as it may reduce the inactive state of GluA3-AMPAR by upregulating cAMP (Rebola et al. 2003). Two stimulating electrodes, (two-contact Pt/Ir cluster electrode, Frederick Haer), were placed between 100-200 µm down the apical dendrite and 100-300 µm apart laterally. AMPAR-mediated EPSCs were measured as the peak inward current at −60 mV directly after stimulation. NMDAR-mediated EPSCs were measured as the mean outward current between 40 and 90 ms after the stimulation at +40 mV, and corrected by the same current at 0 mV to compensate for incomplete clamping. Data was acquired using a Multiclamp 700B amplifier (Molecular Devices). Mean EPSC amplitudes contained at least 20 sweeps at each holding potential and were aquired using pClamp 10 software (Molecular Devices). mEPSC data are based on at least 100 events or 10 min of recording and analysed with MiniAnalysis (Synaptosoft). Individual events above a 5pA threshold were manually selected by an experimenter blind to the experimental condition.

2-photon imaging

3D images were collected by two-photon laser scanning microscopy (Femtonics Ltd.) with a mode-locked Ti:sapphire laser (Chameleon; Coherent) tuned at 910 nm using a 20× objective. During imaging, slices were kept under constant perfusion of aCSF (in mM: 118 NaCl, 2.5 KCl, 26 $NaHCO_3$, 1 NaH_2PO_4, supplemented with 4 $MgCl_2$, 4 $CaCl_2$, 20 glucose) at 30°C, gassed with 95%O_2/5%CO_2. For spine densities, apical dendrites were imaged ~180 µm from the cell body (pixel size x,y,z 0.05 × 0.05 × 0.75µm). The density of spines protruding in the horizontal (*x*/*y*) plane were manually quantified from projections of stacked 3D images by an experimenter blind to experimental condition. For analysis and example images, the look up table of each stacked image was optimized for spine recognition (figure 1E, 2E and 4G). To monitor the transportation of virally expressed GFP-GluA3 into dendrites, the soma and >150µm apical dendrite were captured (pixel size x,y,z 0.3 × 0.3 × 0.75µm). The same laser power was used in each condition. The ratio between mean fluorescence intensity of the dendrite (150µm from the soma) and soma was manually quantified. For photobleaching experiments, apical dendrites were imaged 150–250µm from the cell body (pixel size x,y,z 0.05 × 0.05 × 0.5µm). Photobleaching of SEP-fluorescence was achieved by prolonged scanning of isolated spines, until complete bleaching was visually confirmed (Figure SX). To determine the fluorescence recovery after photobleaching (FRAP), similarly sized z-stacks of dendrites were collapsed for each time point. Background-subtracted green fluorescence of spines was quantified, normalized to that of its dendrite and compared across time. All image analysis was performed with ImageJ software (fiji.sc).

HEK-cell co-immunoprecipitation and immunoblotting

Full length GluA3 cDNAs were subcloned into a pRK5-Dest vector, and Grip1 into a pcDNA3.2-V5-Dest vector. HEK cells were passed one day before transfection in DMEM + GlutaMAX (Gibco), 10% FBS (Invitrogen), 1% Penicillin/Streptomycin (Gibco) in 10 cm dishes. 2 h before transfection, the medium of ~60% confluent cells was refreshed. Cells were transfected with ~2.5ug Grip-V5 and GluA3, $GluA3_{S885A}$, or $GluA3_{K887A}$ using PEI 2500. The amount of DNA used for transfection with GluA3 constructs was optimized based on protein expression levels beforehand. After ~48 hours, cells were harvested in 1 ml of a 2% Triton X-100 ice-cold immunoprecipitation buffer (25mM HEPES/NaOH, pH7.4, 150 mM NaCl) containing 2% Triton X-100 and EDTA-free protease inhibitor cocktail (Roche). The resulting samples were incubated for 1 h at 4°C and spun down twice at 20800 x g for 10 min at 4°C. Anti-Grip (4 µg ABN27, Millipore) was added to the supernatants and incubated overnight at 4°C. The next day, protein A/G PLUS-

agarose beads (40 µL; Santa Cruz Biotechnology, Inc.) were added for 1 h at 4°C and washed 4 times with immunoprecipitation buffer containing 1% Triton X-100. Proteins were eluted in SDS sample buffer (55 µL), boiled for 5 min and loaded on a 4-15% Criterion TGX Stain-Free precast gel (BioRad). Protein samples were transferred unto a PVDF membrane (BioRad) overnight at 40V. The blots were blocked in 5% milk in TBST and incubated with primary and secondary antibody in 3% milk in TBST. The following antibodies were used: anti-GluA2/3 (1:2000; CQNFATYKEGYNVYGIESVKI, custom made at Genscript) (Chen et al. 2014), anti-V5 (1:1000; ab27671, Abcam) in combination with goat-anti-rabbit-HRP (DAKO 1:10000) and goat-anti-mouse-HRP (DAKO, 1:10000). Membranes were developed using ECL femto (Thermo Scientific).

Quantification and statistical analysis

Experimental conditions that are depicted in the same graph were performed in parallel and within the same animals. Experimental conditions were compared using two-tailed Student *t* tests for 2 conditions (unpaired, unless indicated paired t-test) or with ANOVAs with post-hoc Tukey for more than 2 conditions. Where indicated 2-way ANOVAs were used to detect interaction effects. *P* values below 0.05 were considered statistically significant.

REFERENCES

Alfonso, S., Kessels, H.W., Banos, C.C., Chan, T.R., Lin, E.T., Kumaravel, G., Scannevin, R.H., Rhodes, K.J., Huganir, R., Guckian, K.M., Dunah, A.W. and Malinow, R., 2014. Synapto-depressive effects of amyloid beta require PICK1. *The European journal of neuroscience,* **39**(1460-9568; 0953-816; 7), pp. 1225-1233.

Alfonso, S.I., Callender, J.A., Hooli, B., Antal, C.E., Mullin, K., Sherman, M.A., Lesne, S.E., Leitges, M., Newton, A.C., Tanzi, R.E. and Malinow, R., 2016. Gain-of-function mutations in protein kinase Calpha (PKCalpha) may promote synaptic defects in Alzheimer's disease. *Sci.Signal.,* **9**(1937-9145; 1945-0877; 427), pp. ra47.

Bloom, G.S., 2014. Amyloid-beta and tau: the trigger and bullet in Alzheimer disease pathogenesis. *JAMA Neurol.,* **71**(2168-6157; 2168-6149; 4), pp. 505-508.

Bradley, C.A., Peineau, S., Taghibiglou, C., Nicolas, C.S., Whitcomb, D.J., Bortolotto, Z.A., Kaang, B.K., Cho, K., Wang, Y.T. and Collingridge, G.L., 2012. A pivotal role of GSK-3 in synaptic plasticity. *Frontiers in molecular neuroscience,* **5**, pp. 13.

Chen, N., Pandya, N.J., Koopmans, F.T.W., Castelo-Szekelv, V., van, d.S., Smit, A.B. and Li, K.W., 2014. Interaction proteomics reveals brain region-specific AMPA receptor complexes. *Journal of Proteome Research,* **13**(12), pp. 5695-5706.

Chung, H.J., Xia, J., Scannevin, R.H., Zhang, X. and Huganir, R.L., 2000. Phosphorylation of the AMPA receptor subunit GluR2 differentially regulates its interaction with PDZ domain-containing proteins. *The Journal of neuroscience : the official journal of the Society for Neuroscience,* **20**(1529-2401; 0270-6474; 19), pp. 7258-7267.

Cisse, M., Halabisky, B., Harris, J., Devidze, N., Dubal, D.B., Sun, B., Orr, A., Lotz, G., Kim, D.H., Hamto, P., Ho, K., Yu, G.Q. and Mucke, L., 2011. Reversing EphB2 depletion rescues cognitive functions in Alzheimer model. *Nature,* **469**(1476-4687; 0028-0836; 7328), pp. 47-52.

Coleman, P.D. and Yao, P.J., 2003. Synaptic slaughter in Alzheimer's disease. *Neurobiology of aging,* **24**(8), pp. 1023-1027.

Coleman, S.K., Hou, Y., Willibald, M., Semenov, A., Moykkynen, T. and Keinanen, K., 2016. Aggregation Limits Surface Expression of Homomeric GluA3 Receptors. *The Journal of biological chemistry,* **291**(16), pp. 8784-8794.

Daw, M.I., Chittajallu, R., Bortolotto, Z.A., Dev, K.K., Duprat, F., Henley, J.M., Collingridge, G.L. and Isaac, J.T., 2000. PDZ proteins interacting with C-terminal GluR2/3 are involved in a PKC-dependent regulation of AMPA receptors at hippocampal synapses. *Neuron,* **28**(0896-6273; 0896-6273; 3), pp. 873-886.

de Wilde, M.C., Overk, C.R., Sijben, J.W. and Masliah, E., 2016. Meta-analysis of synaptic pathology in Alzheimer's disease reveals selective molecular vesicular machinery vulnerability. *Alzheimer's & dementia : the journal of the Alzheimer's Association,* **12**(6), pp. 633-644.

DeKosky, S.T., Scheff, S.W. and Styren, S.D., 1996. Structural correlates of cognition in dementia: quantification and assessment of synapse change. *Neurodegeneration : a journal for neurodegenerative disorders, neuroprotection, and neuroregeneration,* **5**(4), pp. 417-421.

Diering, G.H. and Huganir, R.L., 2018. *The AMPA Receptor Code of Synaptic Plasticity.*

Dixon, R.M., Mellor, J.R. and Hanley, J.G., 2009. PICK1-mediated glutamate receptor subunit 2 (GluR2) trafficking contributes to cell death in oxygen/glucose-deprived hippocampal neurons. *The Journal of biological chemistry,* **284**(21), pp. 14230-14235.

Dong, H., O'Brien, R.J., Fung, E.T., Lanahan, A.A., Worley, P.F. and Huganir, R.L., 1997. GRIP: a synaptic PDZ domain-containing protein that interacts with AMPA receptors. *Nature,* **386**(6622), pp. 279-284.

Ehlers, M.D., Heine, M., Groc, L., Lee, M.C. and Choquet, D., 2007. Diffusional trapping of GluR1 AMPA receptors by input-specific synaptic activity. *Neuron,* **54**(3), pp. 447-460.

Fiuza, M., Rostosky, C.M., Parkinson, G.T., Bygrave, A.M., Halemani, N., Baptista, M., Milosevic, I. and Hanley, J.G., 2017. PICK1 regulates AMPA receptor endocytosis via direct interactions with AP2 α-appendage and dynamin. *The Journal of cell biology,* **216**(10), pp. 3323.

Guntupalli, S., Jang, S.E., Zhu, T., Huganir, R.L., Widagdo, J. and Anggono, V., 2017. GluA1 Ubiquitination Mediates Amyloid-beta-induced Loss of Surface AMPA Receptors. *Journal of Biological Chemistry,* (1083-351; 0021-9258),.

Gutierrez-Castellanos, N., Da Silva-Matos, C.M., Zhou, K., Canto, C.B., Renner, M.C., Koene, L.M.C., Ozyildirim, O., Sprengel, R., Kessels, H.W. and De Zeeuw, C.I., 2017. Motor Learning Requires Purkinje Cell Synaptic Potentiation through Activation of AMPA-Receptor Subunit GluA3. *Neuron,* **93**(2), pp. 409-424.

Hong, S., Dissing-Olesen, L. and Stevens, B., 2016. New insights on the role of microglia in synaptic pruning in health and disease. *Current opinion in neurobiology,* **36**, pp. 128-134.

Hsieh, H., Boehm, J., Sato, C., Iwatsubo, T., Tomita, T., Sisodia, S. and Malinow, R., 2006. AMPAR removal underlies Abeta-induced synaptic depression and dendritic spine loss. *Neuron,* **52**(0896-6273; 0896-6273; 5), pp. 831-843.

Iwakura, Y., Nagano, T., Kawamura, M., Horikawa, H., Ibaraki, K., Takei, N. and Nawa, H., 2001. N-methyl-D-aspartate-induced alpha-amino-3-hydroxy-5-methyl-4-isoxazoleproprionic acid (AMPA) receptor down-regulation involves interaction of the carboxyl terminus of GluR2/3 with Pick1. Ligand-binding studies using Sindbis vectors carrying AMPA receptor decoys. *The Journal of biological chemistry,* **276**(43), pp. 40025-40032.

Jurado, S., Benoist, M., Lario, A., Knafo, S., Petrok, C.N. and Esteban, J.A., 2010. PTEN is recruited to the postsynaptic terminal for NMDA receptor-dependent long-term depression. *The EMBO journal,* **29**(1460-2075; 0261-4189; 16), pp. 2827-2840.

Kamenetz, F., Tomita, T., Hsieh, H., Seabrook, G., Borchelt, D., Iwatsubo, T., Sisodia, S. and Malinow, R., 2003. APP processing and synaptic function. *Neuron,* **37**(0896-6273; 0896-6273; 6), pp. 925-937.

Kessels, H.W. and Malinow, R., 2009. Synaptic AMPA receptor plasticity and behavior. *Neuron,* **61**(1097-4199; 0896-6273; 3), pp. 340-350.

Kessels, H.W., Nabavi, S. and Malinow, R., 2013. Metabotropic NMDA receptor function is required for beta-amyloid-induced synaptic depression. *Proceedings of the National Academy of Sciences of the United States of America,* **110**(1091-6490; 0027-8424; 10), pp. 4033-4038.

Kim, C.H., Chung, H.J., Lee, H.K. and Huganir, R.L., 2001. Interaction of the AMPA receptor subunit GluR2/3 with PDZ domains regulates hippocampal long-term depression. *Proceedings of the National Academy of Sciences of the United States of America,* **98**(0027-8424; 0027-8424; 20), pp. 11725-11730.

Kim, T., Vidal, G.S., Djurisic, M., William, C.M., Birnbaum, M.E., Garcia, K.C., Hyman, B.T. and Shatz, C.J., 2013. Human LilrB2 is a beta-amyloid receptor and its murine homolog PirB regulates synaptic plasticity in an Alzheimer's model. *Science,* **341**(1095-9203; 0036-8075; 6152), pp. 1399-1404.

Kirouac, L., Rajic, A.J., Cribbs, D.H. and Padmanabhan, J., 2017. Activation of Ras-ERK Signaling and GSK-3 by Amyloid Precursor Protein and Amyloid Beta Facilitates Neurodegeneration in Alzheimer's Disease. *eNeuro,* **4**(2), pp. 10.1523/ENEURO.0149-16.2017. eCollection 2017 Mar-Apr.

Knafo, S., Sanchez-Puelles, C., Palomer, E., Delgado, I., Draffin, J.E., Mingo, J., Wahle, T., Kaleka, K., Mou, L., Pereda-Perez, I., Klosi, E., Faber, E.B., Chapman, H.M., Lozano-Montes, L., Ortega-Molina, A., Ordonez-Gutierrez, L., Wandosell, F., Vina, J., Dotti, C.G., Hall, R.A., Pulido, R., Gerges, N.Z., Chan, A.M., Spaller, M.R., Serrano, M., Venero, C. and Esteban, J.A., 2016. PTEN recruitment controls synaptic and cognitive function in Alzheimer's models. *Nature neuroscience,* **19**(1546-1726; 1097-6256; 3), pp. 443-453.

Kopec, C.D., Li, B., Wei, W., Boehm, J. and Malinow, R., 2006. Glutamate receptor exocytosis and spine enlargement during chemically induced long-term potentiation. *The Journal of neuroscience : the official journal of the Society for Neuroscience,* **26**(1529-2401; 0270-6474; 7), pp. 2000-2009.

Kopec, C.D., Real, E., Kessels, H.W. and Malinow, R., 2007. GluR1 links structural and functional plasticity at excitatory synapses. *The Journal of neuroscience : the official journal of the Society for Neuroscience,* **27**(1529-2401; 0270-6474; 50), pp. 13706-13718.

Koszegi, Z., Fiuza, M. and Hanley, J.G., 2017. Endocytosis and lysosomal degradation of GluA2/3 AMPARs in response to oxygen/glucose deprivation in hippocampal but not cortical neurons. *Sci.Rep.,* **7**(2045-2322; 2045-2322; 1), pp. 12318.

Kreegipuu, A., Blom, N., Brunak, S. and Jarv, J., 1998. Statistical analysis of protein kinase specificity determinants. *FEBS letters,* **430**(1-2), pp. 45-50.

Lesne, S., Koh, M.T., Kotilinek, L., Kayed, R., Glabe, C.G., Yang, A., Gallagher, M. and Ashe, K.H., 2006. A specific amyloid-beta protein assembly in the brain impairs memory. *Nature,* **440**(1476-4687; 0028-0836; 7082), pp. 352-357.

Lin, D.T. and Huganir, R.L., 2007. PICK1 and phosphorylation of the glutamate receptor 2 (GluR2) AMPA receptor subunit regulates GluR2 recycling after NMDA receptor-induced internalization. *The Journal of neuroscience : the official journal of the Society for Neuroscience,* **27**(1529-2401; 0270-6474; 50), pp. 13903-13908.

Makino, H. and Malinow, R., 2011. Compartmentalized versus global synaptic plasticity on dendrites controlled by experience. *Neuron,* **72**(1097-4199; 0896-6273; 6), pp. 1001-1011.

Makino, H. and Malinow, R., 2009. AMPA receptor incorporation into synapses during LTP: the role of lateral movement and exocytosis. *Neuron,* **64**(1097-4199; 0896-6273; 3), pp. 381-390.

McCormack, S.G., Stornetta, R.L. and Zhu, J.J., 2006. Synaptic AMPA receptor exchange maintains bidirectional plasticity. *Neuron,* **50**(0896-6273; 0896-6273; 1), pp. 75-88.

McLean, C.A., Cherny, R.A., Fraser, F.W., Fuller, S.J., Smith, M.J., Beyreuther, K., Bush, A.I. and Masters, C.L., 1999. Soluble pool of Abeta amyloid as a determinant of severity of neurodegeneration in Alzheimer's disease. *Annals of Neurology,* **46**(0364-5134; 0364-5134; 6), pp. 860-866.

Moretto, E. and Passafaro, M., 2018. Recent Findings on AMPA Receptor Recycling. *Frontiers in cellular neuroscience,* **12**, pp. 286.

Muller-Schiffmann, A., Herring, A., Abdel-Hafiz, L., Chepkova, A.N., Schable, S., Wedel, D., Horn, A.H., Sticht, H., de Souza Silva, M.A., Gottmann, K., Sergeeva, O.A., Huston, J.P., Keyvani, K. and Korth, C., 2016. Amyloid-beta dimers in the absence of plaque pathology impair learning and synaptic plasticity. *Brain : a journal of neurology,* **139**(Pt 2), pp. 509-525.

Nabavi, S., Kessels, H.W., Alfonso, S., Aow, J., Fox, R. and Malinow, R., 2013. Metabotropic NMDA receptor function is required for NMDA receptor-dependent long-term depression. *Proceedings of the National Academy of Sciences,* **110**(10), pp. 4027.

Osten, P., Khatri, L., Perez, J.L., Kohr, G., Giese, G., Daly, C., Schulz, T.W., Wensky, A., Lee, L.M. and Ziff, E.B., 2000. Mutagenesis reveals a role for ABP/GRIP binding to GluR2 in synaptic surface accumulation of the AMPA receptor. *Neuron,* **27**(2), pp. 313-325.

Perez, J.L., Khatri, L., Chang, C., Srivastava, S., Osten, P. and Ziff, E.B., 2001. PICK1 targets activated protein kinase Calpha to AMPA receptor clusters in spines of hippocampal neurons and reduces surface levels of the AMPA-type glutamate receptor subunit 2. *The Journal of neuroscience : the official journal of the Society for Neuroscience,* **21**(15), pp. 5417.

Rebola, N., Sebastiao, A.M., de Mendonca, A., Oliveira, C.R., Ribeiro, J.A. and Cunha, R.A., 2003. Enhanced adenosine A2A receptor facilitation of synaptic transmission in the hippocampus of aged rats. *Journal of neurophysiology,* **90**(2), pp. 1295-1303.

Regan, P., Piers, T., Yi, J.H., Kim, D.H., Huh, S., Park, S.J., Ryu, J.H., Whitcomb, D.J. and Cho, K., 2015. Tau phosphorylation at serine 396 residue is required for hippocampal LTD. *The Journal of neuroscience : the official journal of the Society for Neuroscience,* **35**(12), pp. 4804-4812.

Reinders, N.R., Pao, Y., Renner, M.C., da Silva-Matos, C.M., Lodder, T.R., Malinow, R. and Kessels, H.W., 2016. Amyloid-beta effects on synapses and memory require AMPA receptor subunit GluA3. *Proceedings of the National Academy of Sciences of the United States of America,* **113**(1091-6490; 0027-8424; 42), pp. E6526-E6534.

Renner, M.C., Albers, E.H., Gutierrez-Castellanos, N., Reinders, N.R., van Huijstee, A.N., Xiong, H., Lodder, T.R. and Kessels, H.W., 2017. Synaptic plasticity through activation of GluA3-containing AMPA-receptors. *Elife.,* **6**(2050-084; 2050-084),.

Scheff, S.W. and Price, D.A., 2003. Synaptic pathology in Alzheimer's disease: a review of ultrastructural studies. *Neurobiology of aging,* **24**(8), pp. 1029-1046.

Scheff, S.W., Price, D.A., Schmitt, F.A. and Mufson, E.J., 2006. Hippocampal synaptic loss in early Alzheimer's disease and mild cognitive impairment. *Neurobiology of aging,* **27**(1558-1497; 0197-4580; 10), pp. 1372-1384.

Seidenman, K.J., Steinberg, J.P., Huganir, R. and Malinow, R., 2003. Glutamate receptor subunit 2 Serine 880 phosphorylation modulates synaptic transmission and mediates plasticity in CA1 pyramidal cells. *The Journal of neuroscience : the official journal of the Society for Neuroscience,* **23**(1529-2401; 0270-6474; 27), pp. 9220-9228.

Setou, M., Dae-Hyung Seog, Tanaka, Y., Kanai, Y., Takei, Y., Kawagishi, M. and Hirokawa, N., 2002. Glutamate-receptor-interacting protein GRIP1 directly steers kinesin to dendrites. *Nature,* **417**(6884), pp. 83.

Shankar, G.M., Li, S., Mehta, T.H., Garcia-Munoz, A., Shepardson, N.E., Smith, I., Brett, F.M., Farrell, M.A., Rowan, M.J., Lemere, C.A., Regan, C.M., Walsh, D.M., Sabatini, B.L. and Selkoe, D.J., 2008. Amyloid-beta protein dimers isolated directly from Alzheimer's brains impair synaptic plasticity and memory. *Nature medicine,* **14**(1546-170; 1078-8956; 8), pp. 837-842.

Shi, S., Hayashi, Y., Esteban, J.A. and Malinow, R., 2001. Subunit-specific rules governing AMPA receptor trafficking to synapses in hippocampal pyramidal neurons. *Cell,* **105**(0092-8674; 0092-8674; 3), pp. 331-343.

Stoppini, L., Buchs, P.A. and Muller, D., 1991. A simple method for organotypic cultures of nervous tissue. *Journal of neuroscience methods,* **37**(0165-0270; 0165-0270; 2), pp. 173-182.

Takashima, A., Noguchi, K., Sato, K., Hoshino, T. and Imahori, K., 1993. Tau protein kinase I is essential for amyloid beta-protein-induced neurotoxicity. *Proceedings of the National Academy of Sciences of the United States of America,* **90**(0027-8424; 0027-8424; 16), pp. 7789-7793.

Terashima, A., Pelkey, K.A., Rah, J.C., Suh, Y.H., Roche, K.W., Collingridge, G.L., McBain, C.J. and Isaac, J.T., 2008. An essential role for PICK1 in NMDA receptor-dependent bidirectional synaptic plasticity. *Neuron,* **57**(1097-4199; 0896-6273; 6), pp. 872-882.

Triller, A. and Choquet, D., 2005. Surface trafficking of receptors between synaptic and extrasynaptic membranes: and yet they do move! *Trends in neurosciences,* **28**(3), pp. 133-139.

Wenthold, R.J., Petralia, R.S., Blahos, J.,II and Niedzielski, A.S., 1996. Evidence for multiple AMPA receptor complexes in hippocampal CA1/CA2 neurons. *The Journal of neuroscience : the official journal of the Society for Neuroscience,* **16**(0270-6474; 0270-6474; 6), pp. 1982-1989.

Zhang, J., Yin, Y., Ji, Z., Cai, Z., Zhao, B., Li, J., Tan, M. and Guo, G., 2017. Endophilin2 Interacts with GluA1 to Mediate AMPA Receptor Endocytosis Induced by Oligomeric Amyloid-beta. *Neural plasticity,* **2017**, pp. 8197085.

Zhou, Z., Liu, A., Xia, S., Leung, C., Qi, J., Meng, Y., Xie, W., Park, P., Collingridge, G. and Jia, Z., 2018. The C-terminal tails of endogenous GluA1 and GluA2 differentially contribute to hippocampal synaptic plasticity and learning. *Nat Neurosci,* **21**(1), pp. 50-62.

SUPPLEMENTAL FIGURES

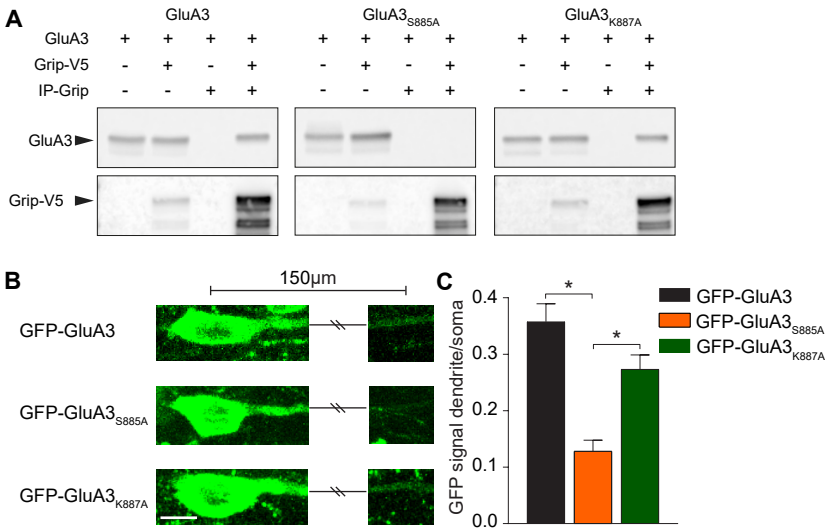

Figure S1. GluA3$_{S885A}$ disables GluA3-GRIP interaction and impairs GFP-GluA3 transportation along dendrites. (A) Blots from GRIP-V5 IPs on HEK cells expressing GFP-GluA3 and/or GRIP-V5, demonstrating the inability of GluA3$_{S885A}$ to bind GRIP-V5. (B) Sample images of GluA3-KO dendrites expressing GFP-GluA3 GFP-GluA3$_{S885A}$ or GFP-GluA3$_{K887A}$. (soma and dendrites have equal look up tables, scale bar: 10 µm). (C) Relative to somatic GFP-GluA3$_{S885A}$ (n=19), the dendritic signal intensity was lower compared to GFP-GluA3 (n=20) and GFP-GluA3$_{K887A}$ (n=20). Data are mean ± SEM. *P < 0.001.

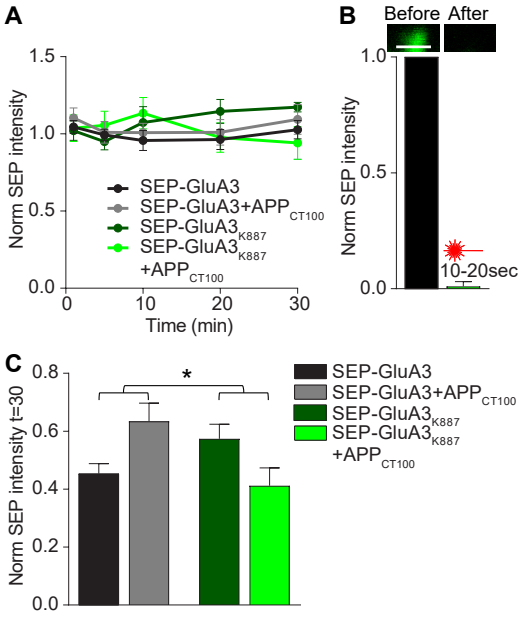

Figure S2. Supplemental FRAP data. (A) During FRAP experiments, dendritic spines were selectively bleached. SEP-GluA3 (black n=14), SEP-GluA3+APP$_{CT100}$ (grey n=16), SEP-GluA3 $_{K887A}$ (dark green n=6), SEP-GluA3$_{K887A}$+APP$_{CT100}$ (green n=12). (B) Top example spine before and after bleaching. Bottom, mean SEP intensity of spines (black) was nearly gone after bleaching (green). n=26 spines. (same look up table, scale bar: 1 µm) (C) The APP$_{CT100}$ induced increased mobile fraction of SEP-GluA3 mobilization was significantly blocked in SEP-GluA3$_{K887A}$. Data are mean ± SEM. *P = 0.01 of two-way ANOVA interaction effect.

Chapter 8

Discussion

DISCUSSION

Adapting to an ever-changing world is crucial for survival. Underlying this capacity to constantly adapt are learning and memory, which allow for the storage and retrieval of information. The modulation of synaptic plasticity is crucial for memory and learning, and this is intrinsically linked to glutamate receptors. These receptors bind to the main excitatory neurotransmitter in the brain, glutamate. AMPA receptors, one of the subtypes of glutamate receptors, are composed of four types of subunits, GluA1 to GluA4. Whilst GluA1 and GluA2 are heavily studied, GluA3 is still quite understudied. This thesis tackled the lack of knowledge regarding this AMPA receptor subunit by looking at its role in synaptic plasticity and synaptic dysfunction in two different brain structures: the hippocampus and the cerebellum.

We show that the GluA3 AMPA receptor subunit is involved in crucial cerebellar motor learning, and that this newly uncovered GluA3-mediated mechanism defies some long-established rules regarding the potentiation of the pf-PC synapse. We propose GluA3 as a major player in hippocampal memory retrieval. We see how the rules proposed for the cerebellum are opposite to the rules uncovered for the hippocampus regarding the GluA1 and GluA3 subunits of the AMPA receptors, in learning. We then see the GluA3 subunit's role in rendering the synapses susceptible to amyloid-β, a peptide crucially involved in Alzheimer's disease. Lastly, we elaborate on these topics for future directions.

8.0 Summary Discussion

In Chapter 1, we aimed at briefly describing the neural bases for learning and memory. We take behavior as a starting point; because behavior is driven by brain activity, changes in behavior likely correspond to changes inside the brain; learning and memory are expressed as changes in the synaptic connections between neurons. We start by describing the brain and its structure, and then deepening to the level of the synapse. We explore synaptic plasticity and transmission, and look at how strengthening and weakening of synapses gives rise to changes in memory and learning. We focus our attention at the glutamatergic activity, namely at the AMPA receptors. We then look at these concepts in the cerebellum, looking at its function in adaptation. We explore the topics of LTP and LTD and the pf-PC synapse. We then shift to the hippocampus, looking at its role in encoding and retrieval of memories, and emphasizing the influence of arousal and stress in learning. Lastly, we review the expression of Alzheimer's disease in the brain,

emphasizing the impact on synaptic transmission, plasticity and memory dysfunction.

We then reviewed the role of the cerebellum in locomotion, describing the cerebellar modules and networks involved. In Chapter 2, we took the perspective of neuro-anatomical and clinical reports as well as cell-specific rodent studies to describe the different modules and networks of the cerebellum involved in the preparation, performance, adaptation and consolidation of locomotion, highlighting their individual contribution to interlimb coordination and to the accuracy, efficiency and regularity of locomotion patterns. We completed this chapter by stressing how the modular organization of the spinocerebellum, responsible for locomotion control, contrasts with that of the vestibulocerebellum, which controls VOR adaptation.

In the next chapter, we used this cerebellar learning task, VOR, to analyze the effect of GCs manipulations, serving additionally as a validation tool of the VOR paradigm. We showed in Chapter 3 different GCs manipulations that didn't impact VOR adaptation. These results raised a substantial number of questions and partially strengthened the idea from previous studies that a minority of functionally intact GCs is sufficient for the maintenance of basic motor performance.

In Chapter 4, we explored the role of the GluA3 AMPARs subunit in cerebellar motor learning. In this chapter, we reveal that adaptation of compensatory eye movements, one of the most widely studied forms of cerebellar motor learning, is dependent on GluA3-containing AMPARs in PCs of the cerebellum. We elegantly demonstrate that the induction and expression of pf-PC LTP is triggered by a rise in cAMP through Epac-mediated activation of postsynaptic GluA3-containing AMPARs, involving a change in conductance and open probability of the GluA3 subunit channel.

We then shifted our focus to the hippocampus. In Chapter 5, we explored the physiological role of the newly identified GluA3-dependent form of synaptic plasticity in the CA1 region of the hippocampus. We also show that GluA3-dependent currents are increased by β-AR activation during arousal. In addition, we found that GluA3-plasticity in the hippocampus regulates the capacity to retrieve a memory.

In Chapters 6 and 7, we looked at the role of the GluA3 subunit in Alzheimer's Disease (AD). We reveal that GluA3-containing AMPARs play a central role in

the Aβ-mediated deficits exhibited in AD-mouse models. In Chapter 6, we show the influence of AMPAR subunit composition on Aβ-mediated synaptotoxicity in three different model systems, namely: a) synaptic depression and spine loss in APP_{CT100}-overexpressing CA1 neurons of organotypic slices; b) block LTP by in exogenously added Aβ-oligomers in acutely isolated brain slices of wild-type mice, but not of GluA3-deficient mice; and c) increased mortality, contextual fear memory deficits and spine loss in APP/PS1-transgenic mice when GluA3 is present in the synapses, but not in its absence. In Chapter 7, we extend these findings and reveal that oligomeric Aβ induces the removal of AMPARs from synapses, requiring the PKCα phosphorylation of the GluA3 subunit at serine 885. We propose that oligomeric Aβ causes synaptic deficits by corrupting the trafficking of GluA3-containing AMPA-receptors at synapses.

8.1 GluA3-mediated synaptic plasticity in the cerebellum

The cerebellum plays an important role in motor learning, most notably participating in the required adjustment to changes in sensorimotor connections. It contributes to the adaptation to the environment by coordinating, planning and tuning motion to the situation ahead. It works as a fine-tuner, constantly adapting to external input.

Among the different players in cerebellar learning, cerebellar granule cells are known to play a pivotal role. As we've reviewed and seen in Chapter 3, they form the input layer of the cerebellum and supply Purkinje cells with the contextual information necessary for motor learning. In the same chapter, we reported five transgenic mouse models targeting granule cell function that show no significant effect on VOR adaptation, a well-known type of cerebellar learning. Several explanations were suggested for these negative effects. It also gave support to the notion that non-significant results are relevant to understand and interpret experiments and should be seen as equally publishable. Finally, it provided a validation for the VOR adaptation protocol used on later chapters.

As emphasized in Chapter 2, in another particular cerebellar-involving task as locomotion, the cerebellum generates the appropriate patterns of the limb movements, dynamically regulates balance, and makes the necessary adjustments to the posture. The role of the cerebellum in locomotor activity is undeniable and not restricted to itself as a single activity. Several studies have shown that locomotion and arousal impact both sensory-evoked responses and spontaneous activity across mouse sensory cortices, with important consequences for sensory perception (e.g. Niell and Stryker, 2010; Ayaz *et al.,*

2013; Bennett, Arroyo and Hestrin, 2013; Schneider, Nelson and Mooney, 2014; Zhou *et al.,* 2014; McGinley *et al.,* 2015; Vinck *et al.,* 2015; Williamson *et al.,* 2015). Albergaria and colleagues add an interesting contribution to the role of locomotor activity in the modulation of another cerebellar learning task, namely during eye blink conditioning (Albergaria *et al.,* 2018). These authors saw that an increase in locomotor speed in head-fixed mice was associated with earlier onset of learning and trial-by-trial enhancement of learned responses. Moreover, eyelid responses evoked by optogenetic stimulation of mossy fiber terminals within the cerebellar cortex were also shown to be modulated by locomotion. This led the authors to conclude that locomotor activity modulates the delay of eyeblink conditioning, suggesting a novel role for behavioral state modulation in associative learning involving locomotor activity.

In Chapter 2 we also saw how PCs of the cerebellum are crucial players for cerebellar motor learning; the manipulation of PC in rodents leads to irregular and smaller movements of different body parts, including the limbs and the eyes. Several studies have dug into the role of PCs in cerebellar learning tasks, as in eye-blink conditioning for example (Jirenhed and Hesslow, 2016), or locomotion (Machado *et al.,* 2015). In this last article, it has been shown that there's a specific failure to predict the consequences of movement across joints, limbs, and body in the Purkinje cell degeneration mouse (pcd), a mutant with postnatal degeneration of virtually all cerebellar PCs (Mullen, Eicher and Sidman, 1976; Machado *et al.,* 2015).

These findings are not surprising, considering that PCs form the sole output of the cerebellar cortex. It has previously been shown that synaptic plasticity at the pf-PC fiber crucially contributes to motor learning (Schonewille *et al.,* 2010). Here we see that the pf-PC synapse requires plasticity of GluA3-containing AMPARs. When GluA3-containing AMPA receptors were selectively removed from PCs or when we pharmacologically blocked the pathway leading to GluA3 plasticity in-vivo, it severely impaired the ability to adapt to the VOR, particularly to the phase-reversal adaptation. This ultimately reflected as an impaired ability to maintain a learned vestibular response in the absence of the visual cue when the GluA3 AMPAR subunit is not present in the synapses.

8.1.1 Potentiation at the pf-PC synapse: the LTP-LTD debate

In Chapter 4 we show that LTP at pf-PC synapses is a required mechanism for cerebellar motor learning, in particular for VOR adaptation. We observed that LTP at the pf-PC synapse, but not LTD, requires plasticity of GluA3-containing AMPARs. This provides the first link between GluA3-dependent LTP and behavioral learning in general. We show that GluA3-dependent synaptic potentiation at pf-PC synapses can occur upon a rise in the cellular level of cAMP. We also show that this cAMP-driven synaptic potentiation does not require an insertion of GluA3-containing AMPARs at the surface of spines, nor does it influence the lateral mobility of GluA3-containing AMPAR. Indeed, cAMP increases channel function of GluA3-containing AMPARs. When GluA3-contaning AMPARs were targeted at the level of the synapse, no structural changes or firing differences were found in awake behaving mice. Though the basal transmission was reduced in PCs lacking GluA3 (both in the global GluA3-KO mice and the cell-specific KO mice), this deficit was probably not the reason for the impairment of LTP or of motor learning, since acutely inhibiting GluA3-plasticity prevented both LTP and motor learning without affecting basal transmission. It was therefore proposed that, in GluA3-KO mice, the reduced basal transmission is the consequence of a prolonged deficit in LTP.

For cerebellar motor learning, LTD at the pf-PC synapse has been considered the dominant plasticity mechanism (Linden and Connor, 1995; Ito, 2002), promoting adaptation of cerebellar learning behaviors as VOR and eye-blink conditioning (De Zeeuw *et al.,* 1998; Ito, 2001; Feil *et al.,* 2003; Boyden *et al.,* 2006). LTP at the pf-PC synapse, on the other hand, has been associated with the extinction of learned associations in previously trained animals (Medina *et al.,* 2000; Han *et al.,* 2007; Schonewille *et al.,* 2010). This reversible change in synaptic efficacy resulting from pf-LTD and pf-LTP is suggested to be the resetting mechanism for motor learning (Sejnowski, 1977a, 1977b; Medina *et al.,* 2000; Houk and Wise, 2015). Indeed, some evidence from fish and rat cerebellum studies demonstrated that pf-LTD and pf-LTP can reverse each other (Lev-Ram *et al.,* 2003; Han *et al.,* 2007). However, our data indicate that LTP is not the reverse process of LTD on a mechanistic level. While LTD involves endocytosis (or removal from synapse) of AMPARs (Man *et al.,* 2000), at least at the short-term scale of tens of minutes, LTP through activation of GluA3-plasticity did not involve trafficking but mainly a prominent increase in open-channel probability of GluA3-containing receptors. This suggests that in the case of GluA3, changes in channel properties are the predominant mechanism to produce synaptic potentiation. These findings reject/disprove the previously described idea that LTP is mechanistically the opposite of LTD at pf to PC synapses (Jörntell and Hansel, 2006).

An increasing amount of studies has been challenging the prominent role of LTD in motor learning (e.g. Schonewille *et al.,* 2011; Hesslow *et al.,* 2013). Indeed, in Chapter 3 we reveal that the adaptation to the VOR was shown to critically depend on LTP, not LTD, at the pf-PC synapse. Through the use of specific knockout mice in which GluA3 was specifically knocked out from their PC, we were able to show that the absence of GluA3 in PCs is necessary for learning. This connects the observation that VOR learning depends on GluA3 with the finding that LTP at pf-PC synapses requires GluA3 plasticity, showing that VOR learning depends on GluA3 specifically in these cells.

Previous studies have proposed a role for cerebellar LTP in the context of bidirectional gain modulation (Boyden *et al.,* 2006). According to this hypothesis, gain-down modulation of the eye movements requires pf-PC LTP, suggesting, conversely, that gain-up modulation would require LTD. Here we show that this hypothesis doesn't fit our results. According to the bidirectional gain modulation hypothesis, one would expect that GluA3-KO mice would show impaired gain-down modulation with integral gain-up adaptation. Our results show that the absence of GluA3 specifically in PCs most significantly impairs gain-up and phase modulation, supporting an opposite kind of role for GluA3-dependent LTP. Others have proposed a possible role in cerebellar motor learning of LTP at the pf-PC synapse, making use of various cell-specific mouse mutant studies (Kramer *et al.,* 2007; Schonewille *et al.,* 2010; Peter *et al.,* 2016). Direct evidence for LTP at the pf-PC synapse is brought in by Schonewille and colleagues (Schonewille *et al.,* 2010), corroborating our results. These authors created a mutant mouse in which calcineurin activity is selectively impaired in PCs (L7-PP2B). They observed, besides deficits in gain decreases, profound deficits in VOR gain increases and a virtual absence of phase reversal learning, while the acquisition of conditioned eyeblink responses and their timing were also affected. By comparison, the behavioral deficits of the potentiation-deficient L7-PP2B mice exceed those of the depression-deficient kinase mutants both during VOR adaptation and eyeblink conditioning (De Zeeuw *et al.,* 1998; Feil *et al.,* 2003; Koekkoek *et al.,* 2003; Hansel *et al.,* 2006).

A recent study threw some more arguments into this mix and suggested that potentiation in PCs complements other forms of cerebellar plasticity in controlling synaptic input strengths and excitability in a dynamic manner (Boele *et al.,* 2018); according to this view, the cerebellum uses these plasticity mechanisms to shape the spike activity patterns of the inhibitory PC output required for motor learning. Though we didn't look at this directly, in Chapter 4 we were able to shed a light

on more downstream PC processes than those tackled in the studies mentioned above (see Gao, van Beugen and De Zeeuw, 2012 for a comprehensive review) by targeting GluA3-containing AMPAR at the level of the synapse itself. This targeting allowed us to observe that the basal transmission was reduced in PCs lacking GluA3, with no evidence of structural changes or firing differences, leading to the proposal that the reduced basal transmission in GluA3-KO mice is the consequence of a prolonged deficit in LTP, reinforcing both the role of GluA3 and of LTP.

8.1.2 The cAMP synergy

Postsynaptic GluA3-dependent synaptic potentiation was shown to be dependent on a rise in cAMP. In Chapter 4 we go even further and uncover Epac as the intermediary factor that translates a rise in cAMP into synaptic potentiation of GluA3-containing AMPARs in PCs. More specifically, Epac activation was revealed as being responsible for the postsynaptic LTP at the pf-PC synapse through activation of GluA3-containing AMPARs; absence of Epac-dependent synaptic potentiation without any change in basal transmission is sufficient to impair learning capabilities.

The finding that an Epac-mediated change in single channel conductance and open probability of GluA2/3-containing AMPARs may underlie LTP at the pf-PC synapse raises the question how this change in AMPAR configuration comes about. Interestingly, under basal conditions the distribution of GluA3-containing AMPAR openings seems to be biased towards the lowest conductance state opening, in which only two out of four ligand binding domains (LBDs) present in the AMPAR tetramer are activated by AMPA. Since GluA3-containing AMPARs predominantly consist of two GluA3 and two GluA2 subunits, only the GluA2 LBDs may effectively bind glutamate under basal conditions. Epac activation may trigger a conformational change in the two GluA3 subunits present in each tetramer, such that they become responsive to glutamate binding at the LBD, as suggested by the observation that enhancing cAMP levels exerts GluA3-containing receptors to produce higher conductance openings, which resembles the behavior of GluA1-containing receptors.

As we've seen, a rise in intracellular cAMP produces synaptic potentiation by increasing the open-channel probability of the GluA3 subunit. This points to a new model for GluA3-dependent synaptic plasticity. It is widely accepted that intracellular calcium signaling is a key mechanism for LTP induction in PCs (Coesmans *et al.,* 2004; van Woerden *et al.,* 2009). It lacks to be explained how

low calcium signals in PCs are translated into activation of adenylyl cyclase to raise cAMP levels. Interestingly, it has been shown that the titanic activity of parallel fibers required for LTP induction produces local calcium increases that are dependent on low-threshold CaV3.1 T-type calcium channels (Hildebrand *et al.,* 2009). Moreover, blockage or global deletion of these channels inhibits LTP induction and motor learning (Ly *et al.,* 2013). An interesting candidate to convert calcium activity in a rise in cAMP could be Adcy1, a calcium/calmodulin-dependent adenylyl cyclase (Masada *et al.,* 2012).

Therefore, in Chapter 4 we increase the range of PC plasticity processes already known to depend on cAMP, such as presynaptic plasticity (Chen and Regehr, 1997; Kaneko and Takahashi, 2004; Lev-Ram *et al.,* 2002), intrinsic plasticity (Belmeguenai *et al.,* 2010) or plasticity at inhibitory synapses (Mitoma and Konishi, 1996). This raises the interesting possibility that Epac2 and/or cAMP in their pre- and postsynaptic domains operate in a synergistic fashion to control synaptic plasticity (Le Guen and De Zeeuw, 2010; Wang *et al.,* 2014). Likewise, the induction protocol of LTP produces an increase in intrinsic excitability in PCs, via cAMP-mediated PKA modulation of SK potassium channels (Belmeguenai *et al.,* 2010). Since this change in intrinsic excitability occurs at least partly as a secondary process following tetanic PF stimulation, LTP at the pf to PC synapse may act as a feed-forward amplifier of synaptic inputs to modulate firing rate in PCs via cAMP production. Finally, it should be noted that rebound potentiation at the molecular layer interneuron to PC synapse, which occurs following PC depolarization, is also mediated by cAMP-mediated PKA modulation (Hirano and Kawaguchi, 2012). Together, these findings point towards a central role of cAMP following induction of pf to PC LTP, regulating multiple forms of plasticity with different identities and natures in a synergistic fashion (Gao *et al.,* 2012).

8.2 A mechanism for memory retrieval: evidence from GluA3-plasticity in the hippocampus

In line with the findings of Chapter 4, we uncovered a new type of synaptic plasticity in the hippocampus that also depends on GluA3 (Renner *et al.,* 2017). In Chapter 5 we show that GluA3-plasticity is activated under physiological conditions, i.e., upon fear conditioning. We further demonstrate that while GluA3 does not contribute to memory formation, it does control the ability to recall a memory.

GluA3-containing AMPARs, long thought to contribute little to synaptic and extrasynaptic AMPAR currents in hippocampal neurons (Andrásfalvy *et al.,* 2003; Lu *et al.,* 2013), are present at synapses, specifically on the cell surface (Renner et al. 2017). Whereas under basal conditions GluA3-containing AMPARs are electrically quiet in CA1 neurons, GluA3-mediated currents become visible when intracellular cAMP levels are increased. As seen in both the cerebellum and the hippocampus, the increased currents are a consequence of an improved capacity of glutamate to open the AMPAR channel. Upon a rise in cAMP, newly formed GluA3-containing AMPARs showed increased currents at both synaptic and extrasynaptic sites without a change in GluA3 levels at synapses or at the cell surface. These ideas are in line with the AMPAR subunit-specific rules for synaptic plasticity: unlike GluA1-containing AMPARs, GluA3-containing AMPARs do not require LTP-like activity to traffic onto the cell surface and into synapses (Kessels *et al.,* 2009; Makino and Malinow, 2009; Shi *et al.,* 2001).

It's very tempting to speculate further on a broad and basic role of the GluA3 AMPAR subunit. Whereas the role of GluA1 in synaptic plasticity and learning is well established, the role of GluA3-containing AMPARs has remained fairly unclear up until the publication of the articles presented in this thesis. Among the theories on the relevance of having two different types of AMPARs in excitatory neurons, it has been proposed, through indirect evidence, that GluA2/3s replace GluA1/2s in an activity-independent manner (Shi *et al.,* 2001). This constitutive process of activity-independent synaptic AMPAR exchange was hypothesized to be necessary for consolidation and stabilization of memories (McCormack *et al.,* 2006; Takahashi *et al.,* 2003; Kessels and Malinow, 2009). We propose a role of GluA3 in memory retrieval. We agree with the idea that, taken the role of GluA1 in forming memories, GluA3 would stabilize those memories; we argue that this replacement of GluA1s by GluA3s would probably serve to free the GluA1-containing receptors for the formation of new memories. We speculate further and suggest that, though GluA3-KO mice have no issues forming a memory (since they have GluA1s), in these mice their memories are always switched on: without GluA3, they cannot store their memory "offline". As seen above, in wild-type mice, GluA1s are gradually replaced by GluA3s. After replacement, the levels of cAMP (and the levels of NE) determine whether the memory is switched on or switched off. It is in fact already known that NE promotes memory retrieval [reference!], and we think that the GluA3 subunit constitutes a large part of the reason NE does so. Therefore, we propose a crucial role of GluA3 in enabling a memory to be silenced and stored offline, as well as bringing such memory back again when necessary by increasing NE levels.

We can also speculate that GluA3 may help in behavioral flexibility. This idea derives directly from what we detailed above: when you cannot silence a previous memory, it will be difficult to change your behavior. A mechanism for behavior flexibility seems necessary when we look at tasks that require a capacity to change patterns and behaviors in response to the environment, like it happens in cerebellar learning. The GluA3 AMPAR subunit would serve, in this model, as an auxiliary tool for change.

8.2.1 The contrasts between GluA3-mediated plasticity in the hippocampus and in the cerebellum

Chapters 4 and 5 emphasized the newly discovered mechanisms of GluA3-mediated plasticity in the cerebellum and hippocampus respectively. The way this subunit revealed itself in each of these structures was striking: whilst in the hippocampus the GluA3 subunit did not contribute to memory formation at all, the absence of this subunit in the cerebellum renders the synapses unable to learn. Reversely, GluA1 in the hippocampus is essential for learning, whilst in the cerebellum is not at all.

As the cerebellum deals with procedural learning and the hippocampus with declarative learning, we can speculate on the distinct roles of this subunit in these two different types of learning. Indeed, cerebellar learning involves a constant adjustment to changes, which suggests that cerebellar synapses have to be prone to be adjusted and tuned; they can't be too rigid. Hippocampal learning, on the other hand, deals with declarative memories, that shouldn't be easily changed; they have to stay stale. This view supports our previous suggestion of a role of GluA3 in adaptive behavior, in which the synapses have to react and respond to a change of rules.

A finding that supports further the model we propose here, has to do with how GluA1 is also distinctively present in these two types of learning and structures. We saw that no compensatory mechanism is able to overcome the declarative memory deficits observed in GluA1 KO mice (Feyder *et al.,* 2007; Humeau *et al.,* 2007). In contrast, GluA1-KO mice learned to adapt their VOR virtually identically to wild-type littermates. This finding suggests two possible scenarios: either PCs synapse are capable to compensate for the absence of GluA1 through a mechanism that is not present in hippocampal pyramidal or amygdalar cells, or GluA1 is not involved in this form of learning at all. With the evidence presented here, none of these possibilities can be unequivocally discarded. Yet, these findings in GluA1-KO mice emphasize the insufficiency of compensation in the

GluA3-KOs; the fact that their PCs could not compensate for the absence of GluA3 to overcome the lack of LTP and the learning deficits highlights the importance of GluA3 for PC synaptic plasticity and motor learning. Taken together, the picture emerges that the learning rules for AMPAR-mediated plasticity in PCs are inverted compared with those in the hippocampus: cerebellar LTP and learning do not require GluA1, but depend on plasticity of GluA3-containing AMPARs. We strongly suggest that this has to do indeed with the different types of requisites necessary for these two types of learning.

The mechanism through which GluA3-mediated plasticity happened in these two structures proved to also show some differences: whilst cerebellar GluA3-mediated plasticity is Epac/Rap1 dependent, hippocampal GluA3-mediated plasticity was not dependent on Epac/Rap1, but instead on Ras (Renner *et al.,* 2017). It might be that Epac/Rap1's path is suitable for a more procedural type of learning as we see in the cerebellum, and that this way doesn't suit hippocampal memory formations paths. A possible explanation for this could well be that Epac/Rap1 versus Ras makes the difference between a persistent change (LTP in PCs) and a transient change (GluA3 in CA1) respectively. While Ras and Rap1 trigger similar downstream (Erk) signaling pathways, they do so with different temporal patterns (Li *et al.,* 2016). This would translate into activating a transient (Ras) or a persistent (Rap1) form of GluA3-plasticity, which suggests different functions to this subunit contingent on the cell type and brain region in which it is expressed.

Relevant differences between GluA1- and GluA3-mediated plasticity

GluA1-containing AMPA receptors are well understood, and known to play a key role in several forms of experience-dependent plasticity, synaptic plasticity and memory formation (Kessels and Malinow, 2009). Since the interaction between GluA1- and GluA3-mediated plasticity points more and more to a synergy, it is important to understand their differences and contrasts in order to get a clear picture. A summary of these points is presented.

First, in the hippocampus, GluA1-containing AMPARs are inserted into synapses upon induction of LTP or formation of fear memories. In contrast, GluA3-containing AMPARs traffic into synapses in the absence of activity and are present at the synapse in an inactive state under basal conditions.

Second, in contrast to the short cytoplasmic tails (C-tails) of GluA2 or GluA3, the GluA1 subunit has a long C-tail that contains several unique phosphorylation sites by which trafficking of GluA1 to synapses can be regulated.

Third, GluA1-dependent synaptic plasticity is mediated by active trafficking (Shi *et al.,* 2001; Makino and Malinow, 2011) as well as by changes in conductance and open probability at the single receptor level (Benke *et al.,* 1998; Derkach, Barria and Soderling, 1999); GluA3-dependent plasticity, in its turn, does not involve activity-dependent trafficking but an increase in open-channel probability of GluA3-containing receptors.

Fourth, another contrast between GluA1- and GluA3-containing AMPA receptors regards their opening mechanism. Whilst GluA1-containing AMPARs open their channels independently of cAMP levels, GluA3-containing AMPARs open their channels upon the increase of intracellular cAMP levels, suggesting that this type of AMPAR channel plasticity is an exclusive feature of GluA3.

Fifth, in the cerebellum, the presence of GluA1 in the PCs was neither essential for the induction of long-term changes (LTD or LTP) nor there were signs of deficits in motor performance or motor learning in the GluA1-KO mice. At the same time, in the hippocampus, no compensatory mechanism was able to overcome the declarative memory deficits observed in these mice (Feyder *et al.,* 2007; Humeau *et al.,* 2007). The possible role of GluA1 in the cerebellum only became indirectly apparent when, compared to the single GluA1-KO, the double GluA1/GluA3-KO mice (lacking both GluA1 and GluA3 subunits globally) virtually completely lacked glutamatergic currents in PCs; besides this, the double L7-GluA1/GluA3-KO (lacking both GluA1 and GluA3 subunits specifically in the PCs) showed signs of ataxia and motor learning deficits. Given that the single GluA3-KO did not show any sign of motor deficit, these findings indicate that GluA1-containing AMPAR in PCs do contribute to cerebellar motor performance but that their absence can be compensated for by GluA3-containing AMPARs. Speculatively, and alternatively, GluA1 in PCs may be required to maintain a basal synaptic transmission, while not being involved in motor learning.

8.3 GluA3-mediated synaptic susceptibility to amyloid-β

Though we couldn't pinpoint exactly the role of GluA3 in the hippocampus, both behaviorally and functionally, we saw in Chapter 6 that the presence of this subunit at synapses contributed to their susceptibility to amyloid-β. GluA3-deficient neurons displayed resistance against the effects of oligomeric Aβ, and the removal of GluA3-containing AMPARs was seen to be a crucial step in the expression of Alzheimer's disease and its related cognitive symptoms. To our knowledge, this is the first evidence that not all synapses are equally vulnerable to Aβ - only those that contain GluA3.

Activity-dependent recruitment of synaptic AMPA receptors in the processes of synaptic plasticity underlying learning and memory has been shown extensively before (Nicol and Malenka, 1999; Kandel, 2001). We have seen previously that GluA3-containing AMPARs have been proposed to gradually replace GluA1-containing AMPARs at synapses after experience-dependent plasticity (Takahashi, Svoboda and Malinow, 2003; McCormack, Stornetta and Zhu, 2006), validating a role for GluA3 in the homeostatic scaling of synapse strength (Kessels and Malinow, 2009; Makino and Malinow, 2011). Neurons that are more active, that receive more experience/synaptic input, will display increased synaptic enrichment of GluA1 and a lower number of GluA3. Conversely, deprivation of synaptic input will increase neuronal synaptic GluA3 levels and decrease GluA1 levels (Rial Verde *et al.,* 2006; Makino and Malinow, 2011). With all this evidence combined with the finding that GluA3 synapses are susceptible to the effects of Aβ, one can predict that a way to prevent the effects of AD-dementia: to keep synapses active by providing more experience-driven synaptic input.

Related to this, it has been shown that there is a significant decrease in GluA3 synaptosomes concentration in AD tissue of the hippocampus, proposing a correlation between GluA3 and cognitive impairment (Bereczki *et al.,* 2018). This supports the observations of reductions of AMPAR trafficking with synaptic and cognitive disturbances (Henley and Wilkinson, 2013).

Lastly, we've seen that GluA3 is important for memory retrieval. Recently it has been shown that memory failure in early AD models reflects an impairment in memory retrieval (Roy *et al.,* 2016) and not in memory formation ***per se***. This finding fits beautifully with our conclusions regarding the vulnerability of GluA3 to the effects of Aβ. The GluA3 involvement could explain the memory retrieval issues displayed by AD patients.

8.4 Future directions

This thesis has proposed roles for the GluA3 AMPA receptor subunit in the cerebellum and in the hippocampus, both in plasticity and dysfunction of synaptic processes. It departed from a time at which the information regarding this AMPAR subunit was limited; the outcome is groundbreaking and hopefully preceed much work on this subunit and related topics.

While we advanced in understanding the roles of GluA3-mediated plasticity, the mechanism through which these happen is still partly unknown. It remains to be established, for example, what is the mechanism of transduction of the low

calcium signals in PCs into activation of adenylyl cyclase to raise cAMP levels. As mentioned above, an interesting candidate to convert local calcium activity in a rise in cAMP could be calcium/calmodulin-dependent adenylyl cyclase Adcy1 (Masada *et al.,* 2012). Future studies could address this topic.

It was out of the scope of this thesis to analyze the connection between stress and learning in the cerebellum. It is worth to note that β-adrenergic receptors are expressed in cerebellum (Nicholas, Hökfely and Pieribone, 1996). Moreover, manipulation of noradrenergic inputs to the cerebellum has been shown to interfere with cerebellum-dependent motor learning (McCormick and Thompson, 1982; Keller and Smith, 1983; Watson and McElligott, 1984; Pompeiano, 1998). It has been shown before that noradrenaline is highly selective for the instructive climbing fiber (cf) synapses (Carey and Regehr, 2009). As noradrenaline controls the induction of associative plasticity at pf synapses through regulation of cf inputs (Carey and Regehr, 2009), this raises the possibility that activity in locus coeruleus neurons could dynamically regulate associative plasticity based on behavioral context (Aston-Jones and Cohen, 2005). Dysregulation of the cerebellar noradrenergic system could disrupt motor control and learning by interfering with cf control of plasticity at the pf-PC synapse (Carey and Regehr, 2009).

Future structural studies on the GluA3 subunit may reveal whether cAMP triggers a putative conformational change within the subunit that allows either glutamate to access the ligand binding site or glutamate binding to open the channel. The activation of GluA3-plasticity by cAMP is fast - outside-out patches were pulled from whole-cell configuration after allowing cAMP to flow inside the cell for less than 10 seconds. We did not find evidence for cAMP to act directly onto GluA3 or via conventional cAMP pathways in the hippocampus (PKA, HCN channels), but we did find that a blockade of Epac in PCs or Ras in CA1 neurons prevents the cAMP-driven activation of GluA3-plasticity. How Epac or Ras activation triggers GluA3-plasticity remains to be established, requiring further study.

We showed that GluA3-dependent currents are increased by β-AR activation during arousal. Other signaling pathways that lead to a rise in intracellular cAMP, like those activated by dopamine or serotonin release, may theoretically also lead to the activation of GluA3-plasticity. Besides the hippocampus, it's known that GluA3-containing AMPARs are present in most other brain regions, including the cortex, amygdala, striatum, thalamus, brain stem, olfactory bulb, nucleus accumbens and cerebellum (Breese *et al.,* 1996; Reimers, Milovanovic and Wolf, 2011; Schwenk *et al.,* 2014), suggesting that GluA3-plasticity may be operative

throughout the brain. Future studies can pursuit this line of thought. For instance, GluA3-plasticity in the cortex may be responsible for EEG-alterations during sleep (Steenland, Kim and Zhuo, 2008).

While we uncovered the role of GluA3 in PC plasticity and cerebellar motor learning in general, the role of GluA1-mediated plasticity in these cells is still fairly unknown. We consider it would be relevant to explore further the role of this subunit in the cerebellum. We saw that the presence of GluA1 in PCs was neither essential for the induction of LTD or LTP nor were there overt signs of deficits in motor performance or motor learning in the GluA1-KO. Its possible role became only indirectly apparent, when we observed that, in contrast to the single GluA1-KO, the double GluA1/GluA3-KO lacked completely glutamatergic currents in PCs and that the double L7-GluA1/A3-KO showed significant signs of ataxia and deficits in motor learning. One can speculate that perhaps its putative role can only be visible in certain physiological situations (as it occurred with the GluA3 role in the hippocampus). It is also possible that its possible role is not as relevant in the cerebellum due to the type of (procedural) learning that occurs in this structure, in contrast with the (declarative) learning occurring in the hippocampus. Further studies can shed some light on this subject.

Regarding Aβ's link to GluA3, it remains unclear how Aβ-oligomers initiate synaptic deficits, and it is worth to look at it in the future. Aβ-oligomers have a broad range of binding partners at the surface of neurons (Rahman *et al.,* 2015), and a number of these partners have been proposed to be necessary for inducing pathological effects (Benilova, Karran and De Strooper, 2012; Mucke and Selkoe, 2012). For the expression of the Aβ-mediated effects we discussed here to occur, NMDAR activity is required: Aβ-oligomers trigger an NMDAR-dependent signaling pathway that leads to synaptic depression through the removal of both AMPARs and NMDARs from synapses. Since a blockade of AMPAR endocytosis seems to prevent the depletion of NMDARs from synapses and a loss of spines (Hsieh *et al.,* 2007; T. Miyamoto *et al.,* 2016), this suggests that the removal of AMPARs from synapses is critical for this pathway to induce synaptic failure. It might be interesting to look at whether this critical step of NMDAR activation for the removal of AMPARs is independent of the subunit composition or if it is actually the exact point of connection of the GluA3 subunit. Here, the hypothesis would be that NMDAR activity leads to removal of GluA3; GluA3 removal leads to loss of synapses and the loss of synapses leads to the loss of NMDARs. An experimental way to partially test this idea was done in Chapter 7, where we blocked the removal of GluA3 from the synapses through the engineering of a GluA3 receptor that can't be trafficked out of the synapse. It might be interesting to pursue further this line.

Future experiments may also reveal under which physiological conditions the levels of GluA3 change in neurons, and whether differences in the expression levels of GluA3 determine the severity of AD-symptoms. For example, an active brain could in theory reduce the susceptibility for the development of AD, since learning and experiences potentiate the trafficking of GluA1-containing AMPARs to synapses (Rumpel *et al.,* 2005; Mitsushima *et al.,* 2011) and the subsequent removal of GluA3s (Rial Verde *et al.,* 2006; Makino and Malinow, 2011). Lowering the levels of GluA3-containing AMPARs may reduce the vulnerability of neurons for the effects of oligomeric Aβ. Due to its social relevance, we suggest this line of study to be followed up in the future.

This thesis aimed at looking at the role of the GluA3 AMPA receptor subunit, by studying its role in two different structures, the cerebellum and the hippocampus, both regarding synaptic plasticity and dysfunction. We believe that, whilst still many questions remain, some lights were shed regarding this subunit and its role. The discussion issued on basis of the work here presented shows the relevance of this subunit and, more importantly, it raises very crucial questions for the topics of memory and learning that can and should be followed. We are confident that future studies issued following this work will bring relevant knowledge regarding memory formation and synaptic vulnerability, both in conditions of health and disease.

REFERENCES

Abel, T. and Nguyen, P. V (2008) 'Regulation of hippocampus-dependent memory by cyclic AMP-dependent protein kinase', in Sossin, W. S. et al. (eds) ***Essence of Memory***. Elsevier, pp. 97–115. doi: https://doi.org/10.1016/S0079-6123(07)00006-4.

Acsády, L. and Káli, S. (2007) 'Models, structure, function: the transformation of cortical signals in the dentate gyrus', in Scharfman, H. E. B. T.-P. in B. R. (ed.) ***The Dentate Gyrus: A Comprehensive Guide to Structure, Function, and Clinical Implications***. Elsevier, pp. 577–599. doi: https://doi.org/10.1016/S0079-6123(07)63031-3.

Adamczyk, A. ***et al.*** (2012) 'GluA3-deficiency in mice is associated with increased social and aggressive behavior and elevated dopamine in striatum', ***Behavioural Brain Research***, 229(1), pp. 265–272. doi: https://doi.org/10.1016/j.bbr.2012.01.007.

Alba, A. ***et al.*** (1994) 'Deficient cerebellar long-term depression and impaired motor learning in mGluR1 mutant mice', ***Cell***. Elsevier, 79(2), pp. 377–388. doi: 10.1016/0092-8674(94)90205-4.

Albergaria, C. ***et al.*** (2018) 'Locomotor activity modulates associative learning in mouse cerebellum', ***Nature Neuroscience***, 21(5), pp. 725–735. doi: 10.1038/s41593-018-0129-x.

Albus, J. S. (1971) 'A Theory of Cerebellar Function', ***Mathematical Biosciences***, (10), pp. 25–61.

Allen, G. I. and Tsukahara, N. (1974) 'Cerebrocerebellar communication systems.', ***Physiological Reviews***. American Physiological Society, 54(4), pp. 957–1006. doi: 10.1152/physrev.1974.54.4.957.

Aller, M. I. ***et al.*** (2003) 'Cerebellar granule cell Cre recombinase expression', ***Genesis***. John Wiley & Sons, Ltd, 36(2), pp. 97–103. doi: 10.1002/gene.10204.

Alme, C. B. ***et al.*** (2014) 'Place cells in the hippocampus: Eleven maps for eleven rooms', ***Proceedings of the National Academy of Sciences***, 111(52), pp. 18428 LP – 18435. doi: 10.1073/pnas.1421056111.

Amaral, D. G. and Witter, M. P. (1995) ***Hippocampal formation in the rat nervous system***. 2nd edn. Edited by G. Paxinos. San Diego: Academic.

Anand, B. K. ***et al.*** (2017) 'Cerebellar Projections to Limbic System', ***Journal of Neurophysiology***. American Physiological Society, 22(4), pp. 451–457. doi: 10.1152/jn.1959.22.4.451.

Anderson, E. B., Grossrubatscher, I. and Frank, L. (2014) 'Dynamic hippocampal circuits support learningand memory-guided behaviors', ***Cold Spring Harbor Symposia on Quantitative Biology***, 79, pp. 51–58. doi: 10.1101/sqb.2014.79.024760.

Andrásfalvy, B. K. ***et al.*** (2003) 'Impaired regulation of synaptic strength in hippocampal neurons from GluR1-deficient mice', ***Journal of Physiology***, 552(1), pp. 35–45. doi: 10.1113/jphysiol.2003.045575.

Andreescu, C. E. ***et al.*** (2005) 'Otolith deprivation induces optokinetic compensation.', ***Journal of neurophysiology***, 94(5), pp. 3487–96. doi: 10.1152/jn.00147.2005.

Anggono, V. and Huganir, R. L. (2012) 'Regulation of AMPA receptor trafficking and synaptic plasticity', ***Current Opinion in Neurobiology***, 22(3), pp. 461–469. doi: https://doi.org/10.1016/j.conb.2011.12.006.

Anzai, M., Kitazawa, H. and Nagao, S. (2010) 'Effects of reversible pharmacological shutdown of cerebellar flocculus on the memory of long-term horizontal vestibulo-ocular reflex adaptation in monkeys', ***Neuroscience Research***, 68(3), pp. 191–198. doi: https://doi.org/10.1016/j.neures.2010.07.2038.

Aston-Jones, G. and Cohen, J. D. (2005) 'AN INTEGRATIVE THEORY OF LOCUS COERULEUS-NOREPINEPHRINE FUNCTION: Adaptive Gain and Optimal Performance', ***Annual Review of Neuroscience***. Annual Reviews, 28(1), pp. 403–450. doi: 10.1146/annurev.neuro.28.061604.135709.

Ayaz, A. ***et al.*** (2013) 'Locomotion Controls Spatial Integration in Mouse Visual Cortex', ***Current Biology***. Elsevier, 23(10), pp. 890–894. doi: 10.1016/j.cub.2013.04.012.

Azim, E. ***et al.*** (2014) 'Skilled reaching relies on a V2a propriospinal internal copy circuit', ***Nature***. 2014/02/02, 508(7496), pp. 357–363. doi: 10.1038/nature13021.

Bats, C., Farrant, M. and Cull-Candy, S. G. (2013) 'A role of TARPs in the expression and plasticity of calcium-permeable AMPARs: Evidence from cerebellar neurons and glia', ***Neuropharmacology***. Elsevier Ltd, 74, pp. 76–85. doi: 10.1016/j.neuropharm.2013.03.037.

Belmeguenai, A. and Hansel, C. (2005) 'A Role for Protein Phosphatases 1, 2A, and 2B in Cerebellar Long-Term Potentiation', ***The Journal of Neuroscience***, 25(46), pp. 10768 LP – 10772. doi: 10.1523/JNEUROSCI.2876-05.2005.

Benilova, I., Karran, E. and De Strooper, B. (2012) 'The toxic Aβ oligomer and Alzheimer's disease: an emperor in need of clothes', ***Nature Neuroscience***. Nature Publishing Group, a division of Macmillan Publishers Limited. All Rights Reserved., 15, p. 349. Available at: https://doi.org/10.1038/nn.3028.

Benke, T. A. ***et al.*** (1998) 'Modulation of AMPA receptor unitary conductance by synaptic activity', ***Nature***. Macmillan Magazines Ltd., 393, p. 793. Available at: https://doi.org/10.1038/31709.

Bennett, C., Arroyo, S. and Hestrin, S. (2013) 'Subthreshold Mechanisms Underlying State-Dependent Modulation of Visual Responses', ***Neuron***. Elsevier, 80(2), pp. 350–357. doi: 10.1016/j.neuron.2013.08.007.

Bereczki, E. ***et al.*** (2018) 'Synaptic markers of cognitive decline in neurodegenerative diseases: a proteomic approach', ***Brain : a journal of neurology***. 2018/01/09. Oxford University Press, 141(2), pp. 582–595. doi: 10.1093/brain/awx352.

Bettler, B. and Mulle, C. (1995) 'AMPA and kainate receptors', ***Neuropharmacology***, 34(2), pp. 123–139. doi: https://doi.org/10.1016/0028-3908(94)00141-E.

Beyreuther, K. and Masters, C. L. (1991) 'Amyloid Precursor Protein (APP) and BZA4 Amyloid in the Etiology of Alzheimer's Disease: Precursor-Product Relationships in the Derangement of Neuronal Function', ***Brain Pathology***. John Wiley & Sons, Ltd (10.1111), 1(4), pp. 241–251. doi: 10.1111/j.1750-3639.1991.tb00667.x.

Blair, M. G. ***et al.*** (2013) 'Developmental changes in structural and functional properties of hippocampal AMPARs parallels the emergence of deliberative spatial navigation in juvenile rats.', ***The Journal of neuroscience : the official journal of the Society for Neuroscience***, 33(30), pp. 12218–28. doi: 10.1523/JNEUROSCI.4827-12.2013.

Boele, H.-J. ***et al.*** (2018) 'Impact of parallel fiber to Purkinje cell long-term depression is unmasked in absence of inhibitory input', ***Science advances***. American Association for the Advancement of Science, 4(10), pp. eaas9426–eaas9426. doi: 10.1126/sciadv.aas9426.

Botterell, E. H. and Fulton, J. F. (1938) 'Functional localizaton in the cerebellum of primates. II. Lesions of midline structures (vermis) and deep nuclei.', ***Journal of Comparative Neurology***, 69, pp. 47–62.

Bouret, S. and Sara, S. J. (2005) 'Network reset: a simplified overarching theory of locus coeruleus noradrenaline function', ***Trends in Neurosciences***. Elsevier, 28(11), pp. 574–582. doi: 10.1016/j.tins.2005.09.002.

Bower, J. M. (1997) 'Control of Sensory Data Acquisition', in Schmahmann, J. D. B. T.-I. R. of N. (ed.) ***Review of*** . Academic Press, pp. 489–513. doi: https://doi.org/10.1016/S0074-7742(08)60367-0.

Bowie, D. (2008) 'Ionotropic glutamate receptors & CNS disorders', ***CNS & neurological disorders drug targets***, 7(2), pp. 129–143. Available at: https://www.ncbi.nlm.nih.gov/pubmed/18537642.

Boyden, E. S. ***et al.*** (2006) 'Selective engagement of plasticity mechanisms for motor memory storage.', ***Neuron***, 51(6), pp. 823–834. doi: 10.1016/j.neuron.2006.08.026.

Breese, C. R. ***et al.*** (1996) 'Regional gene expression of the glutamate receptor subtypes GluR 1, GluR 2, and GluR 3 in human postmortem brain', ***Journal of Molecular Neuroscience***, 7(4), pp. 277–289. doi: 10.1007/BF02737065.

Bremner, J. D. ***et al.*** (1996) 'Noradrenergic mechanisms in stress and anxiety: I. preclinical studies', ***Synapse***. John Wiley & Sons, Ltd, 23(1), pp. 28–38. doi: 10.1002/(SICI)1098-2396(199605)23:1<28::AID-SYN4>3.0.CO;2-J.

Brown, D. F. ***et al.*** (1998) 'Neocortical synapse density and braak stage in the lewy body variant of Alzheimer disease: A comparison with classic Alzheimer disease and normal aging', ***Journal of Neuropathology and Experimental Neurology***, 57(10), pp. 955–960.

Butts, T., Hanzel, M. and Wingate, R. J. T. (2014) 'Transit amplification in the amniote cerebellum evolved via a heterochronic shift in NeuroD1 expression', ***Development***, 141(14), pp. 2791 LP – 2795. doi: 10.1242/dev.101758.

Cahill, L. ***et al.*** (1994) 'β-Adrenergic activation and memory for emotional events', ***Nature***, 371(6499), pp. 702–704. doi: 10.1038/371702a0.

Cappello, S. ***et al.*** (2006) 'The Rho-GTPase cdc42 regulates neural progenitor fate at the apical surface', ***Nature Neuroscience***, 9(9), pp. 1099–1107. doi: 10.1038/nn1744.

Carey, M. R. and Regehr, W. G. (2009) 'Noradrenergic Control of Associative Synaptic Plasticity by Selective Modulation of Instructive Signals', ***Neuron***. Elsevier, 62(1), pp. 112–122. doi: 10.1016/j.neuron.2009.02.022.

Carlisle, H. J. and Kennedy, M. B. (2005) 'Spine architecture and synaptic plasticity', ***Trends in Neurosciences***. Elsevier, 28(4), pp. 182–187. doi: 10.1016/j.tins.2005.01.008.

Chae, J. H., Stein, G. H. and Lee, J. E. (2004) 'NeuroD: The Predicted and the Surprising', ***Mol. Cells***. Molecules and Cells, 18(3), pp. 271–288.

Cho, J.-H. and Tsai, M.-J. (2006) 'Preferential posterior cerebellum defect in BETA2/NeuroD1 knockout mice is the result of differential expression of BETA2/NeuroD1 along anterior–posterior axis', ***Developmental Biology***, 290(1), pp. 125–138. doi: https://doi.org/10.1016/j.ydbio.2005.11.024.

Coesmans, M. ***et al.*** (2004) 'Bidirectional Parallel Fiber Plasticity in the Cerebellum under Climbing Fiber Control', ***Neuron***. Elsevier, 44(4), pp. 691–700. doi: 10.1016/j.neuron.2004.10.031.

Coleman, P., Federoff, H. and Kurlan, R. (2004) 'A focus on the synapse for neuroprotection in Alzheimer disease and other dementias', ***Neurology***, 63(7), pp. 1155 LP – 1162. doi: 10.1212/01.WNL.0000140626.48118.0A.

Collingridge, G. L. ***et al.*** (2010) 'Long-term depression in the CNS.', ***Nature reviews. Neuroscience***, 11(7), pp. 459–473. doi: 10.1038/nrn2867.

Di Cristo, G. (2007) 'Development of cortical GABAergic circuits and its implications for neurodevelopmental disorders', ***Clinical Genetics***. John Wiley & Sons, Ltd (10.1111), 72(1), pp. 1–8. doi: 10.1111/j.1399-0004.2007.00822.x.

Crombag, H. S. ***et al.*** (2008) 'A necessary role for GluR1 serine 831 phosphorylation in appetitive incentive learning', ***Behavioural Brain Research***, 191(2), pp. 178–183. doi: https://doi.org/10.1016/j.bbr.2008.03.026.

Cullen, W. K. ***et al.*** (1997) 'Block of LTP in rat hippocampus in vivo by β-amyloid precursor protein fragments', ***NeuroReport***, 8(15). Available at: https://journals.lww.com/neuroreport/Fulltext/1997/10200/Block_of_LTP_in_rat_hippocampus_in_vivo_by.6.aspx.

D., M. and Skey, B. G. (1971) 'Simple memory: a theory for archicortex', ***Philosophical Transactions of the Royal Society of London. B, Biological Sciences***. Royal Society, 262(841), pp. 23–81. doi: 10.1098/rstb.1971.0078.

D'Amico, L. A., Boujard, D. and Coumailleau, P. (2013) 'The Neurogenic Factor NeuroD1 Is Expressed in Post-Mitotic Cells during Juvenile and Adult Xenopus Neurogenesis and Not in Progenitor or Radial Glial Cells', ***PLoS ONE***, 8(6), pp. 1–10. doi: 10.1371/journal.pone.0066487.

D'Angelo, E. (2008) 'The critical role of Golgi cells in regulating spatio-temporal integration and plasticity at the cerebellum input stage', ***Frontiers in neuroscience***. Frontiers Research Foundation, 2(1), pp. 35–46. doi: 10.3389/neuro.01.008.2008.

Dale, H. H., Feldberg, W. and Vogt, M. (1936) 'Release of acetylcholine at voluntary motor nerve endings', ***The Journal of Physiology***, 86(4), pp. 353–380. doi: 10.1113/jphysiol.1936.sp003371.

Darmohray, D. M. ***et al.*** (2019) 'Spatial and Temporal Locomotor Learning in Mouse Cerebellum', ***Neuron***. Elsevier. doi: 10.1016/j.neuron.2019.01.038.

DeKosky, S. T. and Scheff, S. W. (1990) 'Synapse loss in frontal cortex biopsies in Alzheimer's disease: Correlation with cognitive severity', ***Annals of Neurology***. John Wiley & Sons, Ltd, 27(5), pp. 457–464. doi: 10.1002/ana.410270502.

Derkach, V. A. ***et al.*** (2007) 'Regulatory mechanisms of AMPA receptors in synaptic plasticity', ***Nature Reviews Neuroscience***. Nature Publishing Group, 8, p. 101. Available at: https://doi.org/10.1038/nrn2055.

Derkach, V., Barria, A. and Soderling, T. R. (1999) 'Ca²⁺/calmodulin-kinase II enhances channel conductance of α-amino-3-hydroxy-5-methyl-4-isoxazolepropionate type glutamate receptors', ***Proceedings of the National Academy of Sciences***, 96(6), pp. 3269 LP – 3274. doi: 10.1073/pnas.96.6.3269.

Dingledine, R. ***et al.*** (1999) 'The Glutamate Receptor Ion Channels', ***Pharmacological Reviews***, 51(1), pp. 7 LP – 62. Available at: http://pharmrev.aspetjournals.org/content/51/1/7.abstract.

Dore, K., Aow, J. and Malinow, R. (2016) 'The Emergence of NMDA Receptor Metabotropic Function: Insights from Imaging ', ***Frontiers in Synaptic Neuroscience*** , p. 20. Available at: https://www.frontiersin.org/article/10.3389/fnsyn.2016.00020.

Douyard, J. ***et al.*** (2007) 'Differential neuronal and glial expression of GluR1 AMPA receptor subunit and the scaffolding proteins SAP97 and 4.1N during rat cerebellar development', ***Journal of Comparative Neurology***. John Wiley & Sons, Ltd, 502(1), pp. 141–156. doi: 10.1002/cne.21294.

Dow, R. S. (1938) 'Effect of lesions in the vestibular part of the cerebellum in primates.', ***Archives of Neurology & Psychiatry***, 40, pp. 500–520.

Dudek, S. M. and Bear, M. F. (1993) 'Bidirectional long-term modification of synaptic effectiveness in the adult and immature hippocampus.', ***The Journal of neuroscience : the official journal of the Society for Neuroscience***, 13(7), pp. 2910–2918.

Dudok, J. J. ***et al.*** (2013) 'MPP3 Is Required for Maintenance of the Apical Junctional Complex, Neuronal Migration, and Stratification in the Developing Cortex', ***Journal of Neuroscience***, 33(19), pp. 8518–8527. doi: 10.1523/JNEUROSCI.5627-12.2013.

Eccles, J. C. (1970) 'Neurogenesis and Morphogenesis in the Cerebellar Cortex', ***Proceedings of the National Academy of Sciences***, 66(2), pp. 294 LP – 301. doi: 10.1073/pnas.66.2.294.

Esposito, M. S., Capelli, P. and Arber, S. (2014) 'Brainstem nucleus MdV mediates skilled forelimb motor tasks', ***Nature***. Nature Publishing Group, a division of Macmillan Publishers Limited. All Rights Reserved., 508, p. 351. Available at: https://doi.org/10.1038/nature13023.

Fanselow, M. S. and Dong, H.-W. (2010) 'Are The Dorsal and Ventral Hippocampus functionally distinct structures?', ***Neuron***, 65(1), pp. 1–25. doi: 10.1016/j.neuron.2009.11.031.Are.

Farrant, M. and Nusser, Z. (2005) 'Variations on an inhibitory theme: phasic and tonic activation of GABAA receptors', ***Nature Reviews Neuroscience***, 6(3), pp. 215–229. doi: 10.1038/nrn1625.

Fatemi, S. H. ***et al.*** (2014) 'Downregulation of GABAA Receptor Protein Subunits α6, β2, δ, ε, γ2, θ, and ρ2 in Superior Frontal Cortex of Subjects with Autism', ***Journal of Autism and Developmental Disorders***, 44(8), pp. 1833–1845. doi: 10.1007/s10803-014-2078-x.

Feil, R. ***et al.*** (2003) 'Impairment of LTD and cerebellar learning by Purkinje cell-specific ablation of cGMP-dependent protein kinase I', ***Journal of Cell Biology***, 163(2), pp. 295–302. doi: 10.1083/jcb.200306148.

Ferrer, I. and Gullotta, F. (1990) 'Down's dyndrome and Alzheimer's disease: dendritic spine counts in the hippocampus', ***Acta Neuropathologica***, 79(6), pp. 680–685. doi: 10.1007/BF00294247.

Feyder, M. ***et al.*** (2007) 'Impaired associative fear learning in mice with complete loss or haploinsufficiency of AMPA GluR1 receptors', ***Frontiers in behavioral neuroscience***. Frontiers Research Foundation, 1, p. 4. doi: 10.3389/neuro.08.004.2007.

Foster, M. (1897) ***A textbook of physiology. Part three: The central nervous system.*** 7th edn. London: Macmillan.

Fox, B. Y. C. A. and Barnard, J. W. (1957) 'A quantitative study of the Purkinje cell dendritic branchlets and their relationship to afferent fibres', ***Journal of anatomy***, 91(1951), pp. 299–313. doi: 10.1039/c1rp90071d.

Freir, D. B., Holscher, C. and Herron, C. E. (2001) 'Blockade of Long-Term Potentiation by β-Amyloid Peptides in the CA1 Region of the Rat Hippocampus In Vivo', ***Journal of Neurophysiology***. American Physiological Society, 85(2), pp. 708–713. doi: 10.1152/jn.2001.85.2.708.

Fünfschilling, U. and Reichardt, L. F. (2002) 'Cre-mediated recombination in rhombic lip derivatives', ***genesis***. John Wiley & Sons, Ltd, 33(4), pp. 160–169. doi: 10.1002/gene.10104.

Galliano, E. ***et al.*** (2013) 'Silencing the majority of cerebellar granule cells uncovers their essential role in motor learning and consolidation.', ***Cell reports***. The Authors, 3(4), pp. 1239–51. doi: 10.1016/j.celrep.2013.03.023.

Gao, Z. ***et al.*** (2012) 'Cerebellar ataxia by enhanced Ca(V)2.1 currents is alleviated by Ca2+-dependent K+-channel activators in Cacna1a(S218L) mutant mice.', ***The Journal of neuroscience : the official journal of the Society for Neuroscience***, 32(44), pp. 15533–46. doi: 10.1523/JNEUROSCI.2454-12.2012.

Gao, Z., van Beugen, B. J. and De Zeeuw, C. I. (2012) 'Distributed synergistic plasticity and cerebellar learning', ***Nature Reviews Neuroscience***. Nature Publishing Group, a division of Macmillan Publishers Limited. All Rights Reserved., 13, p. 619. Available at: https://doi.org/10.1038/nrn3312.

Gauthier, G. M. and Robinson, D. A. (1975) 'Adaptation of the human vestibuloocular reflex to magnifying lenses', ***Brain Research***, 92(2), pp. 331–335. doi: https://doi.org/10.1016/0006-8993(75)90279-6.

Gelinas, J. N. ***et al.*** (2008) 'Beta-adrenergic receptor activation during distinct patterns of stimulation critically modulates the PKA-dependence of LTP in the mouse hippocampus', ***Learning & memory (Cold Spring Harbor, N.Y.)***. Cold Spring Harbor Laboratory Press, 15(5), pp. 281–289. doi: 10.1101/lm.829208.

Gelinas, P. V. and Nguyen, J. N. (2007) 'Neuromodulation of Hippocampal Synaptic Plasticity, Learning, and Memory by Noradrenaline', ***Central Nervous System Agents in Medicinal Chemistry***, pp. 17–33. doi: http://dx.doi.org/10.2174/187152407780059196.

Giovannucci, A. ***et al.*** (2017) 'Cerebellar granule cells acquire a widespread predictive feedback signal during motor learning', ***Nature Neuroscience***. Nature Publishing Group, a division of Macmillan Publishers Limited. All Rights Reserved., 20, p. 727. Available at: https://doi.org/10.1038/nn.4531.

Glenner, G. G. and Wong, C. W. (1984) 'Alzheimer's disease: Initial report of the purification and characterization of a novel cerebrovascular amyloid protein', ***Biochemical and Biophysical Research Communications***, 120(3), pp. 885–890. doi: https://doi.org/10.1016/S0006-291X(84)80190-4.

Goebbels, S. ***et al.*** (2005) 'Cre/loxP-mediated inactivation of the bHLH transcription factor gene NeuroD/BETA2', ***genesis***. John Wiley & Sons, Ltd, 42(4), pp. 247–252. doi: 10.1002/gene.20138.

Goebbels, S. ***et al.*** (2006) 'Genetic targeting of principal neurons in neocortex and hippocampus of NEX-Cre mice', ***genesis***. John Wiley & Sons, Ltd, 44(12), pp. 611–621. doi: 10.1002/dvg.20256.

Gonshor, A. and Melvill, J. G. (1973) 'Changes of human vestibulo—ocular response induced by vision reversal during head rotation.', ***The Journal of physiology***, 234(2), pp. 102P-103P.

Granger, A. J. ***et al.*** (2013) 'LTP requires a reserve pool of glutamate receptors independent of subunit type.', ***Nature***. Nature Publishing Group, 493(7433), pp. 495–500. doi: 10.1038/nature11775.

Gray, E. G. (1959) 'Axo-somatic and axo-dendritic synapses of the cerebral cortex', ***Journal of Anatomy***, 93(Pt 4), pp. 420–433. doi: 10.1038/1831592a0.

Gutierrez-Castellanos, N., Winkelman, Beerend H.J., ***et al.*** (2013) 'Impact of aging on long-term ocular reflex adaptation', ***Neurobiology of Aging***. Elsevier Ltd, 34(12), pp. 2784–2792. doi: 10.1016/j.neurobiolaging.2013.06.012.

Gutierrez-Castellanos, N., Winkelman, Beerend H J, ***et al.*** (2013) 'Size does not always matter: Ts65Dn Down syndrome mice show cerebellum-dependent motor learning deficits that cannot be rescued by postnatal SAG treatment', ***The Journal of neuroscience : the official journal of the Society for Neuroscience***. Society for Neuroscience, 33(39), pp. 15408–15413. doi: 10.1523/JNEUROSCI.2198-13.2013.

Gutierrez-Castellanos, N. ***et al.*** (2017) 'Motor Learning Requires Purkinje Cell Synaptic Potentiation through Activation of AMPA-Receptor Subunit GluA3', ***Neuron***. Elsevier, 93(2), pp. 409–424. doi: 10.1016/j.neuron.2016.11.046.

Hagena, H., Hansen, N. and Manahan-Vaughan, D. (2016) 'β-Adrenergic Control of Hippocampal Function: Subserving the Choreography of Synaptic Information Storage and Memory', ***Cerebral Cortex***, 26(4), pp. 1349–1364. doi: 10.1093/cercor/bhv330.

Haglerød, C. ***et al.*** (2017) 'Presynaptic PICK1 facilitates trafficking of AMPA-receptors between active zone and synaptic vesicle pool', ***Neuroscience***, 344, pp. 102–112. doi: https://doi.org/10.1016/j.neuroscience.2016.12.042.

Hall, R. A. (2004) 'β-Adrenergic receptors and their interacting proteins', ***Seminars in Cell & Developmental Biology***, 15(3), pp. 281–288. doi: https://doi.org/10.1016/j.semcdb.2003.12.017.

Han, V. Z. ***et al.*** (2007) 'Synaptic Plasticity and Calcium Signaling in Purkinje Cells of the Central Cerebellar Lobes of Mormyrid Fish', ***Journal of Neuroscience***, 27(49), pp. 13499–13512. doi: 10.1523/jneurosci.2613-07.2007.

Hansel, C. ***et al.*** (2006) 'αCaMKII Is Essential for Cerebellar LTD and Motor Learning', ***Neuron***, 51(6), pp. 835–843. doi: 10.1016/j.neuron.2006.08.013.

Hansel, C. and Linden, D. J. (2000) 'Long-term depression of the cerebellar climbing fiber-Purkinje neuron synapse', ***Neuron***, 26(2), pp. 473–482. doi: 10.1016/S0896-6273(00)81179-4.

Hansel, C., Linden, D. J. and D'Angelo, E. (2001) 'Beyond parallel fiber LTD: the diversity of synaptic and non-synaptic plasticity in the cerebellum', ***Nature Neuroscience***. Nature Publishing Group, 4, p. 467. Available at: https://doi.org/10.1038/87419.

Hardy, J. A. and Higgins, G. A. (1992) 'Alzheimer's disease: the amyloid cascade hypothesis', ***Science***, 256(5054), pp. 184 LP – 185. doi: 10.1126/science.1566067.

Harris, K. M. and Kater, S. B. (1994) 'Dendritic Spines: Cellular Specializations Imparting Both Stability and Flexibility to Synaptic Function', ***Annual Review of Neuroscience***. Annual Reviews, 17(1), pp. 341–371. doi: 10.1146/annurev.ne.17.030194.002013.

Hein, L. (2006) 'Adrenoceptors and signal transduction in neurons', ***Cell and Tissue Research***, 326(2), pp. 541–551. doi: 10.1007/s00441-006-0285-2.

Henley, J. M. and Wilkinson, K. A. (2013) 'AMPA receptor trafficking and the mechanisms underlying synaptic plasticity and cognitive aging', ***Dialogues in clinical neuroscience***. Les Laboratoires Servier, 15(1), pp. 11–27. Available at: https://www.ncbi.nlm.nih.gov/pubmed/23576886.

Herculano-Houzel, S. and Lent, R. (2005) 'Isotropic Fractionator: A Simple, Rapid Method for the Quantification of Total Cell and Neuron Numbers in the Brain', ***Journal of Neuroscience***, 25(10), pp. 2518–2521. doi: 10.1523/jneurosci.4526-04.2005.

Herrup, K. and Kuemerle, B. (1997) 'The compartmentalization of the cerebellum', ***Annual Review of Neuroscience***. Annual Reviews, 20(1), pp. 61–90. doi: 10.1146/annurev.neuro.20.1.61.

Hesslow, G. ***et al.*** (2013) 'Classical conditioning of motor responses: What is the learning mechanism?', ***Neural Networks***. Elsevier Ltd, 47, pp. 81–87. doi: 10.1016/j.neunet.2013.03.013.

Hildebrand, M. E. ***et al.*** (2009) 'Functional coupling between mGluR1 and Cav3.1 T-type calcium channels contributes to parallel fiber-induced fast calcium signaling within Purkinje cell dendritic spines', ***The Journal of Neuroscience***, 29(31), pp. 9668 LP – 9682. doi: 10.1523/JNEUROSCI.0362-09.2009.

Hirano, T. and Kawaguchi, S. (2012) 'Regulation of Inhibitory Synaptic Plasticity in a Purkinje Neuron', ***The Cerebellum***, 11(2), pp. 453–454. doi: 10.1007/s12311-011-0325-7.

Hirano, T., Yamazaki, Y. and Nakamura, Y. (2016) 'LTD, RP, and Motor Learning', ***The Cerebellum***, 15(1), pp. 51–53. doi: 10.1007/s12311-015-0698-0.

Hollmann, M. and Heinemann, S. (1994) 'Cloned Glutamate Receptors', ***Annual Review of Neuroscience***. Annual Reviews, 17(1), pp. 31–108. doi: 10.1146/annurev.ne.17.030194.000335.

Hoogland, T. M. ***et al.*** (2015) 'Role of Synchronous Activation of Cerebellar Purkinje Cell Ensembles in Multi-joint Movement Control', ***Current Biology***. Elsevier, 25(9), pp. 1157–1165. doi: 10.1016/j.cub.2015.03.009.

Horak, F. B. and Diener, H. C. (1994) 'Cerebellar control of postural scaling and central set in stance', ***Journal of Neurophysiology***. American Physiological Society, 72(2), pp. 479–493. doi: 10.1152/jn.1994.72.2.479.

Houk, J. C. and Wise, S. P. (2015) 'Distributed modular architectures linking basal ganglia, cerebellum, and cerebral cortex: their role in planning and controlling action.', ***Cerebral cortex (New York, N.Y. : 1991)***, 5(2), pp. 95–110. doi: 10.1093/cercor/5.2.95.

Hsiao, K. ***et al.*** (1996) 'Correlative Memory Deficits, Aβ Elevation, and Amyloid Plaques in Transgenic Mice', ***Science***, 274(5284), pp. 99 LP – 103. doi: 10.1126/science.274.5284.99.

Hsiao, K. K. ***et al.*** (1995) 'Age-related CNS disorder and early death in transgenic FVB/N mice overexpressing Alzheimer amyloid precursor proteins', ***Neuron***. Elsevier, 15(5), pp. 1203–1218. doi: 10.1016/0896-6273(95)90107-8.

Hsieh, H. ***et al.*** (2007) 'AMPAR removal underlies Abeta-induced synaptic depression and dendritic spine loss.', ***Neuron***, 52(5), pp. 831–843.

Hu, H. ***et al.*** (2007) 'Emotion Enhances Learning via Norepinephrine Regulation of AMPA-Receptor Trafficking', ***Cell***, 131(1), pp. 160–173. doi: 10.1016/j.cell.2007.09.017.

Huganir, Richard L. and Nicoll, R. A. (2013) 'AMPARs and synaptic plasticity: The last 25 years', ***Neuron***. Elsevier Inc., 80(3), pp. 704–717. doi: 10.1016/j.neuron.2013.10.025.

Huganir, Richard L. and Nicoll, R. A. (2013) 'AMPARs and Synaptic Plasticity: The Last 25 Years', ***Neuron***. Elsevier, 80(3), pp. 704–717. doi: 10.1016/j.neuron.2013.10.025.

Humeau, Y. ***et al.*** (2007) 'A pathway-specific function for different AMPA receptor subunits in amygdala long-term potentiation and fear conditioning.', ***The Journal of neuroscience : the official journal of the Society for Neuroscience***, 27(41), pp. 10947–56. doi: 10.1523/JNEUROSCI.2603-07.2007.

Hussain, L. and Maani, C. (2019) ***Physiology, Noradrenergic Synapse.*** Treasure Island (FL): StatPearls Publishing. Available at: https://www.ncbi.nlm.nih.gov/books/NBK540977/.

Ichikawa, R. ***et al.*** (2016) 'Territories of heterologous inputs onto Purkinje cell dendrites are segregated by mGluR1-dependent parallel fiber synapse elimination', ***Proceedings of the National Academy of Sciences***, 113(8), pp. 2282 LP – 2287. doi: 10.1073/pnas.1511513113.

Imai, F. ***et al.*** (2006) 'Inactivation of aPKCλ results in the loss of adherens junctions in neuroepithelial cells without affecting neurogenesis in mouse neocortex', ***Development***, 133(9), pp. 1735 LP – 1744. doi: 10.1242/dev.02330.

Ishikawa, T. ***et al.*** (2011) 'IgSF molecule MDGA1 is involved in radial migration and positioning of a subset of cortical upper-layer neurons', ***Developmental Dynamics***. Wiley Online Library, 240(1), pp. 96–107. doi: 10.1002/dvdy.22496.

Ito, M. ***et al.*** (1974) 'Visual influence on rabbit horizontal vestibulo-ocular reflex presumably effected via the cerebellar flocculus', ***Brain Research***, 65(1), pp. 170–174. doi: https://doi.org/10.1016/0006-8993(74)90344-8.

Ito, M. (1982) 'Questions in modeling the cerebellum', ***Journal of Theoretical Biology***, 99(1), pp. 81–86. doi: https://doi.org/10.1016/0022-5193(82)90390-3.

Ito, M. (1984) 'The modifiable neuronal network of the cerebellum.', ***The Japanese Journal of Physiology***, 34(5), pp. 781–92.

Ito, M. (1989) 'Long-Term Depression', ***Annual Review of Neuroscience***. Annual Reviews, 12(1), pp. 85–102. doi: 10.1146/annurev.ne.12.030189.000505.

Ito, M. (1998) 'Cerebellar learning in the vestibulo–ocular reflex', ***Trends in Cognitive Sciences***, 2(9), pp. 313–321.

Ito, M. (2000) 'Mechanisms of motor learning in the cerebellum.', ***Brain research***, 886(1–2), pp. 237–245. Available at: http://www.ncbi.nlm.nih.gov/pubmed/21645105.

Ito, M. (2001) 'Cerebellar Long-Term Depression: Characterization, Signal Transduction, and Functional Roles', ***Physiological Reviews***. American Physiological Society, 81(3), pp. 1143–1195. doi: 10.1152/physrev.2001.81.3.1143.

Ito, M. (2002) 'Historical Review of the Significance of the Cerebellum and the Role of Purkinje Cells in Motor Learning', ***Annals of the New York Academy of Sciences***. John Wiley & Sons, Ltd (10.1111), 978(1), pp. 273–288. doi: 10.1111/j.1749-6632.2002.tb07574.x.

Jacobsen, J. S. ***et al.*** (2006) 'Early-onset behavioral and synaptic deficits in a mouse model of Alzheimer's disease', ***Proceedings of the National Academy of Sciences of the United States of America***, 103(13), pp. 5161 LP – 5166. doi: 10.1073/pnas.0600948103.

Jansen, J. and Brodal, A. (1940) 'Experimental studies on the intrinsic fibers of the cerebellum. II. The cortico-nuclear projection', ***Journal of Comparative Neurology***. John Wiley & Sons, Ltd, 73(2), pp. 267–321. doi: 10.1002/cne.900730204.

de Jeu, M. and De Zeeuw, C. I. (2012) 'Video-oculography in mice.', ***Journal of visualized experiments : JoVE***, (65), p. e3971. doi: 10.3791/3971.

Jirenhed, D.-A. and Hesslow, G. (2016) 'Are Purkinje Cell Pauses Drivers of Classically Conditioned Blink Responses?', ***Cerebellum (London, England)***. 2015/09/23. Springer US, 15(4), pp. 526–534. doi: 10.1007/s12311-015-0722-4.

Jörntell, H. and Hansel, C. (2006) 'Synaptic Memories Upside Down: Bidirectional Plasticity at Cerebellar Parallel Fiber-Purkinje Cell Synapses', ***Neuron***, 52(2), pp. 227–238. doi: 10.1016/j.neuron.2006.09.032.

Jurd, R. and Moss, S. J. (2010) 'Impaired GABA(A) receptor endocytosis and its correlation to spatial memory deficits', ***Communicative & integrative biology***. Landes Bioscience, 3(2), pp. 176–178. Available at: https://www.ncbi.nlm.nih.gov/pubmed/20585515.

Kadowaki, M. ***et al.*** (2007) 'N-cadherin mediates cortical organization in the mouse brain', ***Developmental Biology***, 304(1), pp. 22–33. doi: https://doi.org/10.1016/j.ydbio.2006.12.014.

Kakegawa, W. and Yuzaki, M. (2005) 'A mechanism underlying AMPA receptor trafficking during cerebellar long-term potentiation', ***Proceedings of the National Academy of Sciences of the United States of America***, 102(49), pp. 17846 LP – 17851. doi: 10.1073/pnas.0508910102.

Kamenetz, F., Tomita, T., Hsieh, H., Seabrook, G., Borchelt, D., Iwatsubo, T., Sisodia, S., Malinow, R., ***et al.*** (2003) 'APP Processing and Synaptic Function', ***Neuron***. Elsevier, 37(6), pp. 925–937. doi: 10.1016/S0896-6273(03)00124-7.

Kamenetz, F., Tomita, T., Hsieh, H., Seabrook, G., Borchelt, D., Iwatsubo, T., Sisodia, S. and Malinow, R. (2003) 'APP Processing and Synaptic Function', ***Neuron***, 37(6), pp. 925–937. doi: 10.1016/S0896-6273(03)00124-7.

Kandel, E. R. (2001) 'The Molecular Biology of Memory Storage: A Dialogue Between Genes and Synapses', ***Science***, 294(5544), pp. 1030 LP – 1038. doi: 10.1126/science.1067020.

Kantardzhieva, A. ***et al.*** (2006) 'MPP3 is recruited to the MPP5 protein scaffold at the retinal outer limiting membrane', ***The FEBS Journal***. John Wiley & Sons, Ltd (10.1111), 273(6), pp. 1152–1165. doi: 10.1111/j.1742-4658.2006.05140.x.

Ke, M. C., Guo, C. C. and Raymond, J. L. (2009) 'Elimination of climbing fiber instructive signals during motor learning.', ***Nature neuroscience***. Nature Publishing Group, 12(9), pp. 1171–9. doi: 10.1038/nn.2366.

Keller, E. L. and Smith, M. J. (1983) 'Suppressed visual adaptation of the vestibuloocular reflex in catecholamine-depleted cats', ***Brain Research***, 258(2), pp. 323–327. doi: https://doi.org/10.1016/0006-8993(83)91159-9.

Kessels, H., Nabavi, S. and Malinow, R. (2013) 'Metabotropic NMDA receptor function is required for beta-amyloid-induced synaptic depression', ***Proc Natl Acad Sci U S A***, 110(10), pp. 4033–4038. doi: 10.1073/pnas.1219605110.

Kessels, H. W. and Malinow, R. (2009) 'Synaptic AMPA receptor plasticity and behavior.', ***Neuron***. Elsevier Inc., 61(3), pp. 340–50. doi: 10.1016/j.neuron.2009.01.015.

Killian, J. E. and Baker, J. F. (2002) 'Horizontal Vestibuloocular Reflex (VOR) Head Velocity Estimation in Purkinje Cell Degeneration (pcd/pcd) Mutant Mice', ***Journal of neurophysiology***, 87(2), pp. 1159–1164.

Kim, C.-H. ***et al.*** (2001) 'Interaction of the AMPA receptor subunit GluR2/3 with PDZ domains regulates hippocampal long-term depression', ***Proceedings of the National Academy of Sciences***, 98(20), pp. 11725 LP – 11730. doi: 10.1073/pnas.211132798.

Kim, C.-H. ***et al.*** (2005) 'Persistent hippocampal CA1 LTP in mice lacking the C-terminal PDZ ligand of GluR1', ***Nature Neuroscience***, 8(8), pp. 985–987. doi: 10.1038/nn1432.

Kim, J. A. ***et al.*** (2017) 'Structural Insights into Modulation of Neurexin-Neuroligin Trans-synaptic Adhesion by MDGA1/Neuroligin-2 Complex', ***Neuron***. Elsevier Inc., 94(6), pp. 1121-1131.e6. doi: 10.1016/j.neuron.2017.05.034.

Kim, J. J. and Thompson, R. E. (1997) 'Cerebellar circuits and synaptic mechanisms involved in classical eyeblink conditioning', ***Trends in Neurosciences***. Elsevier, 20(4), pp. 177–181. doi: 10.1016/S0166-2236(96)10081-3.

Klemann, C. J. H. M. and Roubos, E. W. (2011) 'The gray area between synapse structure and function—Gray's synapse types I and II revisited', ***Synapse***. John Wiley & Sons, Ltd, 65(11), pp. 1222–1230. doi: 10.1002/syn.20962.

Koekkoek, S. K. E. ***et al.*** (2003) 'Cerebellar LTD and Learning-Dependent Timing of Conditioned Eyelid Responses', ***Science***, 301(5640), pp. 1736 LP – 1739. doi: 10.1126/science.1088383.

Kopec, C. D. ***et al.*** (2007) 'GluR1 links structural and functional plasticity at excitatory synapses.', ***The Journal of neuroscience : the official journal of the Society for Neuroscience***, 27(50), pp. 13706–18. doi: 10.1523/JNEUROSCI.3503-07.2007.

Kramer, P. ***et al.*** (2007) 'Estradiol Improves Cerebellar Memory Formation by Activating Estrogen Receptor ', ***Journal of Neuroscience***, 27(40), pp. 10832–10839. doi: 10.1523/jneurosci.2588-07.2007.

Kwak, S. and Weiss, J. H. (2006) 'Calcium-permeable AMPA channels in neurodegenerative disease and ischemia', ***Current Opinion in Neurobiology***, 16(3), pp. 281–287. doi: https://doi.org/10.1016/j.conb.2006.05.004.

Lalonde, R. and Strazielle, C. (2007) 'Spontaneous and induced mouse mutations with cerebellar dysfunctions: behavior and neurochemistry.', ***Brain research***, 1140, pp. 51–74. doi: 10.1016/j.brainres.2006.01.031.

Lang, C. E. and Bastian, A. J. (1999) 'Cerebellar Subjects Show Impaired Adaptation of Anticipatory EMG During Catching', ***Journal of Neurophysiology***, 82(5), pp. 2108–2119. doi: 10.1152/jn.1999.82.5.2108.

Laurie, D. J., Seeburg, P. H. and Wisden, W. (1992) 'The distribution of 13 GABAA receptor subunit mRNAs in the rat brain. II. Olfactory bulb and cerebellum', ***The Journal of Neuroscience***, 12(3), pp. 1063 LP – 1076. doi: 10.1523/JNEUROSCI.12-03-01063.1992.

Lee, H.-K. (2012) 'Ca2+-permeable AMPA receptors in homeostatic synaptic plasticity', ***Frontiers in Molecular Neuroscience***, 5(February), pp. 1–11. doi: 10.3389/fnmol.2012.00017.

Lee, J.-K. ***et al.*** (2000) 'Expression of neuroD/BETA2 in mitotic and postmitotic neuronal cells during the development of nervous system', ***Developmental Dynamics***. John Wiley & Sons, Ltd, 217(4), pp. 361–367. doi: 10.1002/(SICI)1097-0177(200004)217:4<361::AID-DVDY3>3.0.CO;2-8.

Lee, S.-J. R. ***et al.*** (2009) 'Activation of CaMKII in single dendritic spines during long-term potentiation', ***Nature***. Macmillan Publishers Limited. All rights reserved, 458, p. 299. Available at: https://doi.org/10.1038/nature07842.

Lein, E. S. ***et al.*** (2006) 'Genome-wide atlas of gene expression in the adult mouse brain', ***Nature***. Nature Publishing Group, 445, p. 168. Available at: https://doi.org/10.1038/nature05453.

Leitges, M. ***et al.*** (2004) 'A unique PDZ ligand in PKCα confers induction of cerebellar long-term synaptic depression', ***Neuron***, 44(4), pp. 585–594. doi: 10.1016/j.neuron.2004.10.024.

Leppä, E. ***et al.*** (2016) 'Increased Motor-Impairing Effects of the Neuroactive Steroid Pregnanolone in Mice with Targeted Inactivation of the GABA(A) Receptor γ2 Subunit in the Cerebellum', ***Frontiers in pharmacology***. Frontiers Media S.A., 7, p. 403. doi: 10.3389/fphar.2016.00403.

Lev-Ram, V. ***et al.*** (2003) 'Reversing cerebellar long-term depression', ***Proceedings of the National Academy of Sciences***, 100(26), pp. 15989–15993. doi: 10.1073/pnas.2636935100.

Levitt, P. (2005) 'Disruption of Interneuron Development', ***Epilepsia***. John Wiley & Sons, Ltd (10.1111), 46(s7), pp. 22–28. doi: 10.1111/j.1528-1167.2005.00305.x.

Linden, D. J. and Connor, J. A. (1991) 'Participation of postsynaptic PKC in cerebellar long-term depression in culture', ***Science***, 254(5038), pp. 1656 LP – 1659. doi: 10.1126/science.1721243.

Linden, D. J. and Connor, J. A. (1995) 'Long-Term Synaptic Depression', ***Annual Review of Neuroscience***. Annual Reviews, 18(1), pp. 319–357. doi: 10.1146/annurev.ne.18.030195.001535.

Lisman, J. (1989) 'A mechanism for Hebb and anti-Hebb processes underlying learning and memory.', ***Proc. Natl. Acad. Sci. USA***, 86(December), pp. 9574–9578. doi: 10.1073/pnas.86.23.9574.

Lisman, J. E. and Zhabotinsky, A. M. (2001) 'A Model of Synaptic Memory: A CaMKII/PP1 Switch that Potentiates Transmission by Organizing an AMPA Receptor Anchoring Assembly', ***Neuron***. Elsevier, 31(2), pp. 191–201. doi: 10.1016/S0896-6273(01)00364-6.

Lisman, J., Yasuda, R. and Raghavachari, S. (2012) 'Mechanisms of CaMKII action in long-term potentiation', ***Nature Reviews Neuroscience***. Nature Publishing Group, a division of Macmillan Publishers Limited. All Rights Reserved., 13, p. 169. Available at: https://doi.org/10.1038/nrn3192.

Litwack, E. D. ***et al.*** (2004) 'Identification and characterization of two novel brain-derived immunoglobulin superfamily members with a unique structural organization', ***Molecular and Cellular Neuroscience***, 25(2), pp. 263–274. doi: https://doi.org/10.1016/j.mcn.2003.10.016.

Llinas, R. (1964) 'MECHANISMS OF SUPRASPINAL ACTIONS UPON SPINAL CORD ACTIVITIES. DIFFERENCES BETWEEN RETICULAR AND CEREBELLAR INHIBITORY ACTIONS UPON ALPHA EXTENSOR MOTONEURONS', ***Journal of Neurophysiology***. American Physiological Society, 27(6), pp. 1117–1126. doi: 10.1152/jn.1964.27.6.1117.

Lowel, S. and Singer, W. (1992) 'Selection of intrinsic horizontal connections in the visual cortex by correlated neuronal activity', ***Science***, 255(5041), pp. 209 LP – 212. doi: 10.1126/science.1372754.

Lu, W. ***et al.*** (2009) 'Subunit Composition of Synaptic AMPA Receptors Revealed by a Single-Cell Genetic Approach', ***Neuron***. Elsevier, 62(2), pp. 254–268. doi: 10.1016/j.neuron.2009.02.027.

Lu, W. ***et al.*** (2011) 'Potentiation of synaptic AMPA receptors induced by the deletion of NMDA receptors requires the GluA2 subunit', ***Journal of neurophysiology***. 2010/10/27. American Physiological Society, 105(2), pp. 923–928. doi: 10.1152/jn.00725.2010.

Lu, W. ***et al.*** (2013) 'Subunit composition of synaptic AMPA receptors revealed by a single-cell genetic approach', 62(2), pp. 254–268. doi: 10.1016/j.neuron.2009.02.027.Subunit.

Ly, R. ***et al.*** (2013) 'T-type channel blockade impairs long-term potentiation at the parallel fiber-Purkinje cell synapse and cerebellar learning', ***Proceedings of the National Academy of Sciences of the United States of America***. 2013/11/25. National Academy of Sciences, 110(50), pp. 20302–20307. doi: 10.1073/pnas.1311686110.

Machado, A. S. ***et al.*** (2015) 'A quantitative framework for whole-body coordination reveals specific deficits in freely walking ataxic mice', ***eLife***, 4(OCTOBER2015), pp. 1–22. doi: 10.7554/eLife.07892.

Makino, H. and Malinow, R. (2011) 'Compartmentalized versus Global Synaptic Plasticity on Dendrites Controlled by Experience', ***Neuron***. Elsevier, 72(6), pp. 1001–1011. doi: 10.1016/j.neuron.2011.09.036.

Malinow, R. and Malenka, R. C. (2002) 'AMPA Receptor Trafficking and Synaptic Plasticity', ***Annual Review of Neuroscience***. Annual Reviews, 25(1), pp. 103–126. doi: 10.1146/annurev.neuro.25.112701.142758.

Malleret, G. ***et al.*** (2001) 'Inducible and Reversible Enhancement of Learning, Memory, and Long-Term Potentiation by Genetic Inhibition of Calcineurin', ***Cell***. Elsevier, 104(5), pp. 675–686. doi: 10.1016/S0092-8674(01)00264-1.

Man, H.-Y. ***et al.*** (2000) 'Regulation of AMPA Receptor's Mediated Synaptic Transmission by Clathrin-Dependent Receptor Internalization', ***Neuron***. Elsevier, 25(3), pp. 649–662. doi: 10.1016/S0896-6273(00)81067-3.

Man, H.-Y., Sekine-Aizawa, Y. and Huganir, R. L. (2007) 'Regulation of α-amino-3-hydroxy-5-methyl-4-isoxazolepropionic acid receptor trafficking through PKA phosphorylation of the Glu receptor 1 subunit', ***Proceedings of the National Academy of Sciences***, 104(9), pp. 3579 LP – 3584. doi: 10.1073/pnas.0611698104.

Manabe, T. ***et al.*** (1993) 'Modulation of synaptic transmission and long-term potentiation: effects on paired pulse facilitation and EPSC variance in the CA1 region of the hippocampus', ***Journal of Neurophysiology***. American Physiological Society, 70(4), pp. 1451–1459. doi: 10.1152/jn.1993.70.4.1451.

Mapelli, J. ***et al.*** (2016) 'Heterosynaptic GABAergic plasticity bidirectionally driven by the activity of pre- and postsynaptic NMDA receptors', ***Proceedings of the National Academy of Sciences***, 113(35), pp. 9898 LP – 9903. doi: 10.1073/pnas.1601194113.

Marr, D. (1969) 'A theory of cerebellar cortex', ***Journal of Physiology***, 202, pp. 437–470.

Martin, T. A. ***et al.*** (1996) 'Throwing while looking through prisms', ***Brain***, 119(4), pp. 1183–1198. doi: 10.1093/brain/119.4.1183.

Marx, J. (1992) 'Alzheimer's debate boils over', ***Science***, 257(5075), pp. 1336 LP – 1338. doi: 10.1126/science.1529329.

Masada, N. ***et al.*** (2012) 'Distinct mechanisms of calmodulin binding and regulation of adenylyl cyclases 1 and 8', ***Biochemistry***, 51(40), pp. 7917–7929. doi: 10.1021/bi300646y.

Massey, P. V and Bashir, Z. I. (2007) 'Long-term depression: multiple forms and implications for brain function', ***Trends in Neurosciences***. Elsevier, 30(4), pp. 176–184. doi: 10.1016/j.tins.2007.02.005.

McCormack, S. G., Stornetta, R. L. and Zhu, J. J. (2006) 'Synaptic AMPA receptor exchange maintains bidirectional plasticity.', ***Neuron***, 50(1), pp. 75–88. doi: 10.1016/j.neuron.2006.02.027.

McCormick, D. A., Steinmetz, J. E. and Thompson, R. F. (1985) 'Lesions of the inferior olivary complex cause extinction of the classically conditioned eyeblink response', ***Brain Research***, 359(1), pp. 120–130. doi: https://doi.org/10.1016/0006-8993(85)91419-2.

McCormick, D. A. and Thompson, R. F. (1982) 'Locus coeruleus lesions and resistance to extinction of a classically conditioned response: Involvement of the neocortex and hippocampus', ***Brain Research***, 245(2), pp. 239–249. doi: https://doi.org/10.1016/0006-8993(82)90806-X.

McGinley, M. J. ***et al.*** (2015) 'Waking State: Rapid Variations Modulate Neural and Behavioral Responses', ***Neuron***. Elsevier, 87(6), pp. 1143–1161. doi: 10.1016/j.neuron.2015.09.012.

McIntyre, C. K., Hatfield, T. and McGaugh, J. L. (2002) 'Amygdala norepinephrine levels after training predict inhibitory avoidance retention performance in rats', ***European Journal of Neuroscience***. John Wiley & Sons, Ltd (10.1111), 16(7), pp. 1223–1226. doi: 10.1046/j.1460-9568.2002.02188.x.

McNaughton, B. L. and Morris, R. G. M. (1987) 'Hippocampal synaptic enhancement and information storage within a distributed memory system', ***Trends in Neurosciences***, 10(10), pp. 408–415. doi: https://doi.org/10.1016/0166-2236(87)90011-7.

Medina, J. F. ***et al.*** (2000) 'Mechanisms of cerebellar learning suggested by eyelid conditioning', ***Current Opinion in Neurobiology***, 10(6), pp. 717–724. doi: https://doi.org/10.1016/S0959-4388(00)00154-9.

Medina, J. F. and Lisberger, S. G. (2008) 'Links from complex spikes to local plasticity and motor learning in the cerebellum of awake-behaving monkeys.', ***Nature neuroscience***, 11(10), pp. 1185–92. doi: 10.1038/nn.2197.

Meng, Y., Zhang, Y. and Jia, Z. (2003) 'Synaptic transmission and plasticity in the absence of AMPA glutamate receptor GluR2 and GluR3.', ***Neuron***, 39(1), pp. 163–76. Available at: http://www.ncbi.nlm.nih.gov/pubmed/12848940.

Miles, F. A. and Fuller, J. H. (1974) 'Adaptive plasticity in the vestibulo-ocular responses of the rhesus monkey', ***Brain Research***, 80(3), pp. 512–516. doi: https://doi.org/10.1016/0006-8993(74)91035-X.

Milner, B. and Scoville, W. B. (1957) 'Loss of recent memory after bilateral hippocampal lesions', ***Journal of Neurology, Neurosurgery and Psychiatry***, 20(11), p. 11. doi: 10.1136/jnnp-2015-311092.

Mitsushima, D. ***et al.*** (2011) 'Contextual learning requires synaptic AMPA receptor delivery in the hippocampus.', ***Proceedings of the National Academy of Sciences of the United States of America***, 108(30), pp. 12503–8. doi: 10.1073/pnas.1104558108.

Miyamoto, D. ***et al.*** (2016) 'Top-down cortical input during NREM sleep consolidates perceptual memory', ***Science***, 352(6291), pp. 1315 LP – 1318. doi: 10.1126/science.aaf0902.

Miyamoto, T. ***et al.*** (2016) 'Increasing the Receptor Tyrosine Kinase EphB2 Prevents Amyloid-β-induced Depletion of Cell Surface Glutamate Receptors by a Mechanism That Requires the PDZ-binding Motif of EphB2 and Neuronal Activity', ***The Journal of biological chemistry***. 2015/11/20. American Society for Biochemistry and Molecular Biology, 291(4), pp. 1719–1734. doi: 10.1074/jbc.M115.666529.

Miyata, T., Maeda, T. and Lee, J. E. (1999) 'NeuroD is required for differentiation of the granule cells in the cerebellum and hippocampus', ***Genes & development***. Cold Spring Harbor Laboratory Press, 13(13), pp. 1647–1652. Available at: https://www.ncbi.nlm.nih.gov/pubmed/10398678.

Moolman, D. L. ***et al.*** (2004) 'Dendrite and dendritic spine alterations in alzheimer models', ***Journal of Neurocytology***, 33(3), pp. 377–387. doi: 10.1023/B:NEUR.0000044197.83514.64.

Moran, P. M. ***et al.*** (1995) 'Age-related learning deficits in transgenic mice expressing the 751-amino acid isoform of human beta-amyloid precursor protein', ***Proceedings of the National Academy of Sciences***, 92(12), pp. 5341 LP – 5345. doi: 10.1073/pnas.92.12.5341.

Morton, S. M. (2006) 'Cerebellar Contributions to Locomotor Adaptations during Splitbelt Treadmill Walking', ***Journal of Neuroscience***, 26(36), pp. 9107–9116. doi: 10.1523/jneurosci.2622-06.2006.

Morton, S. M. and Bastian, A. J. (2004) 'Cerebellar control of balance and locomotion.', ***The Neuroscientist : a review journal bringing neurobiology, neurology and psychiatry***, 10(3), pp. 247–59. doi: 10.1177/1073858404263517.

Morton, S. M. and Bastian, A. J. (2006) 'Cerebellar Contributions to Locomotor Adaptations during Splitbelt Treadmill Walking', ***The Journal of Neuroscience***, 26(36), pp. 9107 LP – 9116. doi: 10.1523/JNEUROSCI.2622-06.2006.

Mucke, L. and Selkoe, D. J. (2012) 'Neurotoxicity of amyloid β-protein: Synaptic and network dysfunction', ***Cold Spring Harbor Perspectives in Medicine***, 2(7), pp. 1–17. doi: 10.1101/cshperspect.a006338.

Mueller, D., Porter, J. T. and Quirk, G. J. (2008) 'Noradrenergic Signaling in Infralimbic Cortex Increases Cell Excitability and Strengthens Memory for Fear Extinction', ***The Journal of Neuroscience***, 28(2), pp. 369 LP – 375. doi: 10.1523/JNEUROSCI.3248-07.2008.

Mulkey, R. M., Herron, C. E. and Malenka, R. C. (1993) 'An essential role for protein phosphatases in hippocampal long-term depression', ***Science***, 261(5124), pp. 1051 LP – 1055. doi: 10.1126/science.8394601.

Mullen, R. J., Eicher, E. M. and Sidman, R. L. (1976) 'Purkinje cell degeneration, a new neurological mutation in the mouse.', ***Proceedings of the National Academy of Sciences of the United States of America***, 73(1), pp. 208–12. Available at: http://www.pubmedcentral.nih.gov/articlerender.fcgi?artid=335870&tool=pmcentrez&rendertype=abstract.

Murchison, C. F. ***et al.*** (2004) 'A Distinct Role for Norepinephrine in Memory Retrieval', ***Cell***. Elsevier, 117(1), pp. 131–143. doi: 10.1016/S0092-8674(04)00259-4.

Nabavi, S. ***et al.*** (2013) 'Metabotropic NMDA receptor function is required for NMDA receptor-dependent long-term depression.', ***Proceedings of the National Academy of Sciences of the United States of America***, 110(10), pp. 4027–32. doi: 10.1073/pnas.1219454110.

Nabavi, S., Fox, R., Proulx, C. D., ***et al.*** (2014) 'Engineering a memory with LTD and LTP.', ***Nature***. Nature Publishing Group, 511(7509), pp. 348–352. doi: 10.1038/nature13294.

Nabavi, S., Fox, R., Alfonso, S., ***et al.*** (2014) 'GluA1 trafficking and metabotropic NMDA : addressing results from other laboratories inconsistent with ours GluA1 trafficking and metabotropic NMDA : addressing results from other laboratories inconsistent with ours', (December 2013), pp. 5–8.

Nagao, S. (1989) 'Behavior of floccular Purkinje cells correlated with adaptation of vestibulo-ocular reflex in pigmented rabbits', ***Experimental Brain Research***, 77(3), pp. 531–540. doi: 10.1007/BF00249606.

Nedelescu, H. ***et al.*** (2010) 'Endogenous GluR1-containing AMPA receptors translocate to asymmetric synapses in the lateral amygdala during the early phase of fear memory formation: An electron microscopic immunocytochemical study', ***Journal of Comparative Neurology***. John Wiley & Sons, Ltd, 518(23), pp. 4723–4739. doi: 10.1002/cne.22472.

Nicholas, A. P., Hökfely, T. and Pieribone, V. A. (1996) 'The distribution and significance of CNS adrenoceptors examined with in situ hybridization', ***Trends in Pharmacological Sciences***, 17(7), pp. 245–255. doi: https://doi.org/10.1016/0165-6147(96)10022-5.

Nicol, R. A. and Malenka, R. C. (1999) 'Expression Mechanisms Underlying NMDA Receptor-Dependent Long-Term Potentiation', ***Annals of the New York Academy of Sciences***. John Wiley & Sons, Ltd (10.1111), 868(1), pp. 515–525. doi: 10.1111/j.1749-6632.1999.tb11320.x.

Nicoll, R. A., Kauer, J. A. and Malenka, R. C. (1988) 'The current excitement in long term potentiation', ***Neuron***. Elsevier, 1(2), pp. 97–103. doi: 10.1016/0896-6273(88)90193-6.

Niell, C. M. and Stryker, M. P. (2010) 'Modulation of Visual Responses by Behavioral State in Mouse Visual Cortex', ***Neuron***. Elsevier, 65(4), pp. 472–479. doi: 10.1016/j.neuron.2010.01.033.

O'Keefe, J. and Dostrovsky, J. (1971) 'The hippocampus as a spatial map. Preliminary evidence from unit activity in the freely-moving rat', ***Brain Research***, 34(1), pp. 171–175. doi: https://doi.org/10.1016/0006-8993(71)90358-1.

Oda, T. ***et al.*** (1994) 'Purification and Characterization of Brain Clusterin', ***Biochemical and Biophysical Research Communications***, 204(3), pp. 1131–1136. doi: https://doi.org/10.1006/bbrc.1994.2580.

Oda, T. ***et al.*** (1995) 'Clusterin (apoJ) Alters the Aggregation of Amyloid β-Peptide (Aβ1-42) and Forms Slowly Sedimenting Aβ Complexes That Cause Oxidative Stress', ***Experimental Neurology***, 136(1), pp. 22–31. doi: https://doi.org/10.1006/exnr.1995.1080.

Otis, J. M., Fitzgerald, M. K. and Mueller, D. (2013) 'Inhibition of Hippocampal β-Adrenergic Receptors Impairs Retrieval But Not Reconsolidation of Cocaine-Associated Memory and Prevents Subsequent Reinstatement', ***Neuropsychopharmacology***. American College of Neuropsychopharmacology, 39, p. 303. Available at: https://doi.org/10.1038/npp.2013.187.

Papaleonidopoulos, V. and Papatheodoropoulos, C. (2018) 'β-adrenergic receptors reduce the threshold for induction and stabilization of LTP and enhance its magnitude via multiple mechanisms in the ventral but not the dorsal hippocampus', ***Neurobiology of Learning and Memory***, 151, pp. 71–84. doi: https://doi.org/10.1016/j.nlm.2018.04.010.

Peter, S. ***et al.*** (2016) 'Dysfunctional cerebellar Purkinje cells contribute to autism-like behaviour in Shank2-deficient mice', ***Nature communications***. Nature Publishing Group, 7, p. 12627. doi: 10.1038/ncomms12627.

Pettem, K. L. ***et al.*** (2013) 'Interaction between autism-linked MDGAs and neuroligins suppresses inhibitory synapse development', ***Journal of Cell Biology***, 200(3), pp. 321–336. doi: 10.1083/jcb.201206028.

Pike, C. J. ***et al.*** (1991) 'In vitro aging of ß-amyloid protein causes peptide aggregation and neurotoxicity', ***Brain Research***, 563(1), pp. 311–314. doi: https://doi.org/10.1016/0006-8993(91)91553-D.

Pike, C. J. ***et al.*** (1993) 'Neurodegeneration induced by beta-amyloid peptides in vitro: the role of peptide assembly state', ***The Journal of Neuroscience***, 13(4), pp. 1676 LP – 1687. doi: 10.1523/JNEUROSCI.13-04-01676.1993.

Pompeiano, O. (1998) 'Noradrenergic influences on the cerebellar cortex: Effects on vestibular reflexes under basic and adaptive conditions', ***Otolaryngology–Head and Neck Surgery***. SAGE Publications Inc, 119(1), pp. 93–105. doi: 10.1016/S0194-5998(98)70178-0.

Porrero, C. ***et al.*** (2010) 'Mapping of fluorescent protein-expressing neurons and axon pathways in adult and developing Thy1-eYFP-H transgenic mice', ***Brain Research***, 1345, pp. 59–72. doi: https://doi.org/10.1016/j.brainres.2010.05.061.

Price, D. L. (1986) 'New Perspectives on Alzheimer's Disease', ***Annual Review of Neuroscience***. Annual Reviews, 9(1), pp. 489–512. doi: 10.1146/annurev.ne.09.030186.002421.

Price, D. L. and Sisodia, S. S. (1998) 'MUTANT GENES IN FAMILIAL ALZHEIMER'S DISEASE AND TRANSGENIC MODELS', ***Annual Review of Neuroscience***. Annual Reviews, 21(1), pp. 479–505. doi: 10.1146/annurev.neuro.21.1.479.

Qian, H. ***et al.*** (2012) 'β2-Adrenergic receptor supports prolonged theta tetanus-induced LTP', ***Journal of neurophysiology***. 2012/02/15. American Physiological Society, 107(10), pp. 2703–2712. doi: 10.1152/jn.00374.2011.

Ramón y Cajal, S. (1911) ***Histologie du systéme nerveux de l'homme & des vertébrés***. Paris: Maloine.

Ramón y Cajal, S. (1933) ***Histology***. Baltimore: Wood.

Raymond, J. L. and Lisberger, S. G. (1998) 'Neural Learning Rules for the Vestibulo-Ocular Reflex', 18(21), pp. 9112–9129.

Raymond, J. L., Lisberger, S. G. and Mauk, M. D. (1996) 'The Cerebellum: A Neuronal Learning Machine?', ***Science***, 272(5265), pp. 1126 LP – 1131. doi: 10.1126/science.272.5265.1126.

Reimers, J. M., Milovanovic, M. and Wolf, M. E. (2011) 'Quantitative analysis of AMPA receptor subunit composition in addiction-related brain regions', ***Brain research***. Department of Neuroscience, Rosalind Franklin University of Medicine and Science, 3333 Green Bay Road, North Chicago, IL 60064-3095, USA., 1367, pp. 223–233. doi: 10.1016/j.brainres.2010.10.016.

Reimers, J. M., Milovanovic, M. and Wolf, M. E. (2012) 'NIH Public Access', ***Brain research***, 1367, pp. 223–233. doi: 10.1016/j.brainres.2010.10.016.Quantitative.

Reinders, N. R. ***et al.*** (2016) 'Amyloid-β effects on synapses and memory require AMPA receptor subunit GluA3', ***Proceedings of the National Academy of Sciences***, 113(42), p. E6526 LP-E6534. doi: 10.1073/pnas.1614249113.

Renner, M. C. ***et al.*** (2017) 'Synaptic plasticity through activation of GluA3-containing AMPA-receptors', ***eLife***. eLife Sciences Publications, Ltd, 6, p. e25462. doi: 10.7554/eLife.25462.

Rial Verde, E. M. ***et al.*** (2006) 'Increased Expression of the Immediate-Early Gene Arc/Arg3.1 Reduces AMPA Receptor-Mediated Synaptic Transmission', ***Neuron***. Elsevier, 52(3), pp. 461–474. doi: 10.1016/j.neuron.2006.09.031.Increased.

De Robertis, E. (1954) 'Changes in the synaptic vescicles of the ventral acoustic ganglion after nerve section (an electron microscope study)', ***The Anatomical Record***, 118, pp. 284–285.

Rossignol, E. (2011) 'Genetics and function of neocortical GABAergic interneurons in neurodevelopmental disorders', ***Neural plasticity***. 2011/08/18. Hindawi Publishing Corporation, 2011, p. 649325. doi: 10.1155/2011/649325.

Roy, D. S. ***et al.*** (2016) 'Memory retrieval by activating engram cells in mouse models of early Alzheimer's disease', ***Nature***, 531(7595), pp. 508–12. doi: 10.1038/nature17172.

Rumpel, S. ***et al.*** (2005) 'Postsynaptic receptor trafficking underlying a form of associative learning.', ***Science (New York, N.Y.)***, 308(5718), pp. 83–8. doi: 10.1126/science.1103944.

Sakatani, T. and Isa, T. (2004) 'PC-based high-speed video-oculography for measuring rapid eye movements in mice', ***Neuroscience Research***, 49(1), pp. 123–131. doi: https://doi.org/10.1016/j.neures.2004.02.002.

Sanchis-Segura, C. ***et al.*** (2006) 'Involvement of the AMPA receptor GluR-C subunit in alcohol-seeking behavior and relapse.', ***The Journal of neuroscience : the official journal of the Society for Neuroscience***, 26(4), pp. 1231–8. doi: 10.1523/JNEUROSCI.4237-05.2006.

Sara, S. J. (2009) 'The locus coeruleus and noradrenergic modulation of cognition', ***Nature Reviews Neuroscience***. Nature Publishing Group, 10, p. 211. Available at: https://doi.org/10.1038/nrn2573.

Sarro, G. De ***et al.*** (2005) 'AMPA Receptor Antagonists as Potential Anticonvulsant Drugs', ***Current Topics in Medicinal Chemistry***, pp. 31–42. doi: http://dx.doi.org/10.2174/1568026053386999.

Scannevin, R. H. and Huganir, R. L. (2000) 'Postsynaptic organisation and regulation of excitatory synapses', ***Nature Reviews Neuroscience***. Nature America Inc., 1, p. 133. Available at: https://doi.org/10.1038/35039075.

Scheff, S. W. ***et al.*** (2006) 'Hippocampal synaptic loss in early Alzheimer's disease and mild cognitive impairment', ***Neurobiology of Aging***, 27(10), pp. 1372–1384. doi: https://doi.org/10.1016/j.neurobiolaging.2005.09.012.

Schneider, D. M., Nelson, A. and Mooney, R. (2014) 'A synaptic and circuit basis for corollary discharge in the auditory cortex', ***Nature***. Nature Publishing Group, a division of Macmillan Publishers Limited. All Rights Reserved., 513, p. 189. Available at: https://doi.org/10.1038/nature13724.

Schonewille, M. ***et al.*** (2010) 'Purkinje cell-specific knockout of the protein phosphatase PP2B impairs potentiation and cerebellar motor learning.', ***Neuron***. Elsevier Inc., 67(4), pp. 618–28. doi: 10.1016/j.neuron.2010.07.009.

Schonewille, M. ***et al.*** (2011) 'Reevaluating the Role of LTD in Cerebellar Motor Learning', 70(1), pp. 43–50. doi: 10.1016/j.neuron.2011.02.044.Schonewille.

Schwab, M. H. ***et al.*** (2000) 'Neuronal Basic Helix-Loop-Helix Proteins (NEX and BETA2/Neuro D) Regulate Terminal Granule Cell Differentiation in the Hippocampus', ***The Journal of Neuroscience***, 20(10), pp. 3714 LP – 3724. doi: 10.1523/JNEUROSCI.20-10-03714.2000.

Schweighofer, N., Doya, K. and Lay, F. (2001) 'Unsupervised learning of granule cell sparse codes enhances cerebellar adaptive control', ***Neuroscience***. Pergamon, 103(1), pp. 35–50. doi: 10.1016/S0306-4522(00)00548-0.

Schwenk, J. ***et al.*** (2014) 'Regional diversity and developmental dynamics of the AMPA-receptor proteome in the mammalian brain', ***Neuron***. Elsevier Inc., 84(1), pp. 41–54. doi: 10.1016/j.neuron.2014.08.044.

Segal, M. (2005) 'Dendritic spines and long-term plasticity', ***Nature Reviews Neuroscience***, 6(4), pp. 277–284. doi: 10.1038/nrn1649.

Seja, P. ***et al.*** (2012) 'Raising cytosolic Cl-in cerebellar granule cells affects their excitability and vestibulo-ocular learning', ***EMBO Journal***, 31(5), pp. 1217–1230. doi: 10.1038/emboj.2011.488.

Sejnowski, T. J. (1977a) 'Statistical constraints on synaptic plasticity', ***Journal of Theoretical Biology***, 69(2), pp. 385–389. doi: 10.1016/0022-5193(77)90146-1.

Sejnowski, T. J. (1977b) 'Storing covariance with nonlinearly interacting neurons', ***Journal of mathematical biology***, 4(4), pp. 303–321.

Selkoe, D. J. (1991) 'The molecular pathology of Alzheimer's disease', ***Neuron***. Elsevier, 6(4), pp. 487–498. doi: 10.1016/0896-6273(91)90052-2.

Selkoe, D. J. (2000) 'The Origins of Alzheimer DiseaseA Is for Amyloid', ***JAMA***, 283(12), pp. 1615–1617. doi: 10.1001/jama.283.12.1615.

Selkoe, D. J. (2002) 'Alzheimer's Disease Is a Synaptic Failure', ***Science***, 298(5594), pp. 789 LP – 791. doi: 10.1126/science.1074069.

Selkoe, D. J. (2011) 'Resolving controversies on the path to Alzheimer's therapeutics', ***Nature Medicine***. Nature Publishing Group, a division of Macmillan Publishers Limited. All Rights Reserved., 17, p. 1060. Available at: https://doi.org/10.1038/nm.2460.

Shankar, G. M. ***et al.*** (2007) 'Natural oligomers of the Alzheimer amyloid-beta protein induce reversible synapse loss by modulating an NMDA-type glutamate receptor-dependent signaling pathway.', ***The Journal of neuroscience : the official journal of the Society for Neuroscience***, 27(11), pp. 2866–75. doi: 10.1523/JNEUROSCI.4970-06.2007.

Shepherd, G. (2010) ***Creating modern neuroscience: The revolutionary 1950s***. New York, NY: Oxford University Press.

Sherrington, C. S. (1890) 'On Out-Lying Nerve-Cells in the Mammalian Spinal-Cord', ***JSTOR***, 181, pp. 33–48.

Shi, S. ***et al.*** (2001) 'Subunit-specific rules governing AMPA receptor trafficking to synapses in hippocampal pyramidal neurons.', ***Cell***. Elsevier, 105(3), pp. 331–343. doi: 10.1016/S0092-8674(01)00321-X.

Shimansky, Y. ***et al.*** (2004) 'On-line compensation for perturbations of a reaching movement is cerebellar dependent: Support for the task dependency hypothesis', ***Experimental Brain Research***, 155(2), pp. 156–172. doi: 10.1007/s00221-003-1713-0.

Sillitoe, R. V and Joyner, A. L. (2007) 'Morphology, Molecular Codes, and Circuitry Produce the Three-Dimensional Complexity of the Cerebellum', ***Annual Review of Cell and Developmental Biology***. Annual Reviews, 23(1), pp. 549–577. doi: 10.1146/annurev.cellbio.23.090506.123237.

Sisodia, S. S. and Price, D. L. (1995) 'Role of the beta-amyloid protein in Alzheimer's disease.', ***The FASEB Journal***. Federation of American Societies for Experimental Biology, 9(5), pp. 366–370. doi: 10.1096/fasebj.9.5.7896005.

Snider, R. S. and Maiti, A. (1976) 'Cerebellar contributions to the papez circuit', ***Journal of Neuroscience Research***. John Wiley & Sons, Ltd, 2(2), pp. 133–146. doi: 10.1002/jnr.490020204.

Snyder, E. M. ***et al.*** (2005) 'Regulation of NMDA receptor trafficking by amyloid-beta.', ***Nature neuroscience***, 8(8), pp. 1051–1058. doi: 10.1038/nn1503.

Song, M. Y. ***et al.*** (2012) 'SNP-based large-scale identification of allele-specific gene expression in human B cells', ***Gene***, 493(2), pp. 211–218. doi: 10.1016/j.gene.2011.11.058.

Spires, T. L. ***et al.*** (2005) 'Dendritic Spine Abnormalities in Amyloid Precursor Protein Transgenic Mice Demonstrated by Gene Transfer and Intravital Multiphoton Microscopy', ***The Journal of Neuroscience***, 25(31), pp. 7278 LP – 7287. doi: 10.1523/JNEUROSCI.1879-05.2005.

Steenland, H. W., Kim, S. S. and Zhuo, M. (2008) 'GluR3 subunit regulates sleep, breathing and seizure generation.', ***The European journal of neuroscience***, 27(5), pp. 1166–73. doi: 10.1111/j.1460-9568.2008.06078.x.

Steinberg, J. P. ***et al.*** (2006) 'Targeted In Vivo Mutations of the AMPA Receptor Subunit GluR2 and Its Interacting Protein PICK1 Eliminate Cerebellar Long-Term Depression', ***Neuron***. Elsevier, 49(6), pp. 845–860. doi: 10.1016/j.neuron.2006.02.025.

Stéphan, A., Laroche, S. and Davis, S. (2001) 'Generation of Aggregated β-Amyloid in the Rat Hippocampus Impairs Synaptic Transmission and Plasticity and Causes Memory Deficits', ***The Journal of Neuroscience***, 21(15), pp. 5703 LP – 5714. doi: 10.1523/JNEUROSCI.21-15-05703.2001.

Sutherland, S. (1996) ***The international dictionary of psychology***. New York: Crossroad.

Sze, C.-I. ***et al.*** (1997) 'Loss of the Presynaptic Vesicle Protein Synaptophysin in Hippocampus Correlates with Cognitive Decline in Alzheimer Disease', ***Journal of Neuropathology & Experimental Neurology***, 56(8), pp. 933–944. doi: 10.1097/00005072-199708000-00011.

Takahashi, T., Svoboda, K. and Malinow, R. (2003) 'Experience Strengthening Transmission by Driving AMPA Receptors into Synapses', ***Science***, 299(5612), pp. 1585 LP – 1588. doi: 10.1126/science.1079886.

Takeuchi, A. ***et al.*** (2007) 'Novel IgCAM, MDGA1, expressed in unique cortical area- and layer-specific patterns and transiently by distinct forebrain populations of cajal-retzius neurons', ***Cerebral Cortex***, 17(7), pp. 1531–1541. doi: 10.1093/cercor/bhl064.

Takeuchi, A. and O'Leary, D. D. M. (2006) 'Radial Migration of Superficial Layer Cortical Neurons Controlled by Novel Ig Cell Adhesion Molecule MDGA1', ***The Journal of Neuroscience***, 26(17), pp. 4460 LP – 4464. doi: 10.1523/JNEUROSCI.4935-05.2006.

ten Brinke, M. M. ***et al.*** (2015) 'Evolving Models of Pavlovian Conditioning: Cerebellar Cortical Dynamics in Awake Behaving Mice', ***Cell Reports***. Elsevier, 13(9), pp. 1977–1988. doi: 10.1016/j.celrep.2015.10.057.

Terry, R. D. ***et al.*** (1991) 'Physical basis of cognitive alterations in alzheimer's disease: Synapse loss is the major correlate of cognitive impairment', ***Annals of Neurology***. John Wiley & Sons, Ltd, 30(4), pp. 572–580. doi: 10.1002/ana.410300410.

Thach, W. T., Goodkin, H. P. and Keating, J. G. (1992) 'The Cerebellum and the Adaptive Coordination of Movement', ***Annual Review of Neuroscience***. Annual Reviews, 15(1), pp. 403–442. doi: 10.1146/annurev.ne.15.030192.002155.

Thomas, M. J. ***et al.*** (1996) 'Activity-Dependent β-Adrenergic Modulation of Low Frequency Stimulation Induced LTP in the Hippocampal CA1 Region', ***Neuron***, 17(3), pp. 475–482. doi: https://doi.org/10.1016/S0896-6273(00)80179-8.

Traynelis, S. F. ***et al.*** (2010) 'The Glutamate Receptor Ion Channels', ***Pharmacological Reviews***, 62, pp. 405–496. Available at: http://pharmrev.aspetjournals.org/content/51/1/7.abstract.

Tretter, V. ***et al.*** (2009) 'Deficits in spatial memory correlate with modified {gamma}-aminobutyric acid type A receptor tyrosine phosphorylation in the hippocampus', ***Proceedings of the National Academy of Sciences of the United States of America***. 2009/11/10. National Academy of Sciences, 106(47), pp. 20039–20044. doi: 10.1073/pnas.0908840106.

Treves, A. and Rolls, E. T. (1994) 'Computational analysis of the role of the hippocampus in memory', ***Hippocampus***. John Wiley & Sons, Ltd, 4(3), pp. 374–391. doi: 10.1002/hipo.450040319.

Tronson, N. C. and Taylor, J. R. (2007) 'Molecular mechanisms of memory reconsolidation', ***Nature Reviews Neuroscience***. Nature Publishing Group, 8, p. 262. Available at: https://doi.org/10.1038/nrn2090.

Vanhoose, A. M. and Winder, D. G. (2003) 'NMDA and β₁-Adrenergic Receptors Differentially Signal Phosphorylation of Glutamate Receptor Type 1 in Area CA1 of Hippocampus', ***The Journal of Neuroscience***, 23(13), pp. 5827 LP – 5834. doi: 10.1523/JNEUROSCI.23-13-05827.2003.

Varecka, L. ***et al.*** (1994) 'GABAA/benzodiazepine receptor α6 subunit mRNA in granule cells of the cerebellar cortex and cochlear nuclei: Expression in developing and mutant mice', ***Journal of Comparative Neurology***. John Wiley & Sons, Ltd, 339(3), pp. 341–352. doi: 10.1002/cne.903390304.

Vinck, M. ***et al.*** (2015) 'Arousal and Locomotion Make Distinct Contributions to Cortical Activity Patterns and Visual Encoding', ***Neuron***. Elsevier, 86(3), pp. 740–754. doi: 10.1016/j.neuron.2015.03.028.

Vinueza Veloz, M. F. ***et al.*** (2015) 'Cerebellar control of gait and interlimb coordination', ***Brain structure & function***. 2014/08/20. Springer Berlin Heidelberg, 220(6), pp. 3513–3536. doi: 10.1007/s00429-014-0870-1.

Volianskis, A. ***et al.*** (2015) 'Long-term potentiation and the role of N-methyl-D-aspartate receptors', ***Brain research***. Elsevier/North-Holland Biomedical Press, 1621, pp. 5–16. doi: 10.1016/j.brainres.2015.01.016.

Voogd, J. and Barmack, N. H. (2006) 'Oculomotor cerebellum', in Büttner-Ennever, J. A. B. T.-P. in B. R. (ed.) ***Neuroanatomy of the Oculomotor System***. Elsevier, pp. 231–268. doi: https://doi.org/10.1016/S0079-6123(05)51008-2.

Voogd, J. and Glickstein, M. (1998) 'The anatomy of the cerebellum', ***Trends in Neurosciences***. Elsevier, 21(9), pp. 370–375. doi: 10.1016/S0166-2236(98)01318-6.

van Vreeswijk, C. and Sompolinsky, H. (1996) 'Chaos in Neuronal Networks with Balanced Excitatory and Inhibitory Activity', ***Science***, 274(5293), pp. 1724 LP – 1726. doi: 10.1126/science.274.5293.1724.

Wang, V. Y. and Zoghbi, H. Y. (2001) 'Genetic regulation of cerebellar development', ***Nature Reviews Neuroscience***. Nature Publishing Group, 2, p. 484. Available at: https://doi.org/10.1038/35081558.

Watson, M. and McElligott, J. G. (1984) 'Cerebellar norepinephrine depletion and impaired acquisition of specific locomotor tasks in rats', ***Brain Research***, 296(1), pp. 129–138. doi: https://doi.org/10.1016/0006-8993(84)90518-3.

Welsh, J. P. ***et al.*** (1995) 'Dynamic organization of motor control within the olivocerebellar system', ***Nature***, 374(6521), pp. 453–457. doi: 10.1038/374453a0.

Welsh, J. P. ***et al.*** (2005) 'Normal motor learning during pharmacological prevention of Purkinje cell long-term depression', ***Proceedings of the National Academy of Sciences***, 102(47), pp. 17166–17171. doi: 10.1073/pnas.0508191102.

Wenthold, J., Petralia, S. and Niedzielski, S. (1996) 'Evidence for Multiple Neurons Complexes in Hippocampal', 76(6), pp. 1982–1989.

Whitlock, J. R. ***et al.*** (2006) 'Learning Induces Long-Term Potentiation in the Hippocampus', ***Science***, 313(5790), pp. 1093 LP – 1097. doi: 10.1126/science.1128134.

Williamson, R. S. ***et al.*** (2015) 'Locomotion and Task Demands Differentially Modulate Thalamic Audiovisual Processing during Active Search', ***Current Biology***. Elsevier, 25(14), pp. 1885–1891. doi: 10.1016/j.cub.2015.05.045.

van Woerden, G. M. ***et al.*** (2009) 'βCaMKII controls the direction of plasticity at parallel fiber-Purkinje cell synapses.', ***Nature Neuroscience***. Nature Publishing Group, 12(7), p. 823. doi: 10.1038/nn.2329.

Wu, X. ***et al.*** (2013) 'Homeostatic competition between phasic and tonic inhibition', ***The Journal of biological chemistry***. 2013/07/09. American Society for Biochemistry and Molecular Biology, 288(35), pp. 25053–25065. doi: 10.1074/jbc.M113.491464.

Wulff, P. ***et al.*** (2009) 'Synaptic inhibition of Purkinje cells mediates consolidation of vestibulo-cerebellar motor learning.', ***Nature neuroscience***, 12(8), pp. 1042–9. doi: 10.1038/nn.2348.

Yaeger, D. B. and Trussell, L. O. (2015) 'Single granule cells excite Golgi cells and evoke feedback inhibition in the cochlear nucleus', ***The Journal of neuroscience : the official journal of the Society for Neuroscience***. Society for Neuroscience, 35(11), pp. 4741–4750. doi: 10.1523/JNEUROSCI.3665-14.2015.

Yang, Sunggu ***et al.*** (2014) 'Interlamellar CA1 network in the hippocampus', ***National Academy of Sciences. Proceedings***, 111(35), pp. 12919–12924. doi: 10.1073/pnas.1405468111.

Yang, Y. and Lisberger, S. G. (2014) 'Duration of complex-spikes grades Purkinje cell plasticity and cerebellar motor learning', ***Nature***, 510(7506), pp. 529–532. doi: 10.1038/nature13282.Duration.

Yankner, B. A., Duffy, L. K. and Kirschner, D. A. (1990) 'Neurotrophic and neurotoxic effects of amyloid beta protein: reversal by tachykinin neuropeptides', ***Science***, 250(4978), pp. 279 LP – 282. doi: 10.1126/science.2218531.

Yeganeh-Doost, P. ***et al.*** (2011) 'The role of the cerebellum in schizophrenia: from cognition to molecular pathways', ***Clinics (Sao Paulo)***, 66, pp. 71–77.

Yokoyama, M. ***et al.*** (1996) 'Molecular cloning of a human neuroD from a neuroblastoma cell line specifically expressed in the fetal brain and adult cerebellum', ***Molecular Brain Research***, 42(1), pp. 135–139. doi: https://doi.org/10.1016/S0169-328X(96)00154-4.

De Zeeuw, C. I. ***et al.*** (1998) 'Expression of a protein kinase C inhibitor in Purkinje cells blocks cerebellar LTD and adaptation of the vestibulo-ocular reflex.', ***Neuron***, 20(3), pp. 495–508. Available at: http://www.ncbi.nlm.nih.gov/pubmed/9539124.

De Zeeuw, C. I. and Ten Brinke, M. M. (2015) 'Motor Learning and the Cerebellum', ***Cold Spring Harbor perspectives in biology***. Cold Spring Harbor Laboratory Press, 7(9), pp. a021683–a021683. doi: 10.1101/cshperspect.a021683.

Zhou, M. ***et al.*** (2009) 'Fear conditioning enhances spontaneous AMPA receptor-mediated synaptic transmission in mouse hippocampal CA1 area', ***European Journal of Neuroscience***. John Wiley & Sons, Ltd (10.1111), 30(8), pp. 1559–1564. doi: 10.1111/j.1460-9568.2009.06951.x.

Zhou, M. ***et al.*** (2014) 'Scaling down of balanced excitation and inhibition by active behavioral states in auditory cortex', ***Nature Neuroscience***. Nature Publishing Group, a division of Macmillan Publishers Limited. All Rights Reserved., 17, p. 841. Available at: https://doi.org/10.1038/nn.3701.

8

Abstract

The hippocampus and the cerebellum are two different brain regions that encode different types of memories. Whilst the hippocampus deals with declarative memory, the cerebellum is mainly involved in procedural memory.

In the cerebellum, granule cells give rise to parallel fibers, which form synaptic points with Purkinje cells - the parallel fiber-Purkinje cell synapse. We found five mutations in cerebellar granule cell that did not affect phase reversal, a type of cerebellar learning. However, in looking at Purkinje cells whose GluA3 subunit of the AMPA receptors was knocked out, we saw an impairment of phase reversal adaptation. We show, then, that the GluA3 AMPA receptor subunit is involved in crucial cerebellar motor learning. We also show that this GluA3-mediated mechanism defies some long-established rules regarding the potentiation of the parallel fiber-Purkinje cell synapse.

In the hippocampus, learning depends on the trafficking of GluA1-containing AMPARs to synapses. GluA3-containing AMPARs, however, don't seem to contribute much to synaptic currents, synaptic plasticity or learning, though they are present. We found that, in the hippocampus, the GluA3 subunit doesn't contribute to memory formation but does control memory retrieval. We see how the effects of knocking out GluA3 reveal that the hippocampus AMPAR-mediated rules for learning are opposite to the rules uncovered for the cerebellum regarding the GluA1 and GluA3 subunits of the AMPA receptors.

Lastly, we found that memories coded in the hippocampus are affected by amyloid-β, and that its effects occur through the removal of GluA3 from synapses. We demonstrate GluA3 subunit's role in rendering the synapses susceptible to amyloid-β and how it requires PKCα phosphorylation of the GluA3 subunit at serine 885. We finally propose that Aβ causes synaptic deficits by corrupting the constitutive cycling of GluA3-containing AMPA-receptors at synapses.

Samenvatting

De hippocampus en het cerebellum zijn twee verschillende hersengebieden die verschillende soorten herinneringen coderen. Terwijl de hippocampus zich bezighoudt met declaratief geheugen, is het cerebellum voornamelijk betrokken bij procedureel geheugen.

In het cerebellum ontspringen korrelcellen parallelle vezels, die synaptische verbindingen maken met Purkinje-cellen - zijnde de parallelle vezel-Purkinje-celsynaps. We vonden vijf mutaties in de cerebellaire korrelcellen die geen invloed hadden op de faseomkering, een soort leren van het cerebellum. Kijkende naar Purkinje-cellen waarvan de GluA3-subeenheid van de AMPA-receptoren was uitgeschakeld, zagen we echter een verslechtering van faseomkering aanpassing. We laten zien dat de GluA3 AMPA-receptorsubeenheid betrokken is bij cerebellair motorisch leren. We laten ook zien dat dit door GluA3 gemedieerde mechanisme een aantal gevestigde regels tart met betrekking tot de versterking van de parallelle vezel-Purkinje-celsynaps.

In de hippocampus is leren afhankelijk van het transport van GluA1-bevattende AMPAR's naar synapsen. GluA3-bevattende AMPAR's lijken echter niet veel bij te dragen aan synaptische stromingen, synaptische plasticiteit of leren, ondanks hun aanwezigheid. We hebben geconstateerd dat in de hippocampus de GluA3-subeenheid niet bijdraagt aan geheugenvorming, maar wel aan het ophalen van herinneringen. We zien hoe de effecten van het uitschakelen van GluA3 onthullen dat de door AMPAR gemedieerde regels voor leren van de hippocampus tegengesteld zijn aan de regels die voor het cerebellum zijn ontdekt, met betrekking tot de GluA1- en GluA3-subeenheden van de AMPA-receptoren.

Ten slotte hebben we geconstateerd dat herinneringen gecodeerd in de hippocampus worden beïnvloed door amyloïde-β en dat de effecten hiervan optreden doormiddel van de verwijdering van GluA3 uit synapsen. We demonstreren de rol van GluA3-subeenheden bij het gevoelig maken van de synapsen voor amyloïde-β en hoe het PKCα-fosforylering van de GluA3-subeenheid bij serine 885 vereist. We stellen ten slotte voor dat Ap synaptische tekorten veroorzaakt door de constitutieve cycli van GluA3-bevattende AMPA-receptoren bij synapsen te verstoren.

Propositions

1. Different cerebellar modules and networks exert synergistic roles in the preparation, performance, adaptation and consolidation of locomotion.

   (this thesis)

2. Adaptation of compensatory eye movements is dependent on GluA3-containing AMPARs in Purkinje cells of the cerebellum.

   (this thesis)

3. The GluA3 subunit is a major player in memory retrieval.

   (this thesis)

4. GluA3-containing AMPARs play a central role in the Aβ-mediated deficits exhibited by Alzheimer's Disease.

   (this thesis)

5. Lowering the neuronal or synaptic levels of GluA3-containing AMPARs may reduce the vulnerability of neurons for the detrimental effects of oligomeric Aβ in AD.

   (this thesis)

6. (In the brain) "Nothing is lost, nothing is created, everything is transformed."

   – Lavoisier

7. (The story of how memory and learning work becomes) "Curiouser and curiouser!"

   – Alice in Wonderland

8. "Nothing great was ever achieved without enthusiasm."

   – R.W. Emerson

9. "In the realm of ideas everything depends on enthusiasm; in the real world all rests on perseverance."

   – Johann Wolfgang von Goethe

10. "Questions of science, science and progress, do not speak as loud as my heart."

– The Scientist, Coldplay

11. "It's opener, out there, in the wide, open air."

– Dr. Seuss, Oh, The Places You'll Go!

CV

Carla Maria da Silva Matos van der Voort

10/08/1988
São João da Madeira, Portugal

2017-2019
Data Scientist with Python Track Course, DataCamp
Machine Learning, Coursera/Stanford University
Foundations of Data Science: Computational Thinking with Python, BerkeleyX/eDx

2014-2016
PhD candidate at Kessels' lab at the Netherlands Institute for Neuroscience, Amsterdam, The Netherlands

2013-2014
Research Technician at De Zeeuw's lab at the Netherlands Institute for Neuroscience, Amsterdam, The Netherlands

2012-2013
Research Technician at Carey's lab at the Champalimaud Neuroscience Program, Champalimaud Center for the Unknown, Lisboa, Portugal

2010
Erasmus Exchange at the Research Master in Brain and Cognitive Sciences, Universiteit van Amsterdam, Amsterdam, The Netherlands

2009-2012
Research Master in Cognitive Science, University of Lisbon, Portugal
Thesis: Non-literal comprehension in children with Autism Spectrum Disorders

2005-2009
Licenciatura in Speech Language Therapy, Universidade de Aveiro, Aveiro, Portugal

Publications

- **da Silva Matos, C.M.,** Vinueza Veloz, M.F., Ruigrok, T., De Zeeuw, C.I. (2016). Cerebellar Modules and Networks Involved in Locomotion Control. 10.1007/978-3-319-24551-5_37.

- **da Silva Matos, C.M**., Gutierrez-Castellanos, N., Goebbels, S., Dudok, J.J., Wijnholds, J., Schonewille, M., De Zeeuw, C.I., Winkelman, B.H.J. (2019). Granule cells in VOR adaptation. (in preparation)

- Gutierrez-Castellanos, N., Da **Silva-Matos, C.M**., Zhou, K., Canto, C.B., Renner, M.C., Koene, L., Ozyildirim, O., Sprengel, R., Kessels, H.W., De Zeeuw, C.I. (2017). Motor Learning Requires Purkinje Cell Synaptic Potentiation through Activation of AMPA-Receptor Subunit GluA3. Neuron, 93(2), 409-424.

- Reinders, N.R., Pao, Y., Renner, M.C., **da Silva-Matos, C.M.**, Lodder, T.R., Malinow, R., & Kessels, H.W. (2016). Amyloid-β effects on synapses and memory require AMPA receptor subunit GluA3. Proceedings of the National Academy of Sciences of the United States of America, 113(42), E6526-E6534.

- Reinders, N.R., van der Speck, S., **da Silva Matos, C.M.**, Li, K.W., Smit, A.B., Kessels, H.W. (2019). Amyloid-β causes synaptic depression via phosphorylation of AMPA-receptor subunit GluA3 at Serine 885. (in preparation)

Acknowledgements

This thesis is the result of an odd journey. It was not a straight path, rather one full of twists and turns, with much soul-searching and self-learning: what a wonderful trip! I couldn't have done this without the support of many people that walked with me at each step and that kept me surrounded by gentle presence, support and, above everything, **love**.

I would like to start by thanking Megan Carey. You opened the doors of neuroscience to me and I'm so excited to have you in my committee. I will be forever thankful to you for having taken me under your wing and into this awesome world of science. May our paths cross again and let us finish what we started so many years ago.

Chris de Zeeuw, I'm so thankful for everything you have given me and for all the opportunities you've been sending my way. You never fell short from helpful and you always listened to me and believed in me. You are a terrific scientist and your hard working is inspiring.

Cathrin, thank you so much for your friendship, both in the lab and outside. May we continue to meet and discuss all the ways we can make science better, and the sometimes not so easy ways we can make our children's lives even better.

Helmut, I would like to thank you for the path of growth you set me on. We met at tough stages of our (professional) lives. Our mutual passion for science is undeniable. Having brainstorm sessions about the roles of GluA3 is something that I truly treasure and I will forever remember. May the future brings us both the chance of redemption.

Kessels lab, thank you for being my work family for a while. I learned a lot from each of you and that's very valuable. In our own way, we formed a little tribe, through thick and thin. A special thanks to Eva, with whom I engaged in so many scientific discussions. I like to think we kept each other's "scientific flame" alive, and I'm glad we managed to do it so gracefully and even when crossing countries. I'm very proud of you and all that you accomplished.

Seçil, my paranymph, that since I "picked" from the oh so many PhD candidates never disappointed me. You bring me to my feet, amaze me with your humbleness and grace. I look up to you, to be more like you. Thank you, thank you.

To everybody from the Lohmann and Kole labs with whom I crossed paths. Thank you for all the love and support. Mustafa, we held each other throughout the days and I'm so glad we met. Your tenacity and perseverance are examples to me, your work is an inspiration and you are a role model. I love to have you in my life. Alex, you are amazing, so full of talents and such a cool girl. Talking and being with you is easy, no matter if we are in Amsterdam, Buenos Aires or Lisbon. I'm so happy to have you in my life. Cátia, my other paranymph. What a surprise life gave me by bringing you to mine (and yet you were always so close)! May we continue to forge this friendship and learn from each other at each step, knowing that it's much more what unites us than what sets us apart. You are one of a kind.

Nicolas, you opened your project to me and taught me, by example, how to work hard, permanently changing me. I learned so much from you and I take your work ethics with me. I hold you forever in my heart.

María, my honorary paranymph. I half-jokingly say that I couldn't handle being in the lab without you and that's why I left. Maybe it's not a joke, not even half of a joke. I missed and miss you. I'm forever thankful for having met you and have you and your family in my life. You, Bruno and my little niece Clarinha are family. May life continue to allow us to cross oceans once in a while and pretend for a few instants that we were never apart.

À minha mãe e ao meu pai. Por tudo o que eu podia ter sido e que não sou, e também por muito daquilo em que me tornei. Estou grata pelo caminho que me providenciaram e que me fez o tanto que sou hoje. O mundo nunca será suficiente para vocês, eu sei e compreendo, mas espero que possam ver, eventualmente, que é um tremendo lugar para se começar.

Thank you to Claartje, that guided me on defining my own path. *Muito obrigada à Bárbara e à Joana, que no último ano cuidaram do meu corpo e da minha alma. Muito obrigada à Teresa, que cuida da minha casa e da minha família como se fosse sua. Muito obrigada às minhas amigas e amigos que me acompanharam nesta caminhada. Pipi, Sofia, Rita, outra Sofia, Marcelo, Catarina, tantas e tantos.* It takes a village. *Estou rodeada de pessoas extraordinárias. Que jornada foi esta, que bom terem estado comigo!*

To Liesbeth and Willem, who always cared first (and only) about what was the best for me. You always think I will be fine no matter what I choose. Because of you, I actually believe that. Thank you also to Jeske, my *sister*, for never demanding more than what I could give and for never wanting me any different. And to Davey, that brought another perfectionist to the firm. I'm so very lucky to have you all as my family.

To Maçã, that throughout this quest was my constant reminder of what is important in life. She will never read this but was probably the one who suffered the most with my absences of body and mind throughout this endeavor. And to Limão, that joined our lives halfway this journey to make sure we don't forget to be kind and gentle – towards each other, towards him, and mostly towards the world.

Oh June, a beautiful endless summer started the moment you were born. I'm a better person because you exist in me and in our family. The world became a brighter place since you arrived. This is all for you, my little one. May this venture serve to show you that you can do anything you set yourself to, and we will always be here for you. May it also help you realize that you never ever change for others; instead, you show them the way, lead them to change and kindly guide them to see more kinds of beauty. *Em ti estão todos os sonhos do mundo*.

And lastly I would like to thank you, **Job**. You are my partner in crime and in life, my ever-present. Amsterdam is you and all the paths we took in between. This PhD was just another of our many adventures together - and there are so many more to come. You always see me better than I am, and you are the main force for me to become a better version of myself. I wouldn't want it any other way. From all I may have achieved so far, us two and all we do together is still what makes me the proudest. *Atravessemos juntos o deserto do mundo*.